A PRACTICAL METHOD FOR IMPROVED IMPLEMENTATION OF PILE DRIVING FORMULA

A thesis submitted in fulfilment of the requirements for the degree of Master of Engineering

Hamayon Tokhi
B.Eng.

School of Civil, Environmental and Chemical Engineering
RMIT University, Melbourne
February 2012

DECLARATION

I certify that except where due acknowledgement has been made, the work is that of the author alone; the work has not been submitted previously, in whole or in part, to qualify for any other academic award; the content of the thesis is the result of work which has been carried out since the official commencement date of the approved research program; any editorial work, paid or unpaid, carried out by a third party is acknowledged; and, ethics procedures and guidelines have been followed.

Signed:.....

Hamayon Tokhi

On: 27/02/2012

ACKNOWLEDGMENTS

I wish to express my deepest gratitude to my supervisor, Dr. Gang Ren, for allowing me to work on this research. I am also grateful to him for his guidance, support and encouragement throughout the duration of this research. I am also thankful to Professor Mike Xie for his assistance at various stages of this research work.

My sincere appreciation is due to Dr Julian Seidel for his help in this research. His fruitful discussions were invaluable to this work.

I am grateful to Frankipile, a local piling contractor, for allowing me for several weeks to use their office and allowing the use of their database.

This research project contains some data provided by local, national and international organisations. In this regard, I would like to thank the staff of the Washington State Department of Transportation for providing support for the project.

My appreciation is also due to Professor Samuel Paikowsky from the University of Massachusetts Lowell for providing moral support.

Finally, I would like to thank my wife Shukria; my children Nazo, Wali, Palwasha and Weis; and my parents Fazel and Nadia. Without their support I could not have had the luxury of pursuing the interesting research at RMIT University.

TABLE OF CONTENT

LIST OF FIGURES

LIST OF TABLES

LIST OF PUBLICATIONS

Tokhi H., Ren G., Xie Y.M. (2011), *Improving the Predictability of Hiley Pile Driving Formula in the Quality Control of the Pile Foundation*, Advanced Materials Research, Volume 261-263, pp. 1290-1296.

Tokhi H., Ren G., Xie Y.M. (2011), *A new application of Radar in Improving Pile Dynamic Formula used in the Quality Control of Pile Foundation*, Australian Geomechanic Society (AGS), Volume 46, Issue 4 , pp. 35-49, December 2011.

NOTATION

All notations and all symbols are defined where they first appear in the text. For convenience, they are also listed here together with their definitions. Metric units according to the S.I. system have been used.

a	acceleration;
A_p	cross sectional area of pile;
A_s	pile shaft area;
C	velocity of wave propagation in pile material;
C_1	temporary compression in the pile cap;
C_2	temporary compression in the pile;
C_3	temporary compression in the soil (or rebound);
Cu	undrained shear strength;
E	coefficient of restitution;
e_h	hammer efficiency;
e_d	driving system efficiency;
E_h, E_n, E_r	rated energy of hammer;
E_p	modulus of elasticity for pile material;
E_{pl}	energy losses in pile;
E_{sl}	energy losses in soil;
E_{max}	maximum energy entering a pile;
F1	pile head force at the peak impact or other time;
F2	pile head force at the wave return time or (2L/c) after the F1;

f_s soil friction resistance;

g acceleration due to gravity;

h actual stroke or height of hammer drop;

H maximum stroke;

I element number;

J_c case damping factor;

J_s shaft damping factor;

J_t toe damping factor;

l, L length of pile;

v particles velocity of the material around their points of equilibrium;

V_1 pile head velocity at the peak impact force;

V_2 pile head velocity at a time 2L/c later than V_1 time;

v_i velocity of ram, at moment of impact=$\sqrt{2ge_h hW_r/W_r}$.

v_c velocity of ram and pile, at end of compression period;

v_r velocity of ram at end of period of restitution;

v_p velocity of pile at end of period of restitution;

M_r moment of ram, at moment of impact (=$W_r v/g$);

M_t amount of impulse causing compression;

eM_t amount of impulse causing restitution;

P_1 the peak impact force;

P_2 impact force at a time 2L/c later than P_1;

P_p pile perimeter;

q_s shear stress;

q_u unconfined compressive strength;

Qs shaft quake;

Qt toe quake;

R_u ultimate carrying capacity of pile (ultimate soil resistance);

R safe (factored) working load;

s permanent pile penetration or set;

t time;

t_1 first peak, or impact time on a force vs time curve from the PDA testing results;

t_2 wave return time or 2L/c later than t_1;

W_r weight of ram;

W_p	weight of pile;
Z	vertical distance along pile axis;
Z	impedance = AE/c=Aρc;
ϕ	friction angle;
γ	weight density;
ρ	mass density;
σ	stress;

DEFINITION OF TERMS & ABBREVIATIONS

Bl.Ct:	Blow count (blows/m) =$1000/Set\ (mm)$.
Bl.Rt:	Blow rate (blows/minute).
BN:	Blow number.
BOR:	Beginning of restrike.
CAPWAP:	Case Pile Wave Equation Analysis Program.
ComStr:	Compression stress.
COR:	Coefficient of restitution, it describes the energy absorption of material= $\sqrt{h_2/h_1}$ $where\ h_1$ & h_2 $are\ initial\ and\ final\ heights$.
COV:	Coefficient of Variation. It is a non-dimensional parameter that denotes the relative natural scatter of data. COV=Standard Deviation/ Mean.
Compression (c):	Temporary compression or pile rebound as a result of hammer blow.
DFN:	Final displacement (PDA result).
DMX:	Maximum displacement (PDA result).
Driving Formula:	Energy equation developed based on the Newtonian theory to predict pile capacity as a function of delivered energy to pile, pile set and temporary compression.
Enthru:	Transferred energy into a pile.
EMX:	Maximum measured energy with PDA device.
EOD:	End of driving.
EOID:	End of initial drive.
FOS:	Factor of safety. It is used account for uncertainties from loading conditions, site variation and other geotechnical parameters.
GRLWEAP:	Goble-Rausch-Liking Wave Equation Analysis Program.

IBIS-S:	Relatively new radar equipment used in civil engineering applications, such as bridges, towers and high rise buildings. It was used in piling application for the first time and it can measure pile velocity, displacement, pile set and delivered hammer energy accurately and safely.
Kinetic Energy:	Potential Energy x Efficiency=$hW_r \times e_h$.
LVDT:	Linear variable differential transformer. It is used for measuring linear displacement.
maxCForce:	Maximum compression force.
maxCStrss:	Maximum compression stress.
maxD:	Maximum displacement.
maxEt:	Maximum transferred energy.
maxTForce:	Maximum tension force.
maxTStrss:	Maximum tension stress.
maxV:	Maximum velocity.
MQ:	Match Quality. A number that measures the quality of measured and calculated quantities such as acceleration and force propagation in pile.
Pile:	Pile is an elongated columnar body made from concrete, steel and timber that is driven in ground to transfer vertical loads to deep below ground.
Pile Driving Rig:	Rig used to drive piles. There are many types of rigs available and their differences are mainly due to the types of hammer used.
PDA:	A relatively expensive pile testing method called Pile Dynamic Analysis. Accelerometer and strain sensors are attached to the pile and the signals are captured via a portable computer. A software program uses one-dimensional Wave Equation to match the signals and hence calculate the pile capacity.
Penetration:	Total depth of embedment of pile in the ground.
Potential Energy:	Actual drop height ×Wr= hW_r.
PLT:	Pile load test.
Rated Energy:	Maximum energy a hammer can deliver=HW_r.
Set:	Permanent pile penetration per hammer blow.
SLT :	Static load test.
SPT:	Standard penetrometer test.
TC:	Temporary compression (PDA result)
TenStr:	Tension stress.

ABSTRACT

Piles are widely used in construction of foundations for infrastructure such as buildings, bridges and offshore structures particularly at fill and soft soil sites. Hence accurate and reliable determination of pile capacity is very important for design, construction and the overall estimate of the cost of these foundations. It is common in design practice to predict pile capacity by static analysis in advance of pile driving based on the results of in-situ and laboratory tests. Static load testing is carried out during construction stage on a typically 2-5 per cent of the piles in a reasonably large project to determine ultimate load carrying capacity of pile. One of the oldest methods of pile dynamic testing is the use of dynamic formulae that were developed based on the Newtonian impact theory. The contemporary dynamic methods are based on the application of the stress wave theory to piles, whereby the dynamic testing measurements of force and velocity at the upper end of the pile during pile driving and restrike are used for pile capacity prediction. This dynamic testing by wave equation analysis is a prevalent method of pile capacity and driving stress calculations. Unfortunately, though dynamic methods have been used in practice for many years, actual reliability of dynamic methods is vague because their comparison with static loading tests is made incorrectly in most cases due to the variation of pile capacity with time after the initial driving.

On the other hand, the traditional energy or dynamic formulae have been regarded as being unreliable and less accurate than the more analytical methods based on the wave equation analysis. The main two reasons for the poor performance of the dynamic formulae are the assumption of hammer energy and the inherent flaw that they do not take the dynamic resistance into account. With the advent of new technologies in the construction industry, gradual improvements have been made in the application of the dynamic formulae in many projects that have resulted in greater reliability. This research attempts to improving the reliability of the dynamic formula by accounting for the hammer energy and the dynamic resistance by carrying out a comprehensive GRLWEAP parametric analysis for different hammers, soil and pile types. Also, a new application of radar called IBIS-S is proposed as well as a site test results are presented using the Hiley, Gates and MnDOT formulae. The comparison of the results with the more rigorous PDA, CAPWAP® and the GRLWEAP™ analysis show that with the application of new and precise testing equipments, the dynamic formula can be used with greater accuracy than the Case method. It is also shown that the IBIS-S unit may also be used to estimate and evaluate the empirical parameters used in the

CAPWAP® and GRLWEAP™ analysis. This approach enables evaluation of the pile capacity to be made more accurately using the dynamic equations.

CHAPTER 1

1 INTRODUCTION

1.1 Overview

Casagrande (1964) recalled a prediction, made by Karl Terzaghi, in 1964 on the first anniversary of his death that:

'..the worst enemies of soil mechanics would not be those who were denying the validity of its basic assumptions, because those would die out, but that the worst harm would be done when pure theoreticians discovered soil mechanics, because the effort of such men would undermine its very purpose.'

Piling works also happen to fall in the same field because of the heavy reliance on the geotechnical engineering discipline. In fact piling work is a harmonious mix of art and engineering knowledge.

For thousands of years since piles were first used by humans, they naturally searched to developed ways to estimate the loading capacity of pile once it is in the ground in the most efficient and economic manner. One of the oldest methods is the Dynamic or Energy Formula that is still in common use amongst the piling practitioners and consultants according to research surveys (AbdelSalam et al., 2009, Fleming K. et al., 2008).

The early users of the pile driving formula applied the idea of driving a stake to driving of a pile and made the assumption that the effort required to drive the stake is directly related to the resistance

provided by the ground (Whitaker, 1970). As a result, many empirical formulae termed 'dynamic formulae' have been derived to establish the relationship between the pile driving resistance or penetration under hammering and the ultimate bearing capacity of pile.

Pile Dynamic or Energy Formula is a term used to describe a range of formulas of which Engineering News (ENR), Danish, Gates, Janbu, Hiley, FHWA and WSDOT are well known among many others. Countries with a strong tradition of using the Hiley Formula are particularly Hong Kong, UK and Australia while Gates, Janbu, FHWA and WSDOT are commonly used in the US. (Fung W.K., 2004, Lowery L.L. J r . et al., 1968, Whitaker, 1970)

These dynamic equations are generally categorised into theoretical equations, empirical equations and those consisting of the combination of the two. The theoretical basis for the derivation of the pile driving formulas is based on the Newtonian principles of impact between two rigid bodies, for example the driving hammer and the pile. Thus driving formulas are simple idealisation of complex interactions between hammer, pile and the ground.

Experience and pile tests over the years have shown that the dynamic formulae in general and the Hiley formula in particular, consistently over predict pile capacity compared to the reference static tests. It is particularly true when the safety factors are applied to the ultimate load calculated by the dynamic formulae. Typically, a safety factor for the Hiley formula is around 3 whilst for the Wave Equation Method it is 2.5 and for static load tests it is about 2 (Paikowsky, 1994, Paikowsky S, 2004, Paikowsky S., 2009). The reason for this over prediction of capacity evaluation by the Hiley formula is that the formula does not take into account the dynamic component of the capacity.

The primary aim of this research is, therefore, to improve the reliability of the dynamic formula. This research program will concentrate on the proposal of a correction factor to adjust for this dynamic component similar to the damping parameter used in the Wave Equation Analysis and validate its reliability experimentally and theoretically. Similarly, the issue of the variation in the hammer energy delivered to pile needs to be improved by the adoption of new technology and validate experimentally.

1.2 Objective

The objectives of this research are:

1. To review and summarise the methods of the pile driving formula and derive a more general method of application.
2. To improve the reliability of the dynamic formula by accounting for the hammer energy and the dynamic resistance by carrying out a comprehensive parametric analysis using wave equation analysis software for various hammer, soil and pile types.
3. To propose a new application of radar instrument called IBIS-S.
4. Carry out empirical analysis of site test results using the Hiley, Gates and MnDOT formulae.
5. Perform PDA, CAPWAP® and the GRLWEAP™ analysis and compare the results.
6. To illustrate that the dynamic formula, particularly the Hiley formula, can be used to show that with the application of new and precise testing equipments.
7. To show the dynamic formula can be used to determine the ultimate loading capacity of piles.

1.3 Scope of Work

The following paragraph provides a summary of the scope of work that has been undertaken during this research study.

- *Piling Database*: Data collection and analysis of piling contractor's database.
- *Software analysis*: Wave equation analysis of 1400 cases.
- Field testing: Parallel testing of pile using PDA and IBIS-S instruments.
- CAPWAP: Wave equation signal matching analysis of the field testing results.

1.4 Thesis Outline

This thesis is presented in seven chapters. After the background and objectives of this research in earlier sections, progression towards the proposed research work is presented in the following order:

Chapter 2 Background

This chapter is presented in the context of pile dynamic methods and in relation to pile driving formula.

Chapter 3 Literature Review

This reviews relevant previous theoretical and experiment works into the pile dynamic formula, including pile testing and installation methods.

Chapter 4 Wave Equation Analysis of Piles

Provide a comprehensive parametric data analysis using wave equation based finite element analysis package named GRLWEAP. Theoretical relationships between energy and pile movement (set) for different hammers, piles and ground conditions are presented.

Chapter 5 Field Instrument Results and Analysis

Present the results of field dynamic testing and analysis by wave equation with respect to the objectives of the research. A new application of radar instrument for pile testing is proposed and the results of parallel testing with the field dynamic testings are presented.

Chapter 6 Summary and Conclusions

The results of the research program are summarised and conclusions drawn.

Recommendation for future research work and some issues raised in this research are suggested.

CHAPTER 2

2 BACKGROUND

2.1 General

In order to present the setting for this research, it is deemed necessary to present a discussion on the application of different dynamic pile testing methods in practice with particular emphasis on the dynamic formula, which is the particular subject of presented research. The methods are divided according to the design and construction stages of a project. The methods that require dynamic field measurement, which is based on the wave equation, can be broadly categorised as those that are based on a simplified analysis and those that are based on further elaborate computer signal matching calculations. Finally, a brief discussion of pile driving equipment is given to complete the setting of the presented research.

2.2 Pile Types

Pile foundations are employed in various situations where the weight of a superstructure need to be transported to stronger soil layers deep underground. It is the best foundation solution in areas prone to erosion and earthquake and also is the only possible foundation option for offshore structures.

Piles are generally categorised as displacement and non-displacement piles. Driven precast and close-ended tube piles fall into the displacement category, in which, large volume of soil is displaced during installation. Steel piles with thin cross sections such as H and open-ended tube as well as screw and bored piles are categorised as non-displacement piles. These piles cause little or

no disturbance to the surrounding soil during piling process. A summary of advantages and disadvantages of different pile types are presented in Table 2.1.

Table 2.1 Summary of advantages and disadvantages of different pile types (after Broms, 1981)

Pile Type	Advantages	Disadvantages
Timber piles	The piles are easy to handle and to cut Relatively inexpensive	The piles will rot above the ground water level. Have a limited bearing capacity. Can easily be damaged during driving by stones and boulders. The piles are difficult to splice and are attacked by marine borers in salt water.
Steel piles	The piles are easy to handle and can easily be cut to the desired length. Can be driven through dense layers. The lateral displacement of the soil during driving is low (steel H- or I-piles). Can relatively easily be spliced (welded or bolted).	The piles will corrode, will deviate relatively easy during driving. Are relatively expensive.
Prefabricated concrete piles	Do not corrode or rot. Are easy to splice. Relatively inexpensive. The quality of the concrete can be checked before driving. Not affected by the ground water conditions.	Relatively difficult to cut. Displacement of the soil during driving. Can be damaged during driving. Replacement piles may be required. Sometimes problems with noise and vibration .
Cast-in-place concrete piles a) Permanently cased (casing left in the ground) b) Temporarily cased or uncased (casing retrieved)	Can be inspected before casting. Can easily be cut or extended to the desired length. Relatively inexpensive. Low noise level. The piles can be cast before excavation.	Relatively expensive. Time consuming. Can not be used immediately after the installation. Limited length. The pile can be damaged by "necking" during the withdrawal of the casing. Adjacent piles can be damaged during driving. Difficult to check the integrety of the pile.

2.3 Pile Material

Depending on the applicability in a given situation, one of the three different pile types timber, concrete or steel is selected to construct a pile foundation.

2.3.1 Timber Piles

Timber is well suited for construction of jetty and other on-shore structures for their energy absorbing qualities. They relatively inexpensive pile construction material and its durability and resistance to decay can be improved with preservatives such as arsenates and creosotes or can be even shotcreted. All the methods of application of preservative are the same in principle. The piles

to be treated are loaded into a large steel cylinder and preservatives are applied under pressure until the required absorption has been obtained.

The main drawback of timber pile is the limit of length and structural capacity. It is therefore the most suitable option for the construction of residential building in marshland area and marine environment. In US and Scandinavian countries both softwood and hardwood are still commonly used. In Australia treated hardwood is commonly used. Pile lengths vary up to 15m and pile sections are generally square (250mm-500mm) although round section can be also be used.

Driving of timber piles are carried out with a drop or light hydraulic hammers. For driving through dense soil, a steel band around the head and shoe attached to the tip of the pile are needed to mitigate against head crushing and toe disintegration.

2.3.2 Concrete Piles

Concrete piles are the most versatile and are useful in carrying fairly heavy loads through soft soil to harder strata. Concrete piles can be cast to a specification on site or at a yard. The main two types of concrete pile are precast and cast in-situ. Precast piles are normally constructed in square constant cross section, or circular with a core hole to save weight. Pile tips may be flat or pointed and it can also adopt a mechanical shoe for hard driving conditions. Concrete piles can be spliced to suit any desired length by mechanical means.

2.3.3 Steel Piles

These types of piles can come in many different sections such as tube, H or I-sections and provide excellent resistance to both compression and tensile forces. Steel piles are less prone to structural damage during driving process and can be spliced to a desired length very conveniently. However, the main disadvantages of steel piles are relatively high cost and vulnerability to corrosion in marine environments.

2.4 Pile Driving System

Piles are nowadays installed by driving, drilling, vibration, screwing, jacking or by a combination and can be augmented by excavation or water jetting. Installation of piles by brutal force requires careful control combined with good deal of experience and judgment. Hence, success depends heavily on the selection of pile driving equipments, hammers, cushion materials as well as a sufficient knowledge of the soil conditions.

Generally the pile driving system consist of lead, hammer cushion, helmet and pile cushion as shown in Figure 2.1. Different lead system are designed and used depending on the situation one site. It is mainly categorised into fixed, semi-fixed and offshore lead.

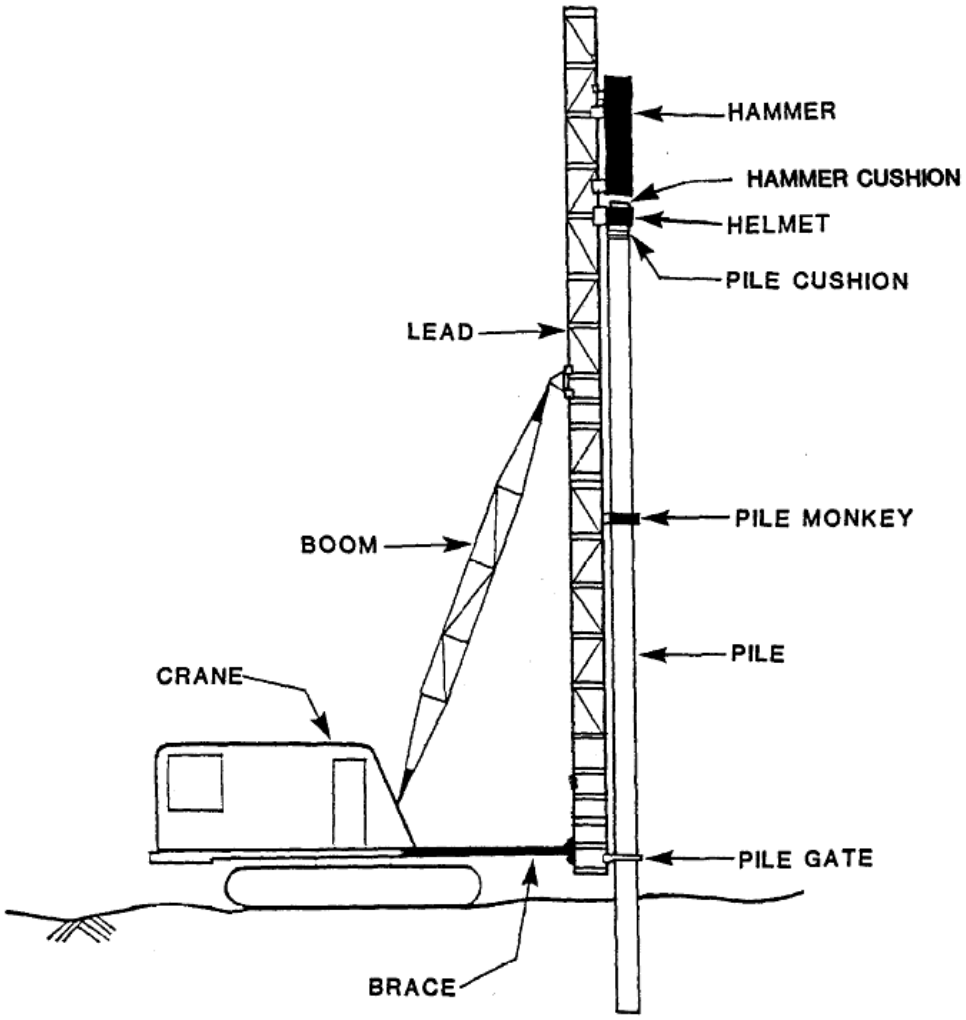

Figure 2.1 Pile support system (after Rausche et al, 1986)

2.4.1 Pile Driving Hammers

Piling hammers play the most important role in the installation of piles because the capacity of the pile depends on the performance of the hammer. The essential role of a hammer is to impart kinetic energy resulting from the gravity fall of the hammer weight. In some hammers this energy is augmented by taking advantage of gravity and further accelerating the mass by mechanical means. However, not all potential energy is converted to kinetic energy and there are losses in driving mechanism due to friction, cushioning and the restitution.

Hammers are categorised into "external combustion", meaning that the power to raise the ram comes from an external source such as rope, steam, air, hydraulic and "Internal combustion" that only apply to diesel hammers. There are further subcategories and Figure 2.2 gives a hierarchy of all common hammer types.

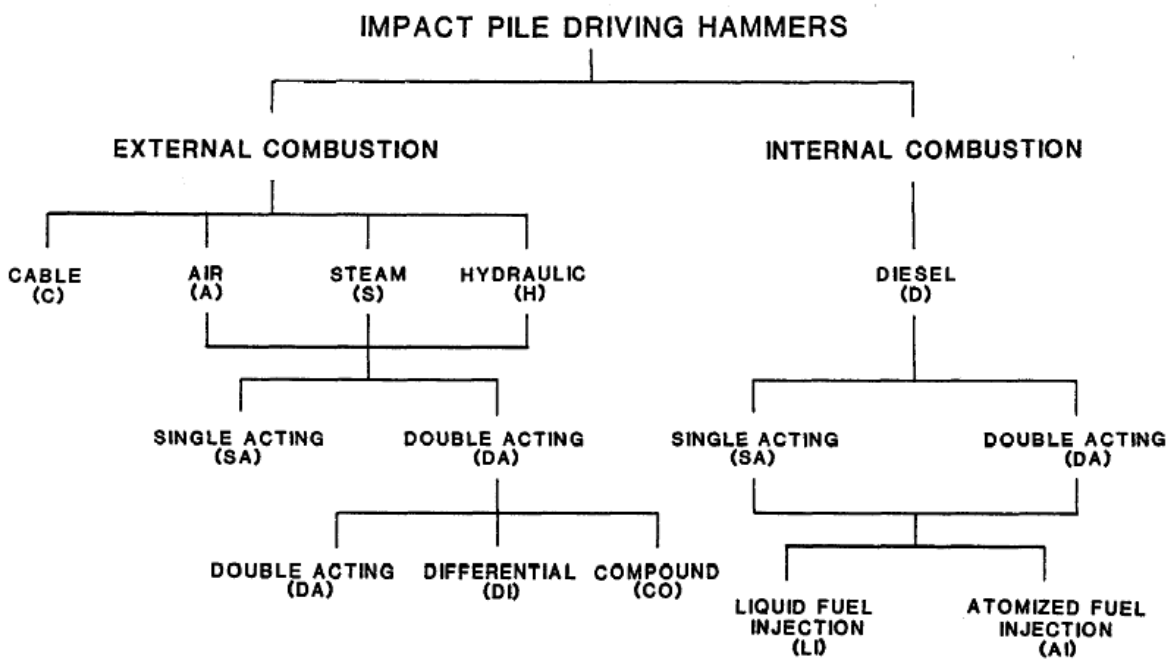

Figure 2.2 Pile driving hammer categories (after Rausche et al,1986)

The efficiency of a diesel hammer, in contrast to the hydraulic hammer, depends on the soil resistance, mass and stiffness of the piles because the ram relies on the reaction force to be lifted up. It is for this reason that the diesel hammers have an advantage over other hammers when driving

concrete piles due to the low impact energy in low resistance soils as it minimises potential damaging tension stresses. Another concern with diesel hammers is that the impact energy may suddenly increase and over-stress the pile. This can be a concern when driving piles through very soft soil to a hard rock bearing layer.

2.4.2 Drop Hammer

A drop hammer is essentially a weight that is repeatedly raised by a rope and then released by tripping it to fall on piles by gravitational force. Dropping weight or drop hammer is the traditional method of pile driving and is still frequently used. A track rig or crane can incorporate the guide for a drop hammer and hoist the pile into position and support it during driving. The impact velocity or delivered energy is strongly influenced by frictional losses in the hoist rope and guide frame.

2.4.3 Single Acting Hammer

Single acting hammer uses steam or air to raise the ram that is connected by a rod to a piston inside a cylinder, shown in Figure 2.3. On upstroke, the steam or air pressures forces the piston up through an inlet valve. When the piston reaches the top of the cylinder near a vent, the valve trips and closes the inlet and opens the cylinder to the exhaust port, which results in hammer falling and driving the pile. These hammers usually have a 0.9m stroke. The blow characteristic is low impact velocity that is more effective than a high-velocity light ram.

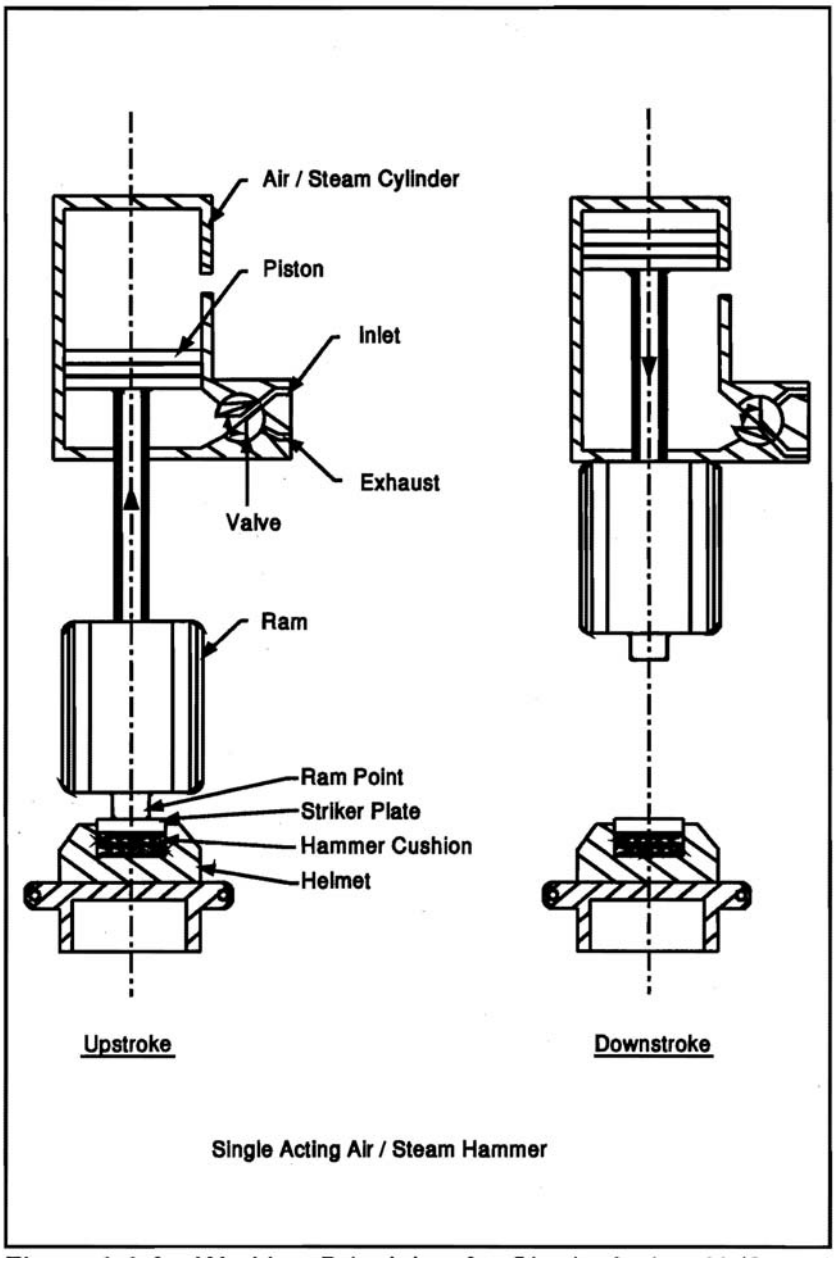

Figure 2.3 Operation principal of single acting hammer (PDI 2005)

2.4.4 Double Acting Hammer

As the name implies, double acting hammers use air, steam or hydraulic to drive the hammer ram both in the up and down strokes. Thus the energy developed is a direct result of gravity fall plus the force developed in the piston by air, steam or fluid pressure. These hammers operate at a high speed compared to the single-acting hammers. However, because the maximum kinetic energy cannot be

more than the stroke times the weight and the hammer weight less than that of a single-acting hammer due to speed of operation, it has led to the development of differential hammers.

2.4.5 Differential Hammer

Differential hammer is similar to double-acting hammer that uses air, steam hydraulic pressure to raise the ram and accelerate the fall of hammer. However, it differs from the double-acting hammer in that it has two pistons located at approximately the top and middle of the cylinder. The upper piston is larger than the lower piston thus the difference in pressures on these two pistons is the net driving force of the ram. The use of heavier rams in the differential hammers result in the advantage of differential hammers over double acting hammers. For hydraulic hammers, only one piston is required to the high operating pressure.

Air and steam differential hammers tend to run slowly in easy driving conditions and increase their speed as the pile resistance increases. For hydraulic hammers, on the other hand, the operating speed is high during easy driving conditions and slows down as the pile resistance increases. Overall, the operating speed of hydraulic differential hammer is 1.5 times the comparable air or steam differential hammers.

Differential hammers can show variability in performance and the ram velocity is affected by the throttle control. The maximum energy developed by these types of hammers cannot exceed the hammer weight times the drop height (PDI 2005).

2.4.6 Diesel Hammer

Diesel hammers are either open-ended (single-acting) or closed-ended (double-acting) type. As the name implies, for the open-ended hammer the top of the cylinder is open, therefore, allowing the piston to rise and then to freely fall by gravity. A diagram showing the working principle of the single acting hammer is shown in Figure 2.4. The basic working principle of the diesel hammer is an internal combustion of diesel fuel between the ram and anvil that results in both pushing the pile down and in raising of ram for the next stroke. The cycle begins by raising the ram by a lifting device inside the cylinder and then allowed to fall. As it falls, the exhaust valves are closed off and diesel fuel is pumped into the combustion chamber. The falling ram compresses the mixture of air

and fuel and upon impact of the ram with anvil, the compressed hot air-fuel mixture is ignited that result in the downward pushing of the pile and the upward moving of the ram for the next stroke cycle.

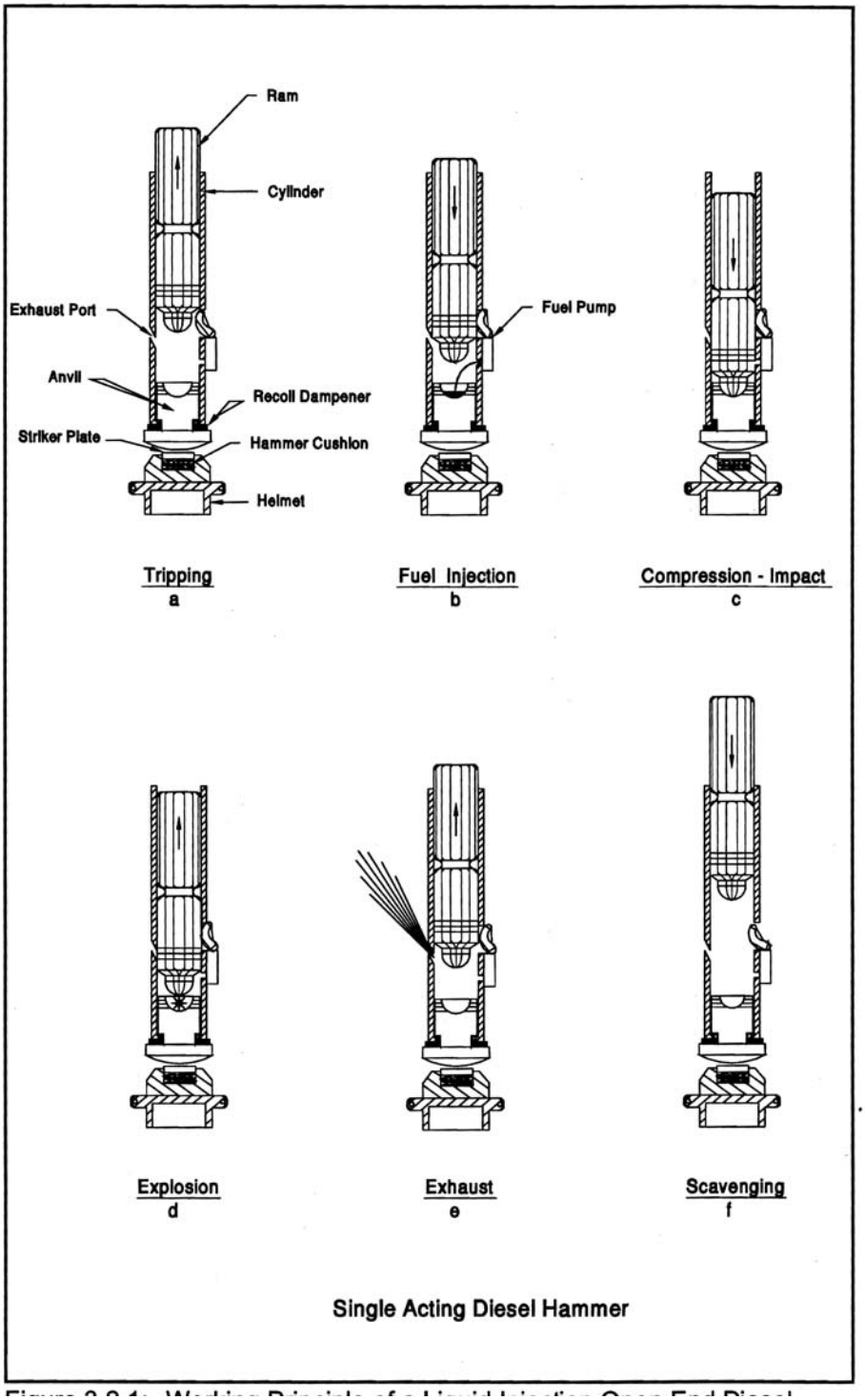

Figure 2.4 Operation of single acting diesel hammer (after PDI, 2005)

The closed-ended diesel hammers operate similarly to open-ended hammers, except, that for the closed-ended hammers, the air above the piston is compressed on the upstroke and it accelerates the ram or piston down as it expands. The pressure generated in the top chamber can be monitored and converted to an equivalent stroke. Figure 2.5 shows a schematic arrangement of the double-acting diesel hammers.

An interesting feature of some diesel hammers is that the single and double acting hammers are convertible. These hammers generate maximum energy under hard driving conditions. The hammer impact can be affected by abnormal pre-ignition which can be caused by either overheated ram or using fuel with low flash-point. The diesel hammers operate at approximately similar speed to the single-acting hammers.

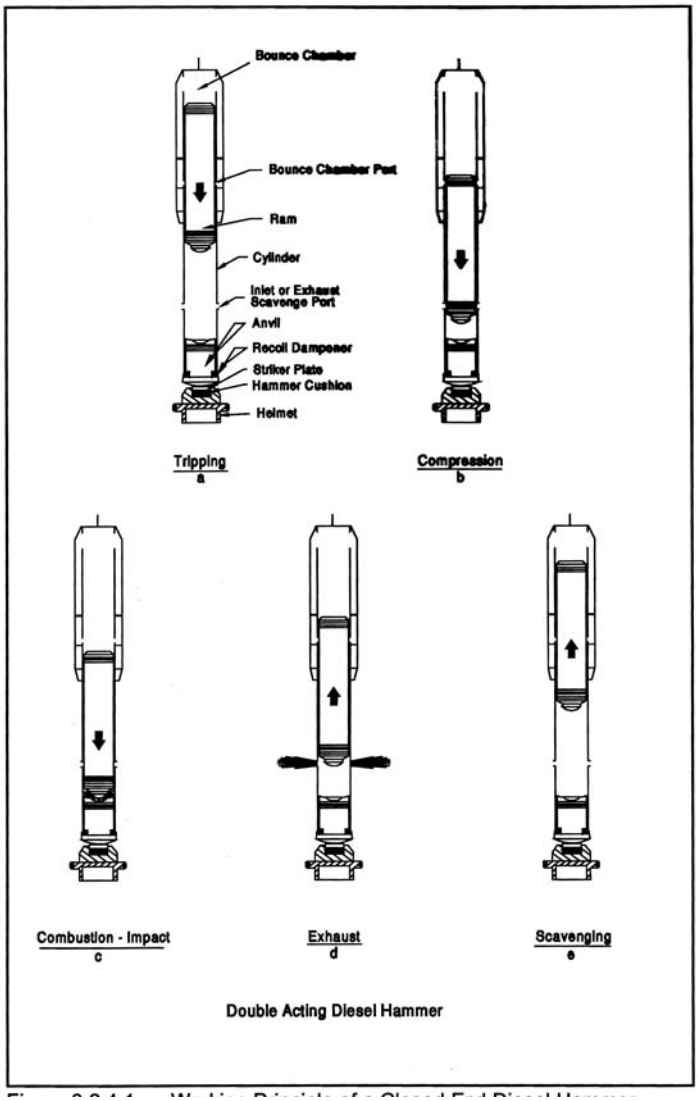

Figure 2.5 Operation of double acting diesel hammer (after PDI, 2005)

2.4.7 Vibratory Hammer

Vibratory hammer consists of contra-rotating eccentric masses that are powered by hydraulic or motor and can be supplied from a mobile generator or hydraulic power pack. The vibrations are produced by the pair of weights mounted on rotating shafts and phased in a fashion that tends to cancel the horizontal forces and to add in the vertical direction. The pile vibrators generally operate at low frequency, below 50Hz with un-damped amplitude of 5 to 30mm or high frequency that operate in the range of resonant frequency of the pile itself (Chellis, 1951, Fleming K. et al., 2008, Salgado R., 2006, Tomlinson, 2001). During vibrating process, granular soil around the pile effectively become like fluid resulting in reduction of shaft friction and improved penetration. For clay soils, however, the effectiveness of the vibratory hammer is generally not good. The main drawback of the vibratory hammer is associated with large energy inputs that are put into pile that results in excessive noise and vibration. It can be a good method to extract piles from the ground. Vibratory hammers are not modelled by the existing wave equation analysis. One of the main disadvantages of the vibratory hammers is that these types of hammers are not yet able to be modelled and analysed by the existing wave-equation methods.

2.4.8 Hammer Cushions

Hammer cushions are used between the helmet (also called cap) and the ram to protect the ram and pile from damage and also to control impact stresses. Commonly used hammer cushion material consist of hardwood about 150mm thick in tight fitting steel ring with its grain parallel to the pile axis to provide maximum stiffness. However, the disadvantages of this cushion are that it becomes crushed and burnt, requiring frequent replacement, and the elastic property of the material changes during driving.

Instead, laminated aluminium and micarta materials are frequently used. These cushions have a consistent energy transmission, elastic property remain nearly constant and have relatively long life compared to the hardwood cushions. As a result, the coefficient of restitution or the efficiency of these cushions is about 0.8 compared to 0.5 for hardwood cushions.

2.4.9 Pile Helmet

Pile helmet is used to hold the head of the pile in position under the ram, to distribute the impact force and align the hammer and the pile. Helmets for H and tube piles are normally snugly fitted to prevent bulging and distortion. However, for concrete piles it should not be tight to prevent pile rotation. Pile drivability is heavily influenced by the mass of the helmet.

2.4.10 Pile Cushions

Pile cushions are used between the pile helmet and the top of concrete pile. It is intended to protect the pile and control impact stresses in the pile. Pile cushions are made from plywood and it is designed to prevent concrete spalling and to limit excessive stresses and yet transmit the hammer impact energy efficiently to the pile. Therefore, it is prudent to achieve a balance between the hammer size, cushion thickness and the pile size.

2.5 Pile Axial Capacity Evaluation

From start to finish, construction of pile foundation generally involves four stages: geotechnical site investigation and associated laboratory testing; design of pile load carrying capacity based on the numerous analytical methods; installation; and pile capacity verification as well as the load-settlement performance and integrity. Pile test may be carried out at any stage of construction whether it is during, preconstruction or post construction. At preconstruction stage, the design of pile capacity is based on the site investigation and laboratory testing that are inherently uncertain and over simplified. Hence it becomes necessary to test piles to ensure compliance is met to the required capacity. Static testing is carried out on insignificant percentage of installed piles (1 to 2%) due to the high cost of testing involved. Other testing like dynamic testing is often undertaken on relatively higher percentage of installed piles (5-10%) (Fleming K. et al., 2008, Hertlein B., 2006, Salgado R., 2006, Timoshenko S.P., 1951). Therefore, dynamic testing eliminates some of the uncertainties in the inherent deficiencies in the design processes. The remaining untested piles (90 to 95%) of piles are installed based on the results of the dynamically tested piles. This is precisely one of the biggest disadvantages of dynamic testing and it is therefore the main justification for the important role of the dynamic formula. This is the main focus of current research. In the following sections, both the traditional and the more recent methods of determining pile capacity are

discussed, with particular emphasis on dynamic pile testing as it relates to the specific focus of the research undertaken.

2.5.1 Static Design

A pile subjected to vertical load will carry the load partly by shear generated along the shaft and partly by normal stresses generated at the base of the pile. Currently numerous analytical methods for calculating ultimate static capacity have been developed. Some of the methods that are used for calculating pile capacity are Terzaghi, Meyerhoff, Vesic, the α , β and λ methods. Table 2.2 gives a summary of the equations used in the different methods. It needs to be emphasised that all of these methods are formulated on in-situ soil parameters, which are often very hard to know with certainty and to account for the variation of capacity with time. More comprehensive details on these methods can be found in Tomlinson (2001). The ultimate load derived from these equations is divided by a suitable factor of safety (FOS) to obtain allowable load on a pile that is subject to an allowable settlement. The magnitude of FOS is dependent on several factors and a FOS between 3 and 4 is commonly used.

Table 2.2 A summary of the some of the static capacity evaluation methods for driven pile (Paikowsky et al 2004).

Method	Side resistance	Tip resistance	Parameters required	Constraints
α-Tomlinson (Tomlinson, 1980/1995)	$q_s = \alpha S_u$	$q_p = 9\ S_u$	S_u; D_b (bearing embedment)	+Bearing layer must be stiff cohesive + Number of soil layers ≤ 2
α-API (Reese et al., 1998)			S_u	
β in cohesive (AASHTO, 1996/2000)	$q_s = \beta\sigma'$		OCR	
λ (US Army Corps of Engineers, 1992)	$q_s = \lambda(\sigma'+2S_u)$		S_u	Only for cohesive soils
β in cohesionless (Bowles, 1996)	$\beta\sigma'$		D_r	
Nordlund and Thurman (Hannigan et al., 1995)	$q_s = K_\delta C_F \sigma' \frac{\sin(\delta+\varpi)}{\cos\varpi}$	$q_p = \alpha_t N'_q \sigma'$	ϕ	
Meyerhof SPT (Meyer-hof, 1976/1981)	$q_s = k\ N$	$q_p = 0.4D/BN'$	N	+ For cohesionless soils + SPT data
Schmertmann SPT (Lai and Graham, 1995)	q_s = function(N)	q_p = fn(N)	N	SPTdata
Schmertmann CPT (McVay and Townsend, 1989)	q_s = function(f_s)	q_p = fn(q_c)	q_c, f_s	CPT data

2.5.2 Static Load Testing

Static load testing began as a way to check that piles could carry their load as designed. The test consists of applying a load equal to the working load plus an equivalent FOS load to the pile top in a manner in which incremental load is applied and held for duration of time and then taken off in similar fashion. The load on pile is made up of heavy load available close to site, usually stacked on a frame called kentledge. Other systems are ground anchors and reaction piles. Figure 2.6 shows a typical set up of the reaction system.

Static load testing is normally undertaken for the reasons of establishing the load-settlement relationship, proof testing to ensure failure is not reached and to check the capacity evaluation by other dynamic and static formula to enable other piles to be installed by empirical methods. It is for these reasons that static load testing is often used as a reference for comparisons of pile capacity evaluations because of the assumption that the testing closely replicates the process of pile loading on a construction site.

However, static load testing can inflict a high cost a significant amount of time right from set up and dismantle to interpretation of results. In addition, the need for significant reaction system imposes even higher cost. Despite all these, the results are often very difficult to interpret by the current methods of analysis. The methods used to calculate the pile capacity from the static load testing are Davison, Chin, Butler-Hoy, Tangent, Slope, D/10 (Allen T. M. , 2005, Allen T. M., 2007, Fleming K. et al., 2008, Fragaszy R.J. , 1988, Fragaszy Richard J. , 1989, Gozeling F.T.M and Van Der Velde E.G., 1996, Lowery L.L. J r . et al., 1968). These methods often give different results which make the interpretation very difficult. In situations of constructing pile in an offshore environment, it may be very difficult to perform static load testing.

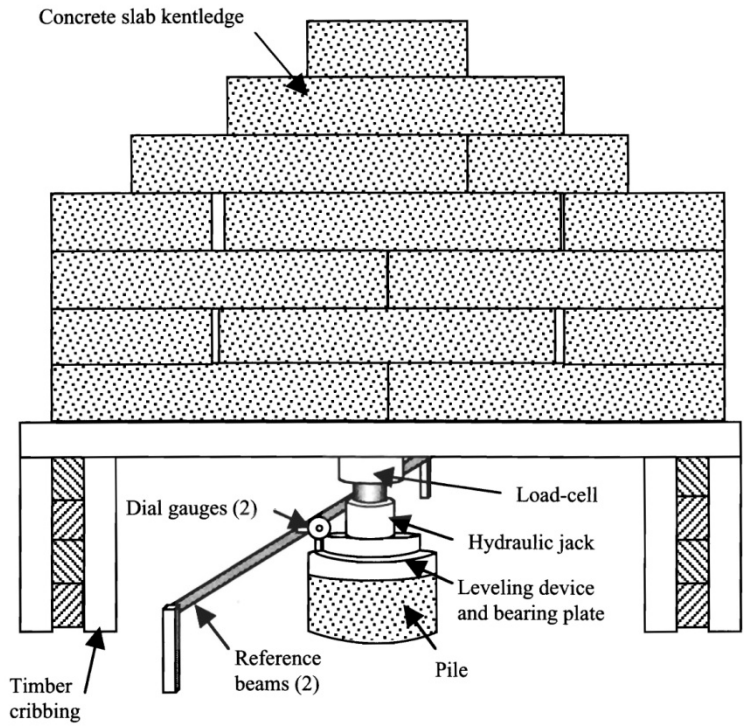

Schematic of a static axial compression load test with a 'kentledge' reaction mass (note that the 2nd reference beam has been omitted for clarity)

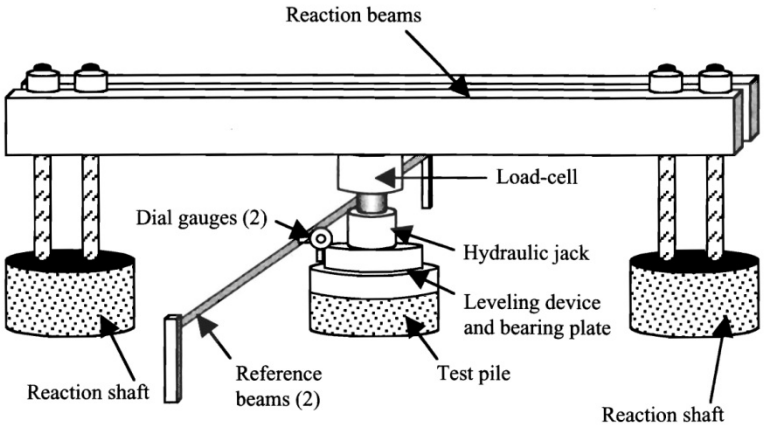

Schematic of a static axial compression load test with reaction shafts (note that the 2nd reference beam and gauges have been omitted for clarity)

Figure 2.6 Typical setups in static load testing (after Hertlein & Davis 2006)

2.5.3 Rapid Load Testing (Statnamic)

Statnamic load testing combines the advantages offered by both static and dynamic load tests. It uses rapid compressive force and the parameters like acceleration and displacements are measured

with accelerometers and displacement transducers. The Statnamic device itself consists of a large mass and a combustion chamber in which a rapid burning fuel is fired to create a compressive force on the pile. The returning mass is caught by a mechanical system before it impacts the pile again. During the short loading, over 2000 data are taken by a data acquisition device and load-displacement curve generated is used to determine the equivalent static load.

Generally, the peak impact velocity generated during Statnamic testing is less than the dynamic pile testing. If the rapid burning fuel is excessive, then the impact velocity may be quite large, thus, resulting in an overestimate of static capacity.

2.5.4 Dynamic Load Testing

This method of determining the pile capacity was developed in the 1970's (Rausche F. et al., 1972). Today, dynamic pile testing is accepted as a valid technique of inferring the static capacity of piles and a standard quality assurance and construction control method for piled foundations. A typical set-up for carrying out a dynamic test involving a ram as well as strain gauges and accelerometers is shown in Figure 2.8.

The dynamic pile testing method is based on the analysis of stress-wave propagation in pile generated by the blow of the pile driving hammer, and reflected from soil resistance acting along and below the pile and from variations in the geometry and material properties of the pile. The theory of stress-wave propagation in the pile is well documented e.g. (Rausche F. et al., 1972, Randolph M.F., 1979, Goble G.G. & Aboumatar H., 1992, Rausche et al., 1997, Hussein M.H., 2004, Fleming K. et al., 2008). An extract from Timoshenko (1951), Verruijt (2005) and PDI inc. (2006) that explain critical and relevant aspects of the theory is included in Appendix A.

Dynamic pile testing has become widely used as a replacement for or supplement to static loading tests because of its inherent savings in cost and time. These dynamic methods allow monitoring pile driving and restrike, and also provide a method of identifying problems during driving for many kinds of piles. To obtain reliable ultimate resistance, it is necessary that the long term pile capacity be fully mobilised. Dynamic testing methods can determine static capacity at the time of testing, in other words either at the end of driving or at restrike. This is a substantial advantage because

dynamic tests can be easily repeated and, consequently, there is an opportunity to obtain pile capacity as a function of time as well as pile embedment.

A special advantage of dynamic pile testing that is not available to static load testing is the ability to test the pile during the exact time of installation. Hence, since piles are installed in soils of all types particularly fine-grained soils below the water table, the piles experience time-dependent capacity changes. Capacity increases (known as set-up, presented in next Chapter 3) are most common. Also, capacity reductions (known as relaxation) are observed in relation to loss of toe capacity in shale/chalk formations. These capacity changes can be monitored by a sequence of dynamic tests commencing at the end of driving, and continuing for days, weeks or even years. Practical limitations make it impossible to statically load test a pile at the completion of installation, or to undertake sequential load tests, unless for a special research application. This feature of dynamic testing enables a direct relationship to be established between pile capacity and the field response (measured as set and temporary compression), and to develop a meaningful correlation between dynamic pile testing and dynamic formulae. Dynamic testing is used not only for estimating pile capacity, but also more generally for construction control, including stress control, damage assessment and pile driving hammer evaluation.

When a pile is dynamically tested during driving or after installation, the capacity of the pile can be approximated using a non-rigorous method called the Case Method and/or more accurately determined using a rigorous method involving signal matching of the measured stress-wave record. These analyses are described subsequently.

2.6 Wave Equation Analysis

The theory of wave propagation provides the proper theory of pile driving. Wave equation was proposed nearly 150 years ago in 1866 by Saint Venant and Boussinesq for longitudinal impact of bars (Timoshenko and Goodier, 1951). Isaacs (1931), an Australian, was the first to point out the application of wave propagation theory to piles and developed a set of graphical charts and formulas to analyse the stresses and displacements in piles. In 1938, E.N. Fox published a solution of the wave equation and because of the physical and numerical complexities it never took off until 1960 when Smith (1960) presented the mathematical method which, with some modifications, could be applied to pile driving problems and solved numerically by computers. Smith modelled the

pile, hammer and cushion as a series of springs and the actions were analysed in 1/40,000sec time steps. Smith compared the process of the numerical pile calculation to that of an animation artist trying to compute the picture motion based on the 1/24 frames per second so that the final motion is smooth and uniform. Smith also used a simple analogy to explain the basic method for obtaining the numerical solution of the pile driving problem; he used the analogy of water wave travelling in one direction and trying to capture the shape of the wave by small 'rigid floats' connected together by flexible links. For the ground resistance, Smith (1960) used Chellis (1951) concept of the elasto-plastic response at pile toe and suggested using soil quake and soil damping or 'viscous damping' to model soil behaviour subject to impact loading. The reason for introducing the additional damping factor, according to Smith, was to consider the time dependant of pile penetration, as is evidently used in vibration problems.

Wave analysis of piles should be strictly three-dimensional due to the fact that the hammer, pile and helmet are essentially three dimensional. Also, more importantly the interaction between the pile and the surrounding ground is also three-dimensional. However, because of symmetry this interaction may be simplified to two-dimension case. The two-dimensional theory of wave propagation has been studied (Fischer, 1984) in an infinite elastic media and it has been found that the pile-soil interaction to be frequency dependant which is a much better approximation than the one-dimensional theory that is velocity dependant.

2.6.1 One-Dimensional Wave Equation

The one-dimensional equation is derived using Newton's second law. A detail of derivation of the one-dimensional analysis applied to piles is given in Appendix A. The longitudinal stress propagation in a pile during pile driving is given by the following governing hyperbolical differential equation:

$$\frac{\partial^2 w}{\partial t^2} - c^2 \frac{\partial^2 w}{\partial z^2} = 0 \qquad 2.1$$

Where $c = \sqrt{E_p/\rho}$ and w(z,t) is the axial displacement of cross section at distance z and time t. E_p and ρ are modulus of elasticity and density of pile material respectively.

Equation 2.1 is easily solvable by the various mathematical methods such as Laplace, Separation of Variables and Method of Characteristics. Timoshenko (1951) and Verruijt (2005) provide details of the solution and propagation of stress wave in elastic solid media for simple boundary conditions that provide a good insight into the behaviour of stress wave induced in solid media as results of impact energy.

The general solution of Equation 2.1 consists of superposition of two waves, one moving downwards and the other moving upwards both with velocity ($c=\sqrt{E_p/\rho}$). Of course, in this fundamental case, there is no damping which means that the waves propagate without change of shape and the wave attenuates over time.

The fundamental finding from the solution of the hyperbolical differential equation is that wave motion moves energy through the material. The speed of that energy movement is the speed of the wave or wave velocity. The individual particles of the material move about their points of equilibrium and retain that position after the wave has passed. This means that the particles move with a velocity, which changes with time. The speed of the particles is normally lower than the speed of the wave. The wave motion does not transport mass, but it rather transports energy as result of the hammer impact.

When soil friction resistances, as in Equation 2.2, are introduced into the partial differential equation, then the solution is neither simple nor practical, except for very simple cases where the friction can be expressed as a function.

$$E_pA_p\frac{\partial^2 w}{\partial z^2}-P_pf_s=\rho A_p\frac{\partial^2 w}{\partial t^2} \qquad 2.2$$

Where, A_p is pile cross section area, E_p is modulus of elasticity, ρ is density of pile material, P_p is pile perimeter and f_s is frictional force acting on perimeter by soil.

In the case where there is ground shear resistance, the solution for above differential equation is carried out by numerical finite difference method and in fact the Smith's approximation in itself turns out to be essentially a finite difference technique.

2.6.2 Boundary Conditions

When the solution of the wave equation in the un-damped case is applied to pile for three simple boundary conditions (i.e. free, fixed, section area or impedance change), an insight into the behaviour of wave propagation and reflection is gained.

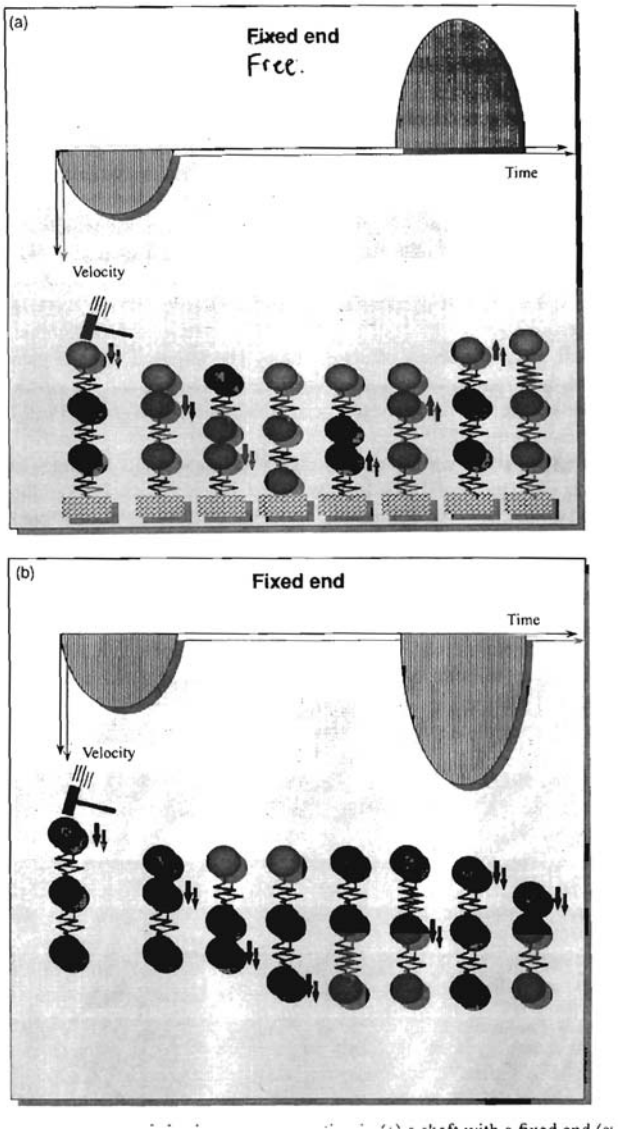

Figure 2.7 Wave stress propagation and reflection in pile with fixed and free end boundary conditions (after Hertlein 2006)

At a free end, as the compressive force reaches the end it become zero because there is no mass to transmit the energy to, and instead the compressive pulse is reflected as a mirror image of the incoming pulse. This reflected wave is hence the same magnitude but opposite sign. Therefore, a compressive force is reflected as a tensile force and vice versa. Furthermore, the particle velocity of

the reflected wave is the same as the incoming pulse, which implies that at the free end the particle velocity is doubled. Another way to look at this is in terms of the wave's energies. Initially the compressive pulse is half kinetic and half potential energy. At the free end all the energy is converted into kinetic energy.

On the other hand, at a fixed end, the situation is opposite in that the displacement and particle velocity are zero. This means that the reflected particle velocity pulse is a mirror image of the incident pulse, and hence the force is doubled.

In other situation where a pile has discontinuity such as an abrupt change in pile impedance or cross section area, the transmitted pulse always has the same sign. For example, compressive pulse leads to a compressive transmitted pulse. In a thinner under pile, the particle velocity is increased while the forces is decreased than the initial pulse. For a thicker under pile, the particle velocity is smaller while the force is larger than the initial pulse. Where the pile impedance changes, the reflection changes sign, for example a thin under pile reflects a downward moving pulse as a tensile pulse, while a thicker under pile reflect a compressive pulse with upward particle velocity.

2.6.3 The CASE Method

Pile Driving Analyser (PDA) is a field tool to measure acceleration and strain with the aid of strain transducers and accelerometers at approximate depth of two pile diameter below the pile head. This method of field measurement was developed by George Goble of Case Western Reserve University in 1964 as a result of a research project funded by Ohio Department of Transportation and FHWA.

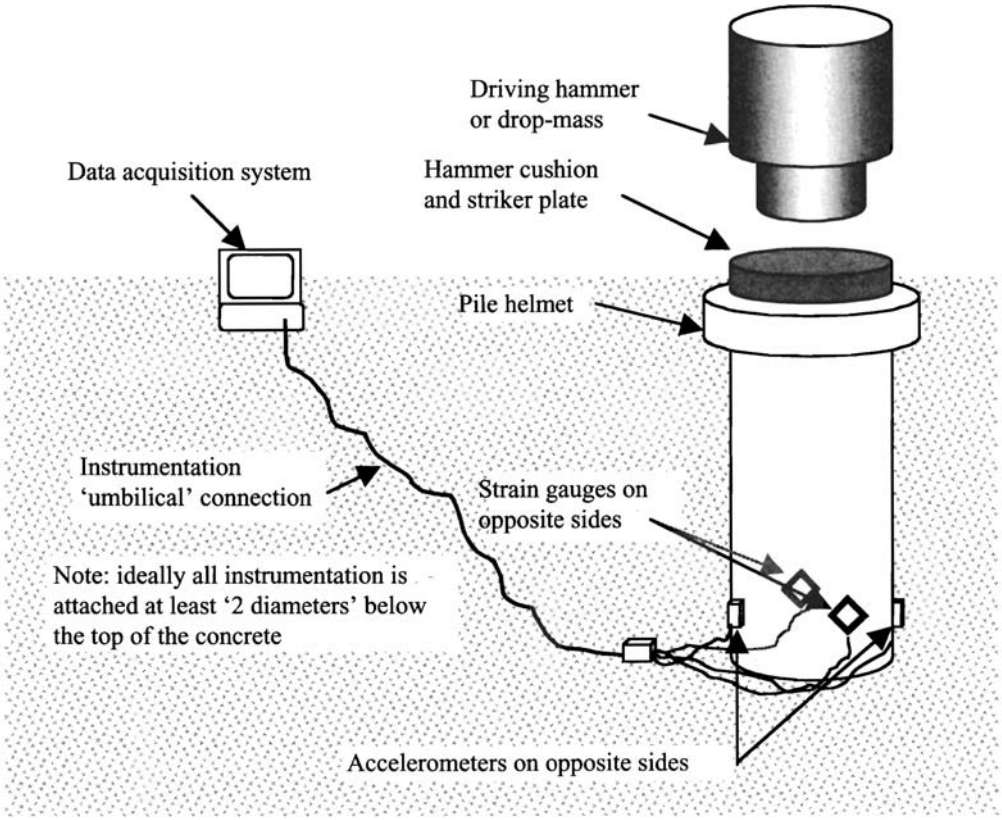

Figure 2.8 Schematic diagram showing typical setup of PDA (Case) method of dynamic testing (Hertlein 2006)

Rausch et al (1985) proposed a method of separating the dynamic and static capacities by introducing a Case damping factor j_c and it was assumed that the entire pile capacity developed at the pile base. The Case damping factor was also assumed to be soil dependant and typical values are given in many standard textbooks on piling foundations.

The Case method is essentially a closed-form solution of the one-dimensional wave equation and it can be written as:

$$Q_u = \frac{1}{2}[(F_2 - ZV_2)(1+j_c) + (F_1 + ZV_1)(1-j_c)] \qquad 2.3$$

Where F_1 and F_2 are pile head forces at the peak impact time and at the wave return time or (2L/c) after the F_1, V_1 and V_2 are the corresponding velocities at peak impact time and wave return time, j_c is the Case damping factor.

The case method is an oversimplification as shown by modelling in Figure 2.9 and the pile capacity deduced by the Equation 2.3 is heavily influenced by the damping factor.

The underlying assumptions in the derivation of the Case method are:

- the pile resistance is lumped at the pile toe,
- the static toe resistance is purely elastic resistance, (Both the wave equation numerical analysis and CAPWAP assume an elasto-plastic model for the static component of the resistance),
- simple mass-spring model is adopted for the hammer-pile-soil system.

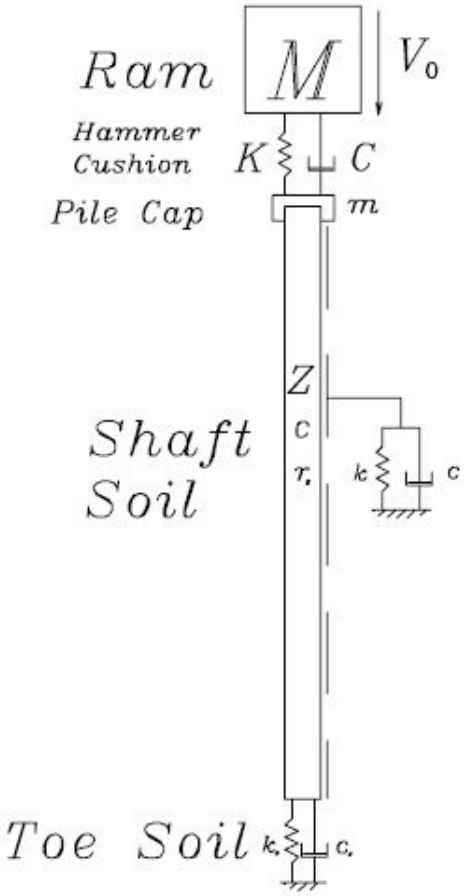

Figure 2.9 Simple hammer-pile-soil system for closed-form solution (after Warrington, 1997)

Pile driving resistance and static capacity can be performed by PDA in-built routine from these measurements by the simplified closed-method solution. This method, as described earlier, is

known as the Case method and there are several procedures that were subsequently developed for different driving conditions and the measured force velocity traces.

The QULT procedure is the dynamic formula equivalent. It uses the measured maximum energy (EMX) and the maximum displacement (DMX) to calculate the ultimate capacity. This value is not reliant and is only used for reference purposes.

Automatic Resistance procedure is employed in cases where the pile skin friction is very low (RAU) or moderate shaft resistance (RA2). This procedure is best suited for hard driving cases and is independent of the damping parameter.

The Maximum Resistance (RMX) is generally most appropriate when large quakes are observed. This ensures full capacity is mobilised. This method is preferred when velocity doesn't become negative prior to the time at which the travelling wave returns.

The RSP is original procedure that uses the peak forces and a soil (grain size) based empirical damping factor is applied to calculate ultimate capacity. It is very sensitive to the damping factor.

One of the limitations of the Case method is that the damping factor, as shown by Paikowsky (2004) and others that it is not a soil property and does not depend on the soil type. However, this method is still useful in that it is simple and provides an estimate of the pile capacity at the time of driving.

In cases where the Case damping factor can be calibrated against actual pile capacity obtained from static testing or other rigorous analysis such as signal matching CAPWAP® method, this method can be used to yield reasonable results for piles. A summary of the advantages and disadvantages of the various dynamic testing methods are given in Table 2.3.

2.6.4 The CAPWAP Method

CAPWAP® (**Ca**se **P**ile **W**ave **A**nalysis) is a signal matching or reverse analysis program for piles using the wave equation theory. In this analysis, the PDA measured force and velocity trace are matched with the calculated forces and velocities based on the Smith model of mass, springs and

dashpots. It models the ground reactions (both skin and toe) as elasto-plastic spring and a linear dashpot. In radiation damping model, an additional dashpot is inserted for the toe to take into account the movement of the surrounding soil. Therefore, the soil model can be described by ultimate resistance, quake and viscous damping factor. The total resistance is the sum of the displacement (quake) dependant static resistance and the viscous velocity dependant dynamic resistance.

Smith quake and damping factors are assumed to be soil type dependant and can be estimated by load tests or perform CAPWAP® analysis by using the PDA monitoring data. However, Paikowsky (1994) showed in a large database of load testing that no correlation exists. CAPWAP® analysis is a linear process to determine the best-fit solution and the parameters it produces are not unique. As a result, there have been numerous studies undertaken to understand the correlations of the Smith model parameters (McVay & Kuo, 1999) and there is still lack of understanding about the factors attributed to these parameters. McVay and Kuo (1999) provide a comprehensive literature review of the many methods. Liang and Sheng (1992) derived a theoretical expression by using the spherical expansion and punching theory to express the toe/skin quakes and damping factors.

Normal CAPWAP® analysis procedure involves selecting a blow record and matching the measured and computed force-velocity trace by changing a number of variables, which under a normal case, would be 11 plus the number of shaft resistances that are dependent on the depth of pile or soil. In cases where additional options are required, such as Residual Stress Analysis (RSA), radiation damping, toe gap and unloading, the variables would, of course, add up even more.

Certainly the pile resistance estimation using CAPWAP signal matching is much more accurate to that from the Case method because of the inherently crude assumptions in the derivation of the method.

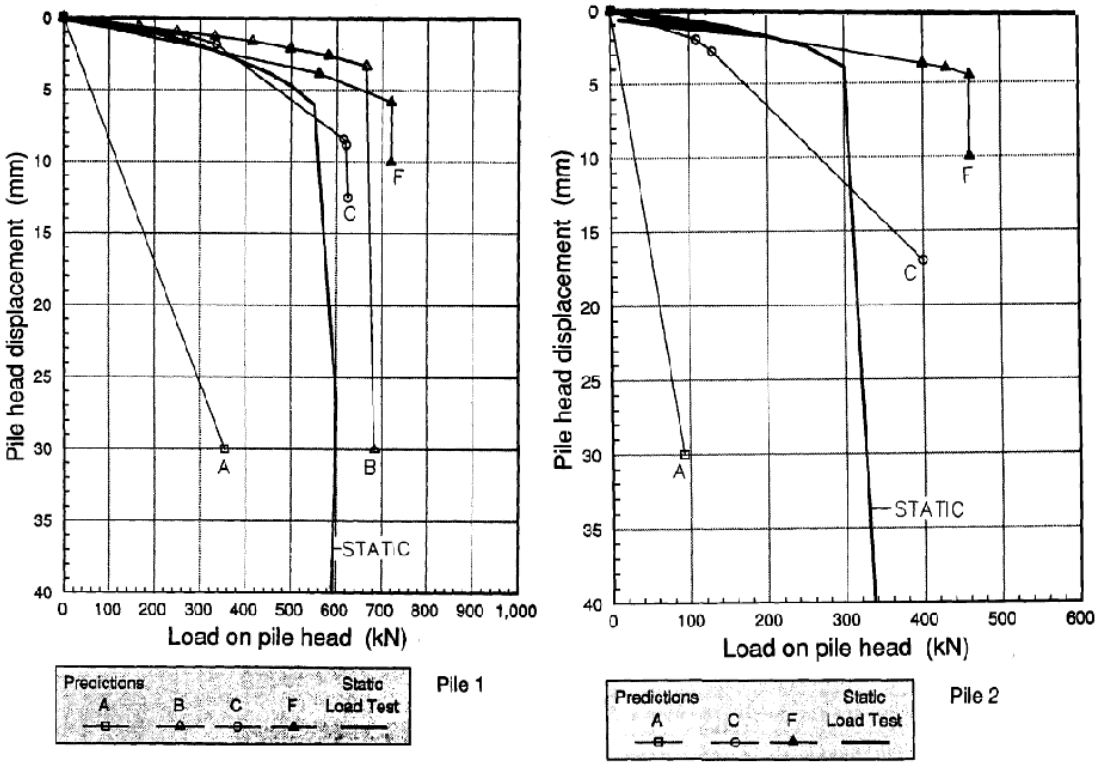

Figure 2.10 Capacity comparisons by dynamic and static test methods (after Baker et al., 1993)

Table 2.3 Advantages and disadvantages of dynamic methods (Paikowsky, 2004)

Category	Method	Advantages	Disadvantages	Comment
Design Stage	WEAP (Smith, 1960, Goble et al., 1976)	- Equipment Match - Drivability Study - Structural Stresses	- Non unique Analysis - Performance sensitive to field conditions	- Required for Construction - Required Evaluation for capacity predictions
Dynamic Equations	ENR (Wellington, 1892)	- Sound Principles - Common use	- Unreliable	- Needs to be examined without a built in FS.
	Gates (Gates, 1957)	- Empirical - Common use	- Depends on original database	- Found to be more reliable than other equations
	FHWA version of Gates Eqn. (FHWA, 1988)	- Correction based on additional data	- Depends on database	- Was found to be reliable
Dynamic Measurements	Signal Matching (e.g. CAPWAP) (Goble et al., 1970)	- Solid principle of matching calculations to measurements by imposing msd. B.C.	- Stationary soil forces - Expensive - Requires time	- Office Method - Found reliable at BOR
	Case Method (Goble et al., 1970, Rausche et al., 1975)	- Simplified Analysis - Field Method	- Requires local calibration - Presumed dependency of soil conditions found baseless	- Was found reliable with local calibration - How to obtain national or international calibration?
	Energy Approach (Paikowsky, 1982, Paikowsky et al., 1994)	- Simplified Analysis - Field Method	- Shows long-term capacity which may not be present at EOD	- Ideal for construction

NOTES: ENR = Engineering News Record; FS = Factor of Safety; BOR = Beginning of Restrike; EOD = End of Driving.

2.6.5 GRLWEAP Method

GRLWEAP™ software is pre-driving computational analysis tool for simulating pile response based on the solution (Smith, 1950) of one-dimensional wave equation. Smith first developed the numerical solution to the wave equation by discrete element idealisation of the hammer-pile-soil system as a series of mass, springs and dashpots. One of the first programs was developed by Goble and Rausche in 1976 was named Wave Equation Analysis Program (WEAP) and later it was updated to WEAP87. Amongst the many available programs, currently GRLWEAP is the most widely used program and improvements such as residual analysis, pile-soil modelling and driveability analysis were incorporated in the later versions (Rausche, 1988; Hussein *et al*., 2004). More detailed discussion on the GRLWEAP method is presented in Chapter 4.

2.6.6 SIMBAT Method

The SIMBAT (**Sim**ulation de **Bat**tage or Driving Simulation) method of pile testing based on the wave equation was developed by J.Paquet, a research manager at the CEBTP (Centre Experimental de Recherche et d'Etudes du Batiment et des Travaux Publics), (Testconsult Limited). The methodology was developed specifically for drilled and augered cast-in-place piles. However, the method has also been extended for other pile types. The main differences of the SIMBAT method as compared to the PDA method are:

- Free fall impact mass,
- Theodolite to measure displacement,
- Electrical resistance strain gauges, and
- Hammer drop height sequence measurement.

The theodolite is setup on a tripod about five to ten metres from the pile and it is struck with the drop mass in incremental weight and the resulting acceleration and strain are captured. SIMBAT uses two accelerometers that are mounted in nylon blocks and it is anchored to the pile. It also uses two strain gauges, but unlike PDA testing where the strain gauges are anchored to the pile, SIMBAT instead uses electrical resistance gauges which are bonded to the pile with some sort of epoxy.

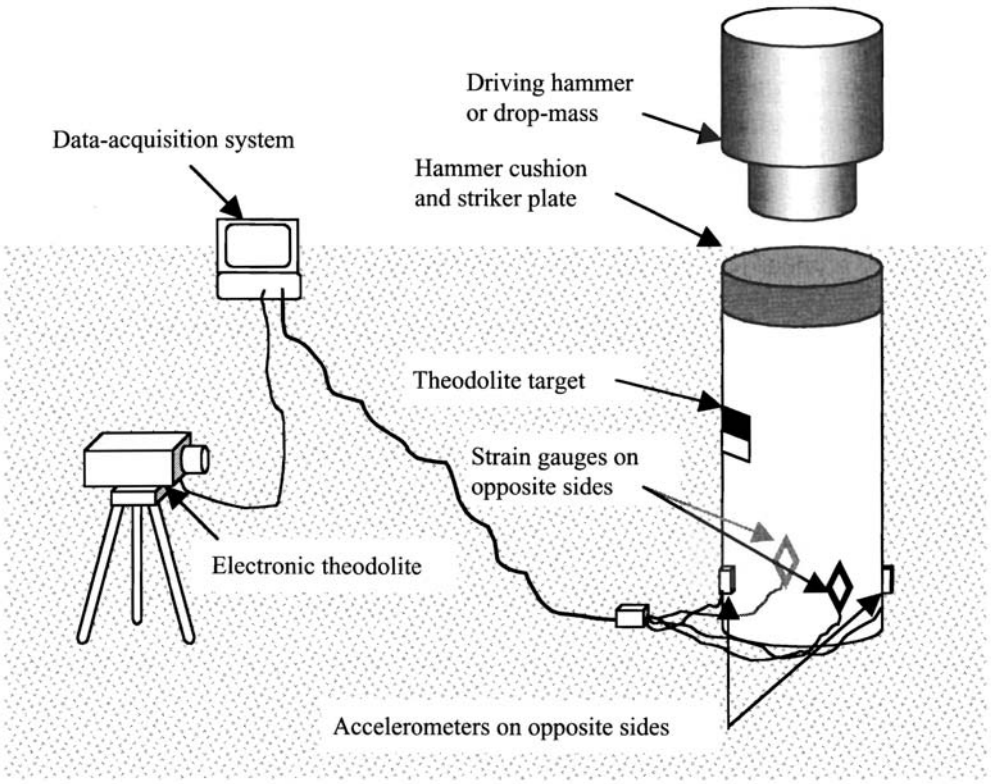

Figure 2.11 Schematic diagram showing a typical setup of Simbat dynamic testing method (Hertlein 2006)

The optical theodolite, shown in the SIMBAT setup in Figure 2.11, is used to measure the pile movements during impact as well as the permanent deflection or set. A small black-white target is attached to the pile and a small halogen light is used to light up the target. The main function of the theodolite is to evaluate pile velocity that is used in the calculation and interpretation pile capacity results. It also serves as check on the pile movements during pile driving.

The SIMBAT method uses two complementary techniques to arrive at the static capacity. First approach is known as 'multi blow', whereby the pile is subjected to a series of ten or more impacts. The second is numerical modelling and signal matching similar to CAPWAP method.

2.7 Comparative study of dynamic test methods

There have been numerous studies under taken by several authors, for example Baker et al.(1993) and Gozeling et al. (1996), comparing current dynamic pile testing methods based on the wave equation as shown in Figure 2.12 and Figure 2.13.

In the study by Baker et al. (1993), four methods that were compared were CAPWAP, Case Method, SIMBAT and TNOWAVE, and in each case the proprietor used its own method to analyse the testing data. Figure 2.12 below shows the results of comparative study carried out by ESSI (Energy Support Services Inc., employing SIMBAT method), GRL (Goble Rausche & Likins Inc., employing the Case method) and TNO (Netherlands Organisation for Applied Scientific Research, employing the TNO method).

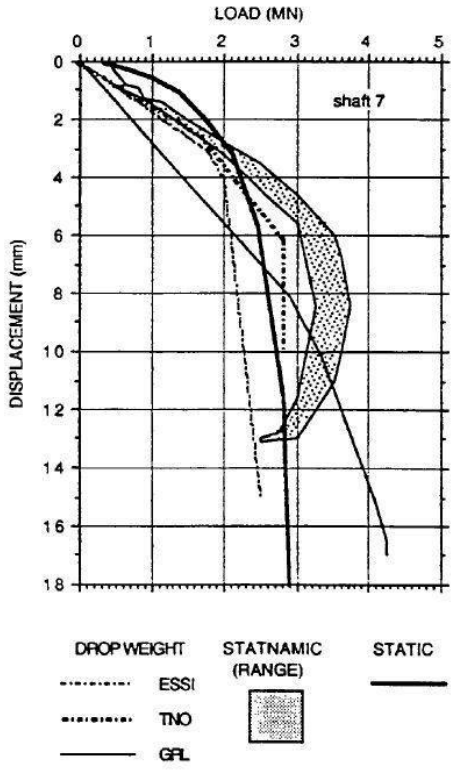

Figure 2.12 Comparative evaluation of pile movement vs. capacity by dynamic and static test methods (after Baker et al., 1993)

As can be seen from the Figure 2.13, there exists a wide scatter about the 45-degree line and no one method stands out between them. Clearly, GRL method performs better on Shaft 2 and performs poorly on the other two Shafts 4 and 7. ESSI's and TNO's methods only perform well on Shaft 7.

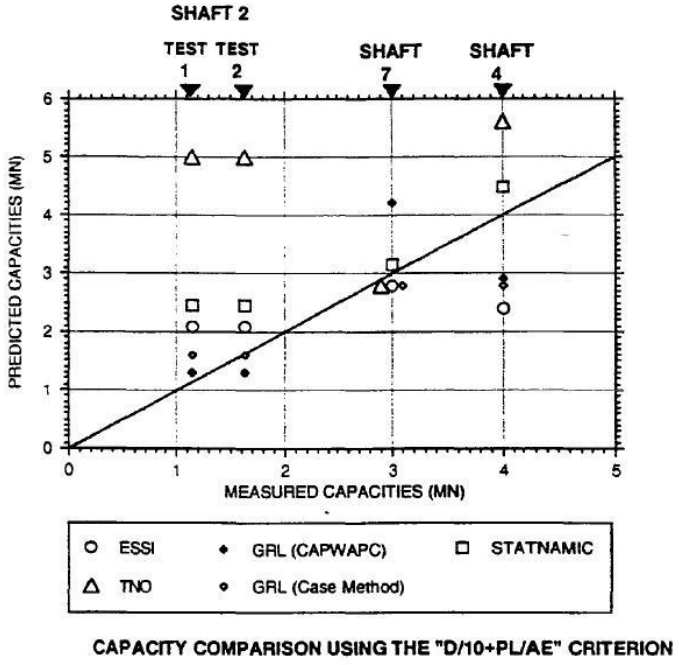

Figure 2.13 Capacity comparison by dynamic and static test methods (after Baker et al., 1993)

Gozeling et al. (1996) carried out a capacity prediction contest involving eleven anonymous participants from all over the world. The aim of the study was to compare the accuracy of pile driving prediction by the various methods using four different types of hammers which were used to drive 20m piles.

The results of the actual and the predicted were compared and the data indicated that the predictions were consistently either too low or too high for the four hammers studied. As it can be seen from Figure 2.14 that no correlation or trend exists between the different pile capacity evaluation methods. Also, a very interesting conclusion, drawn from the test results, was that there was no correlation between the maximum tensile stress in the pile and the energy levels of the four hammers.

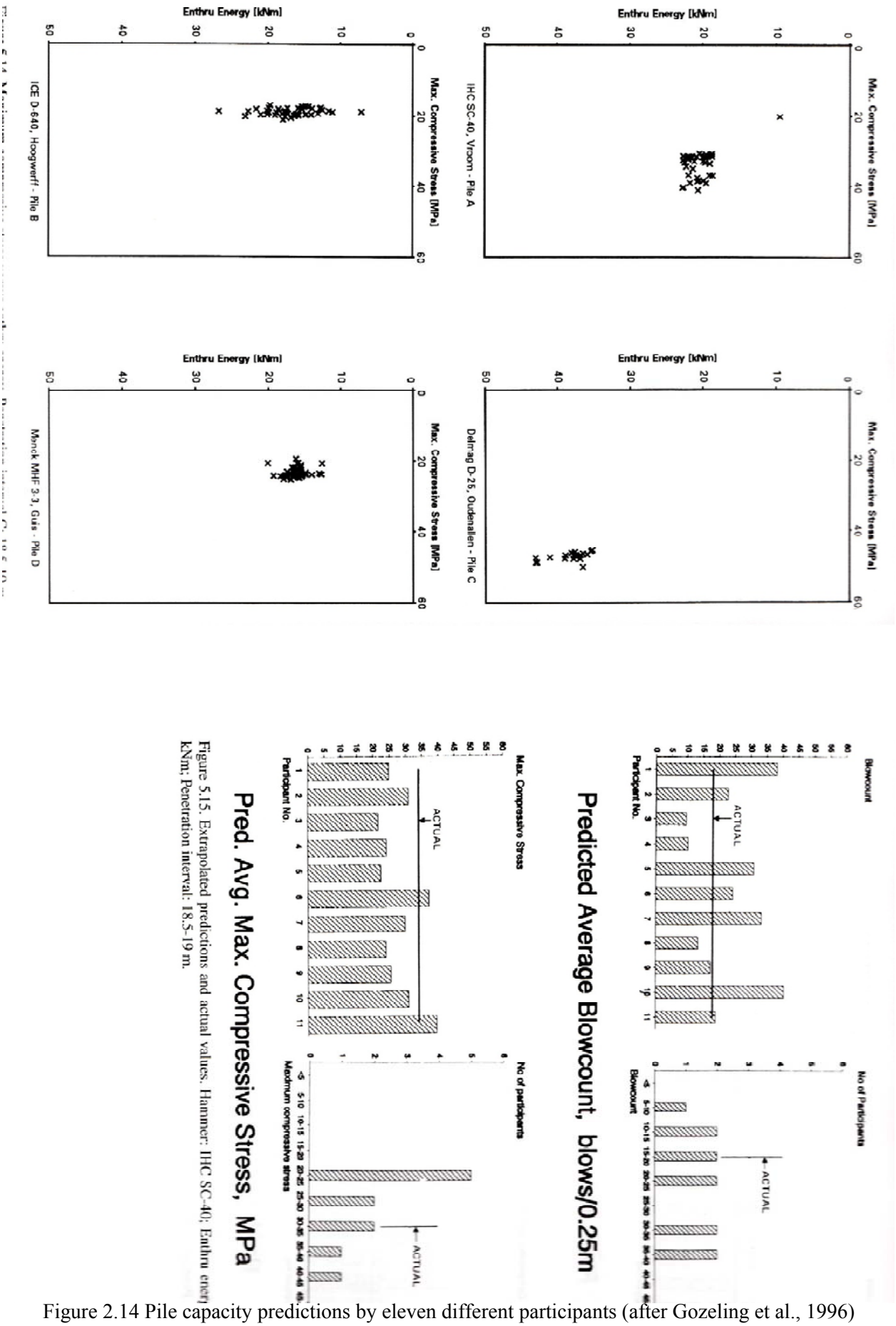

Figure 2.14 Pile capacity predictions by eleven different participants (after Gozeling et al., 1996)

2.8 Dynamic Formula

Pile Dynamic or Energy Formula is a term used to describe a range of formulas including Danish, Engineering News (ENR), Gates, Janbu, Hiley, FHWA and WSDOT are well known among many others (Chellis, 1961, Fragaszy R.J. , 1988, Fragaszy Richard J. , 1989, Gates, 1957, Hiley A., 1925, Vulcanhammer Guide to Pile Driving (Vulcan Iron Works Inc.), 2011). They have been used for hundreds of years to calculate pile capacity during driving. Countries with a strong tradition of using the Hiley Formula are particularly Hong Kong and Australia while Gates, Janbu, FHWA and WSDOT are commonly used in the US.

These dynamic equations are generally categorised into theoretical equations, empirical equations and those consisting of the combination of the two. The empirical and semi-empirical equations are restricted to the conditions and assumption of the original data set and no reference is made here.

The basic concept of the dynamic formula, shown in Figure 2.15 below, is based on the energy equilibrium equation that relates the total resistance of the pile to the energy of falling hammer and pile displacements. Hence the simplest form of the, Equation 2.4, can be derived by calculating the area under the curve O-A-B-C-O in Figure 2.15.

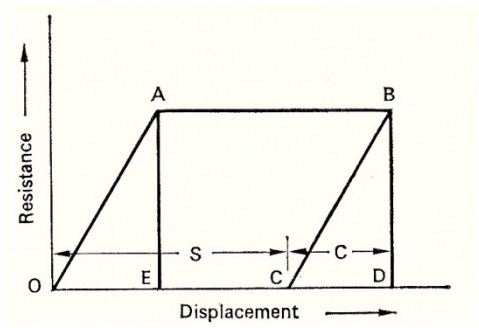

Figure 2.15 Energy equilibrium equation relating to resistance and displacement of pile (Whitaker, 1970)

$$R_u = \frac{W_r H}{(S + C/2)} \qquad 2.4$$

Where, Ru is total resistance or ultimate pile capacity, H is hammer drop height or stroke, S permanent pile displacement or set and C elastic deformation (recoverable movement) of the pile-soil or quake.

A more rational and precise form of Equation 2.4 can be expressed as the Hiley formula (Hiley 1925):

$$R_u = \frac{e_f W_r H}{s + (C_1 + C_2 + C_3)/2} \times \frac{W_r + e^2 W_p}{W_r + W_p} \qquad 2.5$$

Where R_u is total resistance or ultimate pile capacity, e_h is efficiency of hammer, W_r is weight of the hammer, W_p is weight of the pile, H is stroke, s is set, C_1 is elastic compression of pile cushion, C_2 is elastic compression of pile, C_3 is elastic compression of the soil and e is coefficient of restitution (COR) that is material property defined as ratio of initial and final velocities after impact.

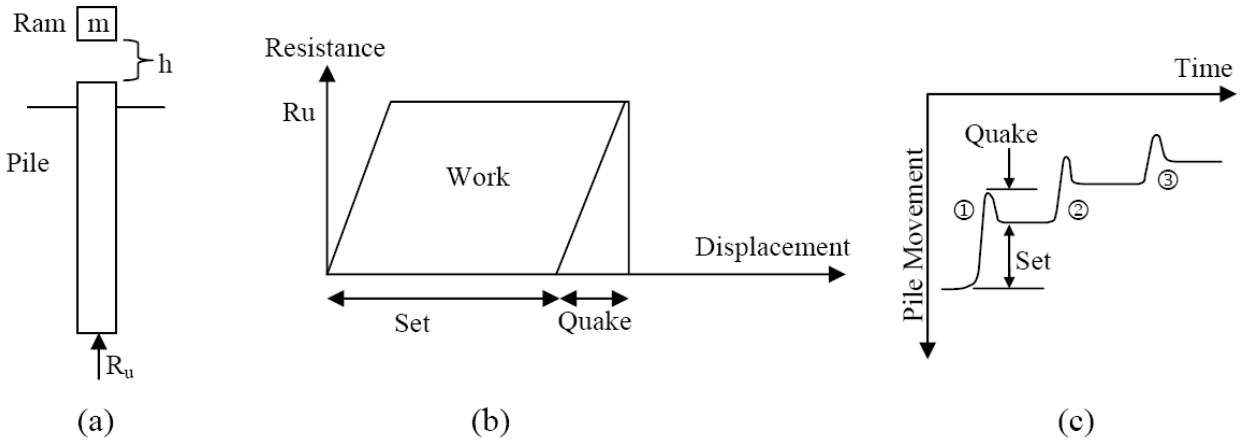

Figure 2.16 Dynamic equation principle: (a) hammer, pile and soil model, (b) assumed elastic-plastic soil response under an impact and (c) pile top movement under continuous hammer impacts (Paikowsky, 2009).

It can be noticed that Equation 2.5 that the terms Wr and Wp on the right accounts for the energy loss between the impact between hammer and pile. However, the empirical term 'e' (COR) is not well established and often are assumed from standard piling textbooks. Paikowsky (1992) and Broms (1988) proposed a simplified Hiley equation based on the actual energy transferred to the pile that can be accurately evaluated by Pile Driving Analyser (PDA):

$$R_u = \frac{E_{max}}{S + C/2} \qquad 2.6$$

In the Equation 2.6, the maximum impact energy, $E_{max,}$ can be evaluated by PDA in the field or calculated from ram impact velocity. The set, *S* and the compression *C* parameters can be determined directly by attaching paper to pile and fixing a horizontal reference beam to the pile and using a pen to mark pile movement on the paper which is attached to the pile. This method of taking set measurement is shown in Figure 2.17 and the pile top movement is illustrated in Figure 2.16. Currently there are devices available (see section 3.6) that can also record the Set and Quake much more accurately and can greatly improve the results from the dynamic formulas. One such device a device, proposed by the author, is the IBIS-S radar and a detail discussion on this instrument is given in Chapter 3.

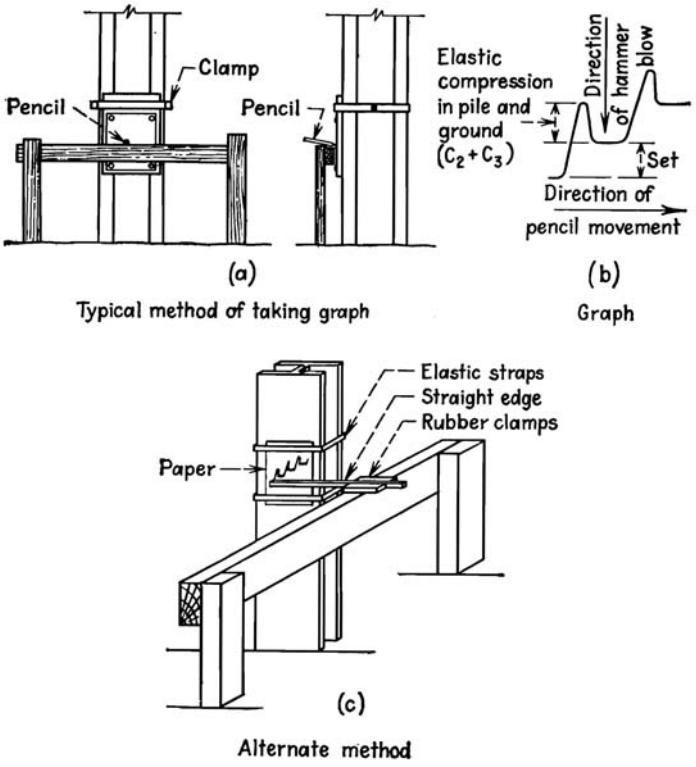

Figure 2.17 Schematic diagram showing typical methods of measuring 'set' and temporary compression in the field (Chellis 1961)

Experience and pile tests data over the years have shown that the dynamic formula in general and the Hiley formula in particular consistently over predict pile capacity compared to the reference static tests. It is particularly true when the safety factors are applied to the ultimate load calculated by the dynamic formulas. Typically a safety factor for the Hiley formula is around 3 whilst for the Wave Equation Method it is typically 2.5 and for static load tests it is about 1.25 to 2. The reason

for this over prediction of capacity evaluation by the Hiley formula is that the formula does not take into account the dynamic component of the capacity. Hence it can be proposed to use a correction factor, say f, to adjust for this dynamic component similar to the damping parameter used in the Wave Equation Method and the Case method as briefly outlined below.

In the case of non-cohesive soils such as sand, gravel, or permeable fill, the dynamic formula bears a reasonably close relationship to those of a static load. However, for cohesive soil there is a large variation due to visco-elasticity of soil. This effect is indicated in Figure 2.18 below, where the resistance gap between the static and dynamic tests is larger for cohesive soil than the non-cohesive soil.

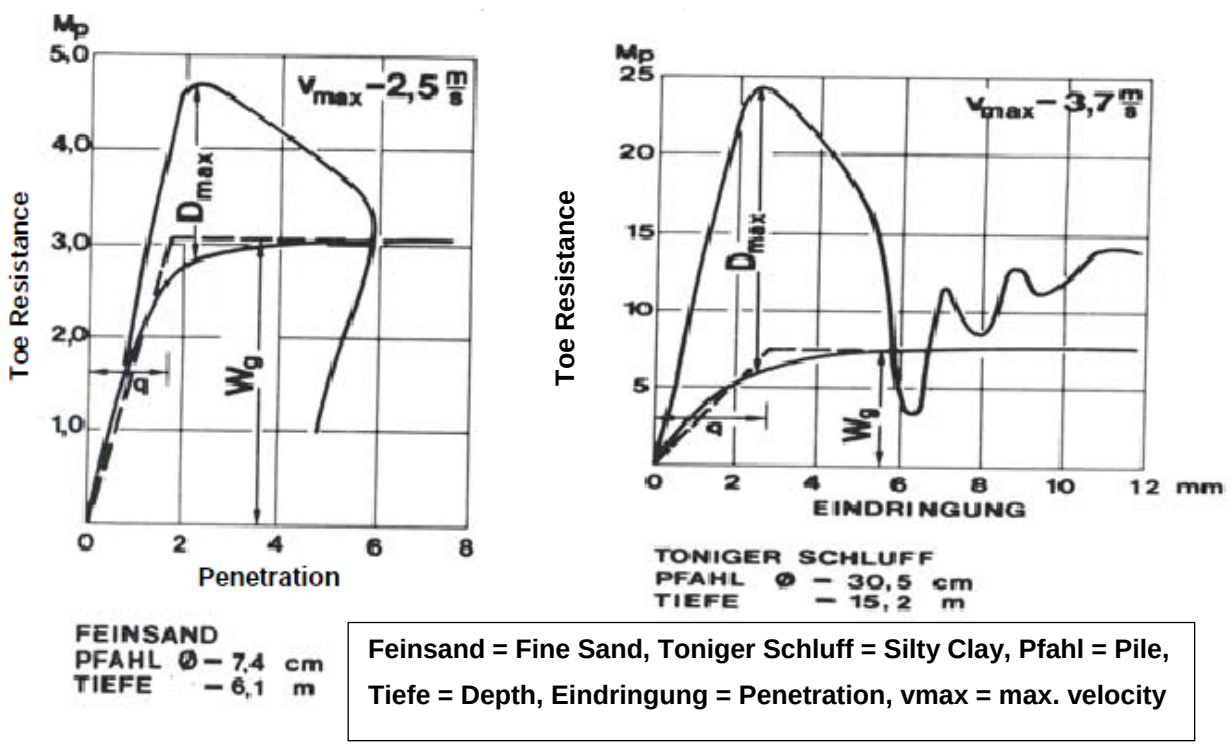

Figure 2.18 Measured dynamic toe resistance versus settlement for non-cohesive and cohesive soils (after Zhang 2009).

By the same token, the factor 'f' is proposed to account for this effect due to the viscous behaviour of soil. The factor is assumed to be function of pile velocity and displacement and the modified Hiley formula can be expressed as:

$$R_u = \frac{1}{f}\left(\frac{E_{max}}{S + C/2}\right) \qquad 2.7$$

Where ‘f’ is proposed factor, Emax is maximum impact energy, S is set and C temporary compression.

Fung et al. (2005) used ’bias factor’ and named it HKCA 2004 formula to account for the dynamic effect of pile driving. Fung et al (2005) evaluated the bias factor by expressing it as a ratio Hiley capacity to CAPWAP or static load capacity and assumed it to be constant. Tejchman (1984) proposed a similar form of the formula and suggested that the ‘parameter’ should be determined from ‘empirical’ data and that it should take the soil conditions, pile and hammer type into account.

However, the current research proposes that the correction factor proposed here is not constant and will vary depending on the pile velocity and displacement. This is the aim of the current research. The author proposes to carry out a comprehensive parametric study based on the wave equation analysis and provide recommendations for the variable for different site conditions, hammers and pile types.

2.8.1 Rationale for use of Dynamic Formula

The need for the continued usage of the dynamic formula is that in any given project only a very limited percentage (0.5 % to 1.0 %) of piles are tested by static load testing and 5 % to 10 % of piles are dynamically tested by PDA measurement and signal matching analysis based on the wave equation. The remaining 90% to 95% of the piles remain untested. Therefore, there is a need to fill the gap and the conventional pile dynamic formulas can fill and satisfy the project quality control requirements.

CHAPTER 3

3 LITERATURE REVIEW

3.1 General

This chapter is divided into three sections. The first section discusses a critical overview on the pile driving formulae, as well as an outline of past and present work by other researchers. The second section is dedicated to a discussion of the findings of previous researchers on the performance of pile dynamic formulae in general and more specifically the Hiley formula. The third section introduces new radar equipment called IBIS-S and a new application is proposed to improving the pile driving formulae used in the field.

3.2 Historical Background

Determination of pile capacity by dynamic formulas is the oldest and most frequently used method. All such formulas assume that the hammer kinetic energy is to be equal to the driving resistance and the soil resistance is equal to pile capacity under static loading. There are a great number of dynamic formulas available with different degrees of reliability. Appendix B provides details on the derivation of most of these formulas.

Engineers over the last two hundred years have applied the idea of driving a stake to driving of a pile and have made the assumption that the effort required to drive the stake is directly related to the resistance provided by the ground (Whitaker, 1970). As a result, many empirical formulae termed

‘driving formulae’ or ‘dynamic formulae’ have been derived to establish the relationship between the driving resistance or penetration when hammering piles and ultimate working load from a structure.

The theoretical basis for the derivation of the pile driving formulae is based on the Newtonian principles of impact between two rigid bodies, for example the driving hammer and the pile. Thus driving formulae are simple idealisation of complex interactions between hammer, pile and the ground. However, due to its simplicity of application, the use of dynamic formulae is still popular with practitioners. Pile driving formula can be used for both Displacement and Non-displacements piles to calculate pile capacity.

A great number of dynamic pile-driving formulas have been proposed and used. Their basic assumption is that the ultimate carrying capacity is equal to the dynamic driving force, and the principle behind them is that the weight of the ram multiplied by the stroke may be equated to the driving resistance multiplied by the set of the tip of the pile.

According to Chellis (1961), the first pile driving formula to become popular was the Sanders Formula, which was proposed by Major John Sanders of the U.S. Army in 1851. The Sanders Formula is in the form:

$$R_a = \frac{W_r H}{8s} \qquad 3.1$$

Where R_a is allowable bearing capacity, W_r is weight of ram, H is the drop height of hammer and s is the set. The number 8 is adopted as the factor of safety to calculate the allowable bearing capacity and this high figure indicates the uncertainties inherent in the formula. Off course, the issue with the Sanders formula is that as the set approaches zero the allowable capacity increases to infinity, which is counter intuitive. Hence A.N. Wellington in 1888 proposed the Engineering News Formula that is used and researched even today.

A list of the most frequently used formulas is given in Table 3.1. Some of the dynamic formulas in the table are empirical, for example the Engineering News, while the others are classified as semi-empirical and those that are purely theoretical formulas.

As it can be noted that some formula assume that the penetration of the pile is linearly proportional to the ram energy, some uses the square root of the ram energy (Gates formula) and some cube root of the stroke or energy.

The underlying theory of the pile dynamic formulas is based on assuming instant propagation of force through the pile, whereas according to the solution of the one-dimensional wave equation, the force actually travels in a wave. The amount of pile skin friction and proportion of plastic to elastic yield of the soil have a great effect on these waves.

Currently, apart from the driving formula, there are two other methods that are used to measure pile performance very accurately: Pile Load Testing (Static, Statnamic) and Pile Dynamic Analysis (PDA) using computer signal matching analysis software CAPWAP. However, the limitations of both of these tests are the high cost involved. In any given project only a very limited percentage (0.5% to 1.0%) of piles are tested by static load testing and 5% to 10% of piles are tested by PDA test and signal matching analysis.

One of the main sources of error in the application of dynamic formula is the determination of the actual energy delivered to piles. Longitudinal studies of PDA testing for large projects demonstrate that during a contract energy delivered can vary up to 30% or more, hence this is a substantial and underlying error in driving formula unless the energy can be established for each pile.

New equipments, such as the IBIS-S radar, provide an opportunity to compute or infer the true hammer energy delivered to each contract pile and also measure the pile penetration (set and temporary compression). By virtue of this method, accurate input into pile driving formula, especially Hiley Formula, is possible:

Table 3.1 List of most commonly used dynamic formula (after Fragaszy et al., 1988)

ENR	$Q_u = \frac{e_h E_h}{s + z}$
Mod. ENR	$Q_u = \frac{e_h E_h}{s + z} \cdot \frac{W + n^2 w}{W + w}$
Hiley	$Q_u = \frac{e_h E_h}{s+(C_1+C_2+C_3)/2} \cdot \frac{W + n^2 w}{W + w}$
Gates	$Q_u = 27 \sqrt{e_h E_h}(1-\log s)$ $e_h = 0.75$ for drop hammers $E_h = 0.85$ for other hammers Q_u (kips), s (in), E_h (ft-kips)
Janbu	$Q_u = \frac{e_h E_h}{K_u s}$ $K_u = C_d \left[1 + \sqrt{1 + \frac{\lambda}{C_d}} \right]$ $C_d = 0.75 + 0.15 \frac{w}{W}$ $\lambda = \frac{e_h E_h L}{AEs^2}$
Danish	$Q_u = \frac{e_h E_h}{s + \sqrt{\frac{e_h E_h L}{2AE}}}$
PCUBC	$Q_u = \frac{e_h E_h \cdot \frac{W + Kw}{W + w}}{S + \frac{Q_u L}{AE}}$ K = 0.25 for steel piles = 0.10 for all other
Eytelwein	$Q_u = \frac{e_h E_h}{s \left[1 + \frac{w}{W} \right]}$ (drop hammers)
	$Q_u = \frac{e_h E_h}{s + \left[0.1 \frac{w}{W} \right]}$ (steam hammers)
Weisbach	$Q_u = \frac{-sAE}{L} + \sqrt{\frac{2e_h E_h AE}{L} + \left[\frac{sAE}{L}\right]^2}$
Navy-McKay	$Q_u = \frac{e_h E_h}{s \left[1 + 0.3 \frac{w}{W} \right]}$

The energy delivered by hammer depends on mainly the mass and velocity of the hammer at impact which is difficult to measure. The energy transferred from the pile to the hammer is the ratio of the actual energy transferred to the pile and the theoretical energy (W×H).

Other dynamic formulas studied for comparison reasons were the Gates and MnDOT formula. Gates (1957) first proposed the empirical formula. The Mn/DOT formula was developed by Paikowsky et al. (2009) as a result of a research project supported by Minnesota Department of Transport and Minnesota State University.

In the literature, three major shortcomings of the energy or dynamic method are the uncertainty of the actual hammer energy input to the pile top, as well as the measurement of pile penetration. Traditionally the hammer energy was assumed constant and the 'set' measurements were not really accurate. Figure 2.17 depicts the set-card method used to evaluate the set and quake values. Also, the dynamic formulas do not take dynamic resistance into account and hence the capacity must be factored for the dynamic component. The magnitude of this factor is thought to be a function of resistance weighed pile velocity. With the IBIS-S radar it is now possible to record the set (S) and temporary compression (C) much more accurately and thus can greatly improve the results from the dynamic formulas.

Lim and Broms (1990) concluded that unless the energy delivered by the hammer is constant (which has been shown to be not the case), the set used in Equation 2.5 and Equation 2.6 cannot be used in defining pile performance.

The well-known dynamic formulas have been criticised in some publications. The reliability of the dynamic formulas is well characterised in publication by Hannigan et al.(1998), in which it was concluded that "... pile capacities determined from dynamic formulas have shown poor correlations and wide scatter when statistically compared with static load test result". However, Hannigan et al. (1998) ignores the fact that this poor performance is due to the fact that the static tests are often carried out days after the initial driving event. Thus the time dependency of pile capacity, discussed in later sections, is often ignored.

Others such as Hussein et al. (1995), Rausche et al. (1997), Hannigan et al. (1998), and Svinkin (2002) provide detailed discussion of the deficiencies of the dynamic formula and its comparison

with the dynamic and static testings. Rausche et al. (1997) in a research project supported by FHWA compiled a database of static analysis method, refined wave equations and PDA measurement method coupled with CAPWAP pile capacity analysis. A reliability of the various capacity prediction methods were compared with the results of static testing. The results of the dynamic formula evaluation showed that, overall, the performance of the dynamic formula was comparable to the other methods. The results presented show that the mean value of the capacity prediction ratio to static by Gates formula were 0.96 (coefficient of variation=0.41) for end-of-drive and 1.33 (coefficient of variation=0.48) for restrike compared to CAPWAP with a mean value of 0.92 (coefficient of variation =0.22) for restrike condition.

Chellis (1951, 1961) suggests that if it can be determined that the dynamic formula results are in reasonable agreement with the wave equation analysis results, then it is permissible to use such simple formula to be quickly applied in the field.

Lowery et al. (1968) presented the results of a study in which it was demonstrated that it was possible to find a range between the Wave Equation Analysis and the Gates formula in which they can be in close agreement.

Tavenas et al. (1972) presented statistical analysis drawn from approximately 478 driving records. Based on a very large foundation built in a homogenous sand deposit it was shown in the paper that the poor quality of the pile driving formulas originates essentially in the estimate of the driving energy. Tavenas et al. (1976) concluded that if the energy estimation is erroneous, then in fact the dynamic formula will also be erroneous.

Paikowsky et al. (1992, 2004) has shown that the reliability of the dynamic formulas can be improved and in fact can be comparable to the stress wave theory calculation. Paikowsky (2004) studied the relationship between the pile resistances to pile penetration with comparison to the pile capacity measured from the static load tests. Based on a large database of tests, the mean values of the ratio of static test capacity to the energy based method at the end of driving (EOD) varied between 1.1 and 1.31.

Paikowsky (2009) carried out analysis, supported by Minnesota Department of Transport, to study relevant case histories in a database (PD/LT2000). Paikowsky (2009) studied four dynamic

equations and based on the analysis of the PD/LT2000 database proposed a new dynamic equation as is indicated in Table 3.2.

Table 3.2 Pile driving formulas investigated and new Mn/DOT formula proposed by Paikowsky (2009)

Equation	Description	Reference
$R_u = \frac{12(W_r * h)}{S + 0.1}$	Drop Hammer	Engineering News-Record (1892)
$R_u = 27.11\sqrt{E_n * e_h}(1 - \log s)$		Gates (1957)
$R_u = 1.75\sqrt{E_n} * \log(10 * N) - 100$	Modified Gates Equation	FHWA (1982)
$R_u = 6.6 * F_{eff} * E * Ln(10N)$		Washington State DOT (Allen, 2005)
$R_u = \frac{10.5E}{S + 0.2} x \frac{W + C * M}{W + M}$	Different format for H and pipe piles	Minnesota DOT (2006)
$R_u = 35\sqrt{E_h} \times \log(10N)$		Proposed General New Mn/DOT Dynamic Equation

Notes:

R_u= ultimate carrying capacity of pile, in kips
W= mass of the striking part of the hammer in pounds
M= total mass of pile plus mass of the driving cap in pounds
E= developed energy, equal to W times H, in foot-kips (1.4)
E= energy per blow for each full stroke in foot-pounds (1.5)
e_h= efficiency
E_n= rated energy of hammer per blow, in kips-foot
C = 0.1 for timber, concrete and shell type piles, 0.2 for steel H piling
Ln= the natural logarithm, in base "e"
W_r= weight of falling mass, in kips
s= final set of pile, in inches
N= blows per inch (BPI)
h= height of free fall of ram, in feet
F_{eff}= hammer efficiency factor

Paikowsky (2009) calculated capacities by these equations in Table 3.2 and performed a load resistance calibration based statistical analysis methods. As result of this research a new equation called Mn/DOT pile driving formula with much better performance was developed.

Zhang et al (2005) proposed a procedure that is based on direct field measurement carried out with measurement device on-board the modern hydraulic piling rigs. The soil resistance are calculated using kinetic and effective energies over 1m of penetration and it is shown that the energy indicator compare well with the measures static load tests.

Current research in the area includes the probabilistic method applied to the energy approach, Liang et al. (1997), in which the authors introduce the Smith pile-soil model and treats the shaft and toe

resistances separately. However, the results are widely scattered. Sakai et al (1996) and Uto et al. (1981, 1992) derived an approximate dynamic formula based on the stress-wave theory. Triantafyllidis (2001) modified Hiley formula, also based on the stress-wave theory, to be used for very long piles driven into weathered mudstone. The interesting aspect of the results is that when viscosity or damping parameter was allowed for, the comparison between Hiley and the static loading result using H-pile matched very well. This is precisely one of the main focuses of the current research by the author.

3.3 Analysis of Energy Losses

The dynamic formulas as well as the more advanced wave-equation analysis all take the energy losses in the driving system, pile and the soil into account to render them reliable.

A typical theoretical analysis of the energy losses together with the formulas for use in various cases is shown in Table 3.3 below. Chellis (1951) provides a good analysis of hammer impact energy and it losses in pile driving process and tries to develop equations to account for the energy losses as a result. In a practical sense, the energy loses can be further simplified and even easily measured with accurate instrumentation as it is described in the subsequent sections.

Table 3.3 Typical analysis of driving formula to include energy losses (Chellis 1951)

Net effective energy available for driving = ultimate resistance to driving final penetration under last blow	*Total kinetic energy applied by hammer*	*Loss in energy due to impact*	*Loss in energy due to imperfectly elastic compression of*		
			Pile head and cap	*Pile*	*Soil*
For use with drop hammers, single-acting steam hammers, and diesel hammers					
$R_u s$	$= e_f W_r h$	$- e_f W_r h \, W_p \frac{(1 - e^2)}{W_r + W_p}$	$- \frac{R_u C_1}{2}$	$- \frac{R_u^2 l}{2AE}$	$- \frac{R_u C_3}{2}$
For use with double-acting and differential-acting steam hammers					
$R_u s$	$= 12 e_f E_n$	$- 12 e_f E_n W_p \frac{(1 - e^2)}{W_r + W_p}$	$- \frac{R_u C_1}{2}$	$- \frac{R_u^2 l}{2AE}$	$- \frac{R_u C_3}{2}$

The efficiency of the driving system is the net energy available to drive a pile. Energy is wasted by friction in the ram, bruising the pile, by the elastic rebound of the hammer and pile, by producing

vibrations and by generating heat. It has been shown in this research that the higher the velocity of ram at impact, the greater the energy loss. Therefore, heavy rams with low drop give higher efficiency than light rams with a high drop. This explains in part the superior efficiency of the hydraulic hammer as well as having rapid succession of blows or high blow counts.

Hölscher et al (1996) and Hajduk et al (2000) have shown that in low driving resistance (easy driving), high acceleration and velocity develop at the tip and in the high resistance case (hard driving), there is small acceleration at the tip, resulting very small mobilisation of the soil mass hence the corresponding energy loss due to soil motion is small.

It has been known that the reason for the discrepancy of the pile driving formulae is that the dynamic formulae do not take dynamic resistance into account and hence the capacity must be factored for the dynamic component. The other reason for the poor reputation of the dynamic formula comes from the variation in hammer performance which have not been detected and also from the time-dependant variations in the pile capacity i.e. comparing end-of-drive capacity with test capacity days, weeks or months later. Without special very accurate measurements, the actual energy delivered to the pile must be estimated from an assumed hammer efficiency and a coefficient of restitution which may be assumed from text books, but can never be known or measured on a project-specific basis.

3.4 Performance Comparison of Dynamic Formulas

Years of correlations between dynamic piles testing the driving formulas have shown that there is a strong relationship between the dynamic testing and the dynamic formulas. Several studies by Olsen (1967), Long (2002) and Tavenas (1972) have been carried out to determine and compare the performance of the dynamic formulas with the higher order pile testing methods.

Olsen (1967) showed that the predicted accuracy is poor and to minimise risk, large safety factors are necessary. However, a more recent study by Long (2002) has shown that the accuracy can be improved and in fact can be as accurate as the Stress-Wave theory calculation.

McVay and Kuo (2000) undertook a comparative study on a database of 247 piles for both EOD and BOR conditions based on the LRFD design, for example, load resistance factor and reliability

factor. The study investigated and compared eight dynamic methods as shown in Table 3.4 below. The study suggested a factor of safety (FOS) of 1 for the FDOT formula, FOS of 3 for Gates and FOS of 2.5 for the PDA Case and CAPWAP methods. These results are highly interesting, as they indicate that the dynamic formula can be improved to match or even perform better than the higher-order wave equation analysis methods.

Table 3.4 Safety factors for dynamic methods (after McVay and Kuo 2000)

Dynamic test method	Equation	Suggested FOS
ENR formula	$R_u = W_r h/(s+0.1)$	6
Modified ENR formula	$R_u = (1.25 e_h E_h)(W_r + e^2 W_p)/(s+0.1)(W_r + W_p)$	6
Gates formula	$R_u = 27\sqrt{e_h E_h}(1\text{-}\log s)$	3
FDOT formula	$R_u = 2E_h/(s+0.1+0.01W_p)$	1
Paikowsky method	$R_u = E_{max}/(s+ (D_{max}\text{-}s)/2)$	-
Sakai method	$R_u = (AE/L)(W_p/2W_r)(D_{max}\text{-}s)$	2.5
PDA Case method	$R_u = 0.5(1\text{-}J_c)(P_1 + Zv_1) + 0.5(1+J_c)(P_2 - Zv_2)$	2.5
CAPWAP method	CAPWAP signal matching software	2.5

McVay and Kuo (2009) concluded that the CAPWAP, PDA and the energy method (Paikowsky, 1992) are approximately twice as efficient as the other dynamic formula such as Gates, FDOT and ENR. McVay asserts that the use of multiple methods, both static and dynamic, and that the capacity evaluated by this procedure would give more reliable result than by a single method. McVay and Kuo (2009) computed the factor of safety based on the LRFD design given in Table 3.5 below.

Table 3.5 Recommended safety factors for dynamic methods (after McVay & Kuo 2000)

Prediction Method	FS at p_f=0.62% BOR	FS at p_f=2.50% BOR	FS at p_f=0.62% EOD	FS at p_f=2.50% EOD	Recommended FS	
					EOD	BOR
CAPWAP	2.48	2.00	1.97	1.58	1.80	2.25
PDA	2.79	2.28	2.24	1.81	2.00	2.50
Paikowsky	3.86	3.09	2.74	2.22	2.50	3.50
FDOT (overall)	1.74	1.31	2.16	1.59	1.90	1.50
FDOT (<200 tons)	2.00	1.65	3.16	2.36	2.75	1.80
FDOT (>200 tons)	1.49	1.14	1.10	0.87	1.00	1.30
ENR (overall)	28.60	20.08	16.02	11.93	14.00	24.00
ENR (<200 tons)	15.35	12.56	18.40	13.80	16.00	14.00
ENR (>200 tons)	28.84	20.12	13.39	10.07	12.00	24.00
Modified ENR (overall)	18.31	12.88	12.53	9.09	11.00	16.50
Modified ENR (<200 tons)	8.70	7.36	20.82	14.60	17.70	8.00
Modified ENR (>200 tons)	18.32	12.81	10.72	7.75	9.20	16.50
Gates (overall)	1.78	1.42	2.28	1.76	2.00	1.60
Gates (<200 tons)	2.12	1.81	2.80	2.27	2.50	2.00
Gates (>200 tons)	1.54	1.24	1.30	1.06	1.20	1.40
FHWAGates (overall)	3.82	3.00	4.20	3.26	3.75	3.40
FHWAGates (<200 tons)	2.40	2.03	5.29	4.24	4.75	2.20
FHWAGates (>200 tons)	3.39	2.69	2.71	2.18	2.50	3.00

Fragaszy et al. (1988) also undertook a comparative study into the reliability of ten pile driving formula as indicated in Table 3.6. The study included 63 pile load tests and the ultimate capacities were calculated using the elastic tangent and double tangent methods. Also a statistical analysis was carried out on the results of the calculated capacities by the various methods, and it was concluded that the Gates formula proved the best while the ENR performed the worst. A summary of the results is given in Table 3.6 below.

Table 3.6 Comparison of results by Fragaszy et al. (1988)

FORMULA	Divisor for 95% safety	Upper limit of safety factors
PCUBC	1.39	3.69
Gates	1.15	3.92
Weisbach	2.97	4.27
Hiley	1.92	4.37
Janbu	1.94	4.56
Danish	2.70	4.88
Eytelwein	5.94	8.07
Modified ENR	4.79	10.41
ENR	8.63	13.23
Navy-McKay	21.45	55.25

For Cohesive soils

FORMULA	Divisor for 95% safety	Upper limit of safety factors
Gates	0.92	2.24
Hiley	2.05	4.42
PCUBC	1.50	4.49
Danish	2.56	4.58
Weisbach	3.06	4.82
Modified ENR	3.12	5.55
Eytelwein	4.27	5.96
ENR	5.79	7.06
Janbu	2.58	9.85
Navy-McKay	14.18	66.02

For non-cohesive soils

It is interesting to note, despite the under performance of the hiley formula, that the results in both soil types are very consistent.

Paikowsky et al. (2004) undertook a comprehensive and the largest study to develop load resistance factors for pile foundations. It comprised collection of case histories into a database called PD/LT2000. The database included static and dynamic analysis tests for concrete, H and tube piles drilled and driven in clay, sand and rock materials as well as the time testing (EOD and BOR).

The main conclusions that were drawn from the PD/LT2000 database study was that the signal matching under-predicted pile capacity, but it performed well for BOR cases. Also, it was remarked that the energy or dynamic method gave a good prediction of capacities during driving (EOD cases) as it can be seen from the Table 3.7 below.

Table 3.7 Performance of dynamic test methods (Paikowsky et al., 2004)

Method		Time of Driving	No. of Cases	Mean	Standard Deviation	COV	Resistance Factors for a given Reliability Index, β		
							2.0	2.5	3.0
Dynamic Measurements	CAPWAP	General	377	1.368	0.620	0.453	0.68	0.54	0.43
		EOD	125	1.626	0.797	0.490	0.75	0.59	0.46
		EOD - AR < 350 & Bl. Ct. < 16 BP10cm	37	2.589	2.385	0.921	0.52	0.35	0.23
		BOR	162	1.158	0.393	0.339	0.73	0.61	0.51
	Energy Approach	General	371	0.894	0.367	0.411	0.48	0.39	0.32
		EOD	128	1.084	0.431	0.398	0.60	0.49	0.40
		EOD - AR < 350 & Bl. Ct. < 16 BP10cm	39	1.431	0.727	0.508	0.63	0.49	0.39
		BOR	153	0.785	0.290	0.369	0.46	0.38	0.32
Dynamic Equations	ENR	General	384	1.602	1.458	0.910	0.33	0.22	0.15
	Gates	General	384	1.787	0.848	0.475	0.85	0.67	0.53
	FHWA modified Gates	General	384	0.940	0.472	0.502	0.42	0.33	0.26
		EOD	135	1.073	0.573	0.534	0.45	0.35	0.27
		EOD Bl. Ct. < 16BP10cm	62	1.306	0.643	0.492	0.60	0.47	0.37
WEAP		EOD	99	1.656	1.199	0.724	0.48	0.34	0.25

Notes: EOD = End of Driving; BOR = Beginning of Restrike; AR = Area Ratio; Bl. Ct. = Blow Count; ENR = Engineering News Record Equation; BP10cm = Blows per 10cm; COV = Coefficient of Variation; Mean = ratio of the static load test results (Davisson's Criterion) to the predicted capacity = $K_{SX} = \lambda$ =bias

Current work and research in the area of pile dynamic formula continue to this day with the aim of improving the existing formula and methods (Allen et al., 2005; Paikowsky et al., 2009).

3.5 Pile Capacity Variations with Time

Piles normally carry their design loads over the long life of the structure it is supporting. Therefore, soil modification by driving and its behaviour over long time around the pile are essential with respect to satisfactory performance of pile. During pile driving, the soil around the pile experiences plastic deformations, remoulding and pore pressure changes. Excess pore water pressure developed during driving reduces the effective soil shear strength and ultimate pile capacity. After the completion of pile driving, soil reconsolidation, as result of the pore water dissipation as well as thixotropy (Mitchell, 1960), are usually accompanied by an increase in pile capacity that is called soil setup. The amount of increase in pile capacity depends on soil properties and pile characteristics. In some soils such as saturated sandy and end-bearing piles in shale, the ultimate pile capacity may decrease (soil relaxation) after the initial driving.

This phenomenon of time-dependent strength gain and loss in soils related to pile driving has been studied and published by Davie (1991), Komurka (2003), Paikowsky et al (1996), Paikowsky et al

(2005), Skov and Denver (1998), Svinkin (1994), Tavenas (1977), Thompson (1985), Tomlinson (2001), Yang (2009) and others. A summary of the empirical equations presenting the capacity variation over time is given in Table 3.8.

Table 3.8 Empirical equations presenting pile capacity change over time Komurka et al (2003)

Empirical Formulas for Predicting Pile Capacities with Time

Author(s)	Equation	Comments
Huang (1988)	$Q_t = Q_{EOD} + 0.236(1 + \log(t)(Q_{max}-Q_{EOD}))$	Q_t = pile capacity at time t, (days) Q_{EOD} = pile capacity at EOD Q_{max} = maximum pile capacity
Svinkin (1996)	$Q_t = 1.4 Q_{EOD} t^{0.1}$ $Q_t = 1.025 Q_{EOD} t^{0.1}$	upper bound lower bound
Guang-Yu (1988)	$Q_{14} = (0.375 S_t + 1) Q_{EOD}$ S_t = sensitivity of soil	Q_{14} = pile capacity at 14 days
Skov and Denver (1988)	$Q_t = Q_o[A\log(t/t_o) + 1]$	where sand: t_o = 0.5, A = 0.2 clay: t_o = 1.0, A = 0.6
Svinkin and Skov (2000)	$R_u(t)/R_{EOD} - 1 = B[\log_{10}(t) + 1]$	

However, this gain or loss in capacity can be difficult to measure as it relies on the assumption that a decrease in pile resistance between the EOD and BOR indicates that relaxation has occurred as long as the same driving system is used in both cases. Such assumptions do not take into consideration variations in the hammer performance or changes in the nature of the pile support.

Currently PDA equipment is used to measure strain and acceleration in piles during driving and use CAPWAP analysis to estimate bearing capacity changes in piles over time. A study by Thompson (1985) indicates that decreases in penetration resistance are more commonly the result of changes in pile driver performance than in soil bearing capacity, and this type of capacity decrease is called apparent relaxation. Thompson presented results of case histories from six sites and showed that in some cases apparent relaxation was observed and only in two cases there were real relaxation that was found to be associated with localised geotechnical conditions.

The decrease of capacity with time after driving has been observed to be associated with the use of single-acting diesel hammers. These hammers tend to decrease in efficiency after extended hard driving.

Paikowsky et al (1996) utilised an extensive database that included EOD, BOR, and PLT information on variety of types and sizes of piles driven in clayey soils and it was shown that the capacity increased with time. Paikowsky et al (2005) showed that piles driven in low permeability soils also gained capacity over time and it was believed to be controlled by the mechanisms of effective stress increase due to the dissipation of excess pore pressures and stress independent phenomena such as strength increase due to thixotropy bonding as reported by Mitchell (1960). Recently, research efforts have been made to quantify time dependent pile capacity and develop a methodology to incorporate this time dependency of pile capacity into pile design by utilising in-situ testing.

3.6 IBIS Radar

The IBIS radar system is recently developed non-contact equipment that measures displacement, velocity, acceleration and vibration in civil engineering applications. It comes in two configurations such as IBIS-L and IBIS-S. The IBIS-L configuration is used for static terrain deformation monitoring and is mainly used in mining and slope stability applications. The IBIS-S configuration is used for dynamic and static monitoring by remote sensing of structures such as buildings, bridges and telecommunication towers.

The IBIS-S radar unit can simultaneously monitor several points, providing the displacement response for each point. The unit operates at frequency of 200Hz, displacement accuracy of 0.01mm and range of up to 1km (IDS, 2008; IDS Australia, 2009). Bernardini et al. (2007) conducted a laboratory test and it showed an excellent quality of the displacement measurements and a good operational stability. IDS Australia (2009) performed some real validation tests with accelerometers and LVDTs and the results showed an excellent match with the accelerometers and LVDTs tests.

The main advantage of IBIS-S, apart from the accuracy, range and resolution, is the fact that it can be operated in all weather conditions over very long distances without the need of accessing the target to install sensor or optical targets. However, if required, then one or several specific points on a target could to be measured by a simple passive radar reflector that can be easily fixed. All the measured quantities are displayed in real time via a computer terminal as indicated in Figure 3.1.

Figure 3.1 Purpose made real-time monitoring of deformation by radar IBIS-S (IDS Australia, 2009).

It should be emphasised that because IBIS-S unit has never been used in piling application and its use was first suggested by the author and trial test was conducted at a test site. Therefore, the purpose built software used for the test was not well suited for the pile testing and the existing software can be easily customised to calculate the required parameters.

A passive reflector was made at RMIT's laboratory in the form of a V-shape and it was bolted to the pile at approximate same vertical distance as the strain transducers and the accelerometer, as shown in Figure 5.2. Continuous readings were taken of all the blows during the two stages.

The radar unit operates on a 12V battery and comes with a hard case. It also comes with an adjustable tripod for easy and quick set up as shown in Figure 3.1.

IDS Australia (2009) presented the performance of IBIS-S with the results of a total station as shown in Figure 3.2. It can be seen that the instrument's performance is excellent and very stable.

Figure 3.2 IBIS-S measurement accuracy (IDS Australia, 2009)

Bernandini (2007) carried out a laboratory performance test in a laboratory on a mass-spring set up as shown in Figure 3.3.

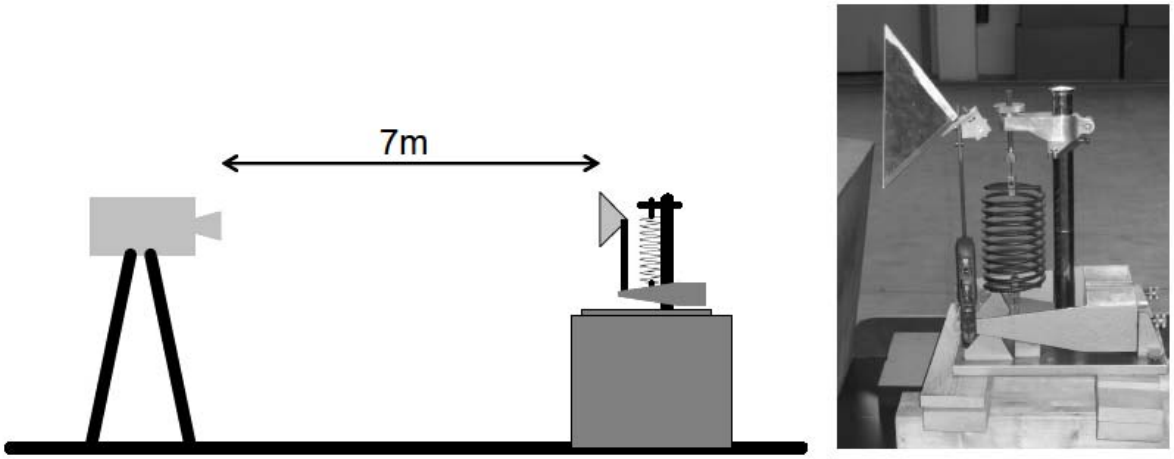

Figure 3.3 IBIS-S radar mass-spring performance test in laboratory (Bernardini, 2007)

The result of the measurement, Figure 3.4, indicates an excellent quality of the displacement measurements and a good operating stability of the equipment. It also confirms the very good quality of the measurements and that the displacement sensitivity of the sensor in the order of 0.01mm.

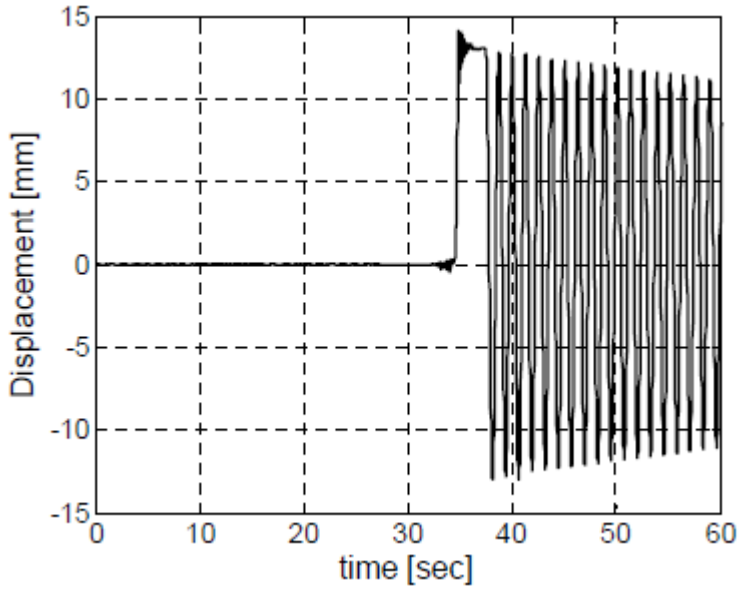

Figure 3.4 The first 60 second of the displacement-time measurement by IBIS-S (Bernardini, 2007)

The new radar system is capable of measuring the displacement response of several points of a structure and provides a direct measurement of displacement, which is often of interest in civil engineering applications.

Chapter 4

4 GRLWEAP Numerical Analysis

4.1 Background

As discussed in the previous chapter, the GRLWEAP program was developed by Goble & Rausche in 1976. The first version was called WEAP and it was later updated to GRLWEAP with many modifications and improvements. The program is founded on the Smiths (1960) solution of the wave equation that is based on the discrete element idealisation of the hammer-soil-pile system, as shown in Figure 4.1.

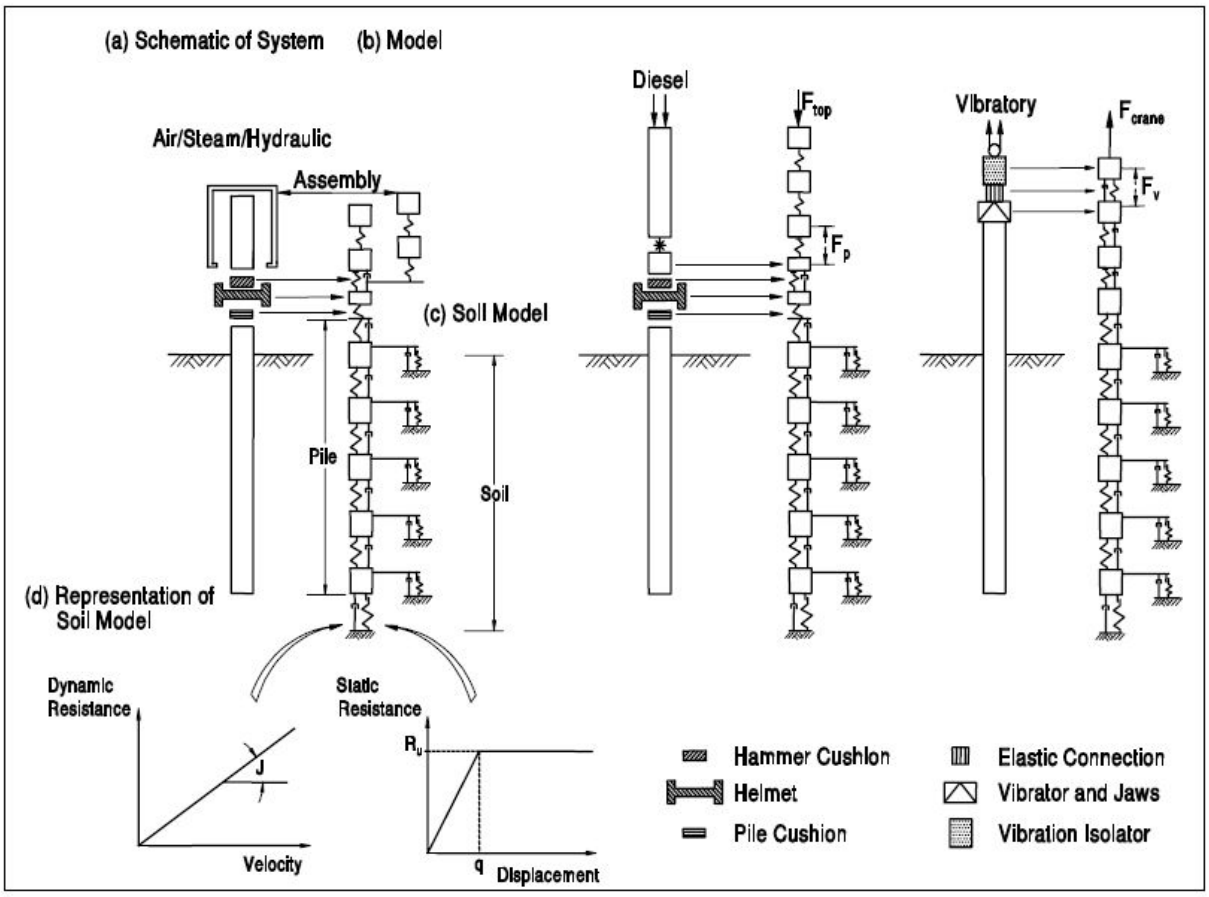

Figure 4.1 GRLWEAP pile, soil and driving system (hammer, helmet & cushion) modelling (PDI 2005)

Although, contrary to the dynamic formulas, GRLWEAP does not directly use the energy approach, but it rather uses the concept of energy losses and energy transfer as results of the pile driving process. The energy balance equation together with the schematic presentation of hammer, driving system, pile and soil is given in Figure 4.2.

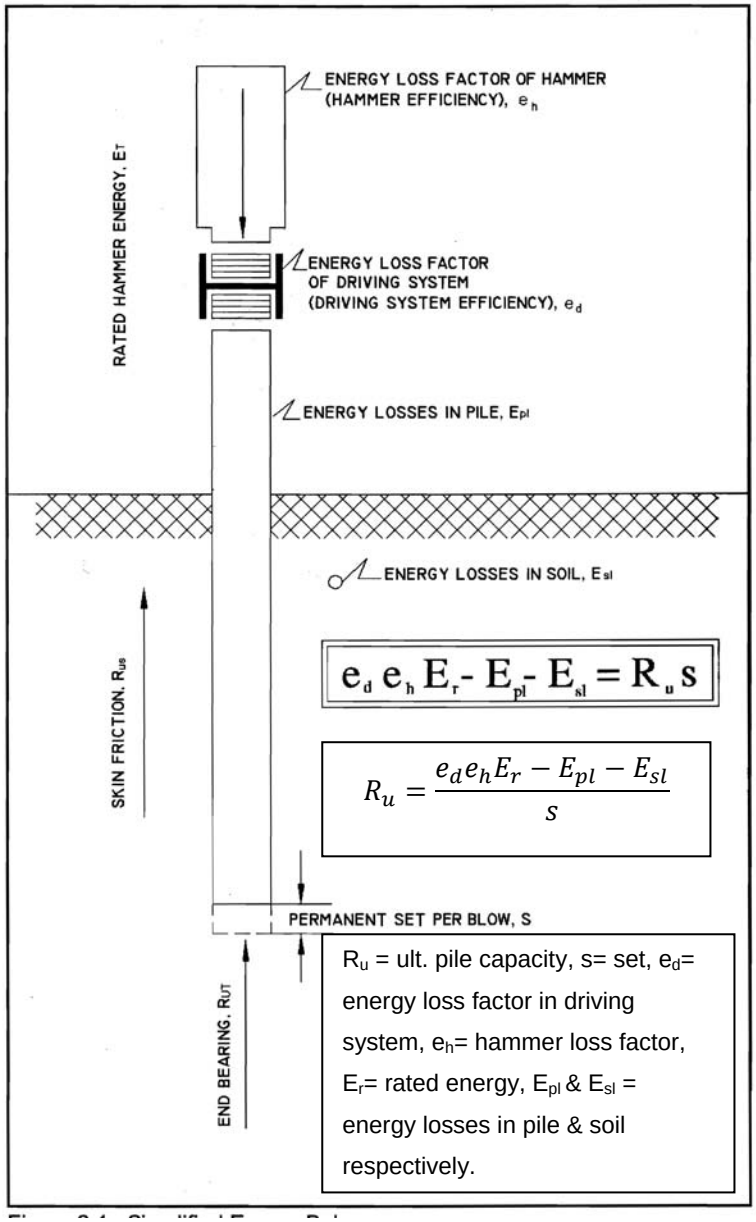

Figure 4.2 Simplified energy balance (PDI, 2006)

In the energy balance equation above, most of the quantities such as E_r, E_p, E_s and the losses e_d and e_h are either known or can be estimated. Therefore, the set, s, can be computed from R_u or vice versa. As a result, plotting the R_u versus the set can be plotted to give what is called Bearing Graph. The most common analysis used in GRLWEAP is the bearing graph which is used to establish driving criteria in the field to ensure quality assurance of piles.

In the bearing graph calculations, an ultimate capacity is assumed and the corresponding set is calculated based on the distributed shaft and toe resistances as per input into the program. This process is repeated for up to ten capacity values. The program also allows for an increase in either

shaft or toe resistances while the other resistance component is held constant for the ten capacities that are input into the program.

Furthermore, the soil model input is also included in the code. The soil model is based on the static formulas available in many standard geotechnical textbooks and is also briefly discussed in Section 2.5.1 of this thesis.

It must be noted that the fundamental difference between the dynamic formula and the wave equation methods are the fact that the energy in the soil, pile and the losses are calculated mathematically. A full detail of the GRLWEAP program background can be found in PDI (2006).

4.2 GRLWEAP Inputs

The main input data in GRLWEAP™ program are hammer, driving system (cushion) and pile details as well as soil parameters. It outputs driving stresses, hammer performance and the pile bearing capacity both graphically and in tabular format. Since 2002, the GRLWEAP™ has included the Residual Stress Analysis (RSA), which is a concept relating to fact that the pile shaft is elastically compressed during hammer strokes and that the resistance distribution between shaft and base vary. RSA analysis is not undertaken for end bearing piles, where the toe capacity significantly larger than the skin friction.

For the hammer, the program provides a large data file which is a compilation of basic properties of many impact hammers, powered by air, steam, hydraulic pressure, or diesel combustion. Once the model is setup, the program then does an analysis of the model that consists primarily of springs, masses and dashpots.

The driving system, consisting of striker plate, cushion, helmet and pile cushion (for concrete piles) that are represented by two non-linear springs and a mass can be entered via the program's input screen. Again, the standard properties of the driving system are inbuilt into the program and can be modified if one wishes so. The cushions can be specified in the program by the area, elastic modulus and the thickness or by the stiffness alone. Pile cushion is only entered for concrete piles and it can be specified by the thickness and the program assumes the elastic modulus value for a

new cushion. However, this assumption may not be correct for the EOD conditions and the program manual suggests a value of approximately 2.5 times the early driving conditions, for example, 500 MPa instead of 200 MPa.

Pile cushions are only used for concrete piles. In the field during pile driving, the cushion properties change over the short life of the cushion material. For example, plywood may compress to half of its initial thickness and its elastic modulus may increase.

The hammer cushion material is usually a hard man made material and the help files of GRLWEAP contain the manufacturers recommended values. If the cushion consists of two sandwiched materials, then the combined properties can be calculated.

The pile cushion is a relatively soft element, usually located underneath the helmet and immediately above the pile top. The pile cushion material is usually wood, most frequently plywood. Also softwood or hardwood boards have been used with the grain perpendicular to the axis of the hammer. In some countries, felt, sisal fabric, rope or other soft materials are used. In general, it is recommended to use only materials for which engineering properties can be accurately determined.

In the analysis, the hammer's transmitted energy to the pile determines the pile stresses. The stiffness of the driving system, non-linearity of material and coefficient of restitution all affect the energy transfer and hence the pile top stresses. Energy losses due to bending, poor surfaces contact, and damaged components etcetera are not well understood.

Pile data consists of total length, cross-section area, toe area, elastic modulus and specific gravity. Many different pile profile options that are available are non-uniform, segmental and open ended piles. Pile mechanical splice and cracks can also be performed by entering 'tension slack', which allows for the extension of the splice with zero tension force.

The coefficient of restitution for the material of the cushion as a decimal number range from 0.1 to 1.0. The cushion coefficient of restitution is a material property, which indicates the fraction of energy that is temporarily stored in the cushion during compression that is not lost. For example, a steel ball dropped onto a steel plate may bounce back to 100% of the drop height. It's COR would

then be 1.0. Numerically, in GRLWEAP, a COR of 0.0 is not an acceptable input. For man-made materials, if nothing else is known, a 0.8 value is a good estimate. For wood COR may be set to 0.5.

Although GRLWEAP performs calculation of soil static resistance in the analysis, but it is only an estimate and the value calculated is found by the author to be non-consistent. So for the bearing graph analysis, a separate static analysis program called DRIVEN (see Appendix D) was used to evaluate the static shaft and toe resistances. Although the pile's ultimate capacity is changed, but the skin and toe resistance distribution is maintained constant throughout the analysis. Another words, as the driving process continue, it is not necessary to recalculate the quake, damping parameters and the skin and toe resistance distribution.

As mentioned earlier, in the GRLWEAP code, two simple static analysis methods are included. One is based on Soil Type (ST) and the other is SPT N-value based (SA) methods. In this research endeavour, only the ST method was used. However, these two methods of pile capacity determination are not very accurate. Therefore, another program called DRIVEN (see Appendix D) was used to calculate the shaft and toe resistances and the values were plugged in the GRLWEAP program.

The ST method is intended for both Driveability and Bearing Graph analyses. It uses the β-Method (static geotechnical capacity as briefly mentioned Section 2.5.1) to calculate the shaft and toe resistance and, hence, the percentage of shaft and toe distribution.

4.3 Analysis Method

The basic result of a wave equation analysis is the bearing graph which relates bearing capacity to blow count for a particular pile depth. In this analysis, an ultimate capacity is assumed then it is distributed along the shaft as per input and the set or blow count is calculated for this ultimate capacity. A higher capacity is selected and it is distributed along the shaft and toe and the again the set is calculated followed by dynamic analysis. GRLWEAP analyses up to ten ultimate capacities and then is plotted against sets or blow counts.

To undertake a GRLWEAP parametric analysis, it was considered to study the effect of different pile-hammer and soil combinations. A summary of the cases that were studied is shown in Table 4.1 below.

Table 4.1 A summary of hammer, pile and soil type combinations in the study

Hammer Type	Hammer Weight	Pile Type	Soil Type	Stroke	Total
Delmag Junttan MKT	3T 5T 10T	-350mm Sq Precast -327mm (12.7mm thick) Tube	Soil combinations as in Table 4.5	1m, 0.5m, 0.25m	Total number of cases analysed in GRLWEAP
3	3	2	36	3	1944

As it can be seen, numerical simulations were carried out using most common hammers such as Delmag, Junttan and MKT together with three rated energies at approximately 3, 5 and 10 tonnes. Also for each hammer three different drop heights of 0.25m, 0.5m and 1m were adopted to produce a wide range of energies and capacities, as shown in Table 4.2.

Table 4.2 Hammer Details

Hammer	Model	Ram Weight(kN)	Max. Stroke(m)	Rated Energy(kNm)
Delmag	D15	29.43	1.2	35.32
	D19-42	49.10	1.2	58.86
	D36-13	98.10	1.2	117.72
Junttan	HHK3	14.69	2.5	36.75
	HHK5	17.8	3.3	58.65
	HHK10	35.29	3.22	113.69
MKT	S-8	35.60	1.0	35.27
	MS500	48.95	1.2	59.68
	S-20	89.00	1.0	81.38

In the case of diesel hammers, the percentages of the maximum hammer strokes were selected. As a result, this systematic analysis produced a total of 1944 cases representing all possible combinations of hammer, pile and soil types, as well as different hammer strokes. After the analysis, the data were sifted through and collated to produce about 20,000 rows by 35 columns of Excel data sheet. A sample of the spreadsheet data sets is shown in Table 4.4. The hammer and pile cushion details that were used in the GRLWEAP analysis are presented in Table 4.3.

Table 4.3 Hammer and Pile Cushion Details

	Concrete pile					Steel pile					
	Delmag		Junttan			MKT		Delmag	Junttan		MKT
	Hammer Cushion	Pile Cushion	Hammer Cushion	HHK10	Pile Cushion	Hammer Cushion	Pile Cushion	Hammer Cushion	Hammer Cushion	HHK10	Hammer Cushion
Material	Nylon	Plywood	Alum/ Conbest	Alum/ Conbest	Plywood	Alum/ Conbest	Plywood	Nylon	Alum/ Conbest	Alum/ Conbest	Alum/ Conbest
Area (cm^2)	1465.5	1225	1590.3	4418.1	1225	-	1225	1464.5	1590.3	4418.1	-
Elastic Mod.(MPa)	3654.2	207	2500	2500	207	-	207	3654.2	2500	2500	-
Thickness(mm)	50.8	94	200	210	94	-	94	50.8	200	210	-
COR	0.8	0.5	0.9	0.9	0.5	0.8	0.5	0.8	0.9	0.9	0.8
Stiffness(kN/mm)	10534.6	269.8	1987.9	5259.6	269.8	6329	269.8	10534.6	1987.9	5259.6	6329

Table 4.4 Sample of the database from GRLWEAP analysis

Hammer Ty	Mod	Ram Weight (k	Rate Energy (k	Potential Energy(k	Kinetic Energy (k	Impact Vel. (m/	Pile Typ	Soil Ty	Rut (kN)	BI Ct (b/m)	Stroke	Ten Str (Mpa)	i	t(ms)	CompStr	i	t(ms)	ENTHRU (kJ)	No	mxTForce	t	mxCForce	t	mxTStrss	t	mxCStrss	t	maxV	t	maxD	t	maxEt	Set(mm)	Hiley(kN)	HCF(-)
JUNTTAN	HHK	29.43	35.32	29.43	23.54	3.96	350 Precst	vl-vl	250	23.8	1	-2.45	4	12	14.72	2	7	14.1	1	0	0	1802	7	0	0	14.7	7	2.64	9	45.5	40	14.1	42.01681	322.2238	1.2888953
JUNTTAN	HHK	29.43	35.32	29.43	23.54	3.96	350 Precst	vl-vl	500	52.2	1	-1.75	3	15	14.94	2	7	14	1	0	0	1817	7	0	0	14.8	7	2.33	9	23.1	22	13.99	19.15709	662.1374	1.3242749
JUNTTAN	HHK	29.43	35.32	29.43	23.54	3.96	350 Precst	vl-vl	750	81.3	1	-1.4	3	15	15.15	2	7	14.1	1	0	0	1831	7	0	0	14.9	7	2.05	9	16.4	16	14.07	12.30012	980.4836	1.3073115
JUNTTAN	HHK	29.43	35.32	29.43	23.54	3.96	350 Precst	vl-vl	1000	109.9	1	-1.5	8	25	15.36	2	7	14.2	1	0	0	1845	7	0	0	15.1	7	1.81	9	13.3	16	14.2	9.099181	1267.903	1.2679035
JUNTTAN	HHK	29.43	35.32	29.43	23.54	3.96	350 Precst	vl-vl	1500	188.9	1	-3.03	5	23	15.76	2	7	13.2	1	0	0	1874	7	0	0	15.3	7	1.44	4	9.8	13	13.23	5.293806	1753.037	1.1686913
JUNTTAN	HHK	29.43	35.32	29.43	23.54	3.96	350 Precst	vl-vl	2000	393.4	1	-2.16	5	21	16.16	2	7	12.1	1	0	0	1903	7	0	0	15.5	7	1.44	4	8.4	10	12.14	2.541942	2218.985	1.1094923
JUNTTAN	HHK	29.43	35.32	29.43	23.54	3.96	350 Precst	vl-vl	2500	1278.5	1	-2.3	4	21	17.12	4	10	11.2	1	0	0	1931	7	0	0	15.8	7	1.43	4	7.5	10	11.18	0.782167	2699.777	1.0799107
JUNTTAN	HHK	29.43	35.32	29.43	23.54	3.96	350 Precst	vl-vl	3000	9999	1	-3.31	4	18	18.74	4	10	10.4	1	0	0	1959	7	0	0	16	7	1.43	4	6.9	10	10.35	0.10001	2957.139	0.9857129
JUNTTAN	HHK	29.43	35.32	7.3575	5.89	1.98	350 Precst	vl-vl	250	77.7	0.25	-0.89	5	13	7.35	1	8	4	1	0	0	900	8	0	0	7.3	8	1.23	10	16.4	28	3.97	12.87001	271.2674	1.0850696
JUNTTAN	HHK	29.43	35.32	7.3575	5.89	1.98	350 Precst	vl-vl	500	186.3	0.25	-0.75	6	30	7.43	1	8	4	1	0	0	911	8	0	0	7.4	8	1.03	10	9	17	3.97	5.367687	552.629	1.105258
JUNTTAN	HHK	29.43	35.32	7.3575	5.89	1.98	350 Precst	vl-vl	750	344.8	0.25	-0.75	5	26	7.52	1	8	3.9	1	0	0	921	8	0	0	7.5	8	0.89	9	6.8	15	3.88	2.900232	799.9809	1.0666412
JUNTTAN	HHK	29.43	35.32	7.3575	5.89	1.98	350 Precst	vl-vl	1000	682.3	0.25	-1.96	6	24	7.6	1	8	3.6	1	0	0	932	8	0	0	7.6	8	0.8	8	5.5	11	3.6	1.465631	1033.646	1.0336465
JUNTTAN	HHK	29.43	35.32	7.3575	5.89	1.98	350 Precst	vl-vl	1166.9	1389.3	0.25	-1.93	6	24	7.66	1	8	3.5	1	0	0	952	8	0	0	7.8	8	0.71	4	4.6	11	3.27	0.719787	1229.373	1.0535372
JUNTTAN	HHK	29.43	35.32	7.3575	5.89	1.98	350 Precst	vl-vl	1500	9999	0.25	-1.18	0	0	8.49	0	0	3.3	1	0	0	939	8	0	0	7.7	8	0.76	8	5.1	11	3.49	0.10001	1342.305	0.8948701
JUNTTAN	HHK	29.43	35.32	14.715	11.77	2.80	350 Precst	vl-vl	250	42.1	0.5	-1.43	4	12	10.46	1	7	7.5	1	0	0	1281	7	0	0	10.5	7	1.79	10	27.2	34	7.45	23.75297	292.4265	1.1697061
JUNTTAN	HHK	29.43	35.32	14.715	11.77	2.80	350 Precst	vl-vl	500	94.2	0.5	-0.53	4	36	10.56	1	7	7.4	1	0	0	1293	7	0	0	10.6	7	1.53	9	14.1	19	7.41	10.61571	599.6186	1.1992372
JUNTTAN	HHK	29.43	35.32	14.715	11.77	2.80	350 Precst	vl-vl	750	154.8	0.5	-0.63	5	27	10.66	1	7	7.4	1	0	0	1306	7	0	0	10.7	7	1.3	9	10.3	16	7.42	6.459948	885.4443	1.1805923
JUNTTAN	HHK	29.43	35.32	14.715	11.77	2.80	350 Precst	vl-vl	1000	227.9	0.5	-1.76	6	24	10.81	2	7	7.2	1	0	0	1318	7	0	0	10.8	7	1.11	9	8.4	14	7.2	4.387889	1126.065	1.1260654
JUNTTAN	HHK	29.43	35.32	14.715	11.77	2.80	350 Precst	vl-vl	1500	627.7	0.5	-2.14	5	23	11.15	2	7	6.5	1	0	0	1343	7	0	0	11	7	1.02	4	6.5	11	6.47	1.593118	1598.889	1.0659263

The soil types and their consistencies were also based on the parameters given in the GRLWEAP program and range of cohesive and non-cohesive soils with various consistencies were selected. A summary of the soil combination as well as the standard soil profile is shown in Table 4.5.

Table 4.5 Soil combinations and cross-section profiles used in the GRLWEAP analysis

Bottom Layer →

Top Layer ↓		CLAY			SAND		
		Soft	Stiff	Hard	VL	MD	VD
	ρ	17-19 kN/m3	19-21 kN/m3	22-23 kN/m3	11-16 kN/m3	17-20 kN/m3	20-23 kN/m3
	SPT-N	2-4	8-15	>30	0-5	5-10	>50
CLAY	Soft	✓	✓	✓	✓	✓	✓
	Stiff	✓	✓	✓	✓	✓	✓
	Hard	✓	✓	✓	✓	✓	✓
SAND	VL	✓	✓	✓	✓	✓	✓
	MD	✓	✓	✓	✓	✓	✓
	VD	✓	✓	✓	✓	✓	✓

VL = very loose
MD = med. dense
VD = very dense

Cross-section

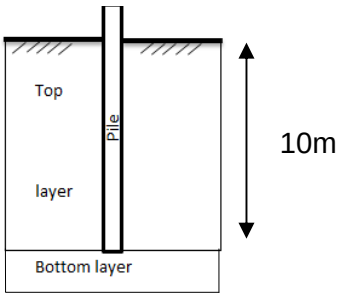

The standard GRLWEAP soil resistance parameters, toe quake value (dependent on the pile toe diameter) and shaft and toe quake damping are shown in Table 4.6 below.

Table 4.6 GRLWEAP resistance parameters for ST analysis for cohesion-less soils

Soil Type	SPT N	Friction angle	Unit Weight	β	N_t	R_s	R_t
		Deg.	kN/m^3			Limit (kPa)	
Very loose	2	25-30	13.5	0.203	12.1	24	2400
Loose	7	27-32	16	0.242	18.1	48	4800
Medium	20	30-35	18.5	0.313	33.2	72	7200
Dense	40	35-40	19.5	0.483	86.0	96	9600
Very Dense	50+	38-43	22	0.627	147.0	192	19000

For cohesive soils, GRLWEAP adopts α-method, also called total stress method, for the ST analysis. For non-cohesive the methods relies on the unconfined compressive strength of soil. The unconfined compressive strength (q_u), the shaft and bearing soil resistance as a function of soil type for cohesive soils are given in Table 4.7.

Table 4.7 GRLWEAP resistance parameters for cohesive soils

Soil Type	SPT N	q_u	Unit Weight	R_s	R_t
		kPa	kN/m^3	kPa	
Very soft	1	12	17.5	3.5	54
Soft	3	36	16	10.5	162
Medium	6	72	18.5	19	324
Stiff	12	144	19.5	38.5	648
Very stiff	24	288	22	63.5	1296
Hard	32+	384+		77	1728

In the GRLWEAP analysis, shaft and toe quakes and damping are the four Smith soil model parameters that are used to model the soil dynamic behaviour. The program standard quake and damping parameters are given in the Table 4.8. It may be noted that no quake or damping values are given by GRLWEAP program for vibratory hammers because of the complex nature of such hammers and the lack of testing experience.

Table 4.8 GRLWEAP recommended Quake values for driven piles

	Soil Type	Pile Type	Quake (mm)
Shaft Quake	All soil types	All types	2.5
Toe Quake	All soil types, soft rock	Non-displacement piles*	2.5
	Very dense & Hard soils	Displacement piles **of diameter or width D	D/120
	Loose or soft soils	Displacement piles *of diameter or width D	D/60
	Hard rock	All types	1.0

*= Non-displacement piles are sheet piles, H-piles or open ended unplugged piles

**= Displacement piles are all other piles including closed-end tube and solid concrete piles

Also, the recommended damping values suggested by GRLWEAP is summarised in Table 4.9 and in general, the Smith damping is used unless the residual stress analysis (briefly discussed in Section 4.2) is required and in which case the Smith Viscous soil damping is used.

Table 4.9 GRLWEAP recommended damping values for driven piles

	Soil Type	Damping Factor (s/m)
Shaft damping	Non-cohesive soils *	0.16
Toe damping	Cohesive soils**	0.65
	All soil types	0.5

*= Non-cohesive soils are sand type soils, **= Cohesive soils are clay type soils

For all the analysis in GRLWEAP, the recommended quake and damping values given in the above Table 4.8 and Table 4.9 were used in this research.

As discussed previously, for the skin and toe resistance, a static analysis program called DRIVEN was used to calculate the shaft and toe resistance ratios. In order to make the analysis consistent, the GRLWEAP resistance parameters for cohesive and non-cohesive soils were adopted and used in DRIVEN program. Table 4.10 shows a summary of the parameters used in the DRIVEN program.

Table 4.10 Input parameters in DRIVEN

Soil Type	SPT(N)	Unit Weight	Cu	Friction angle
	no.	kN/m^3	kPa	degree
Soft	3	17.5	20	-
Stiff	12	20.5	75	-
Hard	32	22	200	-
Very Loose	2	13.5	-	25
Medium	20	18.5	-	30
Very Dense	50	22	-	40

After utilisation of the parameters in DRIVEN, the results were tabulated in total skin/shaft and toe resistance and the ratios for the two pile types were calculated in excel spreadsheet, as shown in

Table 4.11 and Table 4.12, and the results of the DRIVEN program were back-substituted into GRLWEAP for the shaft and toe resistance distribution.

Table 4.11 DRIVEN output of skin and end bearing capacities for precast concrete pile

350mm Precast Concrete Pile

Bottom Layer →

Top Layer ↓

		CLAY									SAND								
		Soft			Stiff			Hard			VL			MD			VD		
ρ(kN/m^3)		17.5			20.5			22			13.5			18.5			22		
Cu/ϕ (kPa/deg)		20			75			200			25			30			40		
		Shaft(kN)	Tip(kN)	Total	Shaft(kN)	Tip(kN)	Total	Shaft(kN)	Tip(kN)	Total	Shaft(kN)	Tip(kN)	Total	Shaft(kN)	Tip(kN)	Total	Shaft(kN)	Tip(kN)	Total
CLAY	Soft	234.78	22.05	256.83	234.97	82.68	317.65	235.19	220.5	455.69	235.36	78.12	313.48	235.8	78.12	313.92	238.48	2449.24	2687.7
		91%	**9%**		**74%**	**26%**		**52%**	**48%**		**75%**	**25%**		**75%**	**25%**		**9%**	**91%**	
	Stiff	964.4	22.05	986.45	965.46	82.68	1048.1	965.27	220.5	1185.8	965.35	78.12	1043.5	965.86	78.12	1044	969.01	2449.24	3418.3
		98%	**2%**		**92%**	**8%**		**81%**	**19%**		**93%**	**7%**		**93%**	**7%**		**28%**	**72%**	
	Hard	775.27	22.05	797.32	775.95	82.68	858.63	775.76	220.5	996.26	773.87	78.12	851.99	776.45	78.12	854.57	779.83	2449.24	3229.1
		97%	**3%**		**90%**	**10%**		**78%**	**22%**		**91%**	**9%**		**91%**	**9%**		**24%**	**76%**	
SAND	VL	281.71	22.05	303.76	282.39	82.68	365.07	282.2	220.49	502.69	281.99	78.12	360.11	280.86	78.12	358.98	284.4	1987.73	2272.1
		93%	**7%**		**77%**	**23%**		**56%**	**44%**		**78%**	**22%**		**78%**	**22%**		**13%**	**87%**	
	MD	618.38	22.05	640.43	619.07	82.68	701.75	618.88	220.49	839.37	618.87	78.12	696.99	619.34	78.12	697.46	622.18	2449.24	3071.4
		97%	**3%**		**88%**	**12%**		**74%**	**26%**		**89%**	**11%**		**89%**	**11%**		**20%**	**80%**	
	VD	2421.9	22.05	2444	2422.58	82.68	2505.3	2422.4	220.49	2642.9	2422.54	78.12	2500.7	2423.1	78.12	2501.2	2426.47	2449.24	4875.7
		99%	**1%**		**97%**	**3%**		**92%**	**8%**		**97%**	**3%**		**97%**	**3%**		**50%**	**50%**	

Table 4.12 DRIVEN output of skin and end bearing capacities for tube pile

327mm@12.7mm Steel Tube Pile (Closed)

Bottom Layer →

Top Layer ↓

		CLAY									SAND								
		Soft			Stiff			Hard			VL			MD			VD		
ρ(kN/m^3)		17.5			20.5			22			13.5			18.5			22		
Cu/ϕ (kPa/deg)		20			75			200			25			30			40		
		Shaft(kN)	Tip(kN)	Total	Shaft(kN)	Tip(kN)	Total	Shaft(kN)	Tip(kN)	Total	Shaft(kN)	Tip(kN)	Total	Shaft(kN)	Tip(kN)	Total	Shaft(kN)	Tip(kN)	Total
CLAY	Soft	193.4	15.12	208.52	193.83	56.69	250.52	193.75	151.16	344.91	193.57	53.56	247.13	193.76	53.56	247.32	194.82	1679.1	1873.92
		93%	**7%**		**77%**	**23%**		**56%**	**44%**		**78%**	**22%**		**78%**	**22%**		**10%**	**90%**	
	Stiff	616.25	15.12	631.37	616.67	56.69	673.36	616.6	151.16	767.76	616.48	53.56	670.04	616.71	53.56	670.27	617.95	1679.1	2297.05
		98%	**2%**		**92%**	**8%**		**80%**	**20%**		**92%**	**8%**		**92%**	**8%**		**27%**	**73%**	
	Hard	544.26	15.12	559.38	544.68	56.69	601.37	544.61	151.16	695.77	544.51	53.56	598.07	544.76	53.56	598.32	546.1	1679.11	2225.21
		97%	**3%**		**91%**	**9%**		**78%**	**22%**		**91%**	**9%**		**91%**	**9%**		**25%**	**75%**	
SAND	VL	138.4	15.12	153.52	138.82	56.69	195.51	138.75	151.16	289.91	138.48	53.56	192.04	138.63	53.56	192.19	139.45	1362.72	1502.17
		90%	**10%**		**71%**	**29%**		**48%**	**52%**		**72%**	**28%**		**72%**	**28%**		**9%**	**91%**	
	MD	292.11	15.12	307.23	292.53	56.69	349.22	292.46	151.16	443.62	292.3	53.56	345.86	292.5	53.56	346.06	293.62	1679.11	1972.73
		95%	**5%**		**84%**	**16%**		**66%**	**34%**		**85%**	**15%**		**85%**	**15%**		**15%**	**85%**	
	VD	1012.86	15.12	1027.98	1013.28	56.69	1069.97	1013.21	151.16	1164.37	1013.11	53.56	1066.67	1013.36	53.56	1066.92	1014.69	1679.11	2693.8
		99%	**1%**		**95%**	**5%**		**87%**	**13%**		**95%**	**5%**		**95%**	**5%**		**38%**	**62%**	

As stated earlier, a total 1944 cases were analysed in GRLWEAP and only the relevant results from an extensive data outputs were collated in a spreadsheet for further analysis. GRLWEAP is capable of producing results both in graphical and tabular data formats. The Figure 4.3 below shows a typical graphical output.

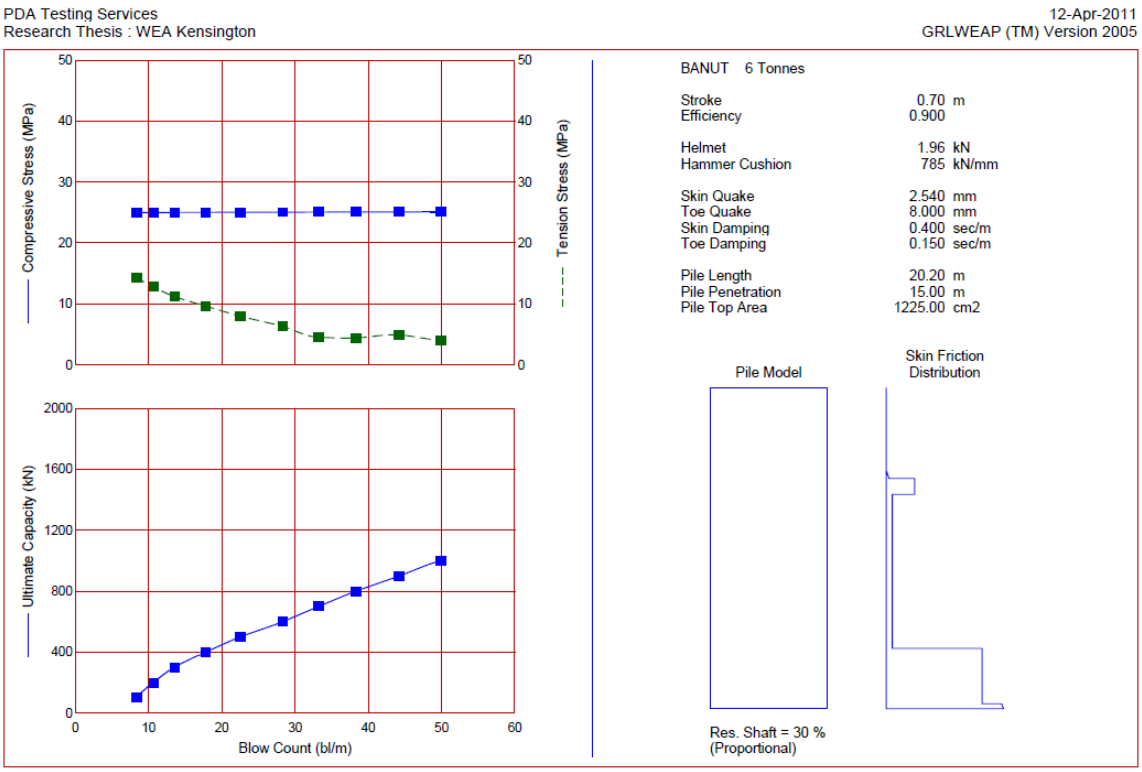

Figure 4.3 GRLWEAP graphical output of results

4.4 Results and Discussions

The results of the GRLWEAP numerical simulations were collated in a spreadsheet and analysed for the following:

1. Three hammer types: Delmag, Junttan and MKT. Within each type, three different ram weights were analysed.
2. Two different piles: Precast concrete and steel tube pile with similar effective sizes.
3. For each hammer type and ram weight, three drop heights were analysed.
4. Three soil resistance models with consistencies of soft, stiff and hard were used for the cohesive soils, and three (very loose, medium dense & very dense) for non-cohesive soils were used.

The results of the GRLWEAP simulations were exported and collated into a spreadsheet for further analysis. The results of the GRLWEAP simulation analysis are shown in Appendix E. The graphs were produced from the calculated Hiley capacities and GRLWEAP capacity ratios versus the set.

4.4.1 Delmag Hammers

Delmag diesel hammers seem to perform very well in driving concrete and steel piles. The maximum hammer energies for the three rams with the weights of three, five and ten tonnes falling from 0.25m, 0.5m and 1m were plotted against maximum ram velocity. As it can be seen from Figure 4.4 and Figure 4.5, that there is reasonable correlation between the maximum energy and the ram impact velocity. Generally, there seems to exceptionally good correlation for low hammer energies than higher energies.

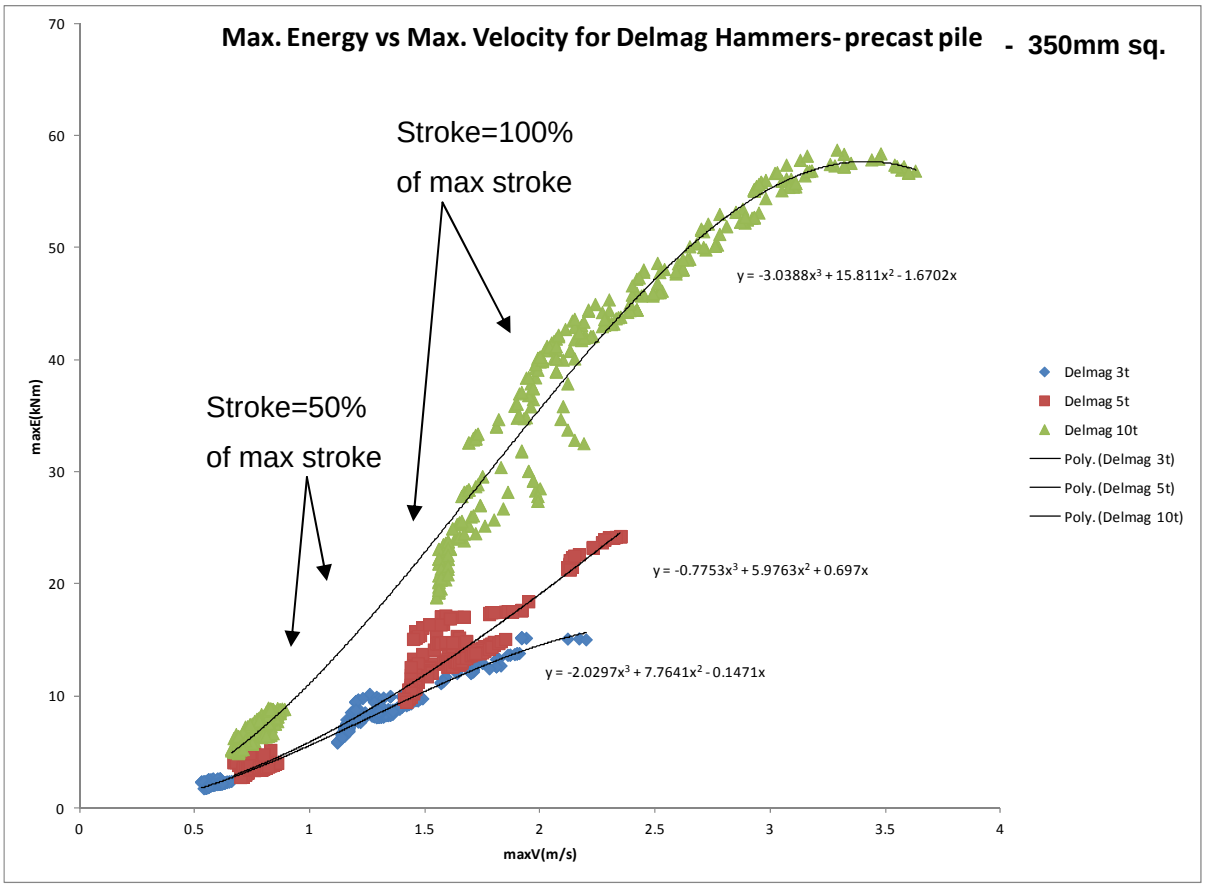

Figure 4.4 Maximum energy versus velocity for Delmag hammer - concrete pile

On the other hand, performance of the Delmag for steel pile is unusual for low R_u capacities and relatively high set values calculated for GRLWEAP. This seems to be a bit of contradiction where

the energy-velocity data seems to reflect which give that there is a minimum energy at the specific set value. It could not be established how this could be possible in the real practical sense.

It should be born in mind that the pile performance in this case is not efficiencies, but rather the implicit relationship between the ram velocity and delivered energy. This relationship is important in the field where once ram velocity can be established and the ram energy can be inferred by the relationship that would make it possible to use the dynamic formulas with greater confidence.

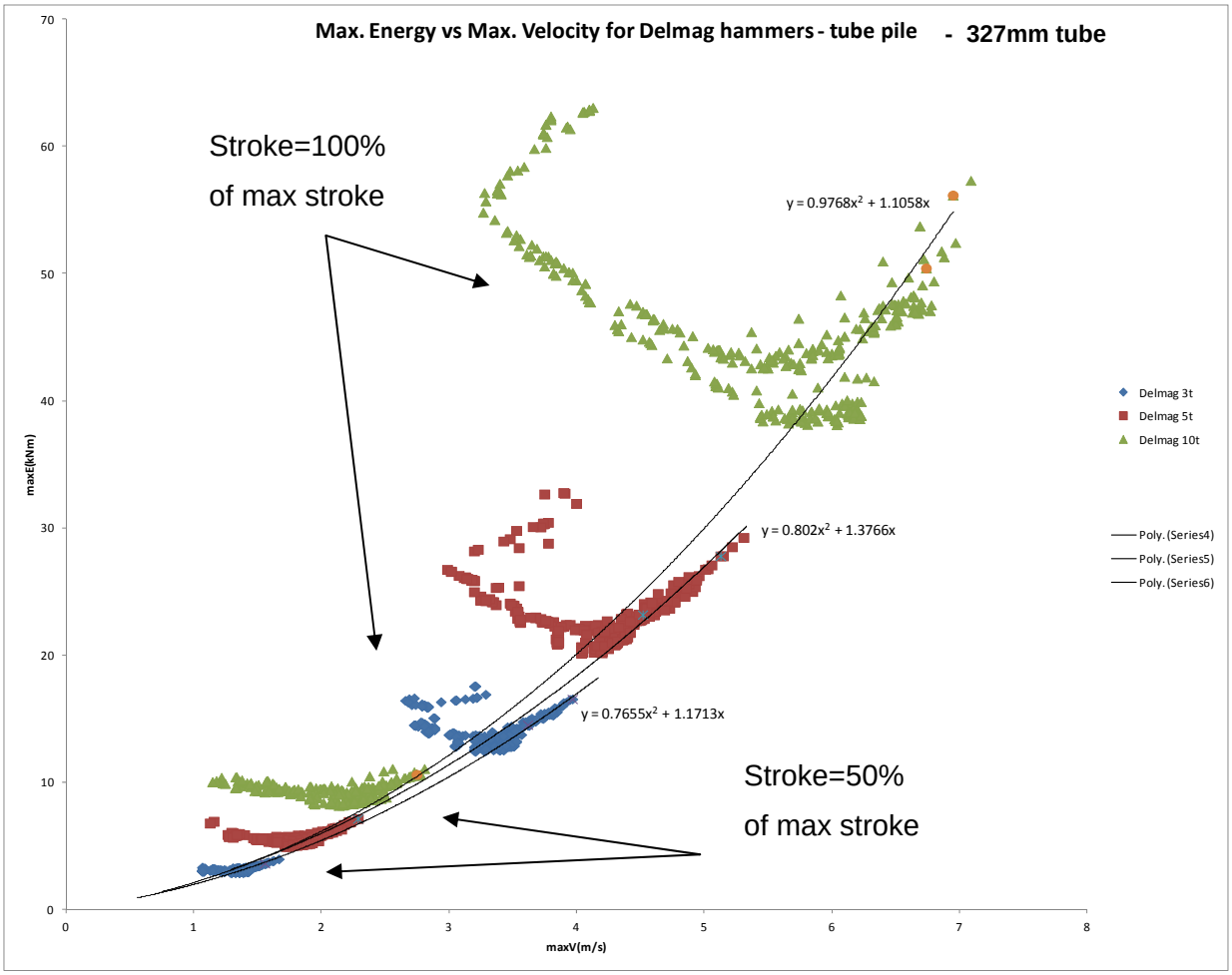

Figure 4.5 Maximum energy versus velocity for Delmag hammer - tube pile

4.4.2 Junttan Hammers

Junttan hammers perform similar to the Delmag hammers for steel piles, but its performance is relatively poor for the precast piles as the data is widely scattered and no clear trend can be

established. However, the velocity-energy graph in figure for the steel pile seems to indicate there is a very good correlation and the relationship may be estimated by the given equation on the graph.

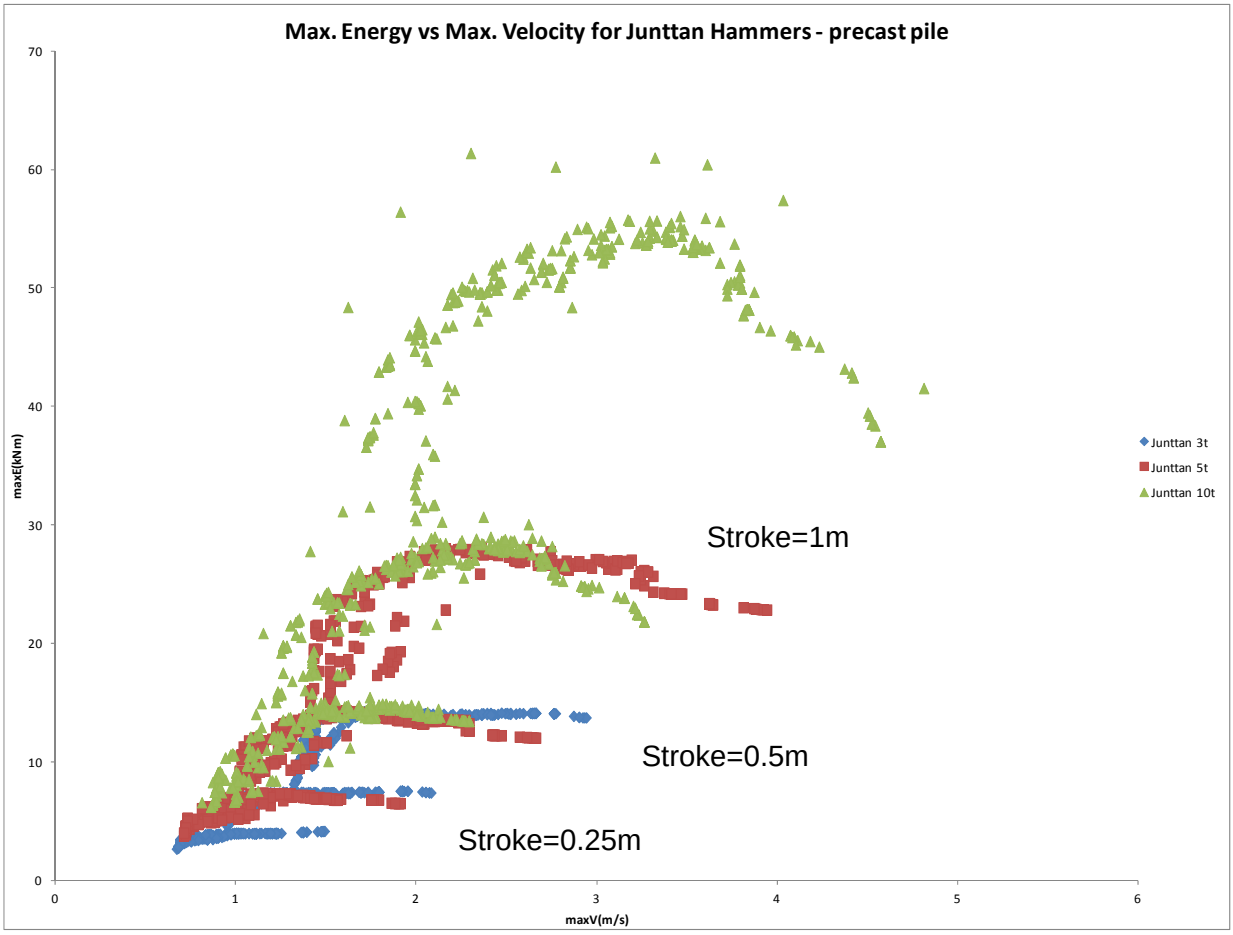

Figure 4.6 Maximum energy versus velocity for Junttan hammer - concrete pile

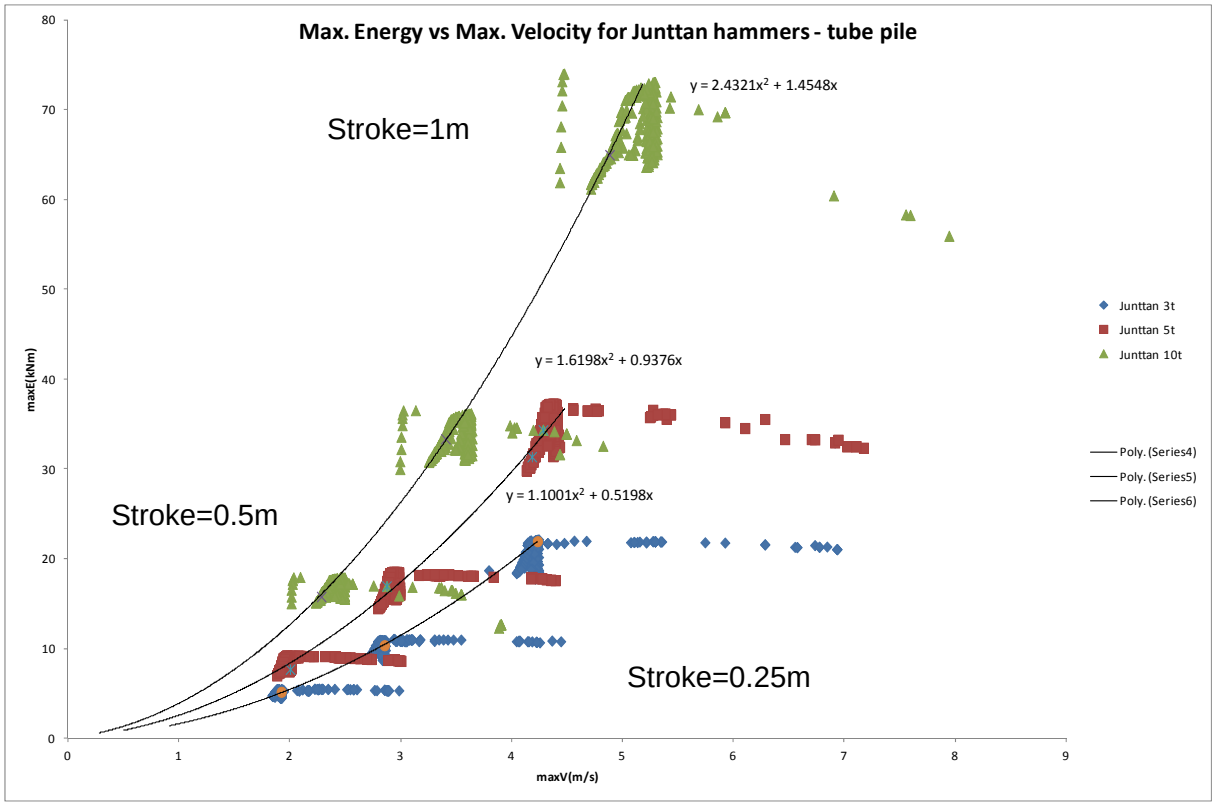

Figure 4.7 Maximum energy versus velocity for Junttan hammer - tube pile

4.4.3 MKT Hammers

Again the energy-velocity relationship for the MKT hammers scattered and no clear correlation exists. It should be emphasised that although there may be a relationship on a small individual case bases, but overall, for a wide range of ground conditions, different rated energies and strokes, there could not be a clear correlation as can be seen from Figure 4.8.

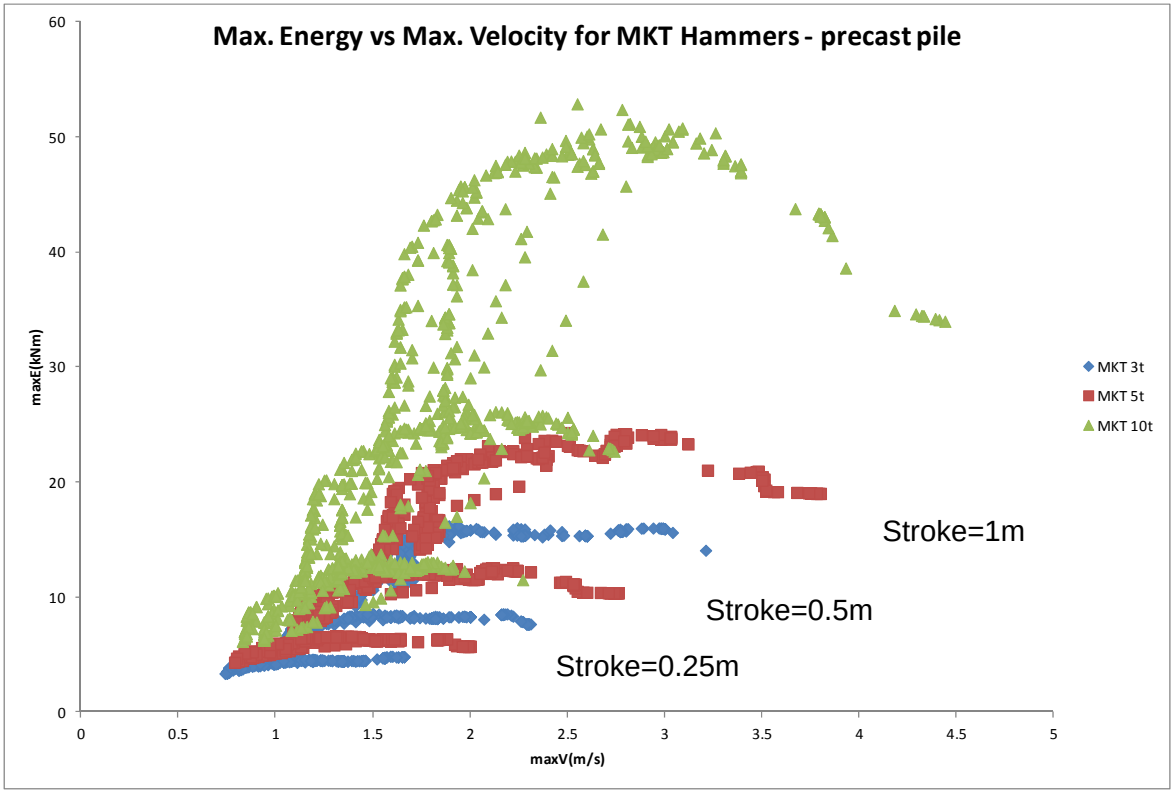

Figure 4.8 Maximum energy versus velocity for MKT hammer - concrete pile

MKT hammers seems to perform exceptionally well for the steel piles. Initially there is clear relationship, as is approximated by the regression line, and then it is a horizontal line indicating that the delivered energy cannot increase indefinitely and reaches a maximum regardless of the ram velocity. This is shown on the Figure 4.9.

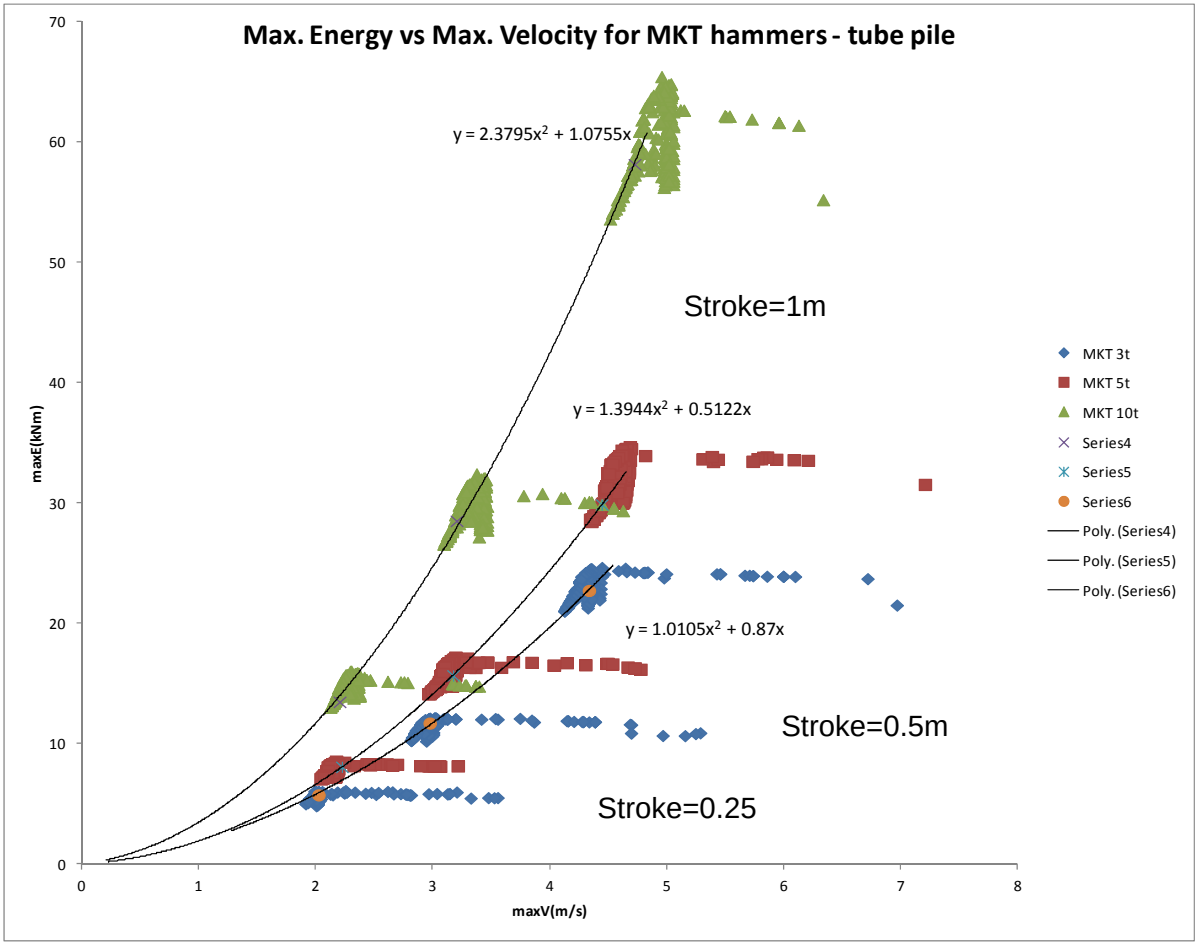

Figure 4.9 Maximum energy versus velocity for MKT hammer - tube pile

4.4.4 Hiley Corrections Factor

Having analysed and established the relative performance of hammers in regards to the velocity-energy relationship, similar analysis were carried out for establishing the hiley correction factor (HCF) for each soil types and hammer types. Appendix E contains the results of the analyses for each soil and hammer types. The graphs were produced by plotting the GRLWEAP and Hiley capacity ration (or HCF) against the sets. Table 4.13 shows a summary of the range of the HCF for the various hammers, pile types and soil conditions.

Table 4.13 Summary of range of Hiley Correction Factors for various driving system and soil types

	Precast Concrete Pile					Tube Steel Pile				
		Top	Bottom	HCF*	Trend		Top	Bottom	HCF	Trend
Delmag	3 tonne	S	S-H	1.51-1.07	Initially steep-linear then horizontal. Nearly constant for low hammer energies.	3 tonne	S	S-H	2.07-1.25	Linear then flat. For low energies initially linear then negative linear.
			VL-VD	1.57-1.00				VL-VD	2.03-1.13	
		H	S-H	1.58-1.06			H	S-H	2.07-1.30	
			VL-VD	1.59-1.02				VL-VD	2.06-1.23	
		VL	S-H	0.95-1.31			VL	S-H	1.07-1.57	
			VL-VD	0.92-1.42				VL-VD	1.08-1.72	
		VD	S-H	0.90-1.19			VD	S-H	1.05-1.38	
			VL-VD	0.90-1.32				VL-VD	1.06-1.60	
Delmag	5 tonne	S	S-H	1.71-1.13		5 tonne	S	S-H	2.29-1.40	
			VL-VD	1.70-1.06				VL-VD	2.26-1.26	
		H	S-H	1.72-1.12			H	S-H	2.25-1.50	
			VL-VD	1.71-1.00				VL-VD	2.28-1.30	
		VL	S-H	0.95-1.37			VL	S-H	1.11-1.68	
			VL-VD	0.95-1.51				VL-VD	1.12-1.88	
		VD	S-H	0.95-1.23			VD	S-H	1.09-1.46	
			VL-VD	0.95-1.39				VL-VD	1.10-1.74	
Delmag	10 tonne	S	S-H	2.09-1.11	Linear then flat. Almost constant for low energies.	10 tonne	S	S-H	2.38-1.28	Power. Negative linear for low energies.
			VL-VD	2.04-1.07				VL-VD	2.26-1.19	
		H	S-H	1.12-2.11			H	S-H	2.40-1.28	
			VL-VD	2.09-1.09				VL-VD	2.35-1.25	
		VL	S-H	1.65-0.95			VL	S-H	1.07-1.70	
			VL-VD	0.97-1.83				VL-VD	1.09-1.74	
		VD	S-H	0.94-1.48			VD	S-H	1.05-1.46	
			VL-VD	0.94-1.68				VL-VD	1.06-1.80	
Junttan	3 tonne	S	S-H	1.96-0.97	Linear then asymptotes	3 tonne	S	S-H	2.59-1.38	Linear then assymptotic.
			VL-VD	1.88-0.99				VL-VD	2.53-1.19	
		H	S-H	1.96-1.18			H	S-H	2.61-1.45	
			VL-VD	1.96-0.93				VL-VD	2.57-1.29	
		VL	S-H	1.60-0.93			VL	S-H	1.10-1.91	
			VL-VD	0.94-1.64				VL-VD	1.07-2.05	
		VD	S-H	0.95-1.26			VD	S-H	1.03-1.62	
			VL-VD	0.92-1.47				VL-VD	1.04-1.82	
Junttan	5 tonne	S	S-H	2.15-1.10		5 tonne	S	S-H	2.54-1.37	
			VL-VD	2.17-0.96				VL-VD	2.50-1.13	
		H	S-H	1.08-2.42			H	S-H	2.60-1.44	
			VL-VD	2.25-1.02				VL-VD	2.50-1.25	
		VL	S-H	1.90-0.93			VL	S-H	1.10-1.93	
			VL-VD	0.90-1.80				VL-VD	1.05-2.14	
		VD	S-H	0.94-1.34			VD	S-H	1.12-1.64	
			VL-VD	0.90-1.60				VL-VD	1.13-1.82	
Junttan	10 tonne	S	S-H	2.30-1.10	Parabolic then asymptotic.	10 tonne	S	S-H	2.41-1.41	Parabolic then linear asymptotic.
			VL-VD	2.30-1.01				VL-VD	2.35-1.15	
		H	S-H	1.05-2.25			H	S-H	2.47-1.45	
			VL-VD	2.13-1.18				VL-VD	2.41-1.27	
		VL	S-H	1.68-0.95			VL	S-H	1.14-1.67	
			VL-VD	1.83-0.94				VL-VD	1.07-1.99	
		VD	S-H	1.43-0.97			VD	S-H	1.13-1.52	
			VL-VD	1.70-0.95				VL-VD	1.14-1.83	
MKT	3 tonne	S	S-H	1.91-1.19	Parabolic then asymptotes down.	3 tonne	S	S-H	2.50-1.48	Parabolic. Power for low energies.
			VL-VD	1.93-1.01				VL-VD	2.44-1.15	
		H	S-H	1.91-1.23			H	S-H	2.54-1.39	
			VL-VD	1.85-1.10				VL-VD	2.48-1.35	
		VL	S-H	1.00-1.46			VL	S-H	1.05-1.82	
			VL-VD	1.63-0.96				VL-VD	1.14-2.04	
		VD	S-H	0.98-1.28			VD	S-H	1.01-1.56	
			VL-VD	0.98-1.48				VL-VD	1.05-1.89	
MKT	5 tonne	S	S-H	1.15-2.25		5 tonne	S	S-H	2.42-1.43	
			VL-VD	2.19-1.00				VL-VD	2.39-1.14	
		H	S-H	1.24-2.25			H	S-H	2.47-1.47	
			VL-VD	2.25-1.06				VL-VD	2.40-1.35	
		VL	S-H	1.02-1.55			VL	S-H	1.11-1.81	
			VL-VD	1.03-1.60				VL-VD	1.13-2.03	
		VD	S-H	1.01-1.32			VD	S-H	1.08-1.52	
			VL-VD	1.56-1.02				VL-VD	1.09-1.87	
MKT	10 tonne	S	S-H	2.33-1.18	Parabolic then asymptotes.	10 tonne	S	S-H	2.38-1.38	Parabolic. Nearly linear for VD soils.
			VL-VD	2.40-1.03				VL-VD	2.32-1.13	
		H	S-H	2.28-1.24			H	S-H	2.60-1.37	
			VL-VD	2.31-1.05				VL-VD	2.39-1.25	
		VL	S-H	0.97-1.52			VL	S-H	1.09-1.76	
			VL-VD	0.98-1.78				VL-VD	1.04-1.98	
		VD	S-H	1.04-1.37			VD	S-H	1.13-1.51	
			VL-VD	0.97-1.53				VL-VD	1.11-1.82	

*= Hiley Correction Fac S= Soft, H= Hard, VL= Very Loose, VD= Very Dense

Overall, the HCF values are fairly uniform across the different hammers and soil types. Delmag 5t, Junttan 3t and MKT 5t have performed really well in terms of the statistical analysis data, as shown in Table 4.14. For the steel tube pile, Delmag 3t, Junttan 10t and MKT 5t have performed better statistically. Also from the Table 4.14 it can be seen that the minimum and maximum range of HCF across the table is between approximately 1.0 to 2.9 and an average of about 1.4. An interesting point about the HFC is that generally the lower unit value is applicable for the sandy soil and the higher value applicable for the clay soils. This indicates that for clay soils the dynamic effect is greater due to the viscous nature of clay soils and hence the factor must be higher for clay soils. On the other hand, for sandy soils, this dynamic effect is very small and hence the HCF approaches a unit.

Table 4.14 Statistical analysis of HCF based on the GRLWEAP data for each hammer type

	Precast Concrete Pile									Steel Tube Pile								
	Delmag			Junttan			MKT			Delmag			Junttan			MKT		
Weight	3t	5t	10t	3t	5t	10t	3t	5t	10t	3t	5t	10t	3t	5t	10t	3t	5t	10t
Min.	0.947	0.897	0.941	0.864	0.831	0.861	0.959	0.926	0.887	1.032	1.016	1.046	0.992	1.013	1.069	0.919	1.052	1.010
Max.	1.719	1.600	2.108	1.965	2.418	2.516	2.909	2.026	2.516	2.099	2.323	2.504	2.676	2.667	2.499	2.802	2.494	2.736
Mean.	1.228	1.164	1.316	1.303	1.384	1.418	1.327	1.282	1.332	1.446	1.555	1.532	1.556	1.514	1.515	1.554	1.527	1.496
STDEV	0.213	0.194	0.298	0.248	0.319	0.314	0.265	0.217	0.283	0.308	0.363	0.391	0.347	0.332	0.299	0.333	0.307	0.294

4.5 Conclusion

In this chapter, the methodology and discussion on the results of numerical analysis using GRLWEAP has been presented.

A total of 1944 cases were analysed based on a combination of different hammer type and weight, pile types, soil types and hammer strokes. The data were collated into a spreadsheet and further analysis were conducted calculate and compare the range of HCF based on these variables.

Based on this study, it has been proposed that GRLWEAP analysis could be carried out to establish the:

1. Hammer performance and efficiency;
2. Transmitted energy to piles;
3. Relationship between hammer velocity and peak energy; and
4. Set versus Resistance of piles.

Once the above have been established, the HCF can be used calculated based on these parameters. Subsequently, the HCF can be used to evaluate pile capacity in the field with greater confidence and reliability. In conjunction with this, radar equipment has been proposed to calculate the set and velocity of a pile on site to make the hiley formula comparable to the wave equation techniques.

Chapter 5

5 FIELD STUDY

5.1 Test Site

A site located at the north-western fringe of Melbourne Central Business District (CBD) was chosen to conduct a trial test of radar IBIS-S. The IBIS-S testing was carried out in parallel with the PDA testing using 350mm square section precast concrete pile. The IBIS (Figure 5) was set up at an offset distance of approximately 20m from the pile.

PDA and IBIS-S testings were carried out at the end-of-driving (EOD) under low driving resistance (easy-driving) and high driving resistance (hard-driving) conditions. The pile was driven by a 6 tonne single-acting hydraulic (Banut) hammer with strokes of 300mm for the easy and 700mm for hard driving conditions. The pile embedded lengths were approximately 15m and 18m for the two pile driving conditions respectively.

5.2 Site Conditions

According to the site geotechnical report, the subsurface condition generally comprised 0.5m thick of borrowed sedimentary rock materials (siltstone), followed by under laying Coode Island Silt (CIS) of 10.5m thickness. The consistency of the CIS material was predominantly soft. Fishermens Bend Silt (FBS) typically 4m in thickness, generally occur below CIS and was of stiff to very stiff consistency. A sedimentary formation deposit called Moray Street Gravels (MSG) that mainly

comprise fine grain sandy materials, underlay the FBS formation. The MSG was approximately 2.5m thick. The Melbourne Formation (Silurian age siltstone) underlay the MSG and forms the bedrock. A generalised ground condition at the site is shown in Figure 5.1below.

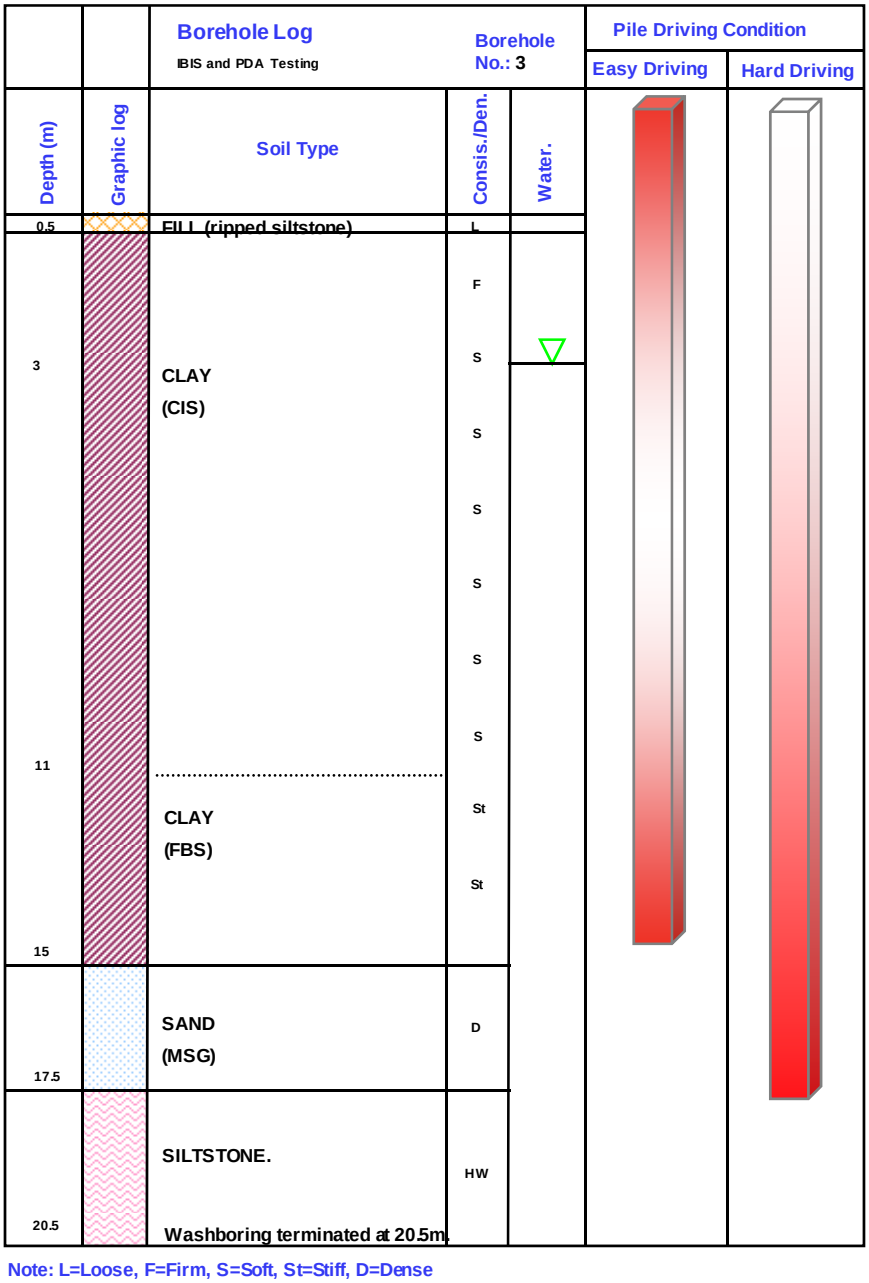

Figure 5.1 Generalised subsurface profile at the test site and the driving conditions analysed

5.3 IBIS Radar

The IBIS radar system is a recently developed non-contact displacement and vibration monitoring device for civil engineering applications. It comes in two configurations such as IBIS-L and IBIS-S. The IBIS-L configuration is used for static terrain deformation monitoring and is mainly used in mining and slope stability applications. The IBIS-S configuration is used for dynamic and static monitoring by remote sensing of structures such as buildings, bridges and telecommunication towers.

The IBIS-S radar unit can simultaneously monitor several points, providing real-time displacement response for each point. The unit operates at frequency of 200Hz giving displacement accuracy of 0.01mm up to range of 1km (IDS, 2008; IDS Australia, 2009). Bernardini *et al*. (2007) conducted a laboratory test and it showed an excellent quality of the displacement measurements and a good operational stability. IDS Australia (2009) performed some real validation tests with accelerometers and LVDTs and the results showed an excellent match with the accelerometers and LVDTs tests.

The main advantage of IBIS-S, apart from the accuracy, range and resolution, is the fact that it can be operated in all weather conditions over very long distances without the need of accessing the target to install sensor or optical targets. However, if required, one or several specific points on a target could be measured by a simple passive radar reflector that can be easily fixed. All the measured quantities are displayed in real time via a computer. Other quantities such as velocity and acceleration records can also be displayed.

It should be emphasised that the IBIS-S unit has never been used in piling application and its use was first suggested by the author and it was suggested to conduct a trial site test. Therefore, the purpose built software used for the test was not well suited for the pile testing to calculate the required parameters.

As a precautionary measure, it was decided to use a passive reflector. Subsequently an L-shape passive reflector was made at RMIT's laboratory and it was bolted to the pile at approximate same vertical distance as the transducers, as shown in Figure 5.2. Continuous readings of all the blows during easy and hard driving test conditions were measured by the IBIS-S radar.

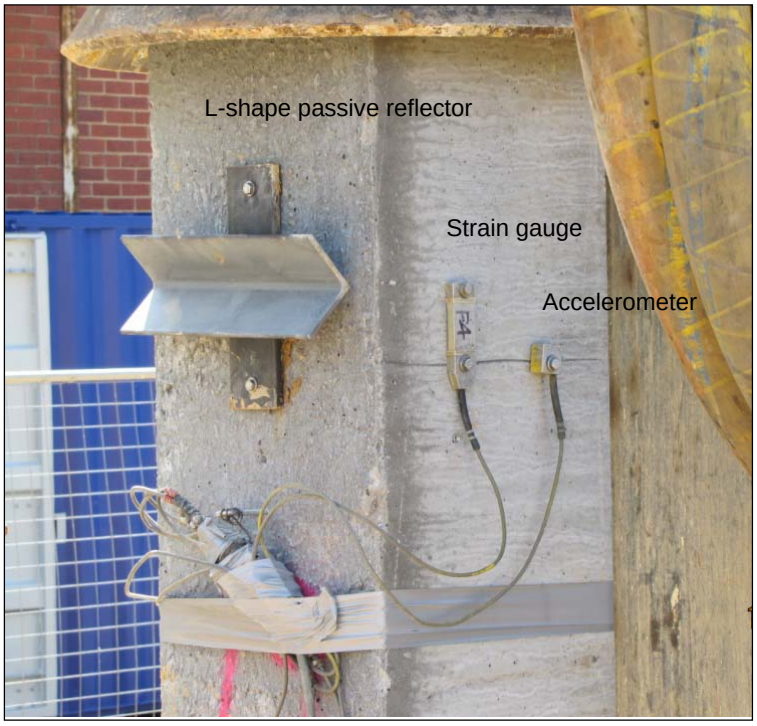

Figure 5.2 A passive reflector target made at RMIT laboratory and PDA transducers

The radar unit operates on a 12V battery and comes with a hard case. It also comes with an adjustable tripod for easy and quick set up as shown in Figure 5.3.

Figure 5.3 IBIS-S radar set-up and real-time monitoring of deformation

5.4 GRLWEAP Analysis

Two GRLWEAP™ analyses were carried out for the easy driving and hard driving conditions based on the soil profile at the site. The standard GRLWEAP™ parameters were input for hammer, cushion and the pile. The soil parameters were based on the in-situ testing results. These cushion, pile and soil parameters were modified till a good match between the GRLWEAP™ program and the PDA results were achieved.

5.5 CAPWAP Analysis

CAPWAP® (**Ca**se **P**ile **W**ave **A**nalysis) is a signal matching or reverse analysis program for piles using the wave equation theory, in which the PDA measured forces and velocities are matched with the calculated forces and velocities based on the Smith model of mass, springs and dashpots. It models the ground reactions (both skin and toe) as elasto-plastic spring and a linear dashpot. In radiation damping model, an additional dashpot is inserted for the toe to take into account the movement of the surrounding soil. Therefore, the soil model can be described by ultimate resistance, quake and viscous damping factor. The total resistance is the sum of the displacement (quake) dependant static resistance and the viscous velocity dependant dynamic resistance.

Smith quake and damping factor are assumed to be soil type dependant and can be estimated by load tests or perform CAPWAP® analysis by using the PDA monitoring data. However, Paikowsky (2004) showed in a large database of load testing that no correlation existed. CAPWAP® analysis is a linear process to determine the best-fit solution and the parameters it produces are not unique. As a result, there have been numerous studies undertaken to understand the correlations of the Smith model parameters (McVay, 1999) and there is still lack of understanding about the factors attributed to these parameters. McVay (1999) provides a comprehensive literature review of the many methods. Liang and Sheng (1992) derived a theoretical expression by using the spherical expansion and punching theory to express the toe/skin quakes and damping.

Normal CAPWAP® analysis procedure involves selecting a blow record and matching the measured and computed force-velocity trace by changing a number of variables, which under a normal case, would be 11 plus the number of shaft resistances that are dependent on the depth of

pile or soil. In cases where additional options are required, such RSA, radiation damping, toe gap and unloading, the variables would, of course, add up even more.

For the CAPWAP® analysis of the PDA results, the author selected and performed two CAPWAP analyses for each driving conditions. Good CAPWAP Match Quality (MQ) of approximately 3.5 was obtained for the records analysed.

Match Quality (MQ) is an objective quality measure of the measured and calculated quantity such as the force and velocity versus time trace. The higher the MQ number, the worst the match is and the lowest possible number is the best match for that particular trace. More details of the calculation of the MQ number can be found in (Pile Dynamics Inc., 2006).

5.6 The CASE Method

Pile Driving Analyser (PDA) is a field tool to measure the acceleration and strain with the aid of strain transducers and accelerometers at approximate depth of two pile diameter below the pile head. This method of field measurement was developed by George Goble of Case Western Reserve University in 1964 as a result of a research project funded by Ohio Department of Transportation and FHWA.

Pile driving resistance and static capacity can be performed by PDA in-built routine from these measurements by simplified closed method solution. This method is known as the Case Method and there are several procedures that were developed for different driving conditions and the measured force velocity traces.

The QULT procedure is the dynamic formula equivalent. It uses the measured maximum energy (EMX) and the maximum displacement (DMX) to calculate the ultimate capacity. This value is not reliant and is only used for reference purposes.

Automatic Resistance procedure is employed in cases where the pile skin friction is very low (RAU) or moderate shaft resistance (RA2). This procedure is best suited for hard driving cases and is independent of the damping parameter.

The Maximum Resistance (RMX) is generally most appropriate when large quakes are observed. This ensures full capacity is mobilised. This method is preferred when velocity doesn't become negative prior to the time at which the travelling wave returns.

The RSP is original procedure that uses the peak forces and a soil (grain size) based empirical damping factor is applied to calculate ultimate capacity. It is very sensitive to the damping factor.

5.7 Field Test Results & Analysis

A tabular summary of the results for the PDA and IBIS-S field testings as well as the CAPWAP signal matching are presented in Table 5.1. Capacity comparison results calculated by the Case, Hiley, Gates and MnDOT methods are also presented in Table 5.1.

The real-time IBIS-S monitoring of the pile head movement is give in Figure 5.4 and Figure 5.5 for the two driving conditions. For the easy-driving condition, the first three blows recorded (BN3 to 5) seem to be invalid and the reasons may be attributed to perhaps target interferences by the hammer hoses and chain used to hold and position the pile.

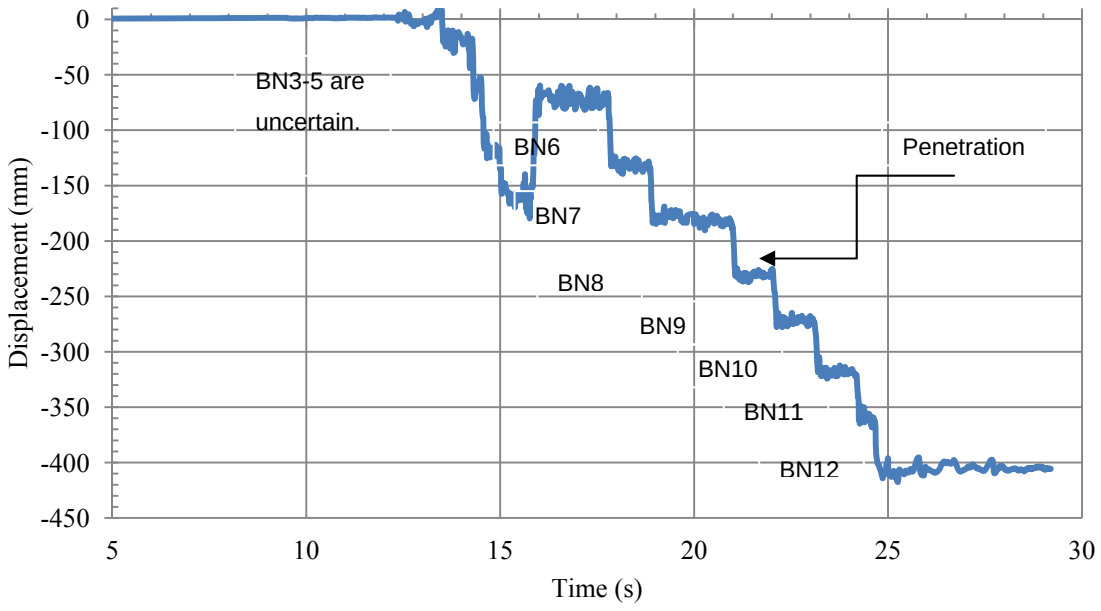

Figure 5.4 IBIS-S Set Measurements for Easy-Driving Condition

Table 5.1 Results of field testing

Blow No. (BN)	Depth	Stroke	Observed set		IBIS-S Measurement			PDA		Max. Energy (EMX)	Max. Force (FMX)	Max. Velocity (VMX)	Case Resistance (RMX)	(RAU)	Capacities						
															QUT	Hiley (set card)	Hiley (Ibis)	Gates	MnDOT	GRLWEAP	CAPWAP
	(m)	(m)	Set (mm)	TC (mm)	Set (mm)	TC (mm)	VMX (m/s)	DMX (mm)	DFN (mm)	(kN-m)	(kN)	(m/s)	(kN)	(kN)	(kN)	(kN)	(kN)	(kN)	(kN)	(kN)	(kN)
3	15	0.3	38.2	0	-	-	-	41.00	38.9	17.016	1852	1.93	283	-	426	445	-	-	-	-	300
4	15	0.3	38.2	0	-	-	-	41.50	40.7	17.115	1876	1.94	295	-	417	448	-	-	-	-	-
5	15	0.3	38.2	0	-	-	-	47.50	45	20.081	2029	2.13	250	-	433	526	-	-	-	-	-
6	15	0.3	38.2	0	43.58	0	1.594	44.70	41.8	19.186	1995	2.09	290	-	444	502	440	471	583	262	-
7	15	0.3	38.2	0	40.3	0	1.842	45.80	44.3	19.131	1969	2.06	281	-	425	501	475	491	609	285	345
8	15	0.3	38.2	0	47.55	0	1.835	43.90	42.8	18.761	1991	2.06	314	-	433	491	395	443	554	235	-
9	15	0.3	38.2	0	38.49	0	1.732	42.70	42.3	18.48	1971	2.02	327	-	435	484	480	495	624	299	-
10	15	0.3	38.2	0	40.75	0	1.633	41.70	41.7	18.247	1947	2.01	337	-	437	478	448	477	605	282	-
11	15	0.3	38.2	0	37.74	0	1.862	40.30	39.7	17.861	1901	1.99	348	-	447	468	473	491	631	305	-
12	15	0.3	38.2	0	46.79	0	1.741	39.70	36.9	17.815	1958	1.99	353	-	465	466	381	435	560	240	-
13	18	0.7	2.4	16	1.82	16.02	2.866	18.70	0.5	36.445	3431	2.58	3387	2615	3806	3504	3708	1818	2496	3276	-
14	18	0.7	2.4	16	2.24	17.8	2.642	19.30	3.3	38.529	3507	2.67	3400	2637	3409	3705	3459	1791	2391	3059	3038
15	18	0.7	2.4	16	1.54	18.43	2.617	18.90	4.2	37.066	3468	2.63	3397	2584	3202	3564	3446	1896	2580	3450	-
16	18	0.7	2.4	16	1.47	20.84	2.576	18.70	3.3	36.5	3418	2.57	3393	2614	3324	3510	3070	1898	2603	3498	-
17	18	0.7	2.4	16	2.31	20.51	2.613	18.70	2.5	36.742	3459	2.60	3423	2653	3469	3533	2924	1737	2375	3027	-
18	18	0.7	2.4	16	2.3	20.73	2.597	18.70	1.8	36.715	3445	2.59	3432	2643	3581	3530	2899	1738	2377	3031	3200
19	18	0.7	2.4	16	2.3	20.73	2.571	18.70	2.9	36.375	3395	2.55	3380	2657	3367	3498	2872	1730	2377	3031	-

For the hard-driving condition, all the seven blows were captured and are presented in Figure 5.5. The pile head velocity and acceleration records can also be obtained from the Ibis-s in-house software or can be calculated from the raw data by other suitable programs or by simple differentiation technique. The transferred energy to the pile can be calculated from the impact velocity records because the transferred energy to the pile is directly dependant on the hammer impact velocity.

The author performed the CAPWAP testing on two of the PDA records for the easy driving and two for the hard driving conditions. The records from the blows were selected on the basis of energy, set and the overall quality of the records. The results together with the damping and quake parameters computed by the CAPWAP are given in Table 5.2. The signal matching quality results are shown in Figure 5.6 and Figure 5.7.

Table 5.2 Soil parameters derived from signal matching CAPWAP

BN	Depth	Stroke	Computed		Shaft			Toe			Total Resist.
			Set	EMX	Damp	Quake	Resist	Damp	Quake	Resist	
			(mm)	(kNm)	(-)	(mm)	(kN)	(-)	(mm)	(kN)	(kN)
3	15	0.3	42.4	16.94	0.42	2.5	161.6	0.15	40.2	138.4	300.00
7	15	0.3	40.69	18.66	0.661	1.62	139.5	0.279	26.25	205.5	345.00
14	18	0.7	2.92	38.38	0.168	6.21	1788	0.229	9.78	1250	3038.0
18	18	0.7	2.833	36.84	0.085	4.84	1037.8	0.455	5.55	2162.2	3200.0

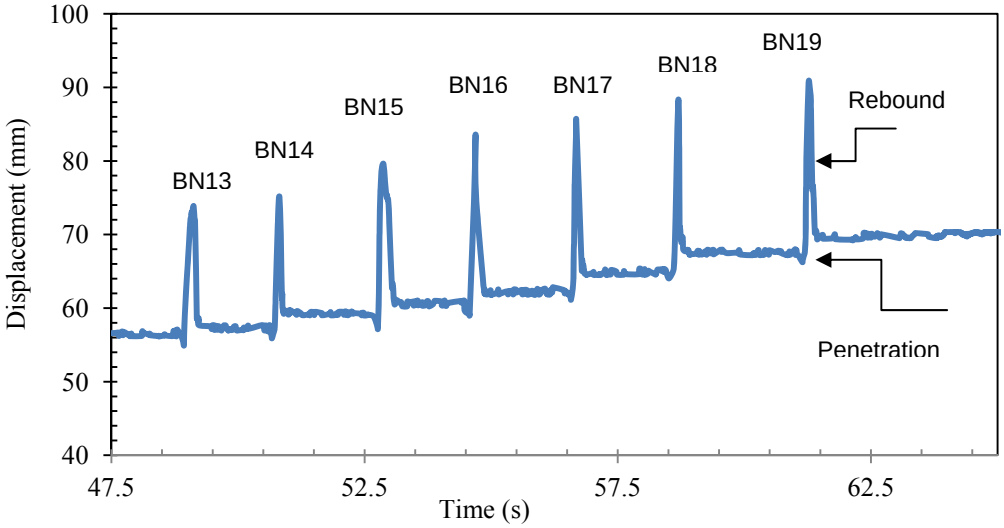

Figure 5.5 IBIS-S Set Measurements for Hard-Driving Condition

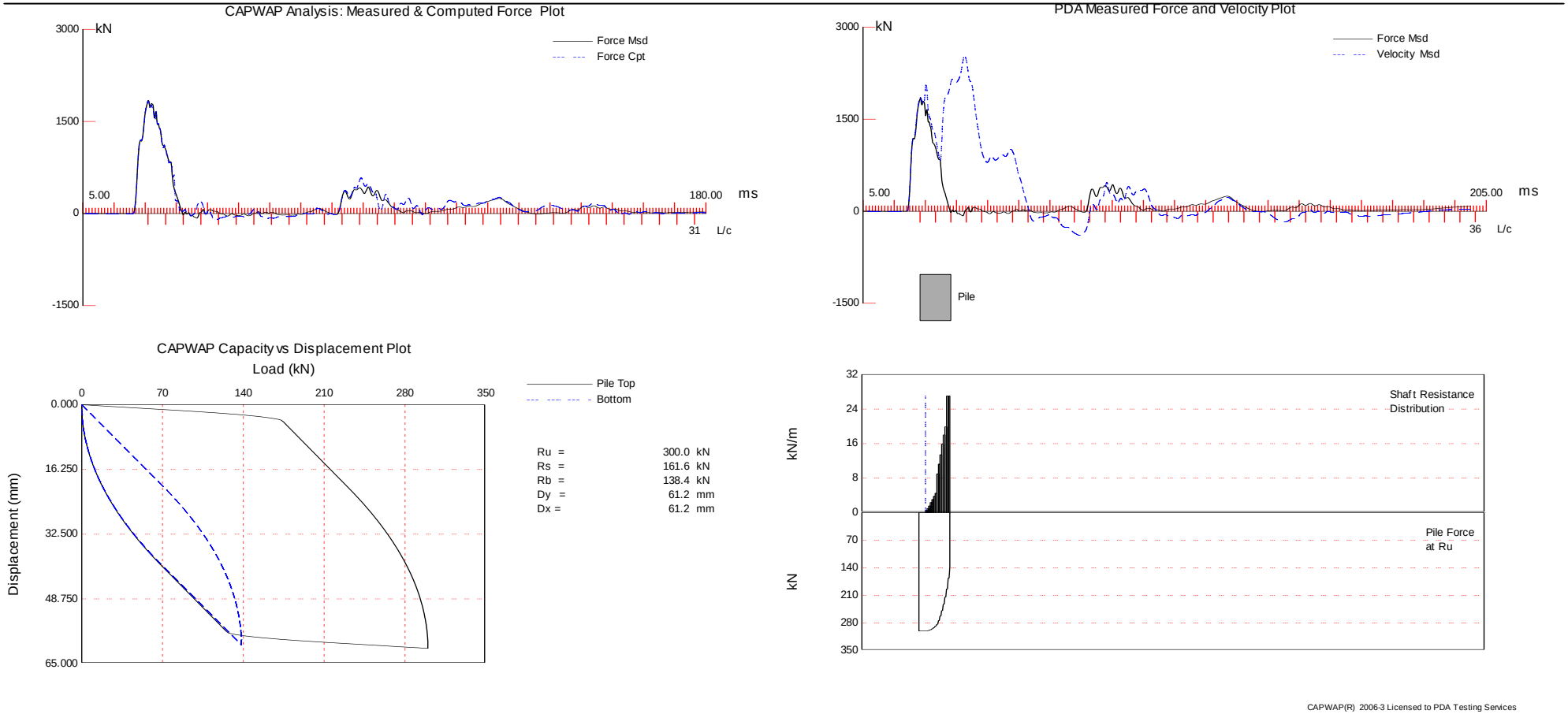

Figure 5.6 Match Quality and results of CAPWAP Analysis for Easy Driving Condition

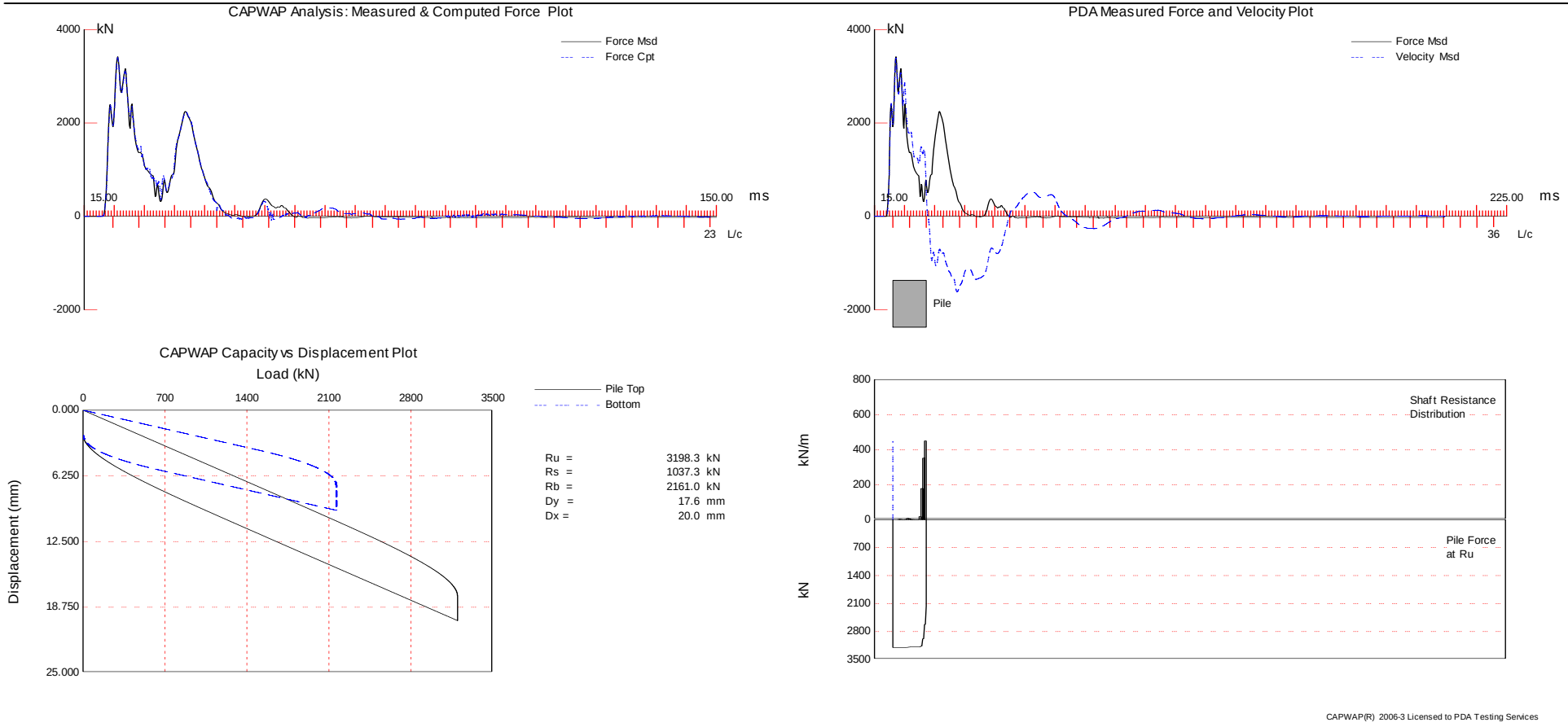

Figure 5.7 Match Quality and results of CAPWAP Analysis for Hard Driving Condition

GRLWEAP analyses were also performed for the easy and hard driving conditions and the Bearing Graph showing the ultimate capacity versus set is presented in Figure 5.8.

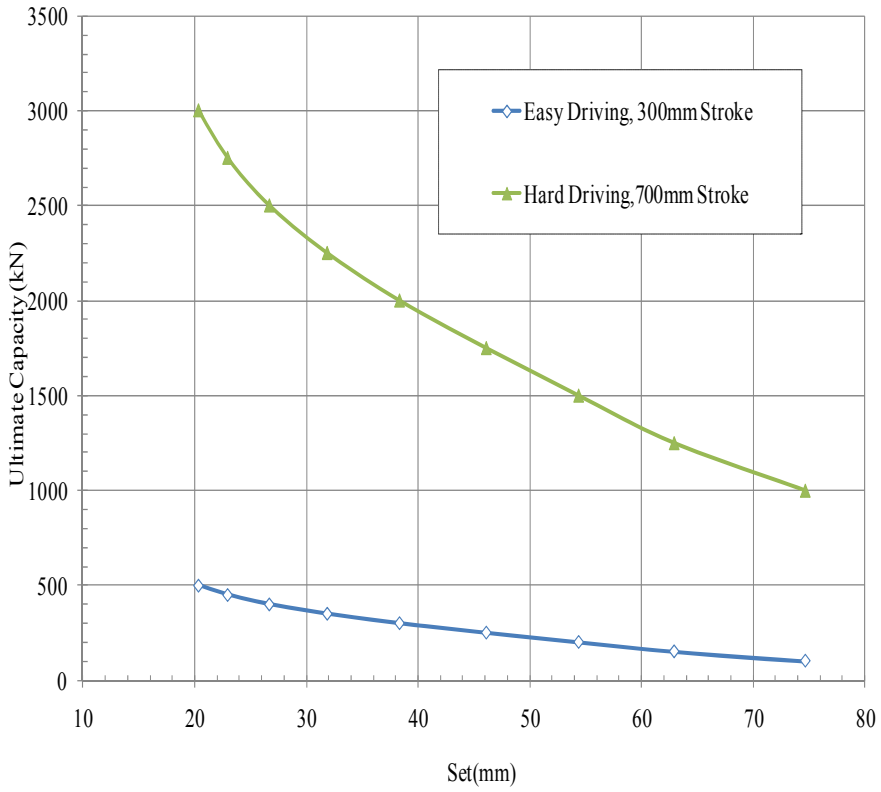

Figure 5.8 GRLWEAP Bearing Graph for Banut6T hammer

The GRLWEAP bearing graph shown in Figure 5.8 is only for single stroke. However, a more general bearing graph can also be established for any particular hammer. The Figure 5.9 and Figure 5.10 show the results of GRLWEAP analysis at various strokes for the Banut 6t hammer.

The ratios of the Hiley, GRLWEAP and the CAPWAP capacities are also plotted in Figure 5.9 and Figure 5.10. From Figure 5.9 it can be seen that the capacity ratio of GRLWEAP and the CAPWAP for the easy-driving condition is about 0.9, which indicates that, although the test results are consistent, GRLWEAP slightly under predicts capacities in easy-driving conditions. However, in hard driving conditions the ratios are nearly one, indicating the results are consistent and in good agreement.

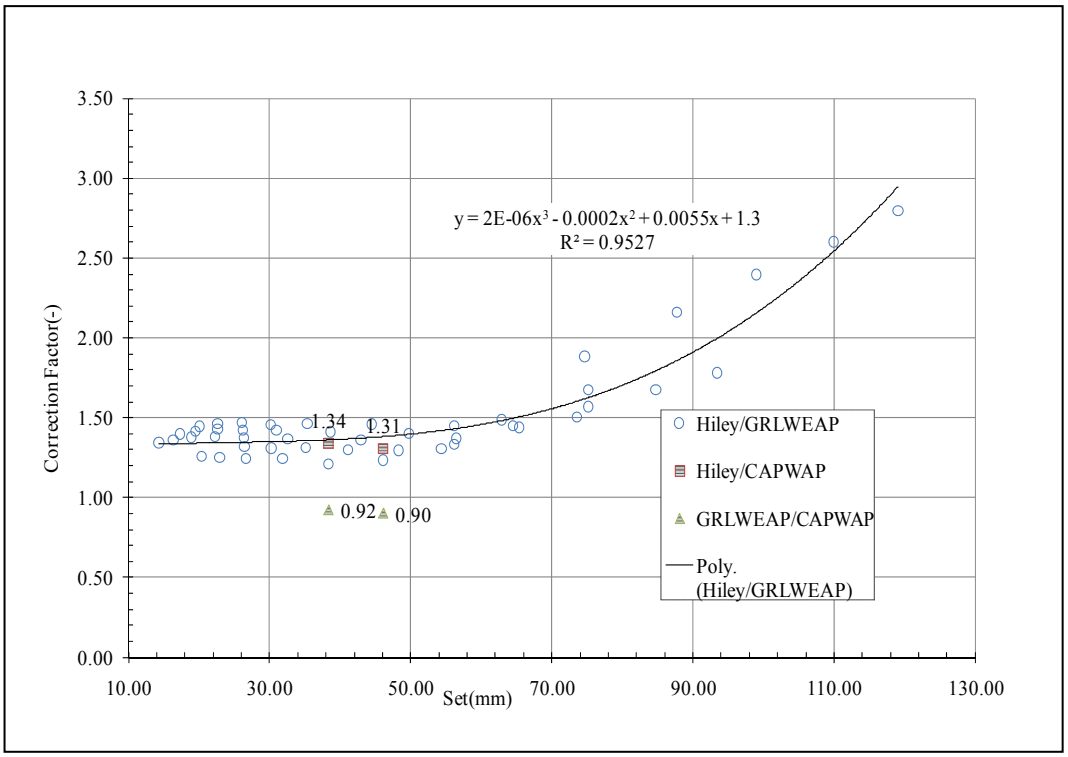

Figure 5.9 GRLWEAP Analysis for easy-driving condition. Hiley Correction Factor vs. Set for Banut6T hammer, 350mm precast pile – Easy driving condition

Similarly, the ratio of Hiley to GRLWEAP (or CAPWAP) is approximately 1.35 which indicates that, irrespective of the driving conditions, the Hiley formula over predicts the capacity by this factor and that this over estimation is consistent.

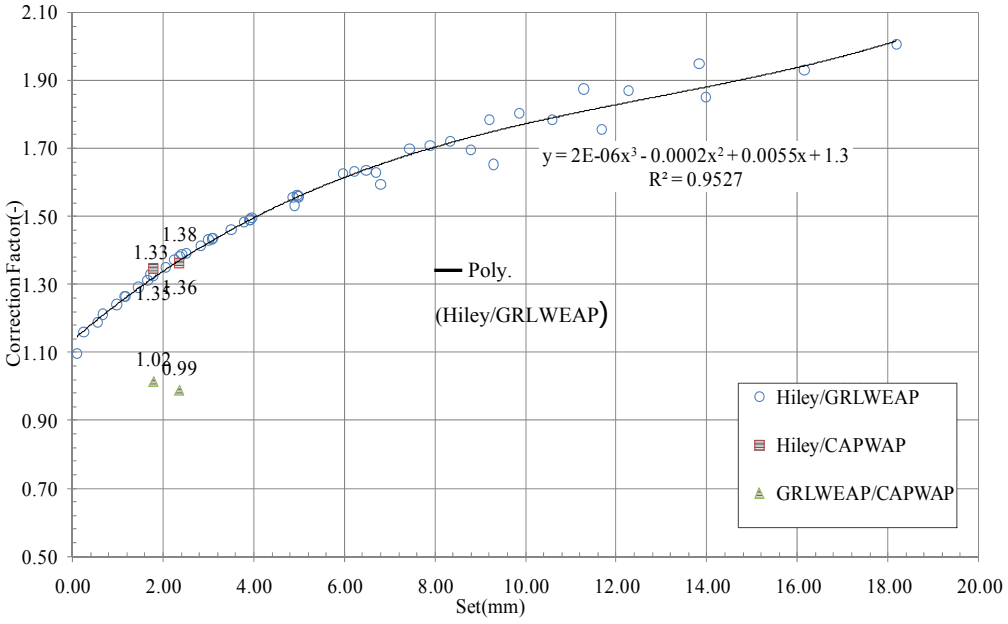

Figure 5.10 GRLWEAP Analysis for hard-driving condition. Hiley Correction Factor vs. Set for Banut6T hammer, 350 precast pile – Hard driving condition

The capacities calculated by the various methods such as the CAPWAP, Gates, GRLWEAP, Hiley and MnDOT methods are plotted and shown in Figure 5.11. The results show that the Hiley formula pile capacity predictions are very good compared to the CAPWAP and consistent throughout the blow records. On the other hand, Gates and MnDOT perform poorly for the easy driving condition, but compare reasonably well in hard driving conditions. It should be mentioned that the Hiley capacities in Figure 5.11are not factored.

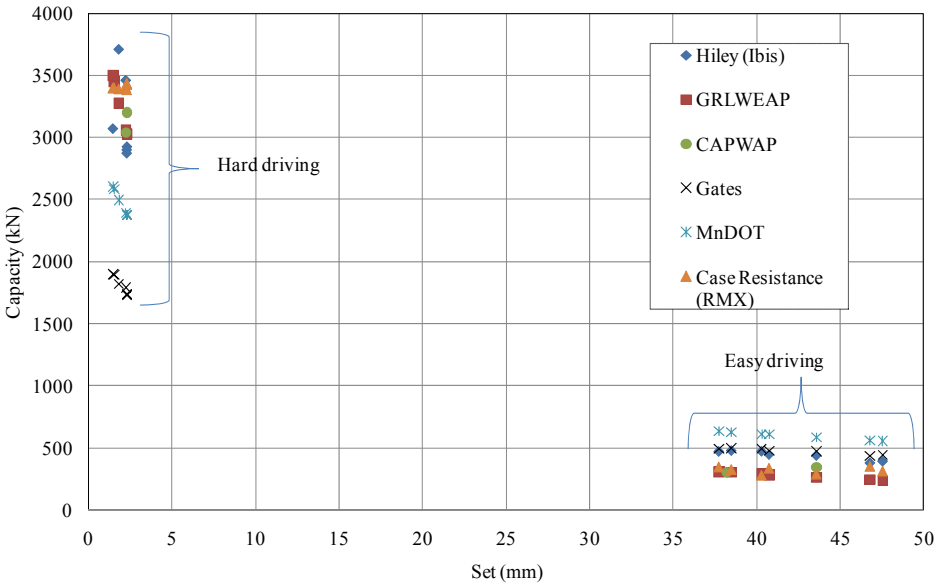

Figure 5.11 Overall Comparisons of Capacities by CAPWAP, Hiley, Gates, GRLWEAP and MnDOT Methods for the Easy and Hard Driving Conditions

The performance of the Banut hammer for the two driving conditions is shown in Figure 5.12. It can be seen that the hammer is very efficient and that the efficiency decreases slightly with increasing velocity.

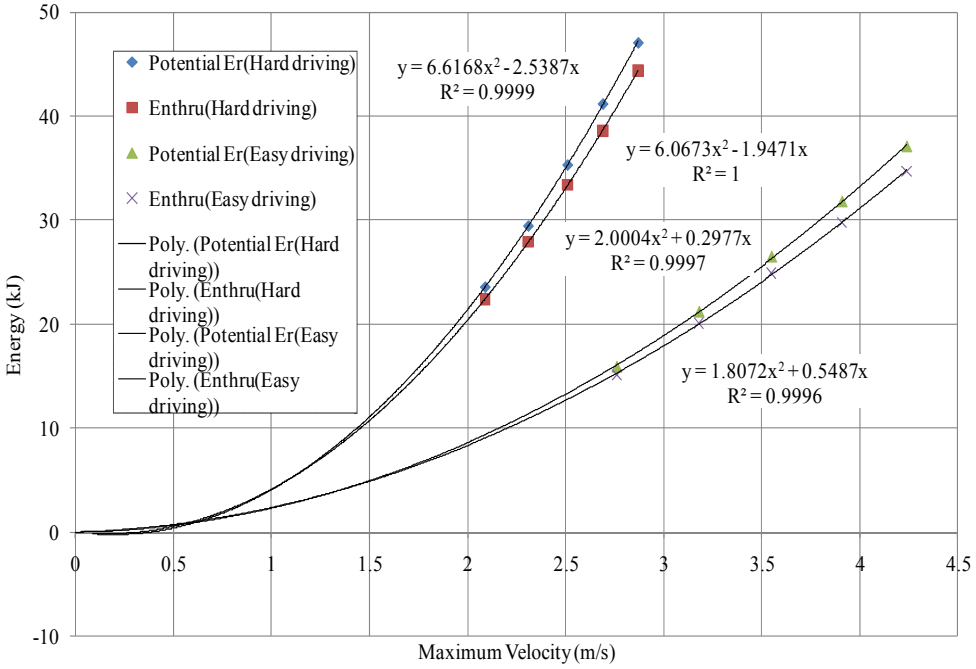

Figure 5.12 GRLWEAP Analysis. Hammer performance and efficiency for Banut 6t

The Hiley Correction Factor shown Table 5.3 are calculated from the field measurements. The factors are based on the GRLWEAP and Hiley capacity predictions for the set measured by IBIS-s. It shows that it slightly under predicts capacity compared to the CAPWAP capacity in easy-driving condition. It is interesting to note that the Hiley factor of about 1.35 is consistent in all conditions compared to both the CAPWAP and GRLWEAP capacities, with the exception of hard driving where the correction factor is about one which indicates that the Hiley capacity is same as the CAPWAP capacity prediction.

Table 5.3 Correction factor calculations based on the field set measurement by Ibis-s

	Hiley Correction Factor (HCF)		
	GRLWEAP Analysis	IBIS-S	
	(GRLWEAP/CAPWAP)	(Hiley/CAPWAP)	(Hiley/GRLWEAP)
Easy Driving	0.83	1.38	1.32-1.33
Hard Driving	0.95-1.01	0.91-1.14	1.31

5.8 Extended Application of IBIS-S

As mentioned earlier, the CAPWAP signal matching program does not produce a unique solution due to the many unknown empirical parameters. Some of the parameters are damping factors, quakes, toe gap and radiation damping. Therefore, due to the high resolution and accuracy of the IBIS-S unit, it is possible that some of these empirical parameters could be directly evaluated. Additionally, it is possible to evaluate the integrity of driven piles from the velocity and acceleration records, especially if a defect has been detected and the need to proof test the untested piles.

Another very useful application of the IBIS-S radar, due to its multi-target measurement capability, is in the assessment of pile mechanical joints. The current VicRoads standard only requires visual inspection under many repetitive hammer blows. In some situations PDA dynamic testing is done concurrently and the results are checked with CAPWAP analysis to ensure the movement complies with a given standard.

CHAPTER 6

6 CONCLUSION

6.1 Summary

The pile driving formulas were derived based on the Newtonian theory of impact. In the past it has been known that the dynamic formula are not very accurate and it consistently over estimate pile capacities. This is particularly true for the Hiley formula.

The reason for this poor performance can be attributed to the fact that often the hammer energy delivered to a pile is estimated rather than determined on case by case bases. It has been shown that this energy can vary enormously from pile to pile and assuming energy to be constant for a given hammer is incorrect. The second reason for the poor results of the dynamic formula is the set and temporary compressions are not determined accurately in the field, and hence lead to erroneous capacity results. The third reason, and the most important, is that the dynamic formula does not account for the dynamic effects, which is similar to the damping factors in the wave equation treatments. Not to mention the fact that in almost all researches, the capacity comparison between dynamic formula and the static testing is deemed to be incorrect because of the time difference of testing and the phenomenon of setup – capacity gain over time.

In this research all these factors have been addressed and tests were undertaken that showed the dynamic formula can be used with greater confidence and can provide comparable results to the wave equation method. Chapter 2 presents the application of dynamic pile testing methods. Chapter 3 compiles a collection of

results on the performance of pile driving formula reported in the literature. Chapter 4 includes a comprehensive numerical analysis of 1944 systematic cases by wave-equation based software called GRLWEAP and factors were calculated for each case to be used in the dynamic formula to account for the dynamic effects. Chapter 5 presents the results of field study as well as measurement results using radar equipment proposed in this research. Further analysis results using CAPWAP and GRLWEAP programs were carried out and a comparison of the results are presented.

The field test data gathered during field test of IBIS-S radar provide an excellent basis for the evaluation of the Hiley formula in prediction of pile capacity for all driving conditions. A comparison of the predictions obtained from the pile driving formulae with the higher order methods such the CAPWAP and GRLWEAP wave-equation analysis showed that the results are very consistent and accurate.

The present investigation thus demonstrates that the pile capacity prediction by the Hiley formula are very reliable provided the variation in the energy input can be accurately measured and allowed for in the calculations. Since under normal pile driving conditions, variability in the driving system and the energies delivered to the pile exists, it is important to account for this variability so that the driving formula can be used with greater confidence.

The results of the correlations between the wave equation and the dynamic formulas are both surprising and very informative. As noted in chapter 4, Table 4.13 and Table 4.14, the ratio of the resistance predicted by the Hiley formula and the wave equation is rather constant. This would indicate that at least for these cases the Hiley formula the consistency is quite surprising, especially considering the amount of research which has been published condemning the method. This is not to imply that the dynamic formulas are without proponent.

In the past the poor quality of the results obtained by pile driving formula was partly related to the erroneous estimate of the driving energy. It is now possible, with the aid of new technology, to measure with high accuracy not only the energy delivered to the pile by each blow, but also the full pile displacement records.

A correction factor to allow for the dynamic effects, similar to the Case damping factor, was back-calculated from the CAPWAP and GRLWEAP analysis. It showed that the correction factor is quite consistent and can be developed for a variety of ground conditions, hammers and pile types. This will allow for the dynamic formula, particularly the Hiley formula to be used with greater accuracy comparable to the wave equation analysis.

More general conclusion of the study in this paper can be as follows:

- The wave-equation analysis only describes the energy transfer mechanism from the hammer to the pile toe in a systematic and accurate fashion and if the dynamic formulae are modified to account for the energy losses, then the dynamic formulae should technically fulfil the same function.
- The dynamic formulae, which ignore the dynamic effects, need to be accounted for in the formulae.
- The energy delivered to the pile and its set measurements need to be accurately determined in order to render the dynamic formulae reliable.
- Create a comprehensive database with driving records for various soil conditions, driving systems as well as different piles and establish driving formula correction factors against the database.
- The correction factors can be established from GRLWEAP and CAPWAP analysis as well as static testing results.

6.2 Future Research

US department of transport (FHWA, FDOT, MnDOT, OSDOT, TRB and WSDOT) are still heavily involved in research into pile driving formula. MnDOT recently published a modified version of the Gates formula, while other works are still ongoing. The current emphasis is to create comprehensive pile databases based on the pile load tests and dynamic testing and to calibrate various pile driving formulae against the database in order to establish the most suitable formula.

Further investigation is required to determine the extent and the influence of different damping factors and cushion materials. The investigation of this zone can provide insight into the energy transfer into the pile.

Further study is required to better understand the distribution of the resistance around and at the base of the pile. Also the effects of pore water pressure and time on the resistance of pile will also need to be investigated.

Appendix A

Stress Wave Theory in Solid Media

Derivation of Wave Equation

A slender pile with uniform cross-section will transmit a pulse or wave down the pile when mechanically impacted by a hammer on the top. It is assumed that because of the much lower stiffness of the surrounding soil, the wave pulse can only travel along the pile axis. Given the distance z measured from the pile head down, let's consider an infinitesimal pile element with length dz bounded by two sections

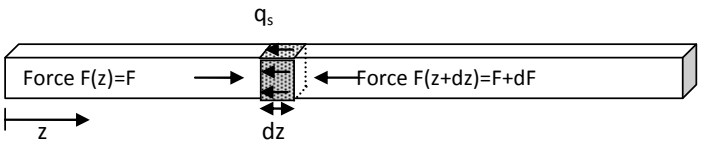

The element is subjected to an external (soil) shear stress q_s applied along the pile shaft. Hence applying Newton's second law to this infinitesimal element yields

$$F-(F+dF)-q_s a_s dz=\rho A dz\frac{\partial^2 w}{\partial t^2} \qquad \text{A.1}$$

Where a_s is the surface area, ρ is mass density of pile and w (z, t) is the axial displacement of cross section at distance z and time t.

Rearrangement and substitution of the elastic stress-strain equation σ=Eε results in the governing differential equation for the pile problem

$$E_p A_p\frac{\partial^2 w}{\partial z^2}-q_s a_s=\rho A_p\frac{\partial^2 w}{\partial t^2} \qquad \text{A.2}$$

Assuming that there is no external force acting on the pile (q_s=0), the above equation can be rewritten in the familiar one-dimensional wave equation

$$\frac{\partial^2 \mathrm{w}}{\partial \mathrm{t}^2}-\mathrm{c}^2\frac{\partial^2 \mathrm{w}}{\partial \mathrm{z}^2}=0,\ \text{where } \mathrm{c}=\sqrt{\mathrm{E_p}/\rho} \qquad \text{A.3}$$

Solution and Interpretation of Wave Equation

The following is an excerpt from Timoshenko (1951) and Verruijt (2005), which explain the interpretation of the stress-wave propagation equation applicable to dynamically loaded piles.

Sudden loading or displacement caused by a force on an elastic solid media generates stress waves that radiates from the impact point in all directions with finite velocities of propagation. Usually there is more than one type of wave with more than one wave velocity. The simplest representation of wave motion in special cases, such as in piles, can be approximated with the one-dimensional hyperbolic partial differential equation in the form shown above.

The one-dimensional wave equation is easily solvable by the various mathematical methods such as Laplace, Separation of Variables and Method of Characteristics. It can be shown by simple substitution that any function in the form of f(z-ct) is a solution of the partial differential equation. By the same token, g(z+ct) is also a solution and because the partial different general solution can be given by

$$w(z,t) = f(z - ct) + g(z + ct) \qquad \text{A.4}$$

The first and second terms of the general solution in equation A.4 represent stress wave travelling in the downward and upward directions, respectively, with constant speed c.

When soil friction resistances are introduced into the partial differential equation, then the solution is neither simple nor practical, except for very simple cases.

In the case where there is ground shear resistance, the solution for above differential equation is carried out by numerical finite difference method and in fact the Smith's approximation in itself turns out to be essentially a finite difference technique.

An interesting aspect of the wave propagation in solid media is reflection and transmission of waves at the surface of discontinuity or change in material

property. Hence, essentially two boundary conditions of interest in pile dynamic are waves approaching free and fixed ends.

When a pulse approaches a free end, there is not inertial mass to overcome, and the energy cannot continue to travel, instead it reflects back. At the exact moment of reflection, the velocity doubles and a compressive wave is reflected as a similar tension wave, and vice versa.

On the other hand, when a pulse approaches a fixed end, the section remains immovable and the wave is reflected without any change.

CAPWAP Notation

The notation of CAPWAP parameters is defined in the CAPWAP manual 2006 (PDI, 2006) and the relevant section has been reproduced.

BT Toe radiation damping. This is the energy radiated by surrounding soil as a result of pile motion A radiation damping model by introducing additional soil mass (MS) and dashpots to represent soil motion to obtain better correlation with static load testing.

CS Shaft quake multiplier. This is used to make unloading lower than the loading quake. The default value of 1 makes loading and unloading equal. It normally varies between 0.1 and 1.0.

CT Toe quake multiplier. Same as CS.

JS Shaft damping factor (case). It is a non-dimensional factor that is independent of the static resistance.

JT Toe damping factor (case)

LS Shaft reloading.

LT Toe reloading

MS Shaft radiation mass. This value of this is dependent on the size of pile. The recommended default value corresponds to a cylinder of soil surrounding the pile and being roughly 0.3m thick.

MT Toe radiation mass. Also see MS.

OP Toe damping type option (0=linear viscous, 1=Smith, 2=combination). The Smith calculation yields better signal match. OP=2 is most frequently used to improve the match around the 2L/c i.e. return wave after impact.

PL Toe plug. This is the mass of soil sticking or trapped underneath the pile causing inertial force thus making the pile appear longer.

PS Shaft plug

QS Shaft quake. Quake or displacement is none zero value with maximum being 10mm and most commonly around 2.5 to 5.0mm.

QT Toe quake. Maximum value of 25mm or more.

SO Shaft damping type option (0=linear viscous, 1=Smith, 2=combination). Also see OP.

SL Shaft radiation damping. Also see BT.

SS Smith shaft damping. The traditional Smith damping that is a velocity and static resistance. However, it is more convenient to use linear viscous coefficients rather than the Smith values so that they can be assigned independent from the magnitude of the static resistance.

ST Smith toe damping.

TG Toe gap. A gap beneath a pile toe driven in very hard end bearing. It exists prior to rebound as it starts to move down again without any resistance.

UN Shaft unloading multiplier. It varies between 0 and 1; with UN=0 there is no downward directed shaft resistance during pile rebound; hence it is applicable in easy driving condition.

3. THE CAPWAP SOIL MODEL

3.1 Basic Relationships

The displacement and velocity of each pile segment relative to the soil (Note: in the Smith approach, the soil surrounding the soil-pile interface is considered fixed; an extension to that fixed soil assumption is CAPWAP's radiation damping model which gives the soil one degree of freedom) is the basis for computing the soil resistance forces. The soil model consists of an elasto-plastic spring and a linear dashpot (Figure 3.1.1) described by three parameters: ultimate resistance R_{ui}, quake q_i, and viscous damping factor J_i. The total static bearing capacity R_{ut} is the sum of all R_{ui}. The total (static plus dynamic) resistance force R_i at segment i is computed from

$$R_i = R_{si} + R_{di} \qquad (3.1)$$

where R_{si} and R_{di} are the time varying static and dynamic soil resistance forces at segment i.

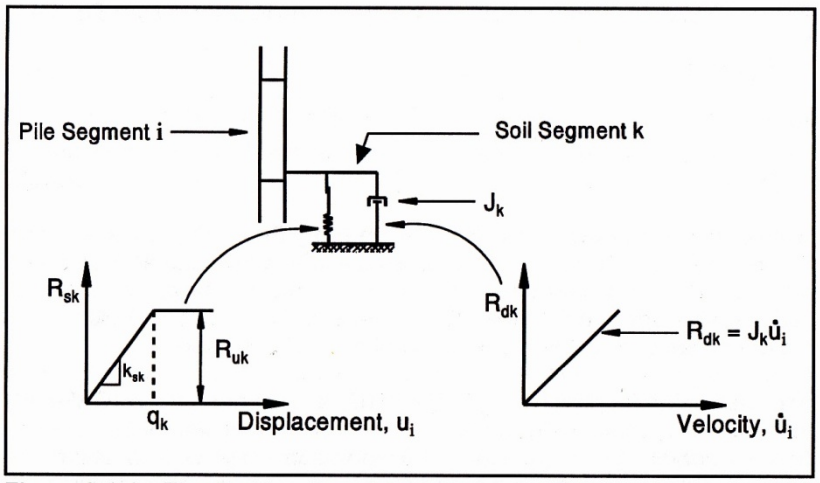

Figure 3.1.1: The Smith soil resistance model - Viscous damping model instead of a strict Smith damping is shown

Soil resistance forces may act at each embedded pile segment. However, since the pile segments are usually rather short and because of the limited resolution of the analysis approach, it may be sufficient to have one soil resistance element at the bottom pile segment for end bearing and one shaft resistance element at every second pile segment for the portion of pile embedded in the soil. Thus, the number of pile segments N_p may be greater than or equal to the number of shaft resistance elements N_s.

Consider a soil element k at pile segment i. Knowing pile segment velocity $\dot{u}_i$, and displacement u_i, and a viscous damping factor J_k, the k-th resistance force becomes

$$R_k = R_{sk} + J_k(\dot{u}_i) \tag{3.2}$$

with the static resistance represented by

$$R_{sk} = k_{sk}\, u_i \tag{3.3}$$

and

$$R_{nk} \le R_{sk} \le R_{uk} \tag{3.4}$$

R_{uk} and R_{nk} are ultimate soil resistance at segment k when the pile is moving downwards (positively) and upwards (negatively), respectively.

3.2 Unloading and Reloading

The lower static resistance bound (or negative uplift capacity[1]) in Eq. 3.4 is

$$R_{nk} = -U_n\, R_{uk} \tag{3.5}$$

with

$$0 \le U_n \le 1 \tag{3.6}$$

Note that U_n is always zero for **end bearing** (no tensile end bearing). Smith's static **shaft** resistance wave equation model assumes that during rebound the uplift capacity is of the same magnitude as the ultimate compressive shaft resistance. Extensive experience in CAPWAP signal matching has shown this hypothesis to be usually not true.

The shaft unloading level multiplier U_n (**"UN"** is the corresponding CAPWAP input quantity) varies between 0 and 1, inclusively (see Figure 3.2.1). U_n = 1 corresponds to the original Smith approach while U_n = 0 allows no downward directed shaft resistance during pile rebound. U_n is assumed to be constant along the shaft. In easy driving, U_n has no effect (no rebound). In hard driving, U_n may be chosen as low as zero. The effect of U_n is most easily observed in the later portion of the record. Lower values raise the later portion of the computed curve because they allow for less negative shaft resistance. Note that Residual Stress Analyses will not be meaningful for very low UN values since residual stresses develop in a pile only in the

---

[1] R_{nk} has nothing to do with the geotechnical term "negative skin friction" which occurs when the upper soil layers settle more than the pile thereby causing a downward directed shear force on the pile surface.

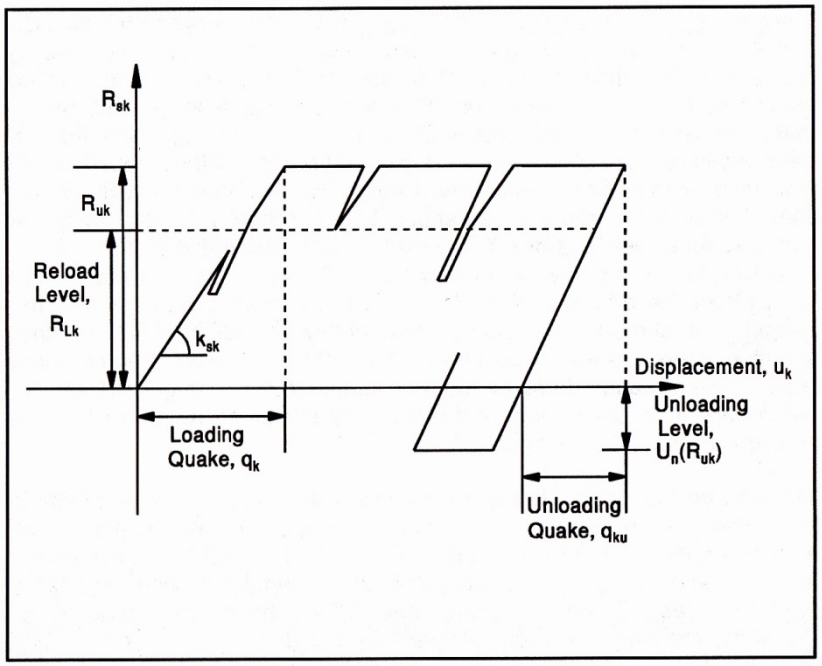

Figure 3.2.1: Static shaft resistance

presence of downward directed shaft resistance values and those are only possible if UN > 0.

The quantity, k_{sk}, in Eq. 3.3 is the soil stiffness of the k-th resistance. For positive (downward) velocities

$$k_{sk} = R_{uk} / q_k \tag{3.7}$$

with q_k being the actual loading quake (**QS** for shaft and **QT** for toe in CAPWAP). Quakes physically and numerically cannot be zero. Under extreme circumstances their maxima may be 1 inch (25 mm) or more on the toe and .3 inches (10 mm) on the shaft. However, most commonly they are in the neighborhood of .1 to .2 inches (2.5 to 5 mm) for the shaft.

For negative (upward, rebound) pile velocities, a modified or unloading quake is calculated.

$$q_{km} = q_k \, c_k \tag{3.8}$$

and the stiffness is then

$$k_{sk} = R_{uk}/q_{km} \tag{3.9}$$

The Skin or Toe Unloading Quake Multipliers (CAPWAP input quantities **CS** and **CT**) are used to assign unloading quakes lower than the loading quakes. The multiplier default is 1.0 which makes loading and unloading quakes equal. The same value **CS** is applied to all skin quakes. A low unloading quake causes a quick shedding of load during rebound and therefore lowers the computed force record at the end of the blow. To avoid zero unloading quakes, which are a numerical impossibility, **CS** and **CT** cannot be zero, in fact they rarely should be less than 0.1. Occasionally, the match requires that **CS** or **CT** are set to values greater than 1.0. This is plausible, for example, when the toe gap, TG (see below), is greater than 0; in effect the quake at the pile toe is then greater than **QT** and the unloading quake can then also be reasonably greater than **QT**. Another situation where it is reasonable that **CS** and **CT** are chosen greater than 1 is when the radiation damping model is employed. The larger **CS** and **CT** values are then compensating for the very simplified model of the soil surrounding the pile-soil interface.

The reloading option specifies the loading level (**LS** or **LT** can be modified in the **Overall Parameter** input section) in a second or later loading cycle. In other words: "Below the reloading level, R_{LK}, the soil stiffness equals the soil's unloading stiffness in a second or later loading cycle within the same blow." Figures 3.2.1 and 3.2.2 illustrates for the shaft and toe, respectively, the static resistance versus relative pile soil displacement model. The reloading levels are normally set to 1.0 and rarely need adjustment. They have little physical meaning and affect only the late record portion. If that portion of the record is difficult to match then **LS** values of 0 or -1 or **LT** = 0 may first be tried before further refinements are attempted.

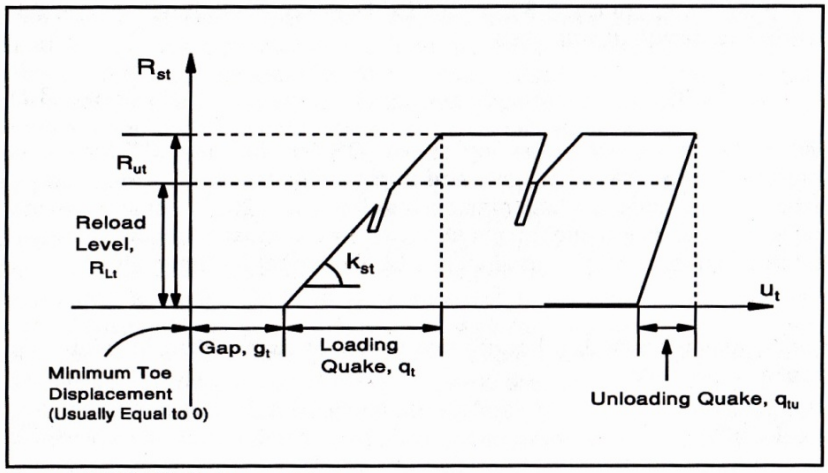

Figure 3.2.2: Static toe resistance

3.3 Toe Model Extension: Gap

For piles on a very hard end bearing layer, a gap, g_t, (**TG** in the CAPWAP program) beneath the pile toe sometimes exists just before the pile toe starts to move downward. As the pile toe moves through the gap distance, the static toe resistance remains zero and increases only after the toe displacement exceeds the gap. For full resistance activation, the sum of the toe gap plus toe quake must be less than the maximum pile toe displacement of the blow. The static soil resistance, subject to the gap g_t, is therefore

$$R_{sk} = k_{sk} (u_i - g_t) \text{ for } g_t < u_i \tag{3.10}$$

where

$$\begin{aligned} R_{sk} &= 0 \quad \text{and} \quad u_i < g_t \\ R_{sk} &= R_{uk} \quad \text{and} \quad u_i > g_t = g_i \end{aligned} \tag{3.11}$$

where k is equal to $N_s + 1$ (pile toe) and i equals N_p (pile bottom segment) R_{sk} is zero for displacements less than the gap and equal to R_{uk} for displacements greater than the sum of gap and toe quake. During unloading, the toe resistance follows the unloading quake. In general wave equation analyses and therefore also in the CAPWAP output, the gap is added to the toe quake. The soil gap is not a soil property but rather a randomly occurring pile toe movement, occurring during rebound. Figure 3.2.2 illustrates the static toe resistance versus pile bottom displacement.

3.4 Plugs (Acceleration Dependent Resistance)

This inertia force may be caused by the mass of the soil sticking to the pile or trapped underneath (displacement piles) or within the pile bottom (open ended pipes). In effect, the soil mass moving with the pile causes a compressive reflection and, if located at the toe, makes the pile appear longer (the toe reflection occurs later if such a mass exists). The effect of the soil mass at the toe could also be modeled by either a pile length increase or a wave speed decrease. A pile impedance increase can also take the place of the soil plug input. However, while the mass effect of the plug input modifies the apparent pile wave speed, an impedance variation does not cause that effect.

The soil mass, m_p, (**PS** and **PL** for the shaft and toe, respectively, in the CAPWAP Main Input section) which might exert an external resistance force (R_{mi}) at time j, acting against a pile segment, i, or at the pile bottom, is

$$R_{mi,\,j} = m_p (\dot{u}_{i,\,j} - \dot{u}_{i,\,j-1}) / \Delta t \tag{3.12}$$

where $\dot{u}_{i,\,j}$ is the pile bottom velocity at time increment j and Δt is the computational time increment. Obviously, the velocity difference between two time steps divided by the time increment is the average acceleration during the time increment and $R_{mi,\,j}$ is therefore an inertia force.

Appendix B

Derivation of Dynamic Formula

The following section from Chellis (1951) is reproduced.

The momentum of the ram at the moment of impact is $W_r v/g$, where v is ram velocity at moment of impact. At the end of the period of compression the momentum of the ram is $(W_r v/g) - M_t$, and the velocity $v_c = [(W_r v/g) - M_t]/(W_r/g)$. Assuming that the pile is able to move a short distance, and that the hammer blows and rebounds of the pile result in a looseness between the pile and the earth, then the momentum of the pile at the end of the period of compression may be taken as M_t, and the velocity of the pile becomes $v_c=M_t/(W_p/g)$.

Since the velocities of the ram and pile are equal at the end of the compression period, at that time $M_t=vW_r W_p/g(W_r+W_p)$.

At the end of the period of restitution, the momentum of the ram is $(W_r v/g)-M_t-eM_t=W_r v_r/g$; therefore,

$$v_r = v - \frac{M_t(1+e)}{W_r/g} = v - \frac{W_p}{W_r+W_p}v(1+e) = \frac{W_r - eW_p}{W_r+W_p}v \qquad \text{B.1}$$

At the end of the period of restitution, the momentum of the pile is $M_t + eM_t = W_p v_p/ g$; therefore,

$$v_p = \frac{M_t(1+e)}{W_p/g} = \frac{W_r}{W_r+W_p}(1+e)v = \frac{W_r+eW_r}{W_r+W_p}v \qquad \text{B.2}$$

Using the above values for v_r and v_p, it is possible to determine the sum of the gross energies in the ram and pile, at the end of the period of restitution, available for expenditure in overcoming ground resistance to driving, and in causing temporary elastic compressions in the driving cap, pile, and soil.

The energy available in the ram and pile at the close of the period of restitution will be equal to

$$\frac{W_r}{2g}v_r{}^2 + \frac{W_p}{2g}v_p{}^2 = \frac{W_r v^2}{2g}\frac{\left(W_r - eW_p\right)^2}{\left(W_r + W_p\right)^2} + \frac{W_p v^2}{2g}\frac{\left(W_r + eW_p\right)^2}{\left(W_r + W_p\right)^2}$$

$$= \frac{W_r v^2}{2g}\frac{(W_r + e^2 W_p)}{(W_r + W_p)}$$

$$= W_r h \frac{W_r e^2 W_p}{W_r + W_p} \qquad \text{B.3}$$

If the above equation for energy available at the close of the period of restitution is written as

$$\frac{W_r v^2}{2g}\left[1 - \frac{W_p(1 - e^2)}{W_r + W_p}\right] \qquad \text{B.4}$$

Then the loss in energy due to impact is

$$\frac{W_r v^2}{2g}\frac{W_p(1 - e^2)}{W_r + W_p} = W_r h \frac{W_p(1 - e^2)}{W_r + W_p} \qquad \text{B.5}$$

And the efficiency of the hammer blow is

$$\frac{W_r + e^2 W_p}{W_r + W_p} = \frac{1}{1 + W_p/W_r} + \frac{e^2}{1 + W_p/W_r} \qquad \text{B.6}$$

(Because of smallness of the term e^2compared to 1, the efficiency has been taken as to serve as the basis of the expression in the denominators of the Eytelwein and Navy-McKay formulas, in each of which, however, it has been modified empirically.)

If not impact or elastic losses occurred, and the mechanical efficiency of the hammer were 100 per cent (e.g. no losses), then following expression could be written

$$R_u s = W_r h \qquad \text{B.7}$$

Denoting the mechanical efficiency by the term e_f , the above expression becomes

$$R_u s = e_f W_r h \qquad \text{B.8}$$

Replacing the terms □□□ by the expression derived for energy available at the close of the period of restitution,

$$R_u s = e_f W_r h \left(\frac{W_r + e^2 W_p}{W_r + W_p} \right) \qquad \text{B.9}$$

This may be transposed to read

$$R_u = \frac{e_f W_r h}{s} \left(\frac{W_r + e^2 W_p}{W_r + W_p} \right) \qquad \text{B.10}$$

However, while the tip of the pile moves downward a distance s, the top of the driving cap moves downward an additional distance C1+C2+C3 owing to temporary elastic compression in the cap, pile, and soil. Within elastic limits, the deformation of each of those materials may be assumed to vary with load. For the cap and pile, the amounts of temporary compression may be computed from expression $C = R_u l/AE$. The work obtained from the kinetic energy of the blow may be written, instead of R_us as R_u(s+C/2), and the above expression becomes

$$R_u = \frac{e_f W_r h}{s + C/2} \left(\frac{W_r + e^2 W_p}{W_r + W_p} \right) \qquad \text{B.11}$$

If the temporary compression C is subdivided into its component elements the following expression results:

$$R_u = \frac{e_f W_r h}{s + \frac{1}{2}(C_1 + C_2 + C_3)} \left(\frac{W_r + e^2 W_p}{W_r + W_p} \right) \qquad \text{B.12}$$

Since there are losses due to efficiency, impact, and elastic compressions of the cap, pile, and soil, these items are deducted as shown in the following expression:

$$R_u = \frac{e_f W_r h}{s} - \frac{e_f W_r h \dfrac{W_p(1 - e^2)}{W_r + W_p}}{s} - \frac{R_u C_1}{2s} - \frac{{R_u}^2 l}{2AEs} - \frac{R_u C_3}{2s} \qquad \text{B.13}$$

And, calling$R_u l/AE = C_2$, by combining terms, we obtain

$$R_u = \frac{e_f W_r h}{s + \frac{1}{2}(C_1 + C_2 + C_3)} \left(\frac{W_r + e^2 W_p}{W_r + W_p} \right) \; Hiley\; formula \qquad \text{B.14}$$

If the rebound coefficients in formula (hiley formula) are modified empirically, and a factor of safety of 3 is assumed, the following Canadian National Building Code formula is obtained:

$$R \; = \frac{4nW_r H}{s + C/2} \; Canadian\; National\; Building\; Code\; formula \qquad \text{B.15}$$

Where $n = \frac{W_r + e^2 W_p}{W_r + W_p}$ for friction piles

$= \frac{W_r + 0.5 e^2 W_p}{W_r + W_p}$ for refusal

$$C = \frac{3R}{A}\left(\frac{l}{E} + 0.0001)\right)$$

H=hammer drop height in feet

If it is assumed that there are no elastic losses in the cap or soil quake, formula (hiley) reduces to

$$R_u = \frac{e_f W_r h}{s} - \frac{e_f W_r h \frac{W_p (1 - e^2)}{W_r + W_p}}{s} - \frac{{R_u}^2 l}{2AEs} \qquad \text{B.16}$$

Now assume the hammer to be mechanically 100 per cent efficient, thus omitting the term e_f, and solve for R_u , in which case,

$$R_u = \frac{AE}{l}\left[-s + \sqrt{s^2 + W_r h \left(\frac{W_r + e^2 W_p}{W_r + W_p} \right) \frac{2l}{AE}} \right] \; Universal\; or\; Stern\; formula \qquad \text{B.17}$$

If the impact is assumed to be perfectly inelastic instead of semi elastic, then $e = 0$, and above formula becomes

$$R_u = \frac{AE}{l}\left[-s + \sqrt{s^2 + \left(\frac{{W_r}^2 h}{W_r + W_p}\right)\frac{2l}{AE}}\right] \quad Redtenbacher\ formula \tag{B.18}$$

If the temporary elastic shortening of the ground is included, as well as of the pile, and these are measured from a load-test diagram near to or beyond the failure point, the above formula becomes

$$R_u = \frac{s}{tan\,\emptyset_e}\left[-1 + \sqrt{1 + \left(\frac{{W_r}^2 h}{W_r W_p}\right)\frac{2\,tan\,\emptyset_e}{AE}}\right] \quad Schenk\ formula \tag{B.19}$$

Where □□= tangent of the gradient of load settlement curve.

If the impact loss is entirely neglected, the Redtenbacher formula becomes

$$R_u = \frac{W_r h}{s}\frac{W_r}{W_r + W_p} \quad Ritter\ formula \tag{B.20}$$

$$R_u = -\frac{sAE}{l} + \sqrt{\frac{2W_r hAE}{l} + \left(\frac{sAE}{l}\right)^2} \quad Weisback\ formula \tag{B.21}$$

If the hammer is assumed to be mechanically 100 percent efficient, thus emitting the term e_f, and if, instead of considering the elastic losses in the cap or soil quake, twice the elastic loss is used, taking into account the full length of the pile, and if fixed values are assumed for e, then the Hiley formula becomes

$$R_u = \frac{12W_r h \dfrac{W_r + KW_p}{W_r + W_p}}{s + \dfrac{24000R_u l}{AE}} \quad International\ Conference\ Uniform \qquad \text{B.22}$$

Building Code formula

Where K= 0.25 for steel and 0.1 for other piles.

On the other hand, assume the impact to be perfectly elastic, and also assume that the pile is fully embedded in the ground and is a friction pile without end bearing, so that the distance from the toe to the centre of resistance is $l/2$, and the Stern formula become

$$R_u = \frac{2AEs}{l}\left(\sqrt{1 + \frac{W_r h l}{s^2 EA}} - 1\right) \quad Rankine\ formula \qquad \text{B.23}$$

By taking the Hiley formula and assuming that the mechanical efficiency is 100 percent (e_f=0), that the impact is perfectly inelastic (e=0), and that there are no elastic losses in the cap, pile, or soil, we obtain

$$R_u = \frac{W_r h}{s}\frac{W_r}{W_r + W_p} \quad Dutch\ formula \qquad \text{B.24}$$

The Ritter formula is the same as the Dutch formula, with the inclusion of terms to add the weight of the pile and ram:

By writing the Dutch formula in the following form, taking h in feet, and assuming a factor of safety of 6, we obtain a formula for drop hammers:

$$R = \frac{2W_r H}{s\left(1 + \dfrac{W_p}{W_r}\right)} \quad Eytelwein\ formula \qquad \text{B.25}$$

The Eytelwein formula is modified as follows for single-acting and double acting hammers:

Single-acting: $R = \frac{2W_r H}{s + 0.1\frac{W_p}{W_r}}$

Double-acting: $R = \frac{2(W_r H + Ap)}{s + 0.1\frac{W_p}{W_r}}$

Where A= effective area of piston,

p= air of steam pressure.

If H is taken in feet, a factor of safety of 6 assumed, and the ratio W_p/W_r in the above formula modified by 0.3s instead of 0.1, we have

$$R = \frac{2W_r H}{s\left(1 + 0.3\frac{W_p}{W_r}\right)} \quad Navy - McKay\ formula \qquad \text{B.26}$$

If in Hiley formula the impact loss is entirely neglected, the mechanical efficiency taken as 100 percent, the elastic losses in the cap, pile and soil represented by a constant term of 1.0, H taken in feet and then multiplied by 12, and a factor of safety of 6 is assumed, the following expression is obtained for use with drop hammers:

$$R = \frac{2W_r H}{s + 1.0} \quad Engineering\ News\ formula \qquad \text{B.27}$$

For use with single-acting hammers, the above formula was modified by its author by changing the term 1.0 to 0.1, and in this form as given below has been widely used for single-acting, double-acting and differential-acting hammers:

Single-acting:

$$R = \frac{2W_r H}{s + 1.0}$$

Double and differential acting:

$$R = \frac{2E_n}{s + 0.1}$$

The above formulas may be expressed as follows, n being the number of blows per foot penetration:

Single-acting:

$$R = \frac{20n}{120+n} W_r H \quad Vulcan\ Iron\ Works\ formula \tag{B.28}$$

Double and differential acting:

$$R = \frac{20n}{120+n} E_n$$

The United States Steel Co. modifies the Engineering News formula by varying the constant in the numerator, as follows:

Drop hammers:

$$R = \frac{FHW_r}{s+1.0} \quad United\ States\ Steel\ formula \tag{B.29}$$

Single-acting:

$$R = \frac{FHW_r}{s+0.1}$$

Double and Differential-acting:

$$R = \frac{FH(W_r + Ap)}{s+0.1}$$

Where F=2 for piles driven to refusal or practical refusal;

=6 for piles driven easy in sands and gravels;

=4 for piles driven easily in hard or sandy clays;

=3 for piles driven easily in mixed medium clays and sand or sand and silt;

=2 for piles driven easily in alluvial deposits;

A= effective piston area;

p= mean steam or air pressure;

Another modification of formula is

$$R = \frac{2W_r H}{s + 0.3} \quad Bureau\ of\ Yards\ and\ Docks\ formula \tag{B.30}$$

The Benabencq formula is

$$R = \frac{W_r H}{2s} + W_r + W_p \quad Goodrich\ formula \tag{B.31}$$

The Sanders formula, proposed in 1851, was obtained by applying a purported factor of safety of 8 to formula ( ),

$$\boldsymbol{R = \frac{W_r h}{8s} \quad Sanders\ formula} \tag{B.32}$$

And Merriman used the same terms with a purported factor of safety of 6,

$$\boldsymbol{R = \frac{W_r h}{6s} \quad Merriman\ formula} \tag{B.33}$$

The Goodrich formula is a simplification of a comprehensive formula which contains 25 terms covering conditions of the pile, hammer, cap and ground, and was intended for use only with wood piles and drop hammers with a fall of about 15 ft and set of 1.0 in. Under these conditions it was believed by its author to have accuracy within 10 per cent of that of the comprehensive formula.

$$R_u = \frac{10W_r H}{3s} \quad Goodrich\ formula \tag{B.34}$$

The Kafka formula is the earliest form in which the elastic rebounds of the pile and soil, measured from a graph taken on the pile, have been found. This formula is

$$R_u = X\left[-1 + \sqrt{1 + \frac{Y}{X(2s + \lambda)}}\right] + W_r + W_p \quad Kafka\ formula \tag{B.35}$$

where $X = (2s + \lambda)\frac{AE}{l}$

$Y = 6W_r h\left(\frac{W_r + e^2 W_p}{W_r + W_p}\right)$

$\lambda = s + C_2 + C_3$

Appendix C

GRLWEAP Background features and Parameters

GRLWEAP Input

The following sections have been re-produced from the GRLWEAP Help Menu.

GRLWEAP was programmed for simple input preparation. Known parameters such as pile length, skin friction distribution, etc. can be entered directly and the program will calculate the necessary model parameters. Since hammer modelling requires the input of relatively complex information, data has been prepared and stored on a file for the most commonly encountered hammer models. Thus, after a hammer has been selected the GRLWEAP hammer model is complete.

- 1.1 Input of Static Soil Resistance
- 1.2 Quake Input
- 1.3 Soil Damping Input
- 1.4 Hammer Data Input
- 1.5 Hammer Parameters
- 1.6 Driving System Data

1.1 Input of Static Soil Resistance

The basic wave equation process requires input of static and dynamic soil resistance parameters. Depending on the Analysis Type, standard static soil parameters may include unit shaft resistance and end bearing or total capacity and static toe/shaft resistance percentage, shaft resistance distribution, and quakes. The dynamic shaft resistance is specified through damping options and damping factors. For the input of the static soil resistance, GRLWEAP offers the following options:

a) For a Bearing Graph
- Up to 10 ultimate capacities
- Shaft resistance percentage whereby, for the second and later ultimate capacity values

analysed, the option exists of:
- varying the shaft and toe resistance proportionally

- varying only the shaft resistance
- varying only the toe resistance
- Shaft resistance distribution
- either simple rectangular or triangular or as a variable distribution
- the distribution is shifted along the pile using the penetration input

1.2 Quake Input

Usually a 0.1 inch (2.5 mm) value is a reasonable input for the shaft quake; this value has been used extensively with good correlations. Measurements have demonstrated that the toe quake can be much larger than 0.1 inches or 2.5 mm. Particularly for displacement piles with a width or diameter of more than 12 inches (300 mm), it is reasonable to assume a toe quake of at least D/120 or even D/60, where D is the width of diameter of the pile. The larger value is reasonable for soft or submerged soils. For open ended pipes, the situation is even more complicated since the pile may or may not plug during driving; for coring or unplugged driving, the usual 0.1 inch (2.5 mm) quake is appropriate. In a restrike test and under static loading conditions, the soil may plug inside the pile bottom. Then D/120 is again a reasonable quake assumption. Large quakes can substantially influence the wave equation results, particularly tension stresses for low resistance values and blow counts for high capacities. Unfortunately, large quakes cannot be predicted from a mere inspection of subsurface investigation data. Instead, large quakes are computed by analysis of dynamic measurements taken during driving or re-striking. When piles are being driven into hard rock, it may be necessary to reduce the quake to values less than 0.1 inches (2.5 mm) to avoid under-predicting the capacity and stresses. Also, for piles with small toe diameters of less than 12 inches (300 mm), or for tapered piles, input of a reduced toe quake may be advisable. It is, however, suggested that quakes never be chosen less than 0.04 inches (1 mm). For vibratory pile driving, a doubling of standard quake values is recommended for cohesive soil. See Help/Soil Information/Soil Parameters and Damping/Quakes for more specific information.

1.3 Soil Damping Input

Input of one average value for shaft damping and one value for toe damping using the standard Smith Damping approach normally yields sufficient accuracy for Bearing Graph or Inspector's Chart analyses. Damping forces are then calculated by GRLWEAP as: with j, i.e. the so-called Smith damping factors, the same value

for all skin elements, Rs effectively normalizes the damping distribution. When assigning an average shaft damping value, it should be remembered that damping forces will be higher where there is a higher static resistance (it has at first a zero value and varies with the pile displacement). The ST static soil resistance analysis calculates reasonable averages.

1.4 Hammer Data Input

Hammer parameters are stored in the hammer data file for most commonly encountered hammer models. All the user has to do is select the desired model. If the hammer model is not contained in the file, the hammer must be coded using the file maintenance program. The data in the hammer file reflects the best knowledge on hammer performance available to the program authors. Actual field performance of a hammer will depend on a variety of operational factors such as its state of maintenance, or the fuel or power supply. Hammer design parameters are also frequently modified. It is therefore imperative that the user insures agreement between predicted and actual hammer performance by field inspection. If necessary, file data may be modified by the user to adjust certain values. However, it is preferable that the user leaves the file data unchanged and uses the Hammer Parameters input under Options to modify parameters such as efficiency, maximum pressure, or stroke.

1.5 Hammer Parameters

- 1.5.1 Hammer Efficiency
- 1.5.2 Diesel Hammers (OED and CED)
- 1.5.3 External Combustion Hammers (ECH)

1.5.1 Hammer Efficiency

The efficiency value accounts for unknowns in the model of hammer and impact process and reduces the potential (usually the rated) energy to the kinetic energy just before impact. The efficiency values can be highly controversial giving the impression that one hammer make is more efficient than another. This is not necessarily so. For example, a hammer with internal ram velocity monitoring may have an assigned efficiency of 0.95, which GRLWEAP applies to the ram energy just before impact, when all other hammer losses have been taken into account by the ram velocity measurement. The hammer may have lost a considerable amount of energy during the ram's downward movement; however, using the measured

ram velocity as a rating, only small additional losses have to be covered by the efficiency input which is therefore relatively high.

1.5.2 Diesel Hammers (OED and CED)

In the data file, all diesel hammers have been assigned a hammer efficiency of 0.8. Differences between individual types are compensated for in the analysis process. Since diesel hammers are continuously analyzed starting at the time when the compression cycle starts which happens a significant time interval prior to impact, the reduction of the ram velocity corresponding to the efficiency happens just before impact. Stroke for open end diesel hammers, and bounce chamber pressure for closed ended diesel hammers, gives a good indication of actual hammer performance. Also, blow rate as printed by the program may be used for construction control, and an automatic stroke indicator (Saximeter™) is a good tool for the purpose of measuring blow rate in the field. However, a hammer in a very poor state of maintenance may have friction losses of such magnitude that blow rate is not an accurate indicator of stroke. It has been noticed that GRLWEAP tends to under-predict strokes, on occasion up to 20%, while stresses and transferred energies are realistic. It is therefore suggested not to adjust the stroke, e.g. by analyzing with an increased combustion pressure, unless the stroke under-prediction exceeds 20%. This is reasonable and conservative particularly when high strokes are possibly the result of pre-ignition. A diesel hammer will perform particularly poorly when it overheats during hard driving and then pre-ignites. Pre-ignition produces large strokes and low transferred energies, and therefore high blow counts. This condition can be modeled by the program using a negative combustion delay for liquid fuel injection or a reduced combustion start volume for atomized injection (Options/Hammer Parameters). Pre-ignition is usually an unexpected situation and cannot be detected in the field without electronic measurements. A number of models; for example, the DELMAG, FEC, and APE D-series hammers and the ICE I-series hammers; have stepwise adjustable fuel pumps. For those hammers, a reduced fuel setting may be chosen under Options/General Options/Stroke (only accessible if a diesel hammer was selected). The Combustion Pressure input can also be adjusted by either changing the absolute pressure value or the percentage in the main input screen or changing both vs. the Depth values for the Driveability analysis. Input of fuel settings less than maximum cause the program to choose a reduced maximum combustion pressure. This input is really only meaningful for hammers that have a stepwise

adjustable fuel pump. Measurement results are limited; therefore, predictions involving diesel hammers should be backed up by field control, particularly where pile stress limitations are critical. It is the user's responsibility to check the actual fuel settings used in the field. For hammers which do not have stepwise adjustable fuel pumps and where reduced hammer energy is necessary or desirable, it is recommended that constant stroke analyses be run, with iteration on pressure, for a variety of strokes. In the field, the desirable stroke or bounce chamber pressure is then attained by fuel pump adjustment.

1.5.3 External Combustion Hammers (ECH)

The wave equation model of ECH hammers is not as complicated as that for diesel hammers, but the correct choice of a proper efficiency, i.e. impact velocity, is not a simple task. For example, a thick cushion may produce a reduced stroke while a thin cushion may allow for early air, steam, or hydraulic injection, i.e. preadmission, and therefore self-cushioning.The ECH category includes an ever increasing number of hammer systems, makes, and models, starting from the simple cat-and-rope driven drop hammer of an SPT rig to sophisticated, hydraulically powered hammers with pneumatic accelerators and electronic controls. Naturally, the unknowns vary widely for these hammers and efficiency values cannot possibly be assigned based on hammer model evaluations or a few measurements at the time of a hammer model's introduction into construction practice. Additional verification and, if needed, modification of the database-supplied values are therefore strongly recommended. Efficiencies were assigned as follows: Options/Numeric for hammer and pile cushions; under Options/Pile Parameters/Additional Input for the pile top; and under Options/Pile Parameters/Splices for cracks, slacks or splices. The input of the Elastic Modulus of a cushioning material may be taken as one half of the tangent modulus determined at a stress level of 5 ksi (35 MPa). The Tables of Helmet and Hammer Cushion Properties and the Table of Cushion Material Properties contain moduli, taken from a variety of sources and reduced by multiplication with 0.5. These sources usually do not reveal how the tests were done or how the moduli were calculated; however, results using the GRLWEAP recommended values are generally acceptable.

(a) 0.67 for traditional single acting air/steam/hydraulic hammers where the motive fluid enters the

power cylinder through valves controlled by the falling ram.
(b) 0.50 for the same hammer as in (a) but double, differential, or compound acting.
(c) 0.95 for all hammers with electronic readout of energy shortly before impact and where this energy
is the basis of the wave equation, or equivalent, stroke input.
(d) 0.80 for all other hydraulic hammers where measurements have shown that preadmission is
precluded and that the downward acceleration will not cause uplift in hard driving.

Note: The user is urged to verify that these efficiency values yield reasonable results. GRL efficiency assignments shall not be used as a quality index of a particular hammer type, make, or model, but rather as a parameter that corrects for lack of a better mathematical hammer model. The hammer cushion, a relatively lightweight and flexible material.

1.6 Driving System Data

Elements between the hammer and the pile top form the driving system and include:

The hammer cushion, a relatively lightweight and flexible material. The helmet accommodating the hammer cushion, including a striker plate to cover and protect the hammer cushion, and pile top adapters (inserts). The helmet is usually heavy and so rigid that its stiffness can be ignored relative to that of the hammer cushion or the ram. The pile cushion, in the case of concrete piles. The Tables of Helmets and Hammer Cushion Properties contain information that has been collected for numerous systems as a help to the program user. The values in these tables are what manufacturers or suppliers recommend as a proper system or what they provide with their hammers. However, different driving system components may be used on the construction site. The user should verify the system components by requiring a data submittal from the pile-driving contractor. The help tables can be easily accessed by pressing function key F3, when the cursor is on a field of driving system parameter input in the main input screen. The mechanical behavior of a cushion material is modeled using its elastic modulus, round out deformation, and coefficient of restitution (see Table of Cushion Material Properties). The

helmet is defined simply by its weight. The additional weights of striker plate, adaptor inserts, hammer cushion or other accessories should be added to yield the helmet weight input value.

The input of the Elastic Modulus of a cushioning material may be taken as one half of the tangent modulus determined at a stress level of 5 ksi (35 MPa). The Tables of Helmet and Hammer Cushion Properties and the Table of Cushion Material Properties contain moduli, taken from a variety of sources and reduced by multiplication with 0.5. These sources usually do not reveal how the tests were done or how the moduli were calculated; however, results using the GRLWEAP recommended values are generally acceptable. Coefficients of Restitution (C.O.R.) are even more difficult to measure than the elastic modulus of a cushioning material. The program uses the C.O.R. to calculate the stiffness of the cushion during expansion, i.e. when the force in the cushioning starts to decrease. Low C.O.R.s produce a very rapid load shedding and therefore a reduction in transferred energy. For wood, the usual recommendation is a C.O.R. of 0.5; however, if the wood cushion is burning or if wood chips are used, the C.O.R. may be lower. Numerical problems may occur in the GRLWEAP analysis if the chosen C.O.R. is less than 0.1. The C.O.R. may not be zero. The cushion thickness is often well defined except for soft cushioning materials such as plywood, which compress severely during their short life as a cushion. Thus, when stress calculations are critical for concrete piles, it is recommended to analyze both early and late driving with different cushion thicknesses, t, and moduli, E. Correlation analyses have shown that it is reasonable to use for a used hammer cushion a combined E/t increase of 2.5 over the new cushion values. For example, when using the nominal, or initial, cushion thickness, the modulus may be used as 30 and 75 ksi (210 and 510 MPa) for early and late driving, respectively. The driveability analysis allows for and should be used with modification of the pile cushion stiffness and C.O.R. as a function of depth of pile driving.

5. Output Options

Several output options control the amount and type of the numerical result file (which may be printed). Usually output is made for each ultimate resistance analysis and summarized after the final Ru value. For driveability analyses this may produce a rather large file and the minimum output option is therefore

sometimes reasonable. The debug option may produce an unreasonably large file. In fact, the debug option is only of use to those intimately familiar with the program.

Note: It is important that the user inspects the numerical output file or any output message that may contain important information about the validity of the results. The minimum output option may not provide all information necessary for a thorough investigation of the analyzed problem.

6. Details of the Driveability Analysis Option

- 6.1 Soil Resistance Input
- 6.2 Gain/Loss Factors
- 6.3 Depths, Modifiers
- 6.4 The Driveability Analysis Procedure

6.1 Soil Resistance Input

The bearing graph is the standard output from wave equation analyses. It can be compared to the result from a dynamic formula which is a relationship between bearing capacity and blow count or pile penetration per blow. Strictly speaking, this relationship is only valid for one particular pile penetration, its associated frictional distribution and end bearing. For the sake of convenience, however, a particular bearing graph is usually applied to a range of penetrations. For the purpose of bearing capacity determination from observed blow counts, the bearing graph approach is satisfactory. However, if the question is whether a pile can be driven to a certain depth, whether unsafe stresses will occur during the installation and how many blows (how much time) it will take to install a pile, the bearing graph approach is cumbersome at best since it would require the calculation of a large number of bearing graphs and then a tedious evaluation. The Driveability analysis of GRLWEAP generates up to 100 bearing graphs automatically and organizes results as a function of a pile penetration. However, instead of a normalized skin friction distribution, the following information is required as an input for the driveability for upto 100 different depth values:

Depth	Unit Shaft Resist	Toe Resist	Skin Quake	Toe Quake	Skin Damping	Toe Damping	Setup Factor	Limit Distance	Setup Time
Ft	ksf	kips	inch	inch	s/ft	s/ft		ft	hours
(m)	(kPa)	(kN)	(mm)	(mm)	(s/m)	(s/m)		(m)	(hours)

While quake and damping values are as described in the corresponding data descriptions, some explanation has to be added for the remaining input values in the above table.

Unit shaft resistance is usually calculated as a long-term shaft resistance value using standard static geotechnical procedures like the GRLWEAP ST and SA procedures, DRIVEN, SPT-97 or UNIPILE, all of which are based on methods referred to as Meyerhoff, Nordlund, Tomlinson, Effective stress, Total stress, etc.. Adjustment of the long-term unit friction to the usually lower shaft resistance during driving (also called Static Resistance to Driving, SRD) is made by GRLWEAP using the setup and gain/loss factor information.

Toe Resistance is also calculated in a static formula as a long-term value. Normally, it is not assumed that the toe resistance changes significantly due to driving except in a few soil types, among them some very dense fine silty sands or shales, in which end bearing may be artificially high during driving and relax after pile installation. If relaxation is indicated then a toe gain/loss factor greater than 1 (it is possibly as high as 2) may be used to simulate the unusually high toe resistance during driving.

Note: When using standard geotechnical methods to calculate unit friction and end bearing, care should be taken not to reduce friction or end bearing values in an attempt to remain conservative. The resistance values should be as realistic if possible; low resistance values may lead to low and therefore non-conservative predictions of blow count and stress.

The setup factor is the ratio of long-term shaft resistance to SRD (static resistance to driving along the shaft) for a certain soil layer. In GRLWEAP the setup factor only describes the loss of shaft resistance and therefore does not affect the end bearing. Often set-up factors are calculated as total capacity calculated from restrike tests divided by the total pile capacity at the end of driving. For example, assume that in a clay the bearing capacity is 2,500 and 1,000 kN during re-strike (after a sufficiently long time after initial driving) and at the end of driving, respectively, then the setup factor is 2.5. Strictly speaking, this setup factor would be incorrect, first because it would include the effects of the capacity change at the pile toe and second, because restrike tests are often not done after sufficiently long

waiting times and therefore do not necessarily represent the long term pile capacity. However, for friction piles in uniform deposits, these setup factors give valuable setup information for driveability analyses. Suppose that a pile has been driven to a certain depth, that driving has been interrupted for a long time ("Wait Time" greater than "Setup Time"), and that driving then again resumes. The shaft resistance will then have reached its full setup capacity. After resumption of driving, the dynamic effects of the moving pile will gradually reduce the shaft resistance until it reaches its fully reduced value (long term resistance divided by setup factor). This process is modelled in GRLWEAP using Setup time and Relative Energy Inputs. It should be done with the first shaft gain/loss factor set to the inverse of the highest setup factor considered in the driveability analysis. Setup Time is even less known than the Setup Factors. However, like the relative energy data it is only required as an input if it is desired to consider the setup effect of driving interruptions. It is known that in some geologic areas (for example in Louisiana, USA) setup materializes very slowly, probably because of a very slow draining of pore water pressures in the fine-grained soils. Indeed in Louisiana it is known that static load tests would indicate unrealistically low capacities unless the waiting time between pile installation and static load test would be at least 6 weeks. In other areas, and particularly in coarse-grained soils, setup may occur much quicker. A rough estimate would be that sands set up within one hour, fine sands or silts within 1 day and clays within 7 days. The Relative Energy is the pile driving energy necessary to break down the soil setup effect completely in a particular layer. To make the input as simple as possible, this energy value is divided by the associated ultimate shaft resistance in that same layer; in this way it is only necessary to enter a distance over which driving would produce a complete loss of set-up. (Note that internally, GRLWEAP calculates the energy as the integral of resistance times pile movement and thus, even if a pile does not permanently penetrate into the ground, some loss of setup will be calculated.) Not much is known about this value; it may be estimated as 3 to 6 ft or 1 to2 m, regardless of soil type or pile size. Setup Time and Relative Energy are inputs that help generate in a more qualitative than quantitative manner a blow count vs. depth curve that shows increasing and decreasing resistance values during driving interruptions. Instead of using these optional inputs it may be satisfactory to analyse both full setup (G/L = 1) and fully reduced resistance (G/L = 1/Setup Factor) and interpolate blow counts manually between these two curves where driving interruptions are expected.

Appendix D

DRIVEN

This appendix presents some of the background features on the static analyses program DRIVEN. The following extracts are reproduced.

The DRIVEN program follows the methods and equations presented by Nordlund (1963, 1979), Thurman (1964), Meyerhof (1976), Cheney and Chassie (1982), Tomlinson (1980, 1985), and Hannigan, et.al. (1997). The Nordlund and Tomlinson static analyses methods used by the program are semi-empirical methods and have limitations in terms of correlations with field measurements and pile variables which can be analysed. The user is encouraged to review further information on this subject in the "Design and Construction of Driven Pile Foundations" manual (Hannigan, et.al. 1997). The application of this software product is the responsibility of the user. It is imperative that the responsible engineer understands the potential accuracy limitations of the program results, independently cross checks those results with other methods, and examines the reasonableness of the results with engineering knowledge and experience. There are no expressed or implied warranties.

New DRIVEN Features

Although DRIVEN has been completely rewritten from the ground up, its legacy lies in the SPILE program. Clearly, the most visible change is the move to a Windows based environment. The SPILE program was also developed by the FHWA and released in 1993. In SPILE, the user entered a soil profile to a planned pile toe depth and “ran” the program for the results of this input. When using the DRIVEN program, the user enters the entire sampled soil profile to the full depth of the profile. Based upon this input, DRIVEN will calculate pile capacities at predetermined depth intervals. This allows the user to view the pile capacity as a function of depth. There are many other new features that have been added. They are discussed below. These options are discussed in full detail within the user's manual.

Multiple Water Tables

Support for three water tables is now included. One water table at the time of sampling, another water table for restrike/driving considerations, and one water table for ultimate capacity considerations.

Soft Compressible Soils/Negative Skin Friction

The user may specify the depth of a soft compressible soil layer at the top of the soil profile. For ultimate calculations, the shaft resistance from this layer can be considered in two different ways, as soft compressible soil or as negative skin friction. If the shaft resistance is considered to be soft compressible soil, the skin friction for this layer is not include in the ultimate skin friction capacity. If the resistance is negative skin friction, the skin friction from this layer is considered to be negative and is subtracted from the total skin friction for ultimate capacity computations. See Chapter 3 for a detail discussion on how the DRIVEN program calculates the ultimate capacity with soft compressible soils/negative skin friction conditions.

Scourable Soils

There are two kinds of scour conditions that the DRIVEN program can consider: short term (local) and long term (channel degradation and contraction) scour. In both cases, there is considered to be no shaft resistance. For the case of short term scour, the weight of the soil is still considered in the effective stress computation. For long term scour, the weight of the soil is not considered when computing effective stress. See Chapter 3 for a detail discussion on how the DRIVEN program calculates the ultimate capacity with scour conditions.

Open End Pipe Piles

The DRIVEN program supports the use of open-end pipe piles in its static analyses. For a detailed background on how DRIVEN computes open-end pipe pile capacities, refer to Chapter 7. This chapter provides comprehensive coverage of the engineering aspects of the DRIVEN software.

Capacities

The DRIVEN program computes three sets of capacities for three different conditions: restrike,
driving, and ultimate.

Restrike

Restrike computes static skin and end bearing resistance for the entire soil profile. Restrike computations do not consider the effects of soft soils or scour conditions.

Driving

The user may enter a loss of soil strength in the soil profile for each soil layer due to the effects of driving. The driving computations are based upon the restrike calculations minus the soil strength loss due to driving.

Ultimate

Ultimate capacity computations consider the effects of soft soil conditions or scour. Hence, this is the ultimate capacity available to resist applied loads.

Output

The DRIVEN program presents the output in both tabular and graphical format. In the tabular format, the user can inspect each set of computations (restrike, driving, and ultimate) individually. The program presents each analysis depth in the profile with some of the contributing factors along with the skin, end, and total resistance. In graphical format, the program allows the user to select between the three sets of computations. The graphs plot the depth versus capacity for the skin, end, and total resistance. The tabular results may be printed using the report button, while the graphical output can be either printed or sent to the Windows clipboard.

Units

DRIVEN includes support of both English and SI units. While using the program, the appropriate units for each data entry field are shown. If desired, the user can change the unit system for a project at any time and the DRIVEN program will convert all the input and output parameters to the new unit system.

Driveability

Finally, DRIVEN will prepare a partial driveability file for use by the GRLWEAP software. DRIVEN requests a few input parameters from the user then generates a data file that contains the soil and pile data that can be used by the GRLWEAP software to perform a driveability study. Please see chapter 5 for a more detailed explanation.

Appendix E

Outputs of GRLWEAP Analyses

1. Concrete Pile

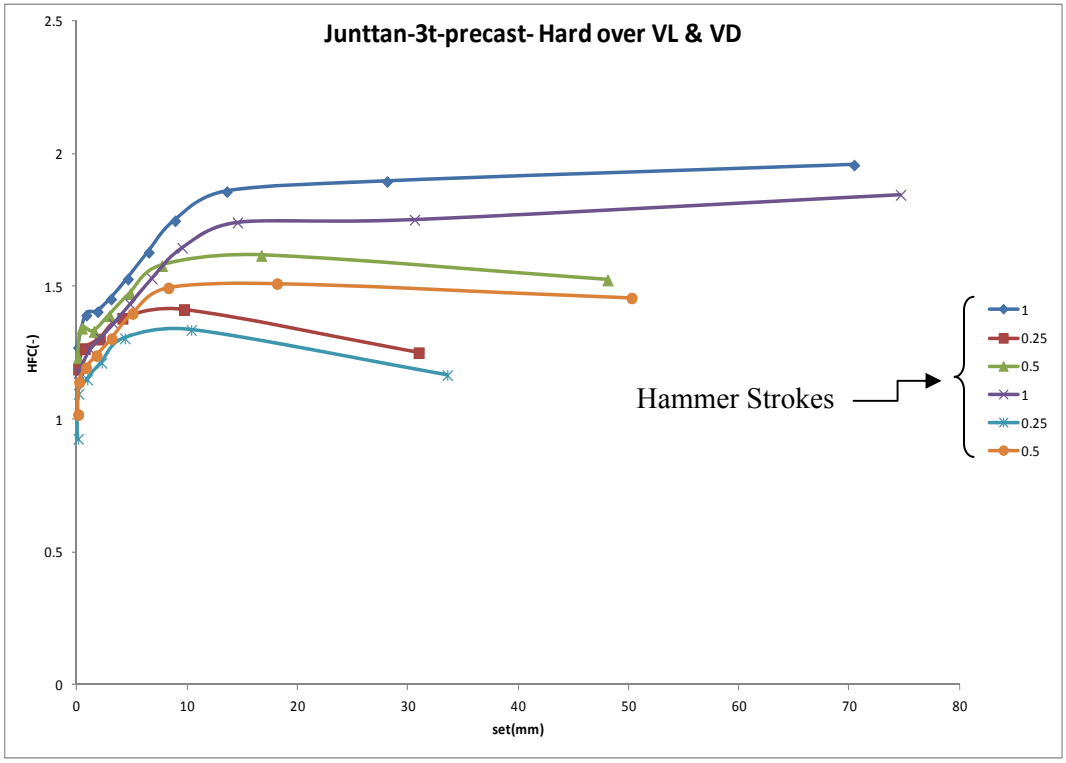

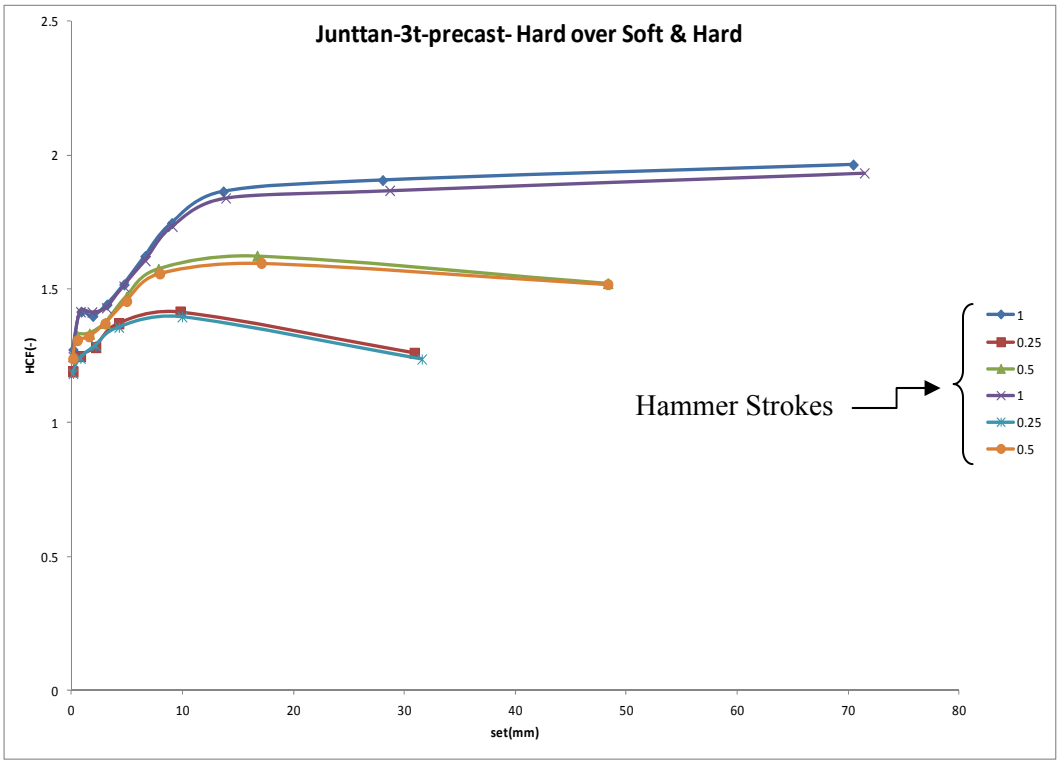
Junttan-3t-precast- Hard over Soft & Hard
HCF(-)
set(mm)
Hammer Strokes
1
0.25
0.5
1
0.25
0.5

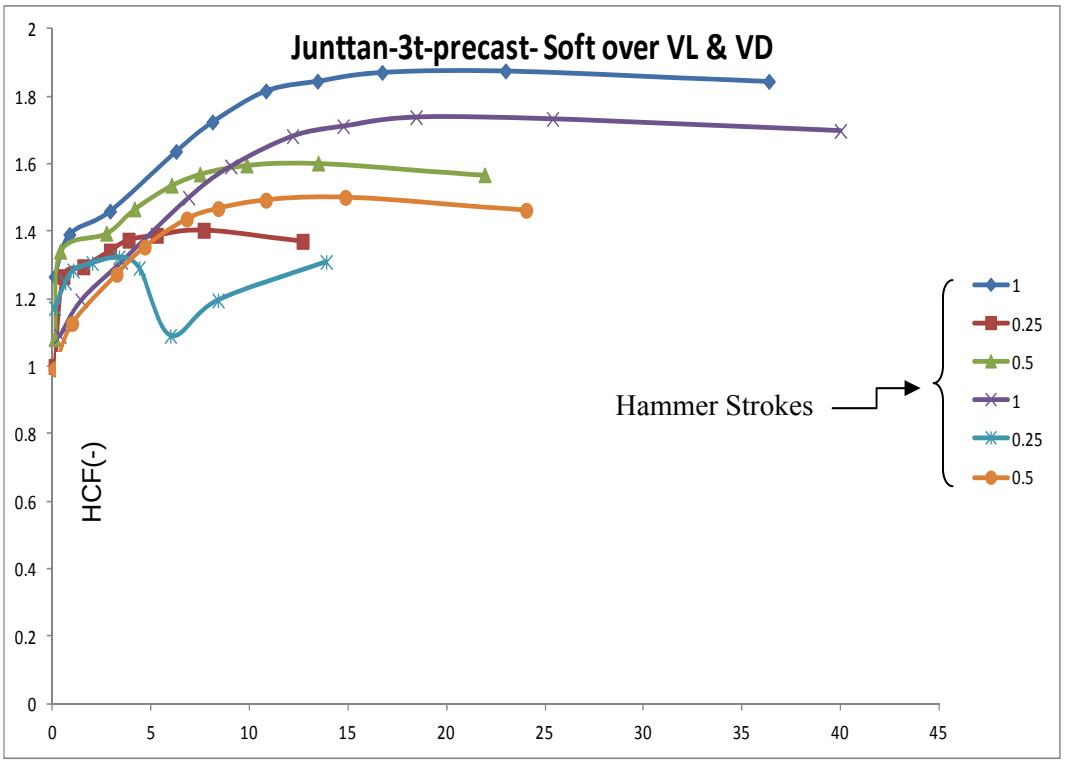
Junttan-3t-precast- Soft over VL & VD
HCF(-)
Hammer Strokes
1
0.25
0.5
1
0.25
0.5

Set(mm)

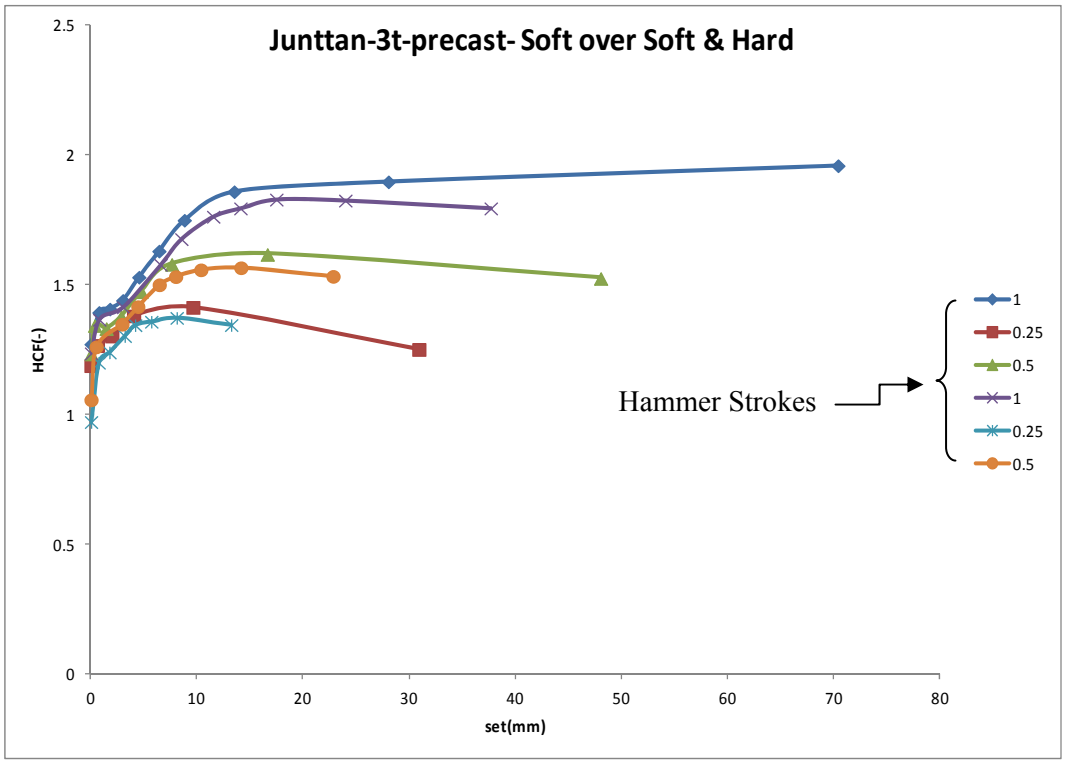
Junttan-3t-precast- Soft over Soft & Hard
HCF(-)
set(mm)
Hammer Strokes
1
0.25
0.5
1
0.25
0.5

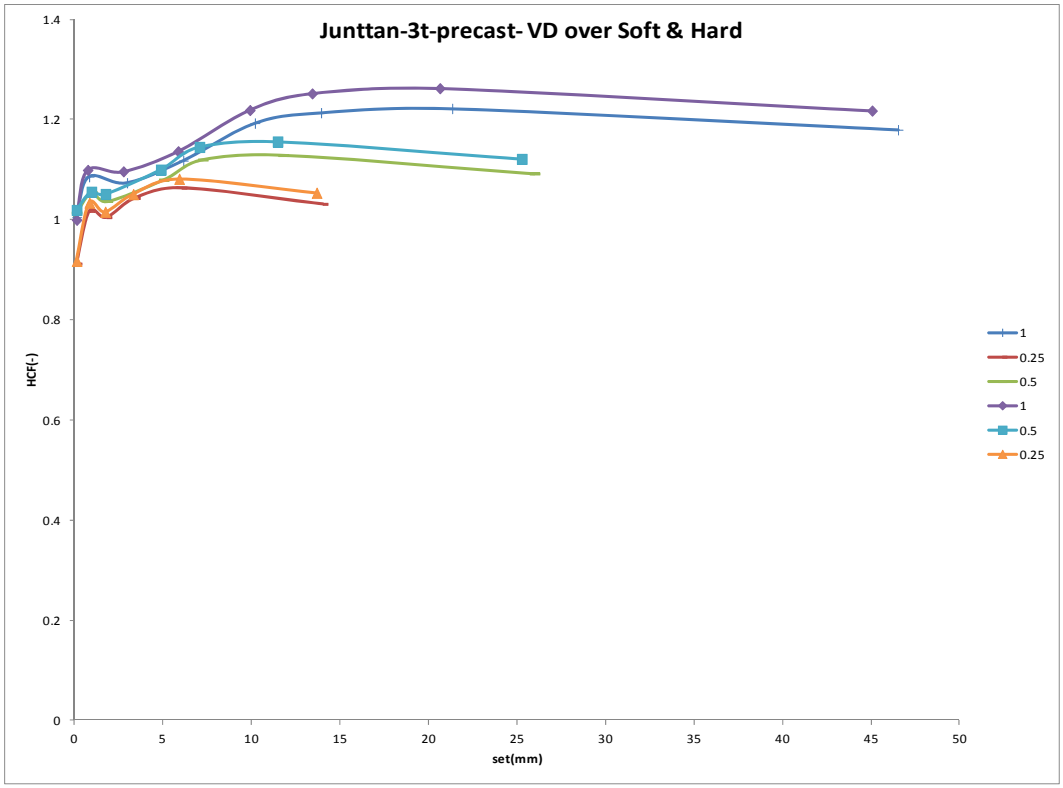
Junttan-3t-precast- VD over Soft & Hard
HCF(-)
set(mm)
1
0.25
0.5
1
0.5
0.25

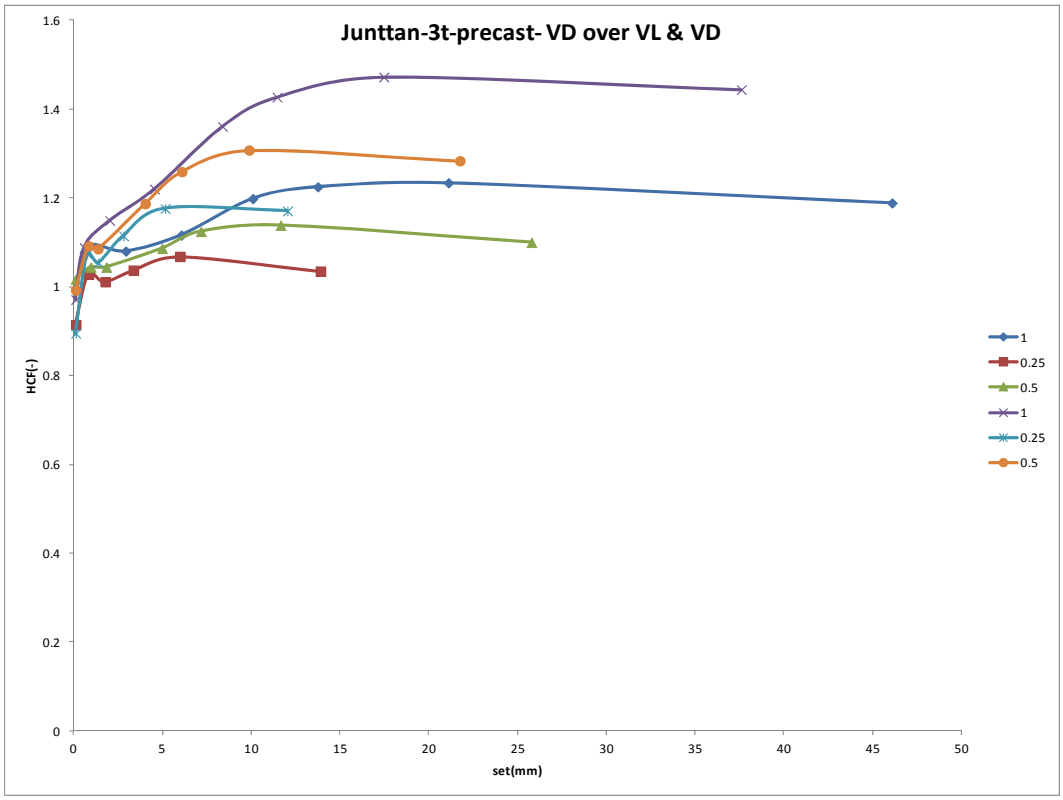
Junttan-3t-precast- VD over VL & VD
HCF(-)
set(mm)
1
0.25
0.5
1
0.25
0.5

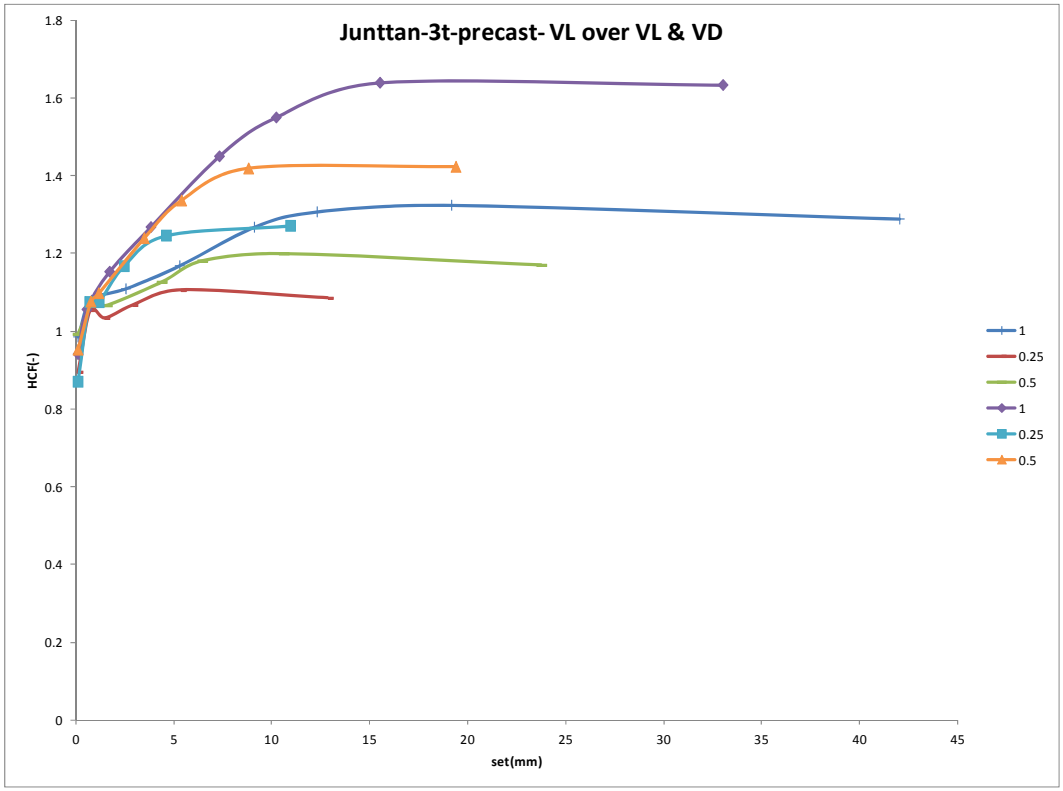
Junttan-3t-precast- VL over VL & VD
HCF(-)
set(mm)
1
0.25
0.5
1
0.25
0.5

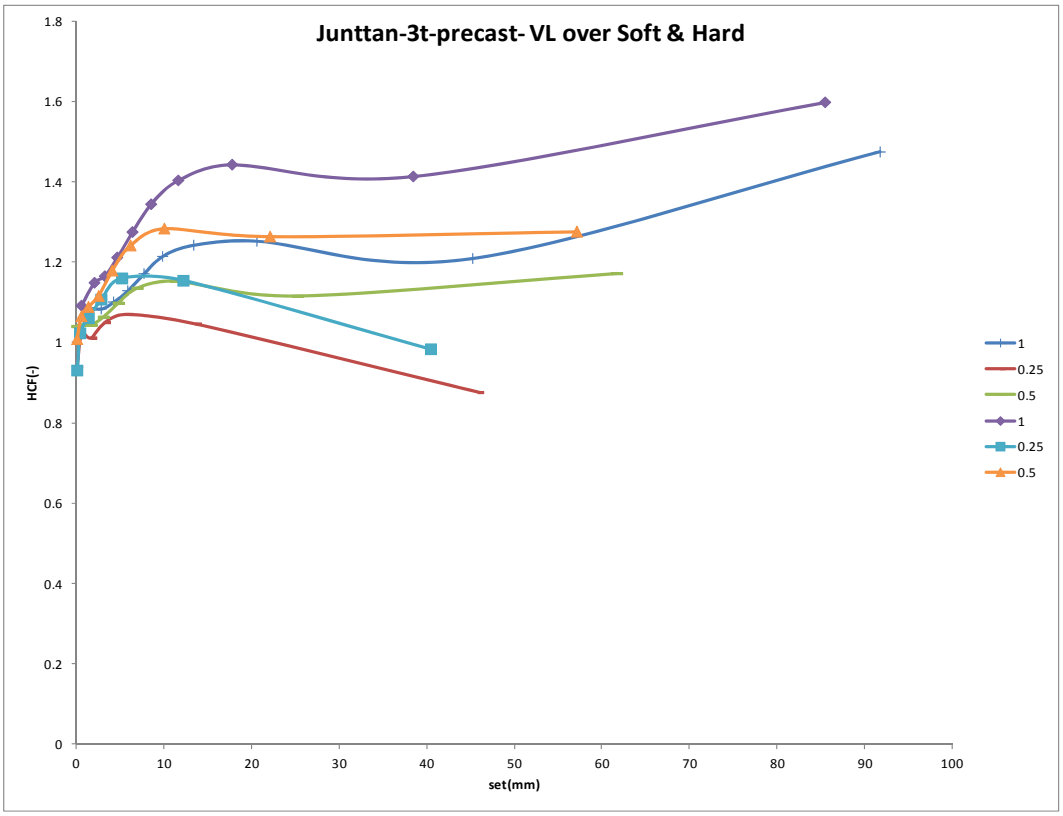
Junttan-3t-precast- VL over Soft & Hard
HCF(-)
set(mm)
1
0.25
0.5
1
0.25
0.5

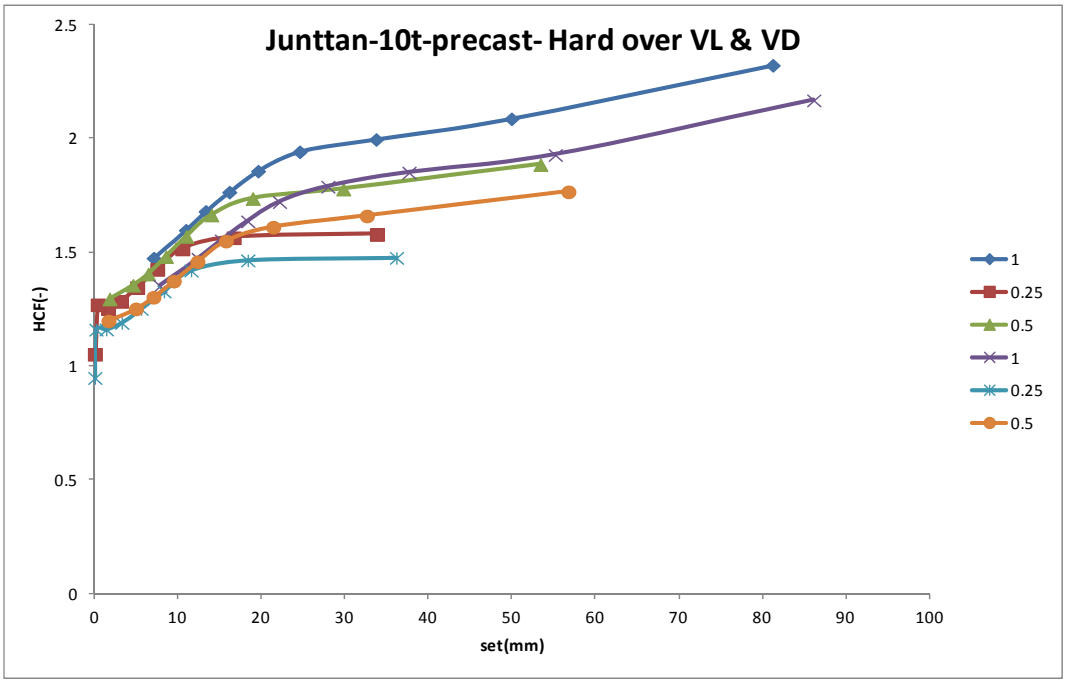
Junttan-10t-precast- Hard over VL & VD
HCF(-)
set(mm)
1
0.25
0.5
1
0.25
0.5

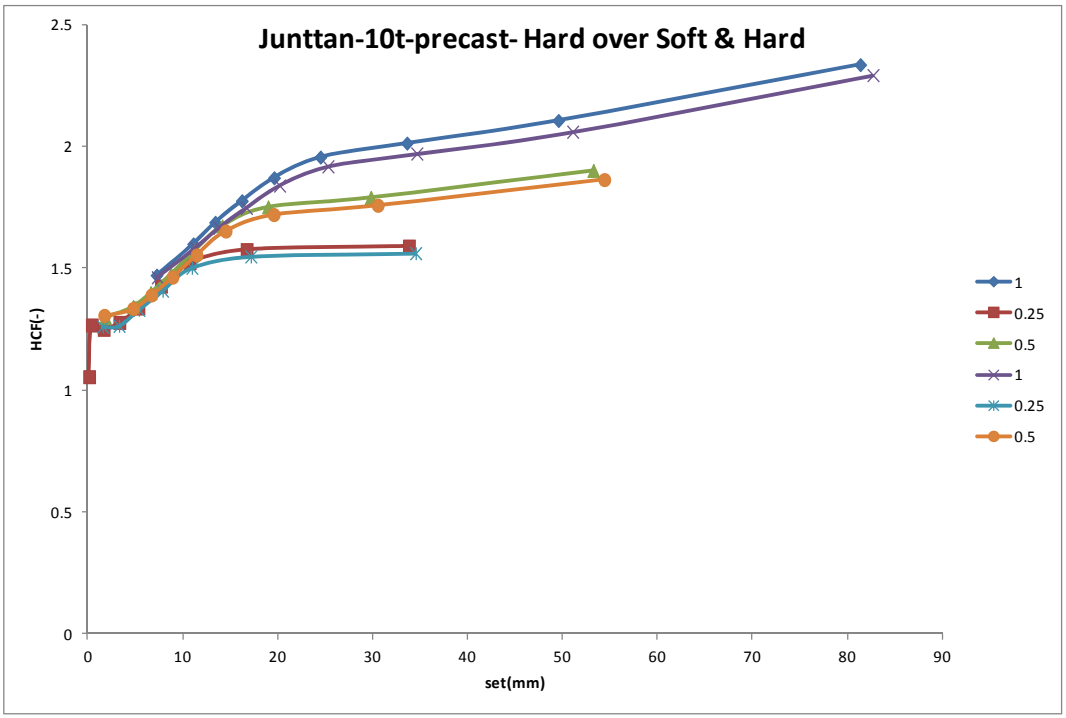
Junttan-10t-precast- Hard over Soft & Hard
HCF(-)
set(mm)
1
0.25
0.5
1
0.25
0.5

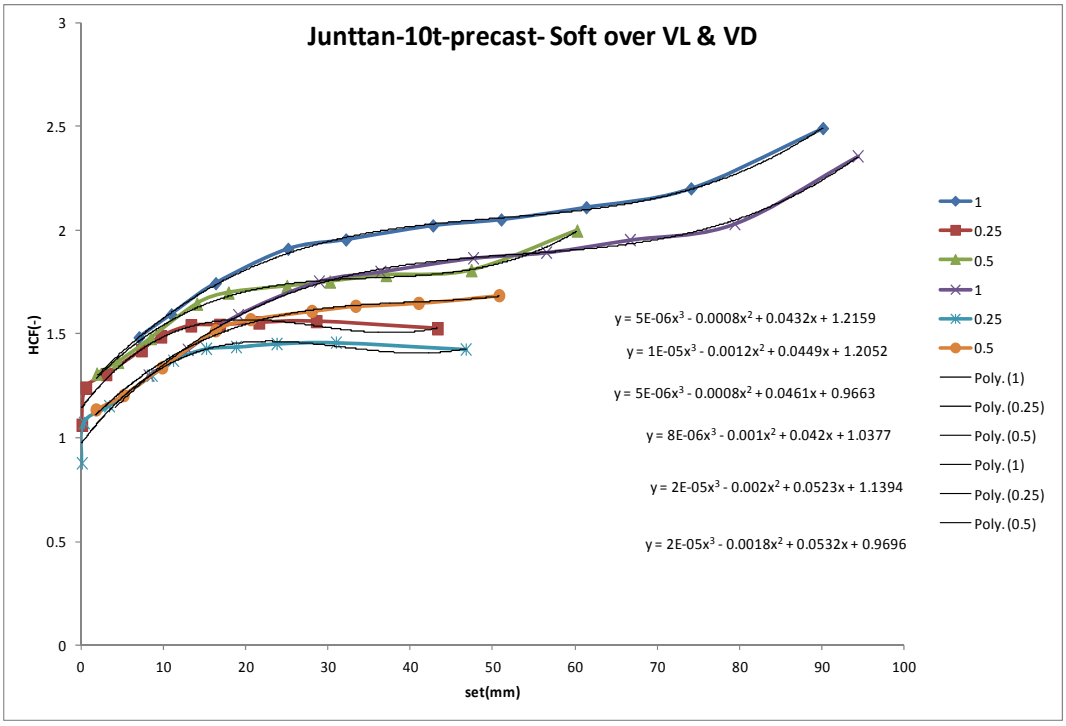
Junttan-10t-precast- Soft over VL & VD
HCF(-)
set(mm)
y = 5E-06x³ - 0.0008x² + 0.0432x + 1.2159
y = 1E-05x³ - 0.0012x² + 0.0449x + 1.2052
y = 5E-06x³ - 0.0008x² + 0.0461x + 0.9663
y = 8E-06x³ - 0.001x² + 0.042x + 1.0377
y = 2E-05x³ - 0.002x² + 0.0523x + 1.1394
y = 2E-05x³ - 0.0018x² + 0.0532x + 0.9696
1
0.25
0.5
1
0.25
0.5
Poly. (1)
Poly. (0.25)
Poly. (0.5)
Poly. (1)
Poly. (0.25)
Poly. (0.5)

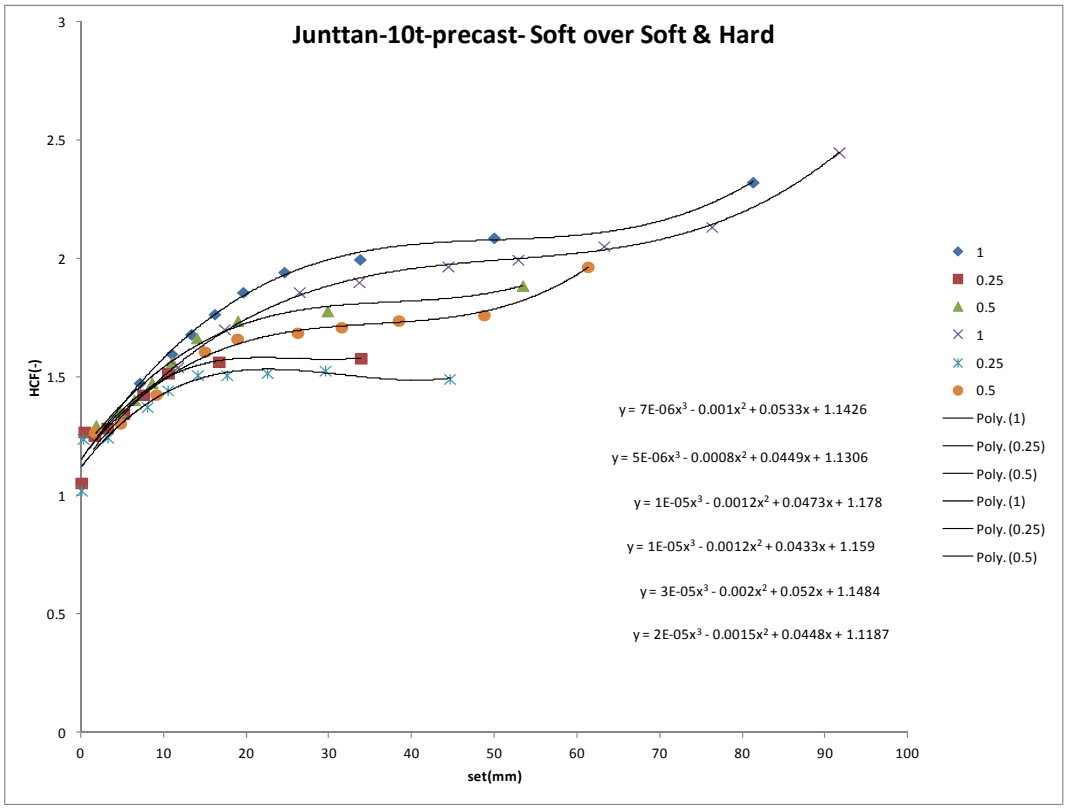
Junttan-10t-precast- Soft over Soft & Hard
HCF(-)
set(mm)
y = 7E-06x³ - 0.001x² + 0.0533x + 1.1426
y = 5E-06x³ - 0.0008x² + 0.0449x + 1.1306
y = 1E-05x³ - 0.0012x² + 0.0473x + 1.178
y = 1E-05x³ - 0.0012x² + 0.0433x + 1.159
y = 3E-05x³ - 0.002x² + 0.052x + 1.1484
y = 2E-05x³ - 0.0015x² + 0.0448x + 1.1187
1
0.25
0.5
1
0.25
0.5
Poly. (1)
Poly. (0.25)
Poly. (0.5)
Poly. (1)
Poly. (0.25)
Poly. (0.5)

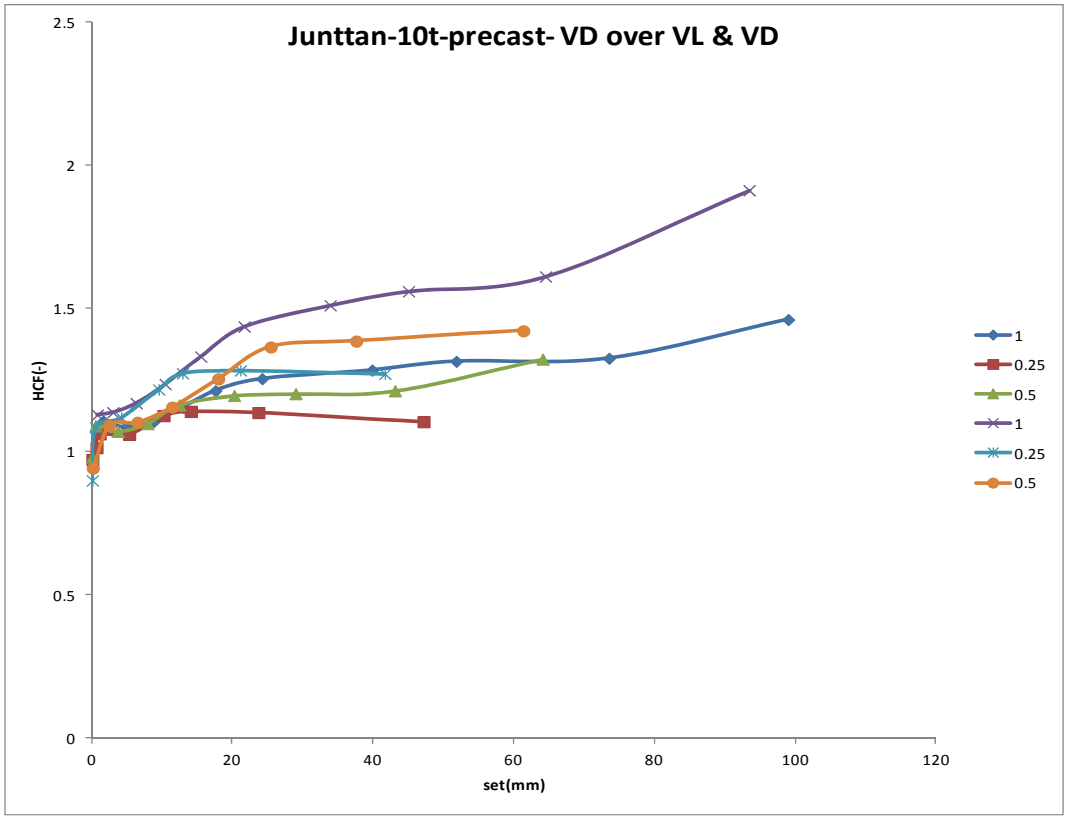
Junttan-10t-precast- VD over VL & VD
HCF(-)
set(mm)
1
0.25
0.5
1
0.25
0.5

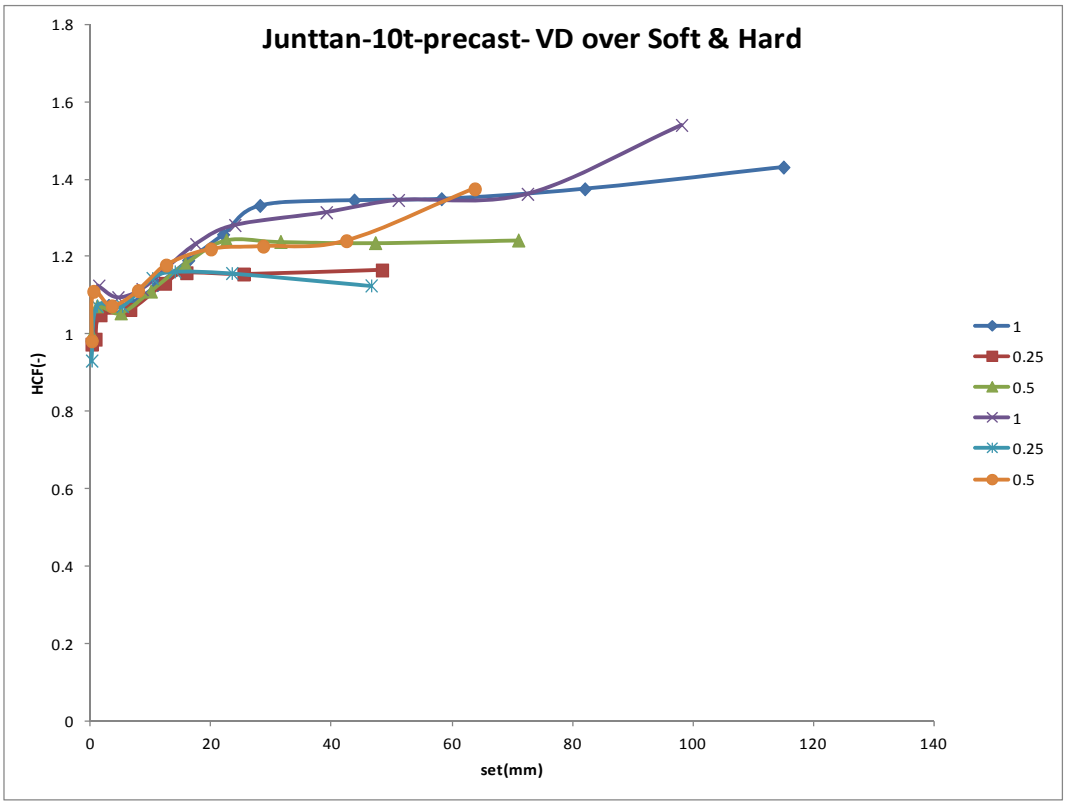
Junttan-10t-precast- VD over Soft & Hard
HCF(-)
set(mm)
1.8
1.6
1.4
1.2
1
0.8
0.6
0.4
0.2
0
0
20
40
60
80
100
120
140
1
0.25
0.5
1
0.25
0.5

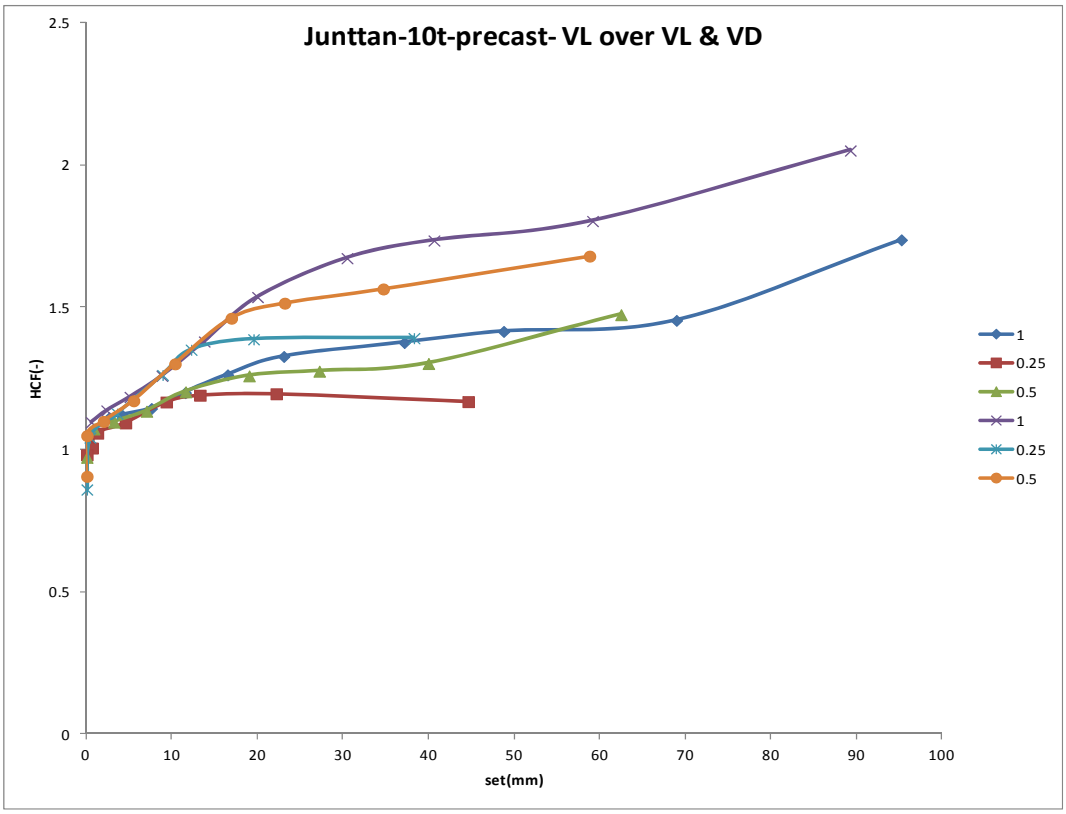
Junttan-10t-precast- VL over VL & VD
HCF(-)
set(mm)
2.5
2
1.5
1
0.5
0
0
10
20
30
40
50
60
70
80
90
100
1
0.25
0.5
1
0.25
0.5

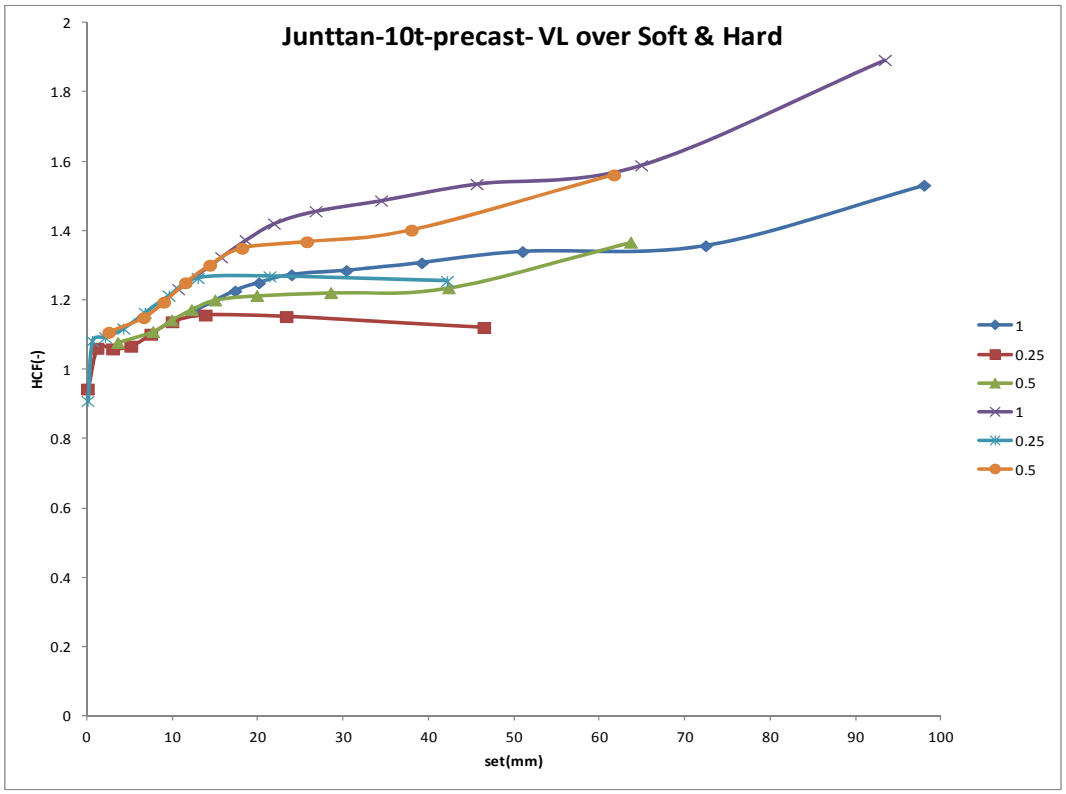
Junttan-10t-precast- VL over Soft & Hard
HCF(-)
set(mm)
0
0.2
0.4
0.6
0.8
1
1.2
1.4
1.6
1.8
2
0
10
20
30
40
50
60
70
80
90
100
1
0.25
0.5
1
0.25
0.5

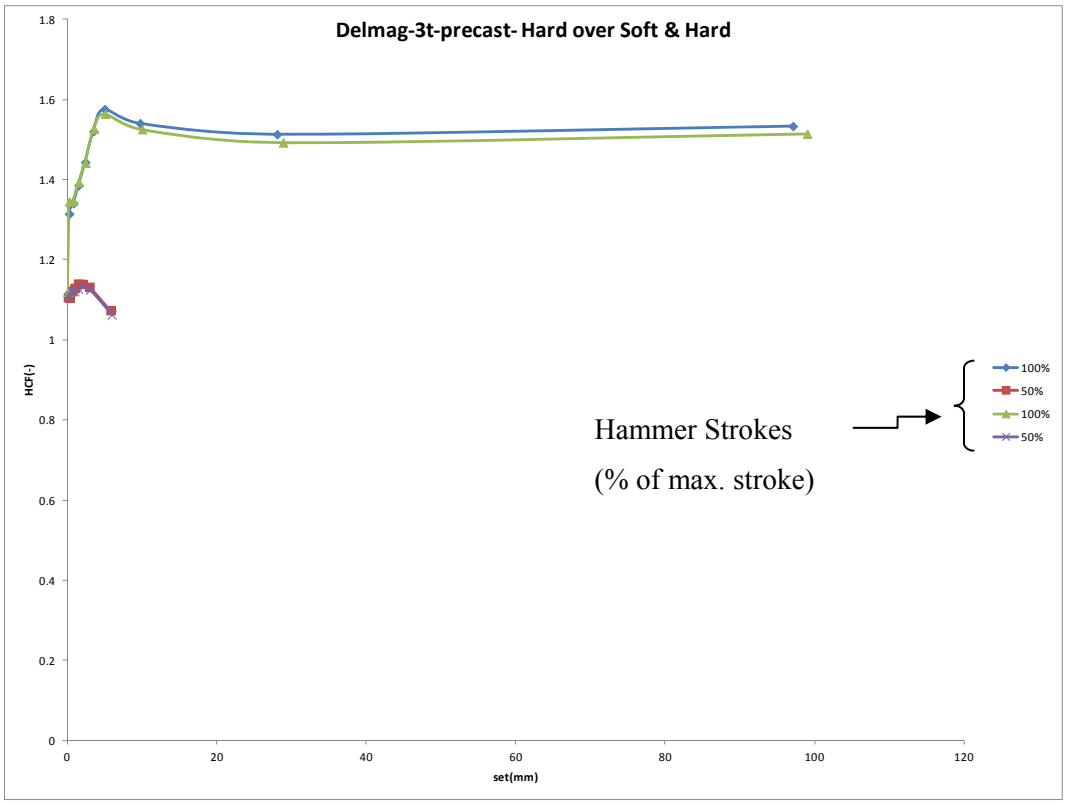
Delmag-3t-precast- Hard over Soft & Hard
HCF(-)
set(mm)
0
0.2
0.4
0.6
0.8
1
1.2
1.4
1.6
1.8
0
20
40
60
80
100
120
Hammer Strokes
(% of max. stroke)
100%
50%
100%
50%

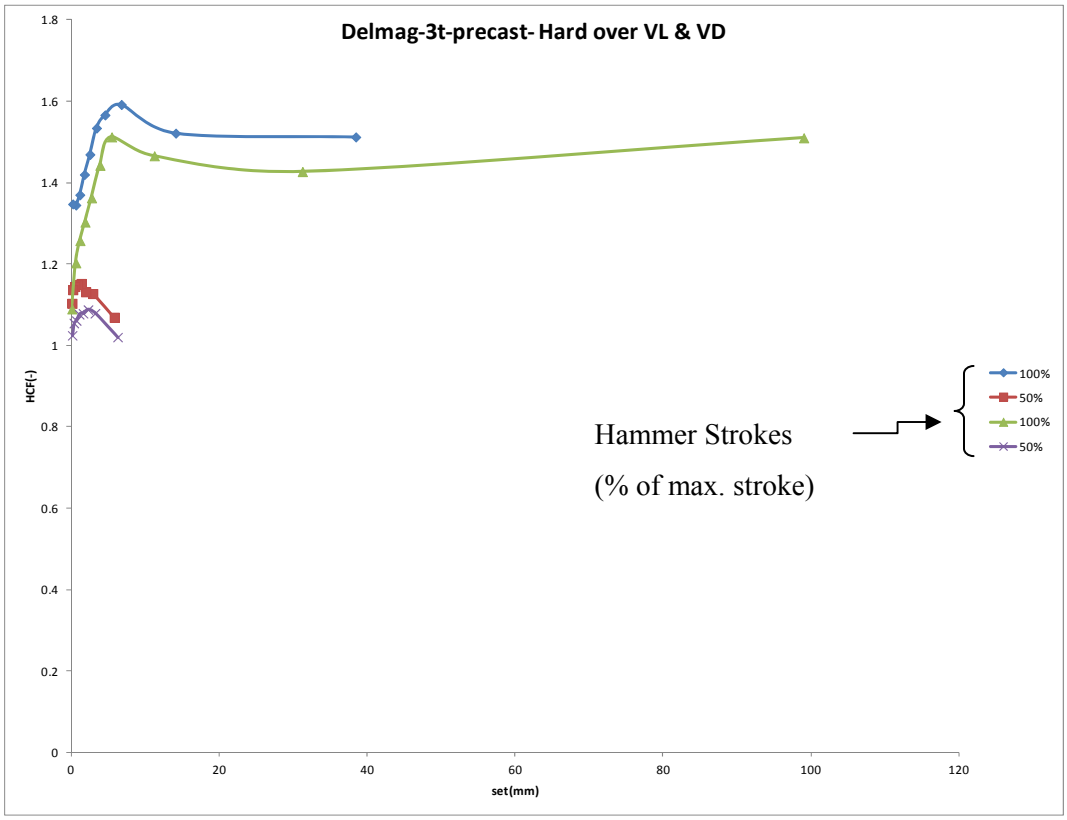
Delmag-3t-precast- Hard over VL & VD
HCF(-)
set(mm)
Hammer Strokes
(% of max. stroke)
100%
50%
100%
50%

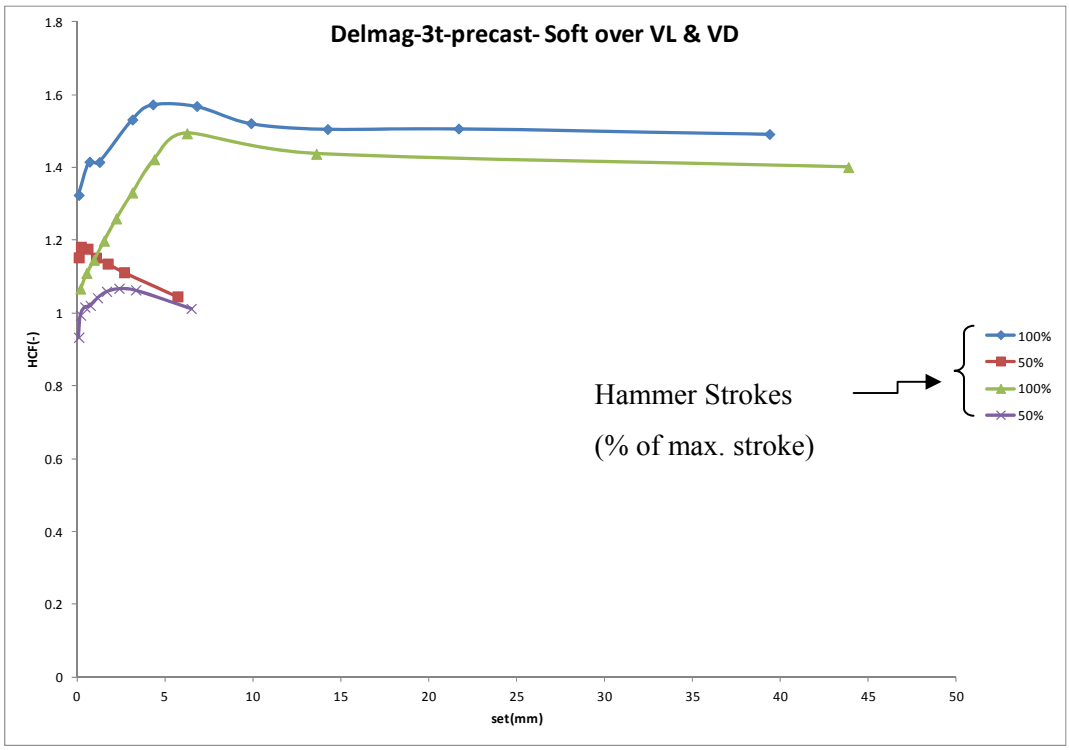
Delmag-3t-precast- Soft over VL & VD
HCF(-)
set(mm)
Hammer Strokes
(% of max. stroke)
100%
50%
100%
50%

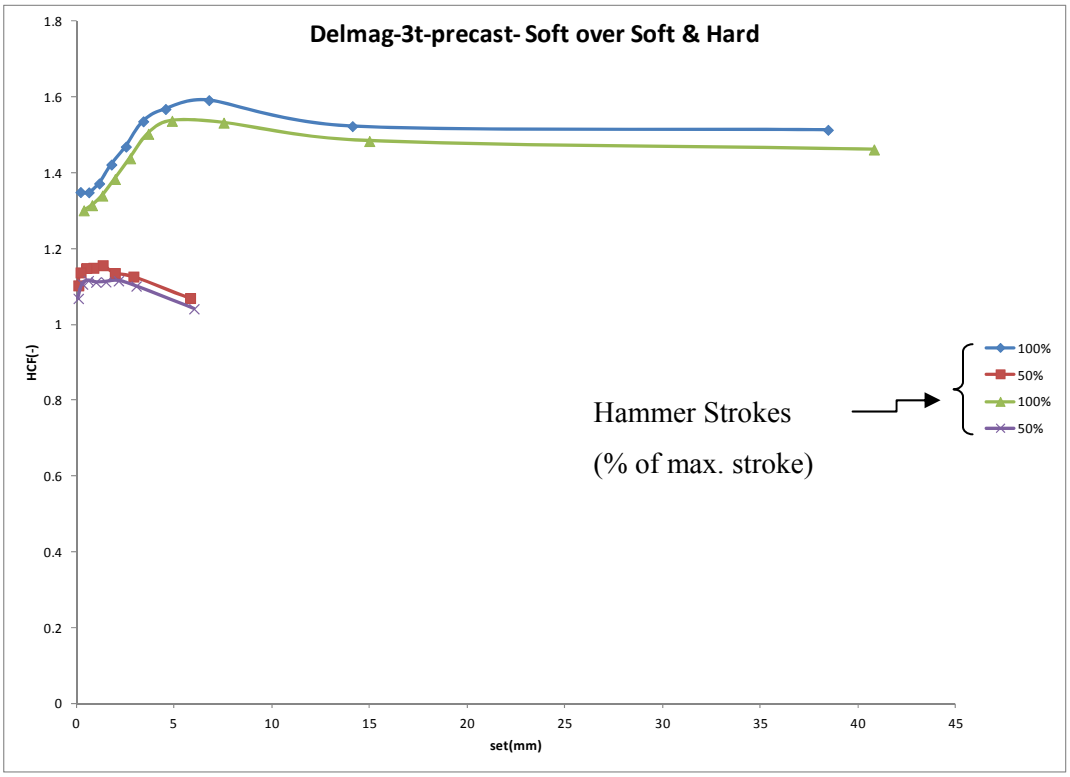
Delmag-3t-precast- Soft over Soft & Hard
HCF(-)
set(mm)
Hammer Strokes
(% of max. stroke)
100%
50%
100%
50%

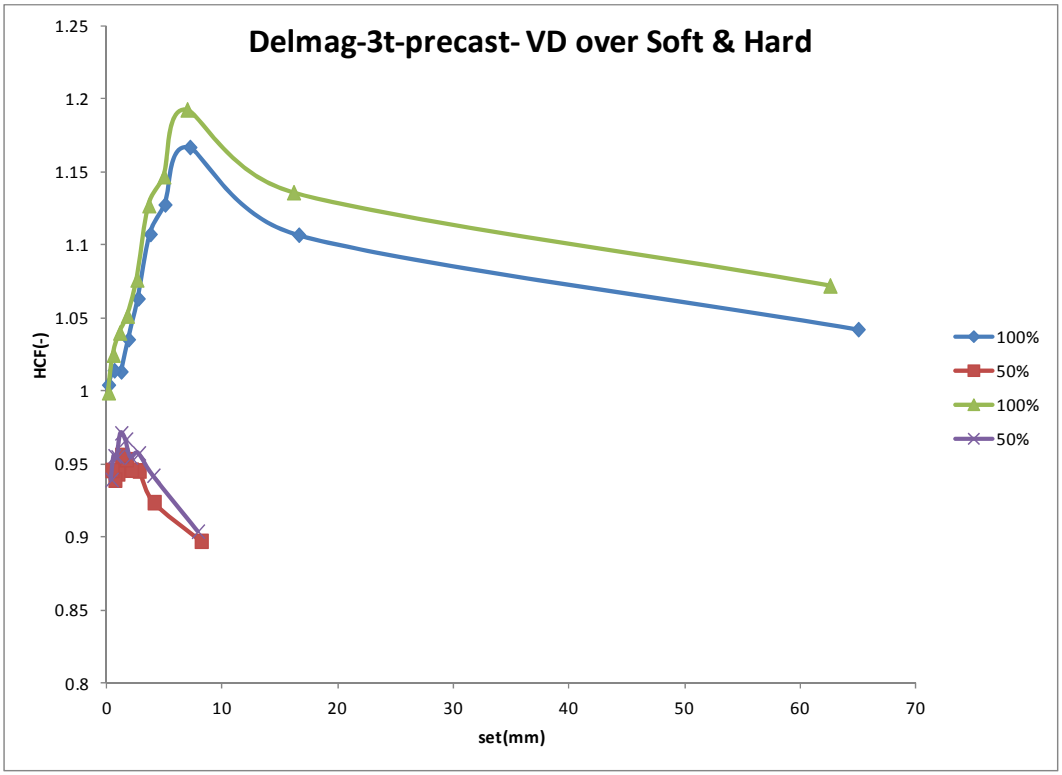
Delmag-3t-precast- VD over Soft & Hard
HCF(-)
set(mm)
100%
50%
100%
50%

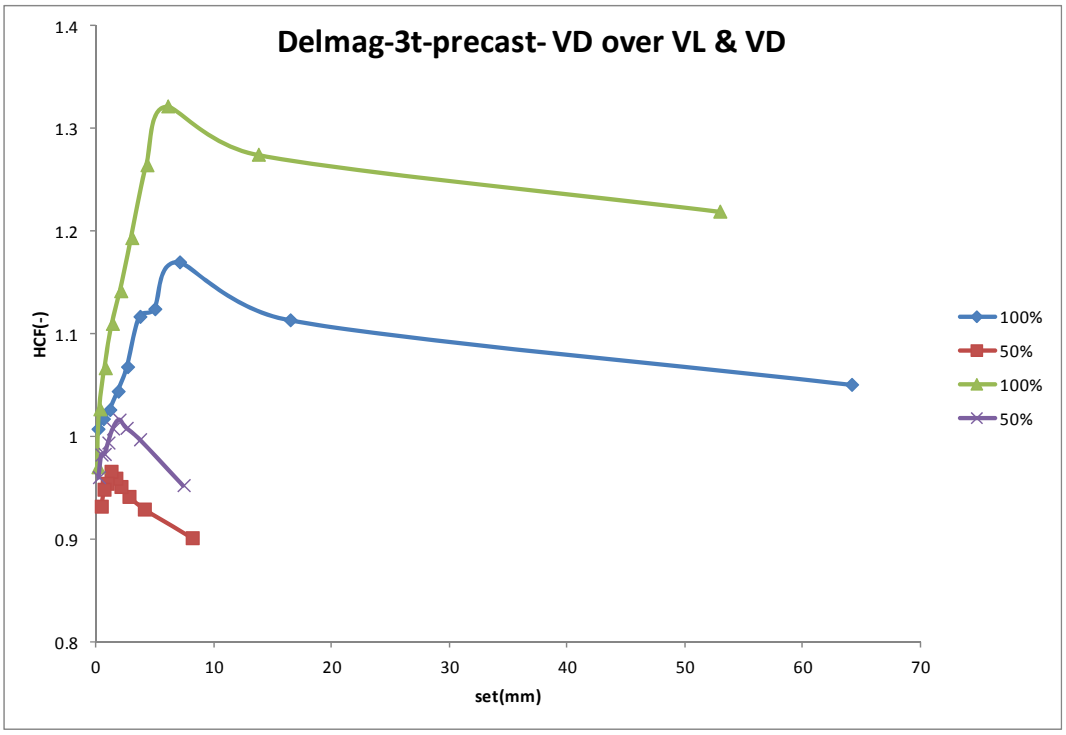
Delmag-3t-precast- VD over VL & VD
HCF(-)
set(mm)
100%
50%
100%
50%

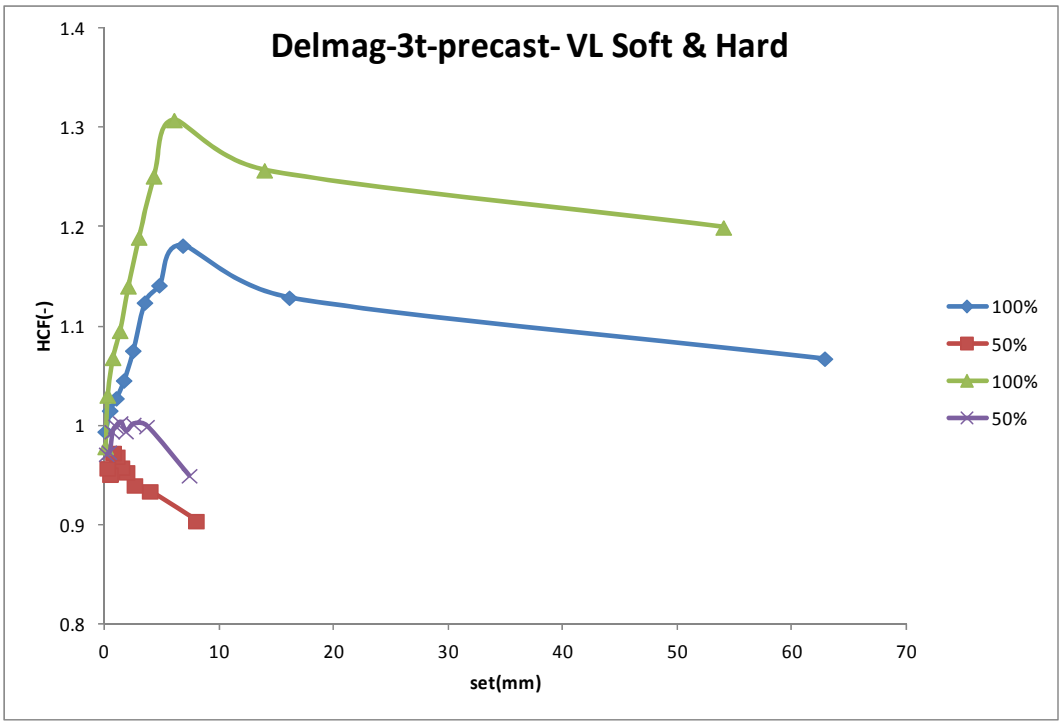
Delmag-3t-precast- VL Soft & Hard
HCF(-)
set(mm)
100%
50%
100%
50%

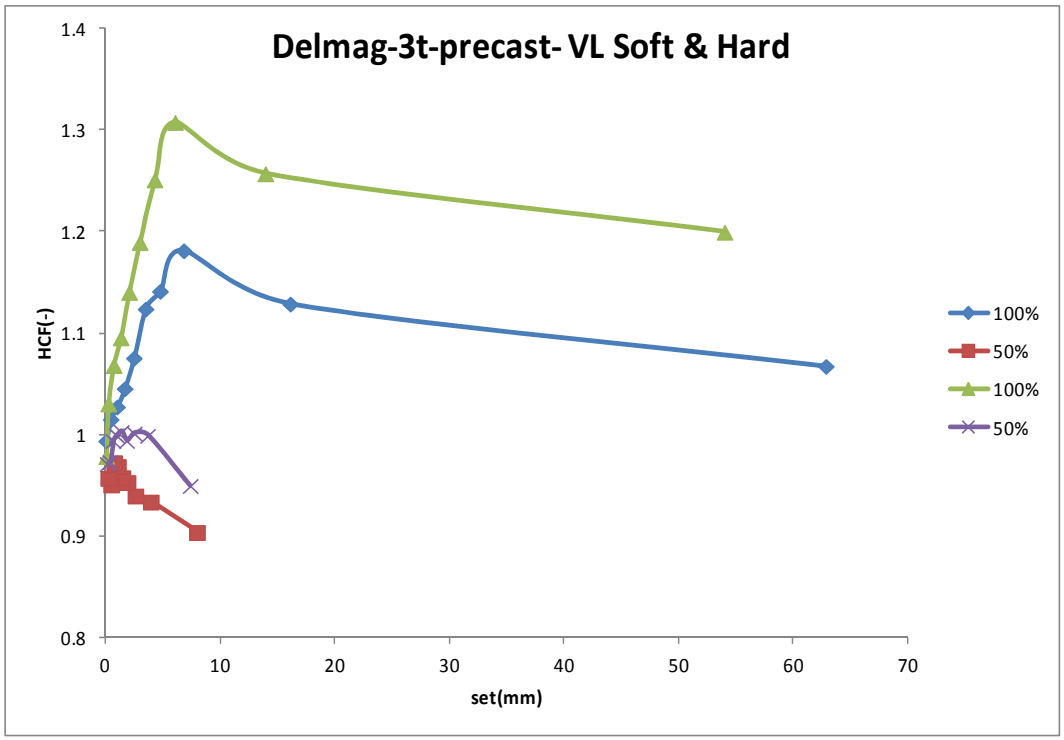
Delmag-3t-precast- VL Soft & Hard
HCF(-)
set(mm)
1.4
1.3
1.2
1.1
1
0.9
0.8
0
10
20
30
40
50
60
70
100%
50%
100%
50%

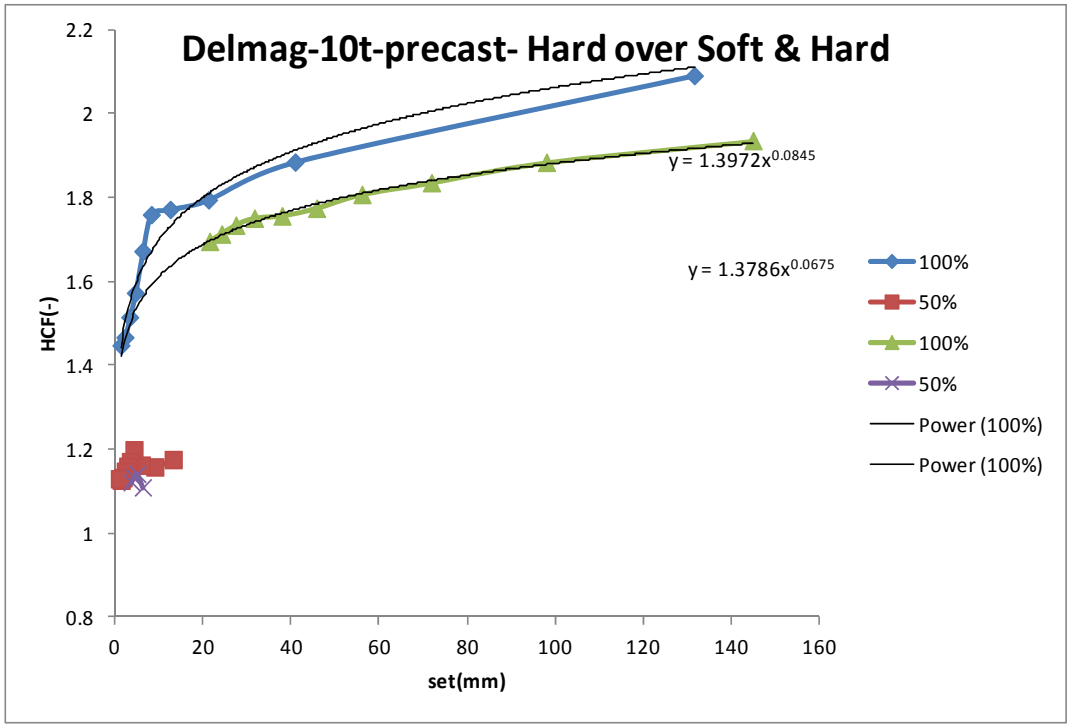
Delmag-10t-precast- Hard over Soft & Hard
HCF(-)
set(mm)
y = 1.3972x^0.0845
y = 1.3786x^0.0675
2.2
2
1.8
1.6
1.4
1.2
1
0.8
0
20
40
60
80
100
120
140
160
100%
50%
100%
50%
Power (100%)
Power (100%)

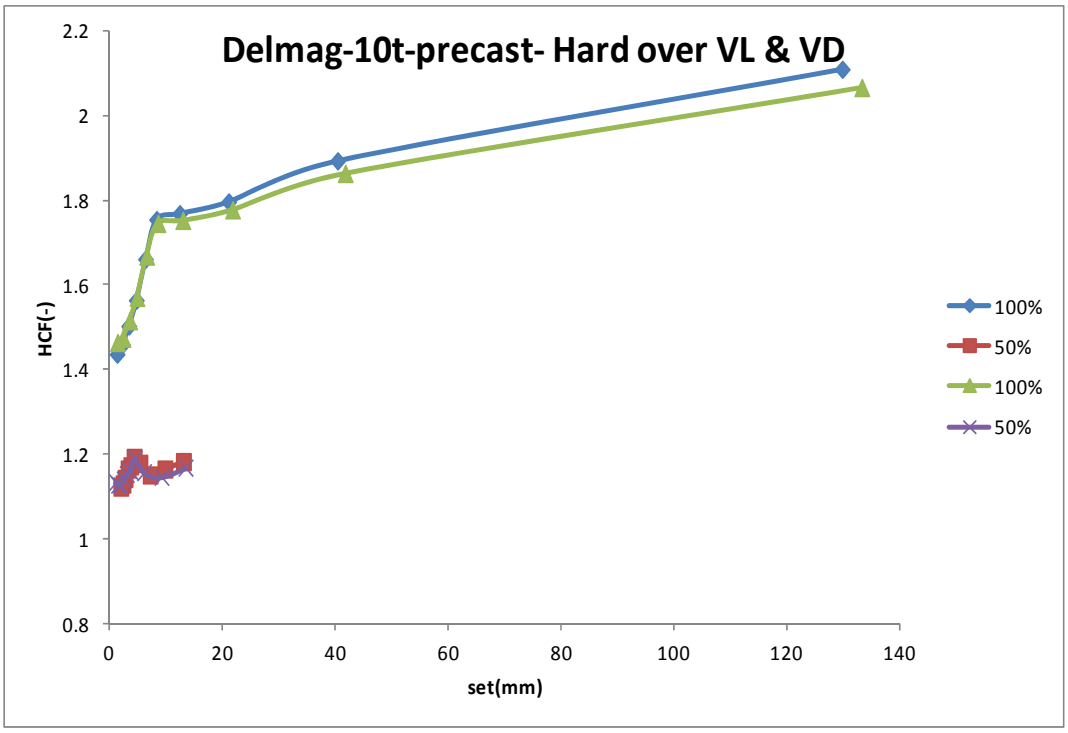
Delmag-10t-precast- Hard over VL & VD
HCF(-)
set(mm)
2.2
2
1.8
1.6
1.4
1.2
1
0.8
0
20
40
60
80
100
120
140
100%
50%
100%
50%

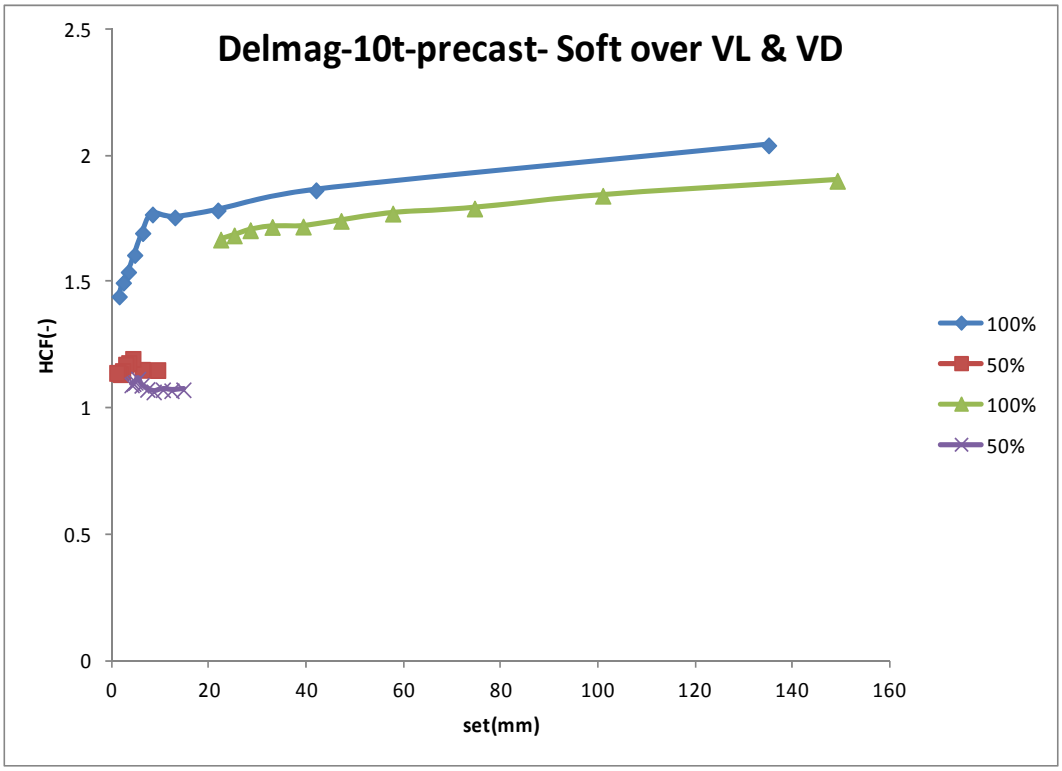
Delmag-10t-precast- Soft over VL & VD
HCF(-)
set(mm)
2.5
2
1.5
1
0.5
0
0
20
40
60
80
100
120
140
160
100%
50%
100%
50%

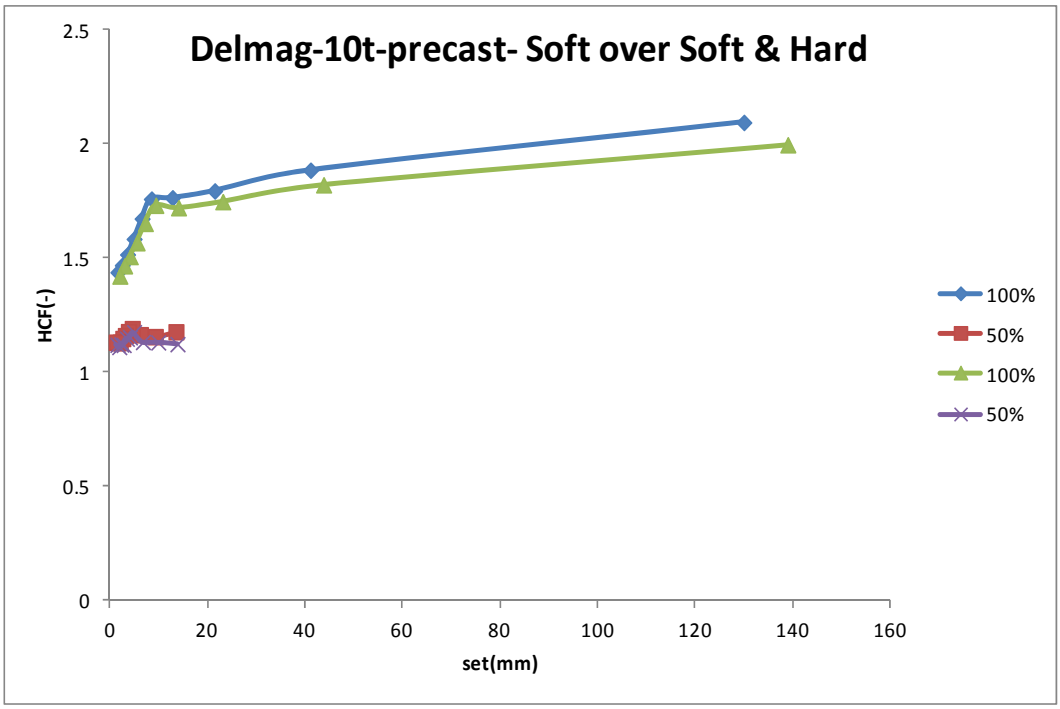
Delmag-10t-precast- Soft over Soft & Hard
HCF(-)
set(mm)
2.5
2
1.5
1
0.5
0
0
20
40
60
80
100
120
140
160
100%
50%
100%
50%

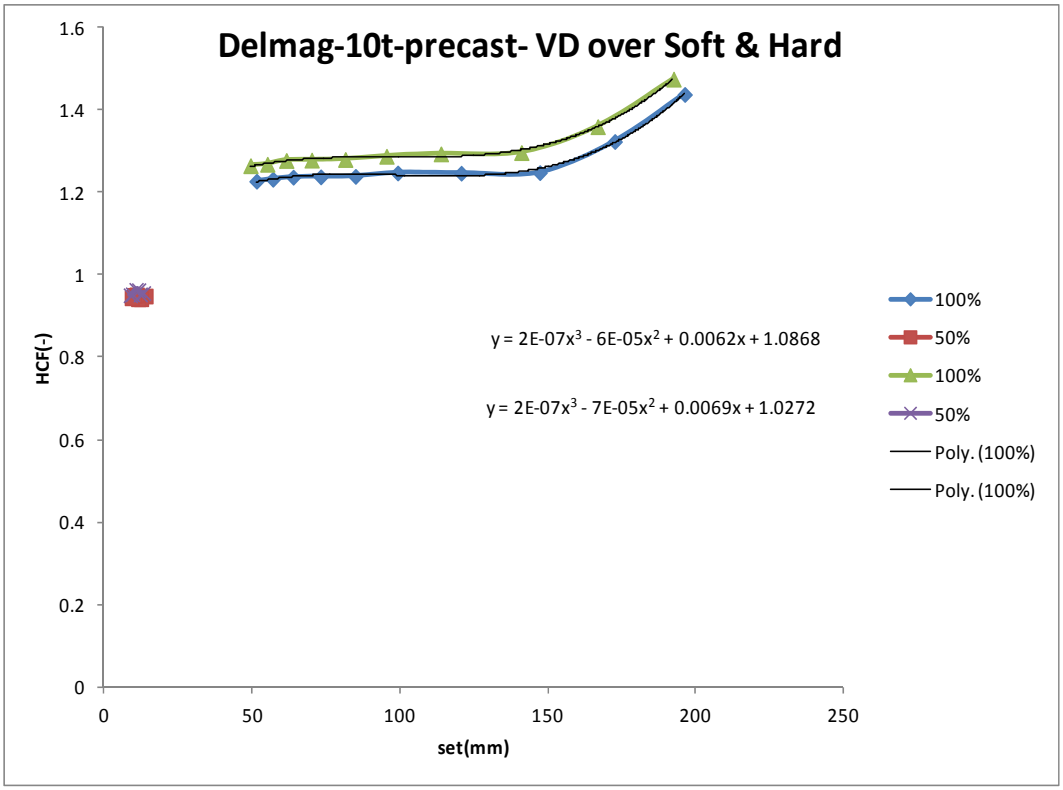
Delmag-10t-precast- VD over Soft & Hard
HCF(-)
set(mm)
1.6
1.4
1.2
1
0.8
0.6
0.4
0.2
0
0
50
100
150
200
250
y = 2E-07x³ - 6E-05x² + 0.0062x + 1.0868
y = 2E-07x³ - 7E-05x² + 0.0069x + 1.0272
100%
50%
100%
50%
Poly. (100%)
Poly. (100%)

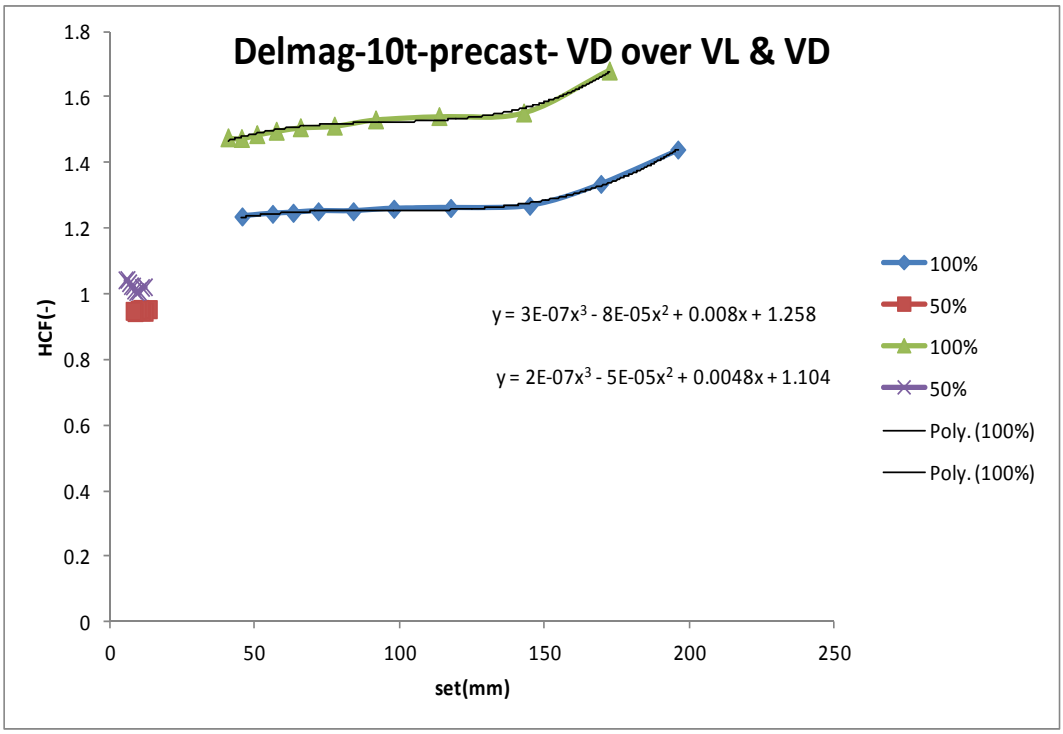
Delmag-10t-precast- VD over VL & VD
HCF(-)
set(mm)
y = 3E-07x³ - 8E-05x² + 0.008x + 1.258
y = 2E-07x³ - 5E-05x² + 0.0048x + 1.104
100%
50%
100%
50%
Poly. (100%)
Poly. (100%)

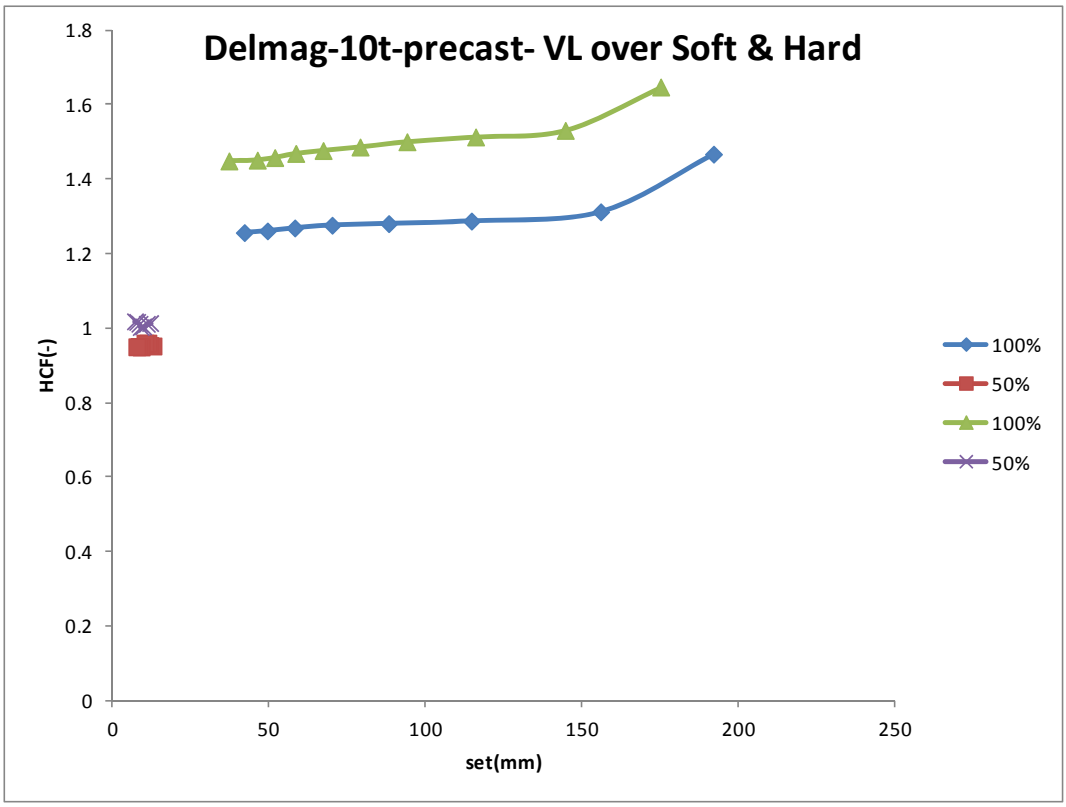
Delmag-10t-precast- VL over Soft & Hard
HCF(-)
set(mm)
100%
50%
100%
50%

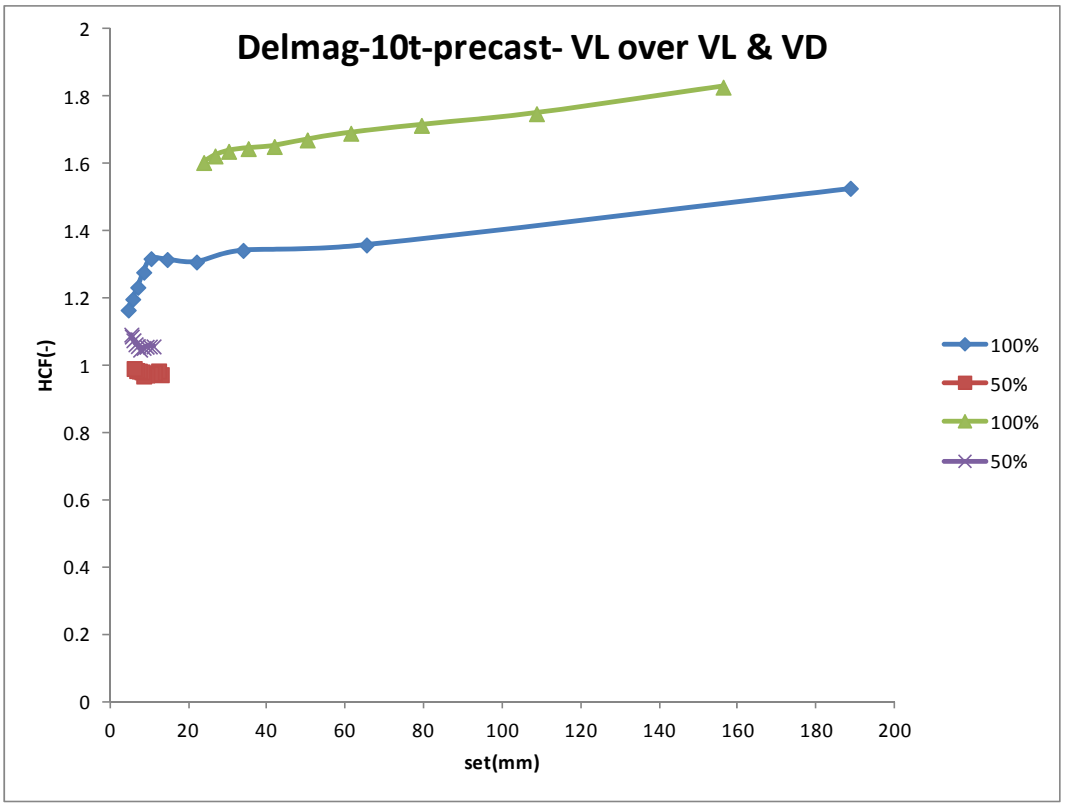
Delmag-10t-precast- VL over VL & VD
HCF(-)
set(mm)
100%
50%
100%
50%

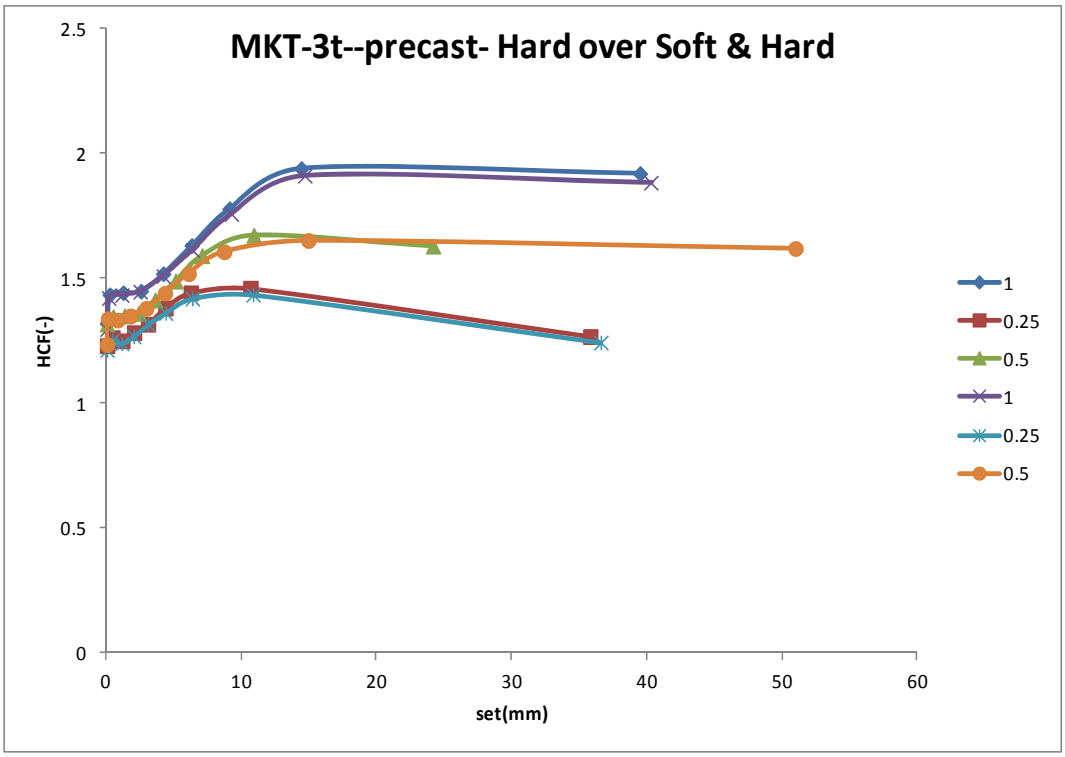
MKT-3t--precast- Hard over Soft & Hard
HCF(-)
set(mm)
1
0.25
0.5
1
0.25
0.5

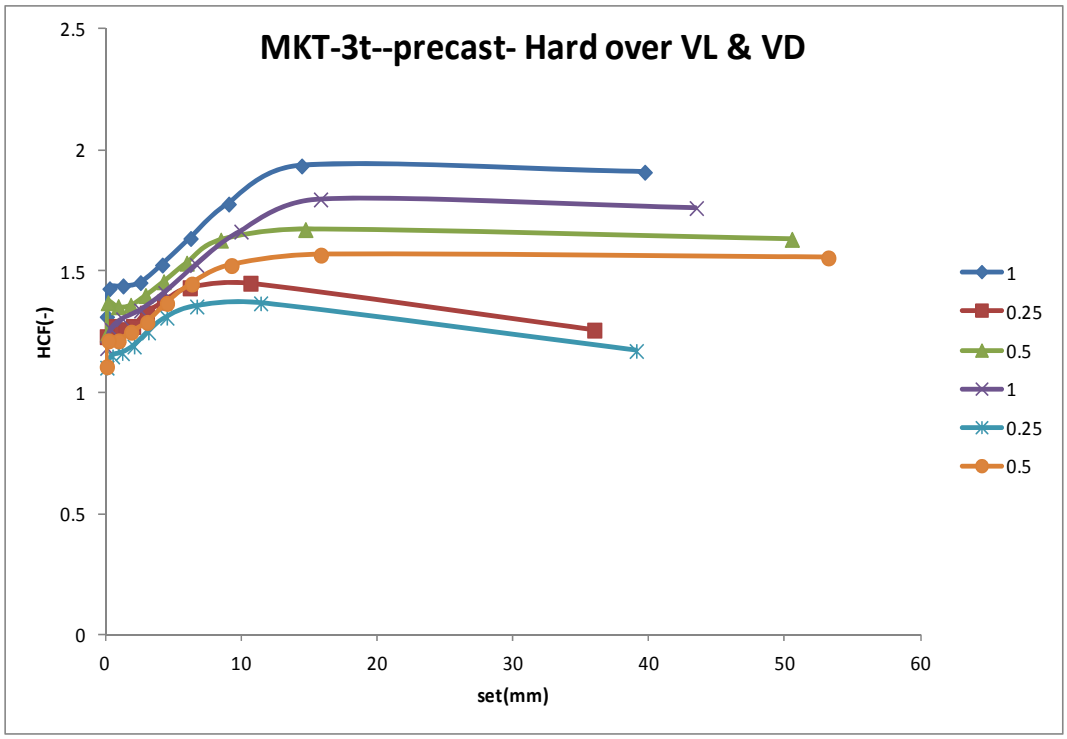
MKT-3t--precast- Hard over VL & VD
HCF(-)
set(mm)
2.5
2
1.5
1
0.5
0
0
10
20
30
40
50
60
1
0.25
0.5
1
0.25
0.5

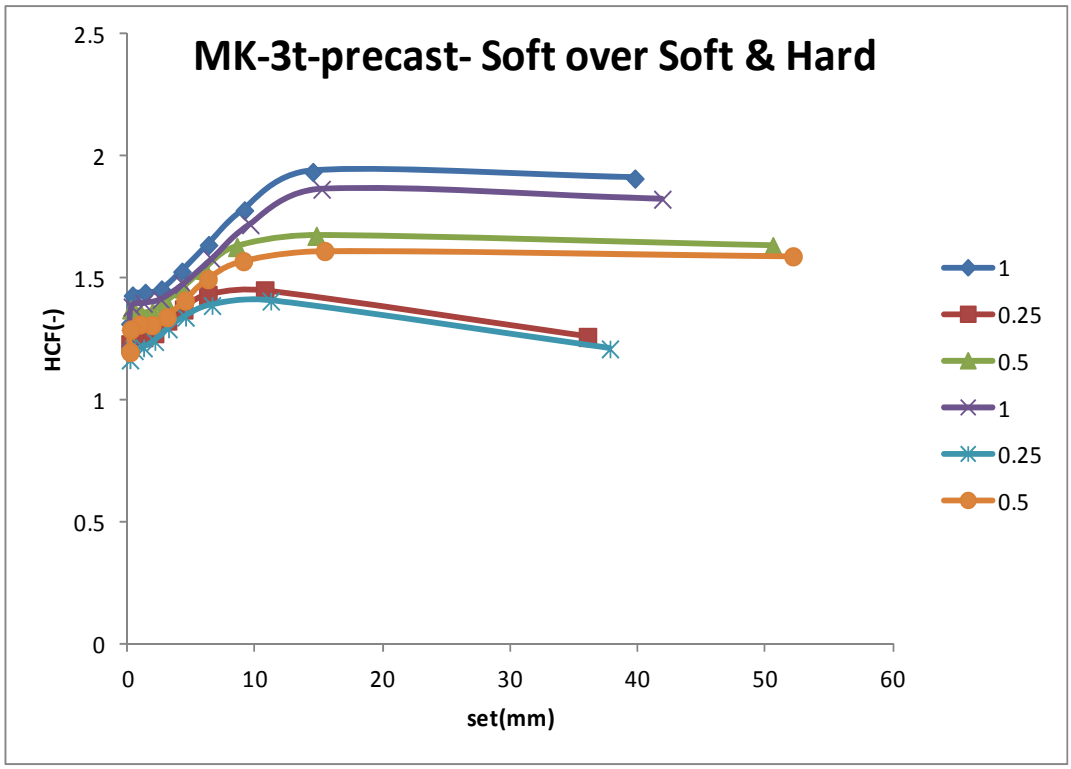
MK-3t-precast- Soft over Soft & Hard
HCF(-)
set(mm)
2.5
2
1.5
1
0.5
0
0
10
20
30
40
50
60
1
0.25
0.5
1
0.25
0.5

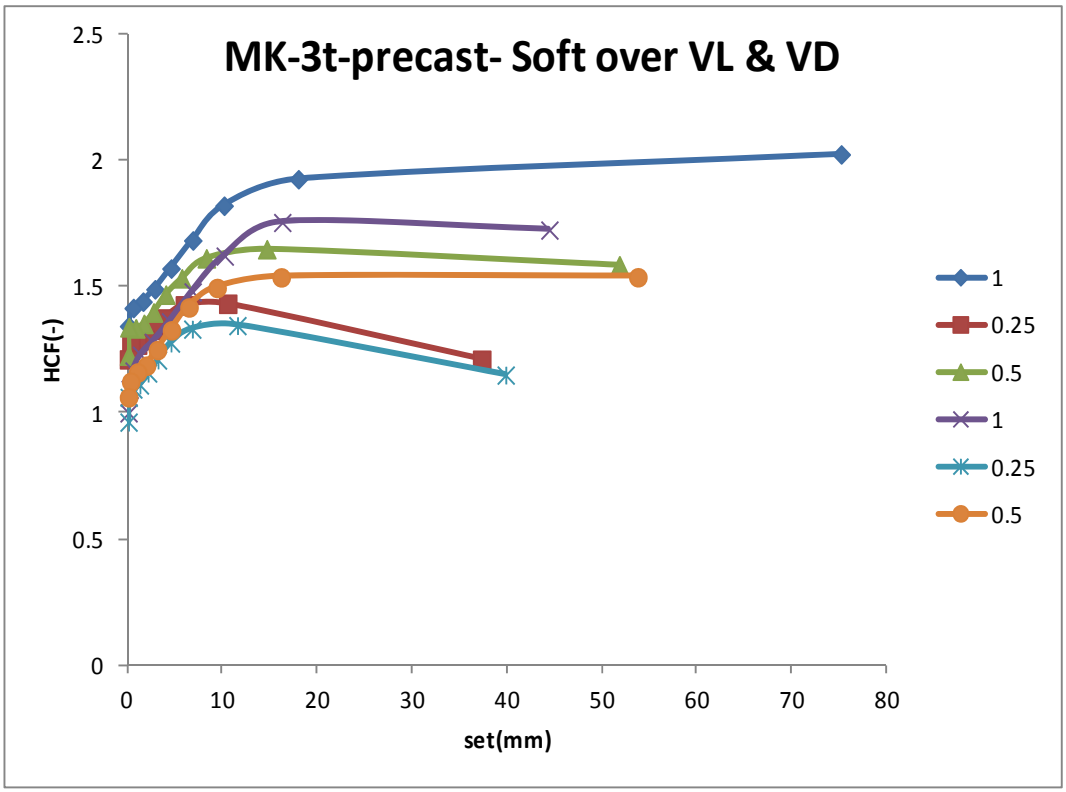
MK-3t-precast- Soft over VL & VD
HCF(-)
set(mm)
2.5
2
1.5
1
0.5
0
0
10
20
30
40
50
60
70
80
1
0.25
0.5
1
0.25
0.5

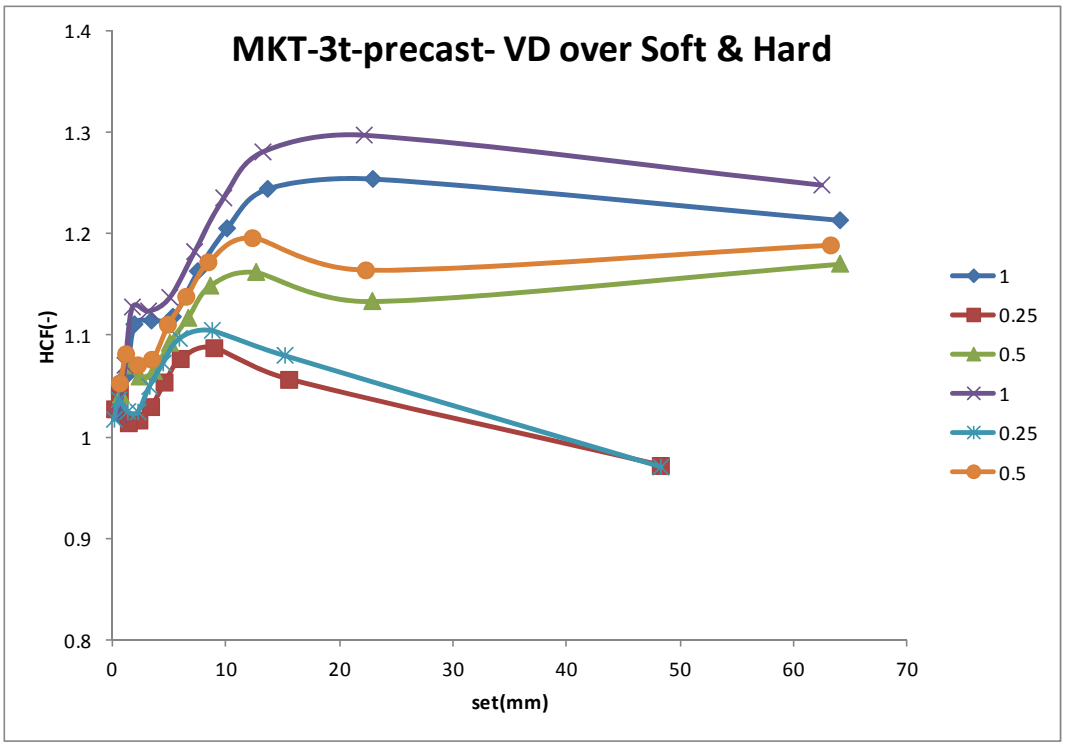
MKT-3t-precast- VD over Soft & Hard
HCF(-)
set(mm)
1.4
1.3
1.2
1.1
1
0.9
0.8
0
10
20
30
40
50
60
70
1
0.25
0.5
1
0.25
0.5

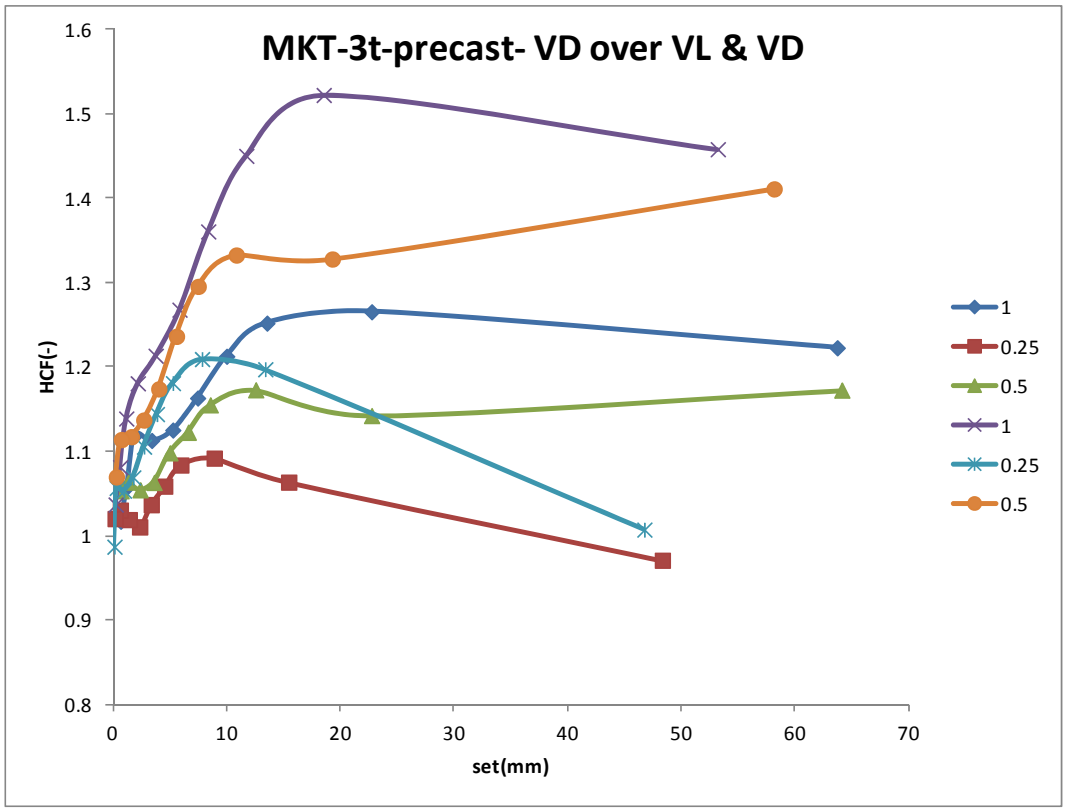
MKT-3t-precast- VD over VL & VD
HCF(-)
set(mm)
1.6
1.5
1.4
1.3
1.2
1.1
1
0.9
0.8
0
10
20
30
40
50
60
70
1
0.25
0.5
1
0.25
0.5

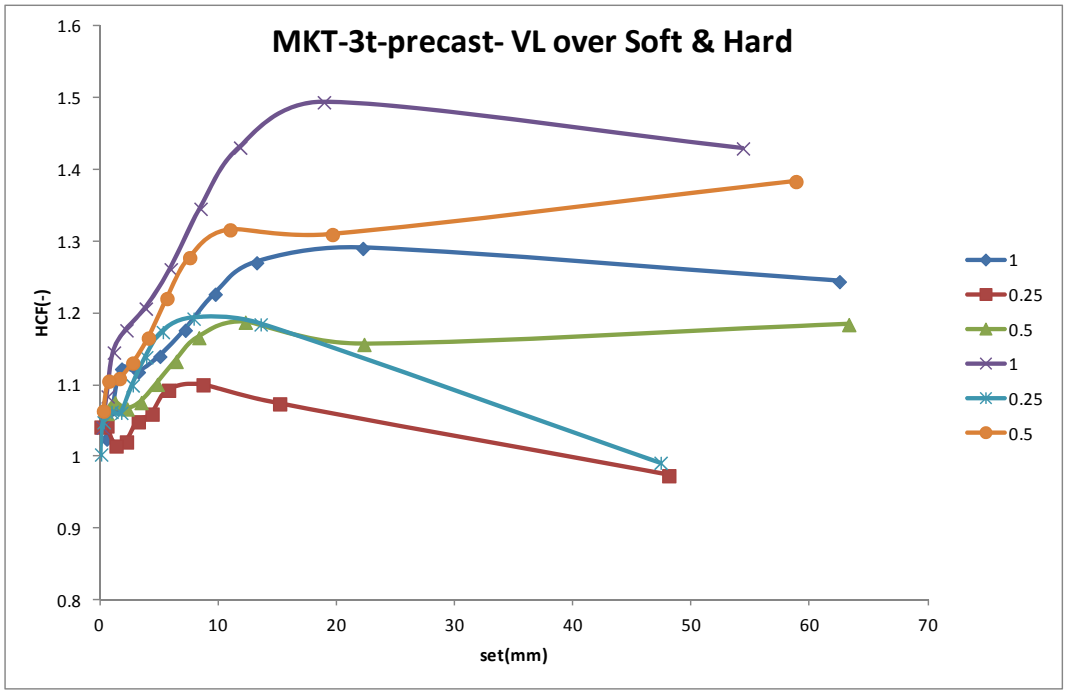
MKT-3t-precast- VL over Soft & Hard
HCF(-)
set(mm)
1.6
1.5
1.4
1.3
1.2
1.1
1
0.9
0.8
0
10
20
30
40
50
60
70
1
0.25
0.5
1
0.25
0.5

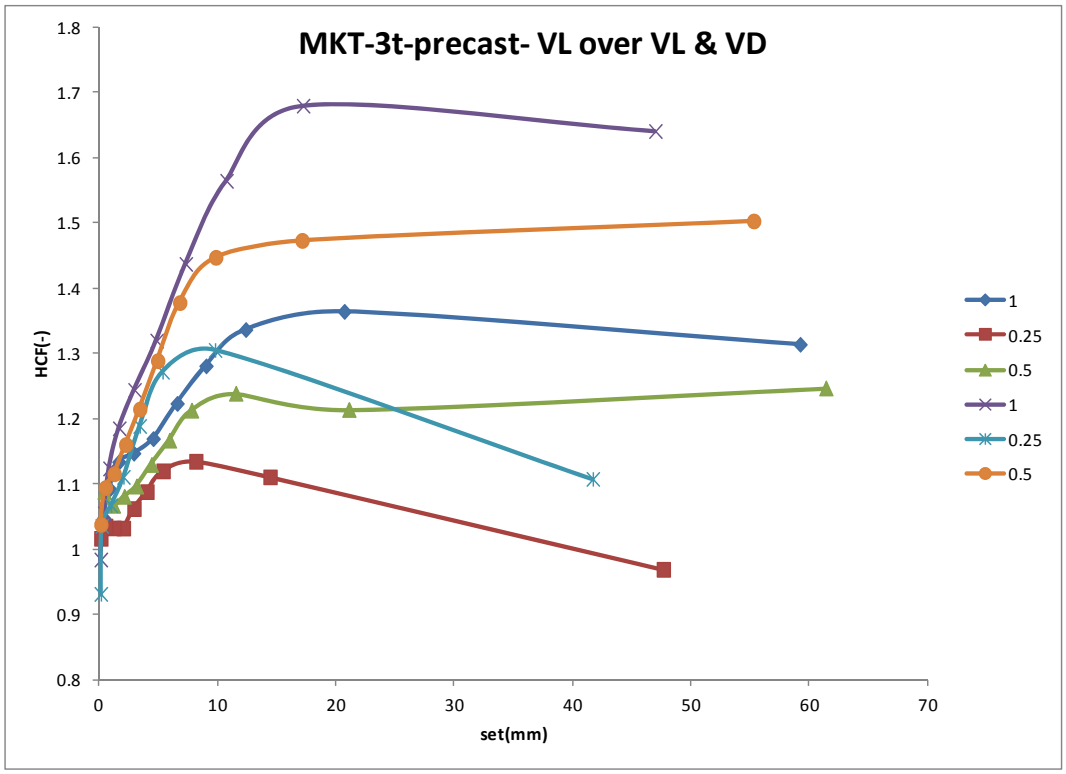
MKT-3t-precast- VL over VL & VD
HCF(-)
set(mm)
1
0.25
0.5
1
0.25
0.5

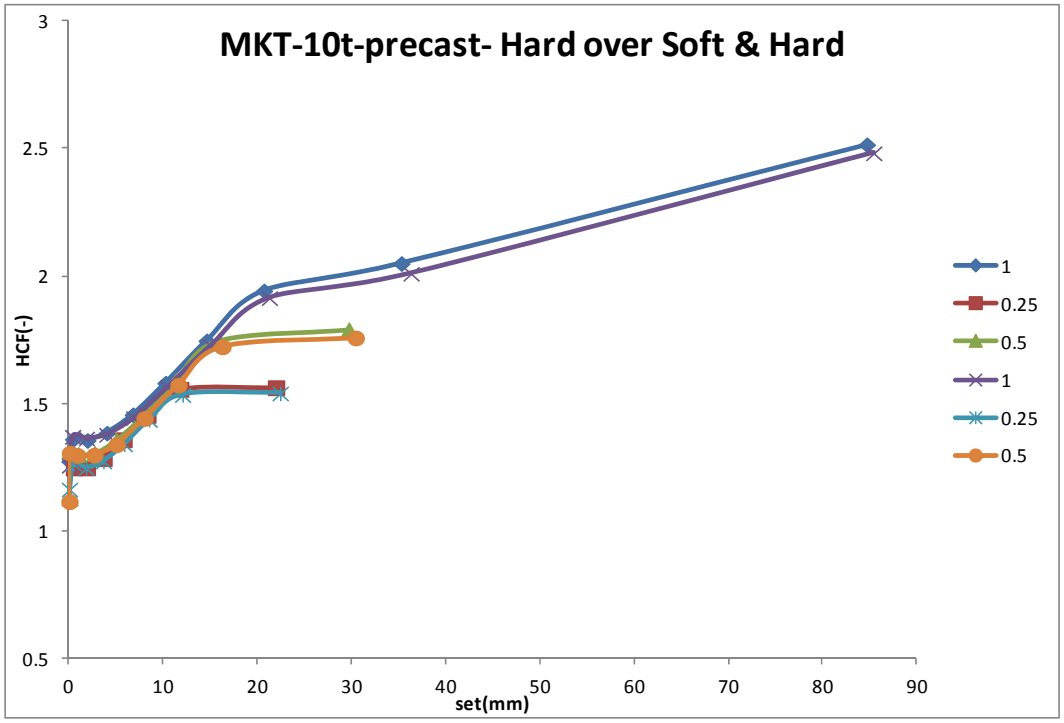
MKT-10t-precast- Hard over Soft & Hard
HCF(-)
set(mm)
1
0.25
0.5
1
0.25
0.5

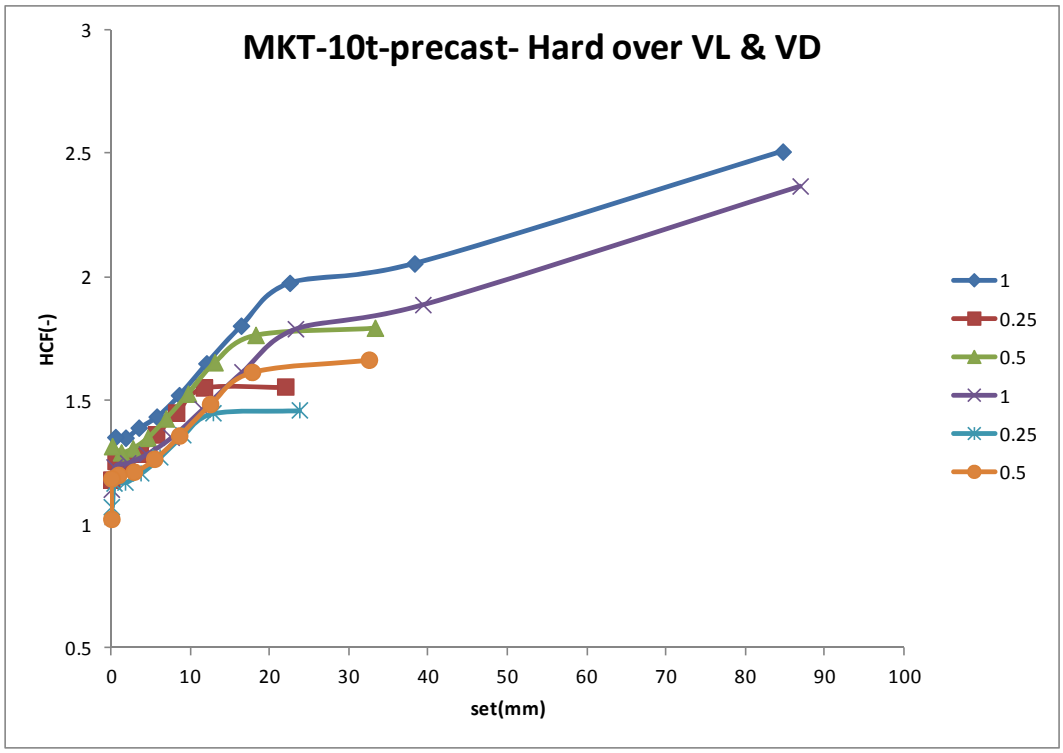
MKT-10t-precast- Hard over VL & VD
HCF(-)
set(mm)
3
2.5
2
1.5
1
0.5
0
10
20
30
40
50
60
70
80
90
100
1
0.25
0.5
1
0.25
0.5

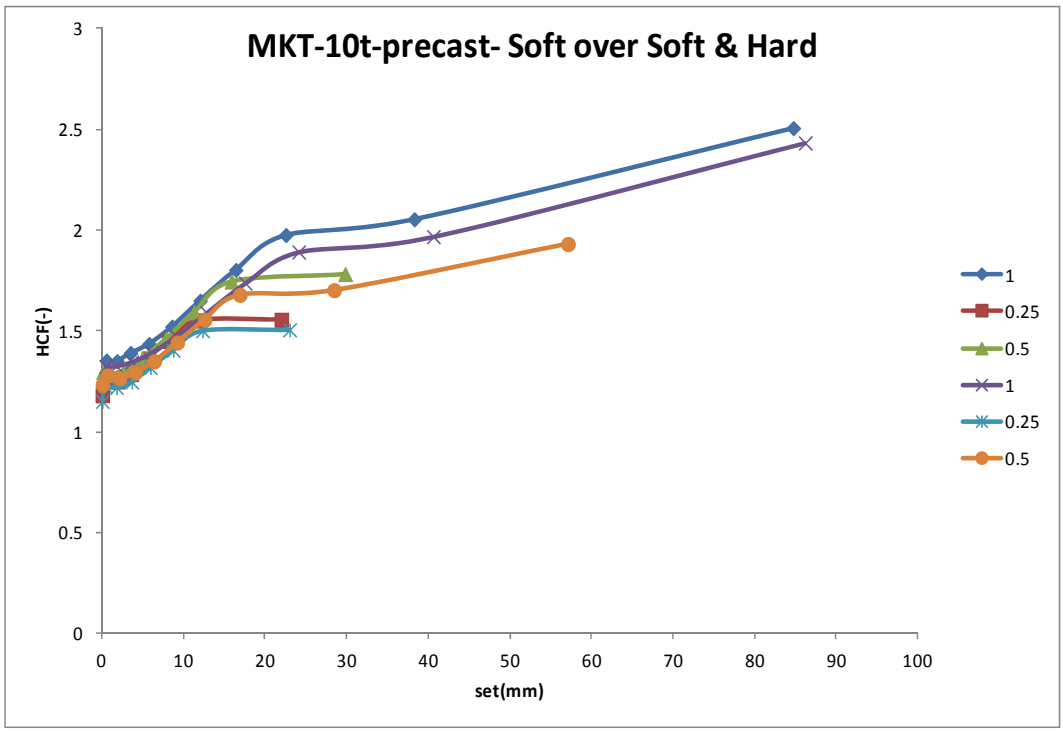
MKT-10t-precast- Soft over Soft & Hard
HCF(-)
set(mm)
3
2.5
2
1.5
1
0.5
0
10
20
30
40
50
60
70
80
90
100
1
0.25
0.5
1
0.25
0.5

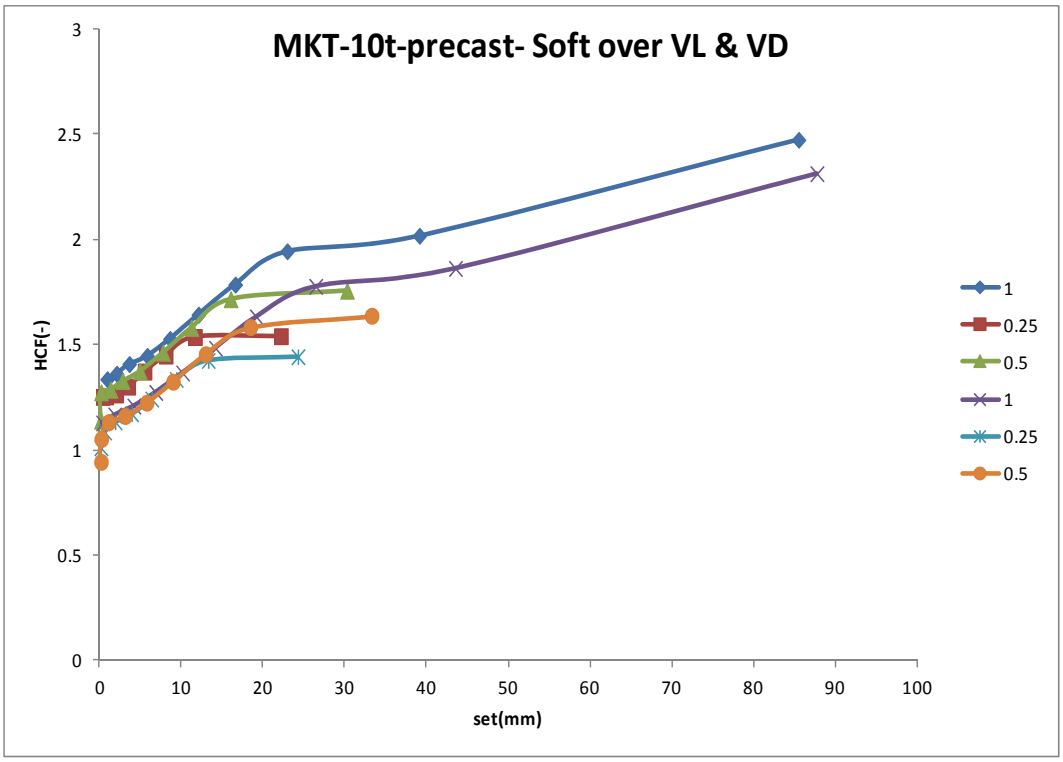
MKT-10t-precast- Soft over VL & VD
HCF(-)
set(mm)
3
2.5
2
1.5
1
0.5
0
0
10
20
30
40
50
60
70
80
90
100
1
0.25
0.5
1
0.25
0.5

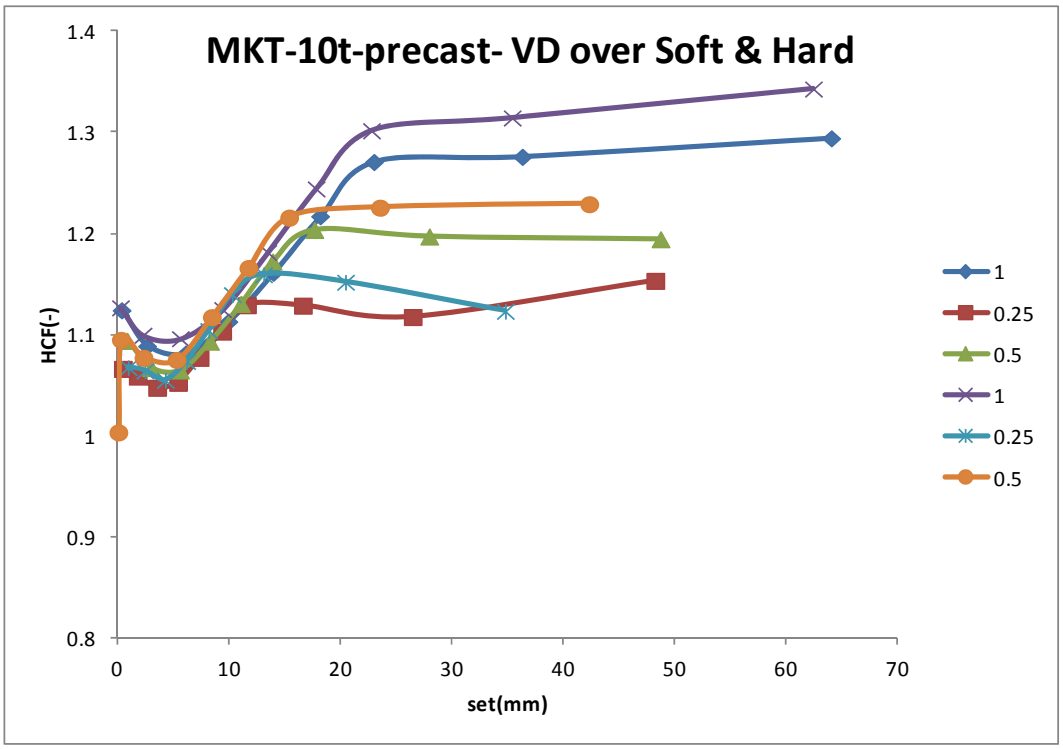
MKT-10t-precast- VD over Soft & Hard
HCF(-)
set(mm)
1.4
1.3
1.2
1.1
1
0.9
0.8
0
10
20
30
40
50
60
70
1
0.25
0.5
1
0.25
0.5

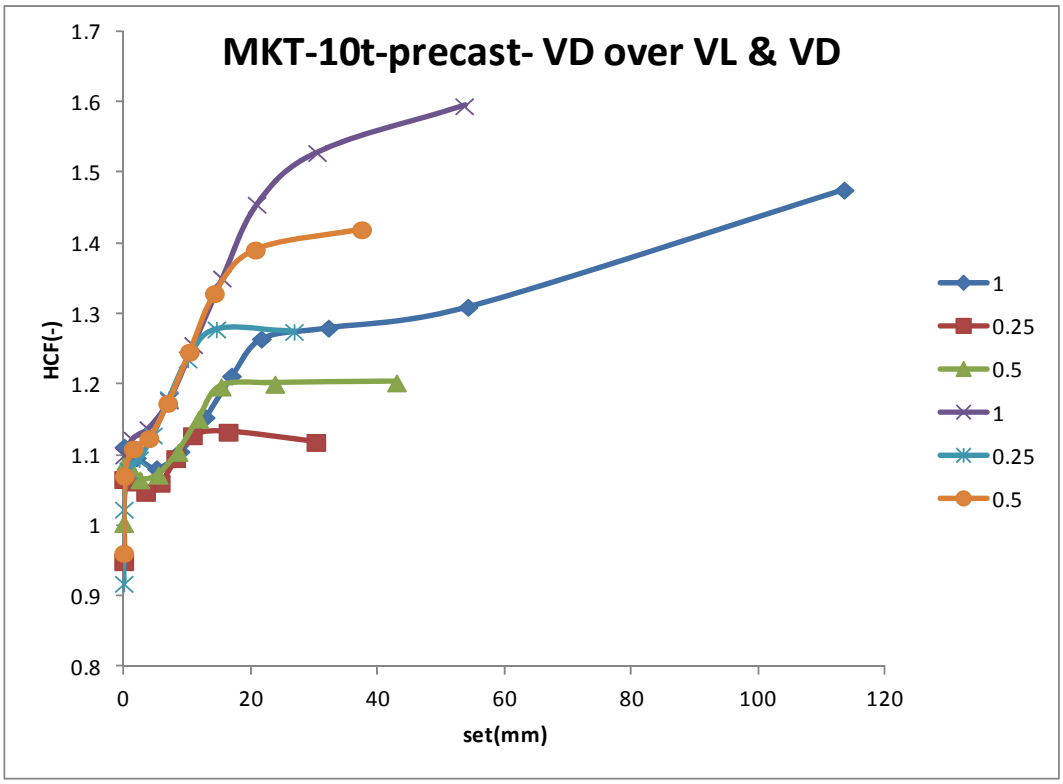
MKT-10t-precast- VD over VL & VD
HCF(-)
set(mm)
1.7
1.6
1.5
1.4
1.3
1.2
1.1
1
0.9
0.8
0
20
40
60
80
100
120
1
0.25
0.5
1
0.25
0.5

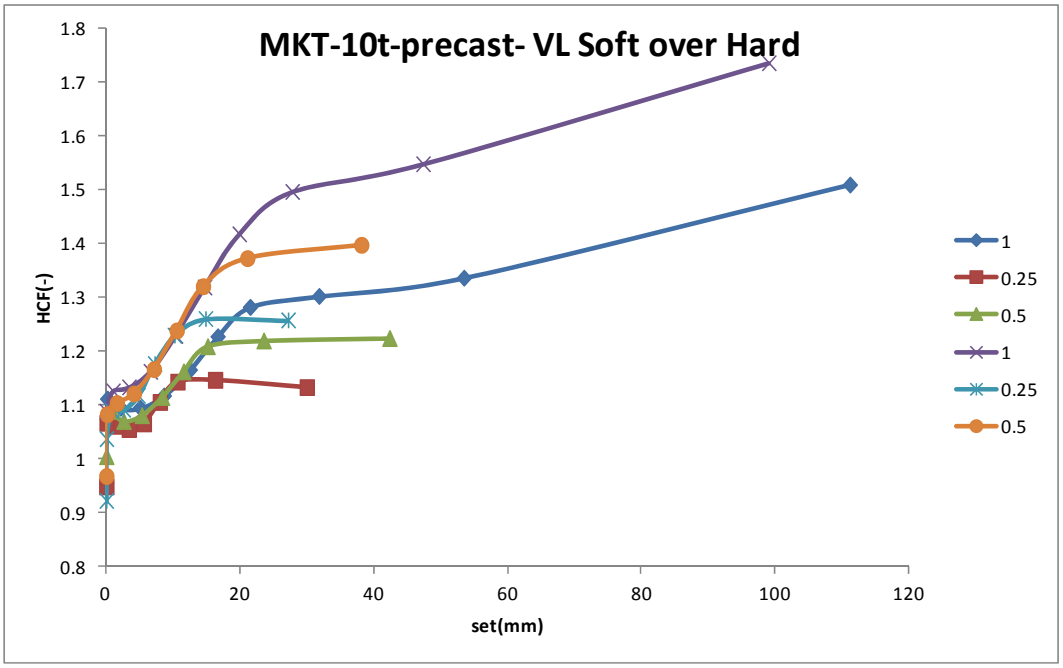
MKT-10t-precast- VL Soft over Hard
HCF(-)
set(mm)
1.8
1.7
1.6
1.5
1.4
1.3
1.2
1.1
1
0.9
0.8
0
20
40
60
80
100
120
1
0.25
0.5
1
0.25
0.5

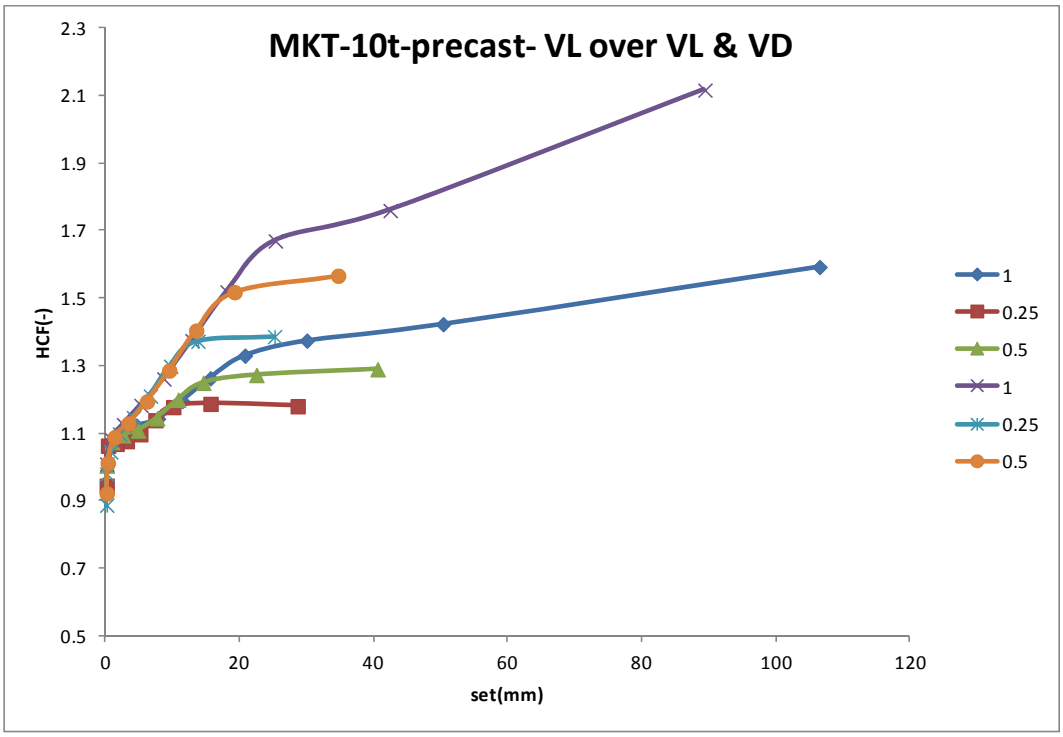

2. *Steel Tube Pile*

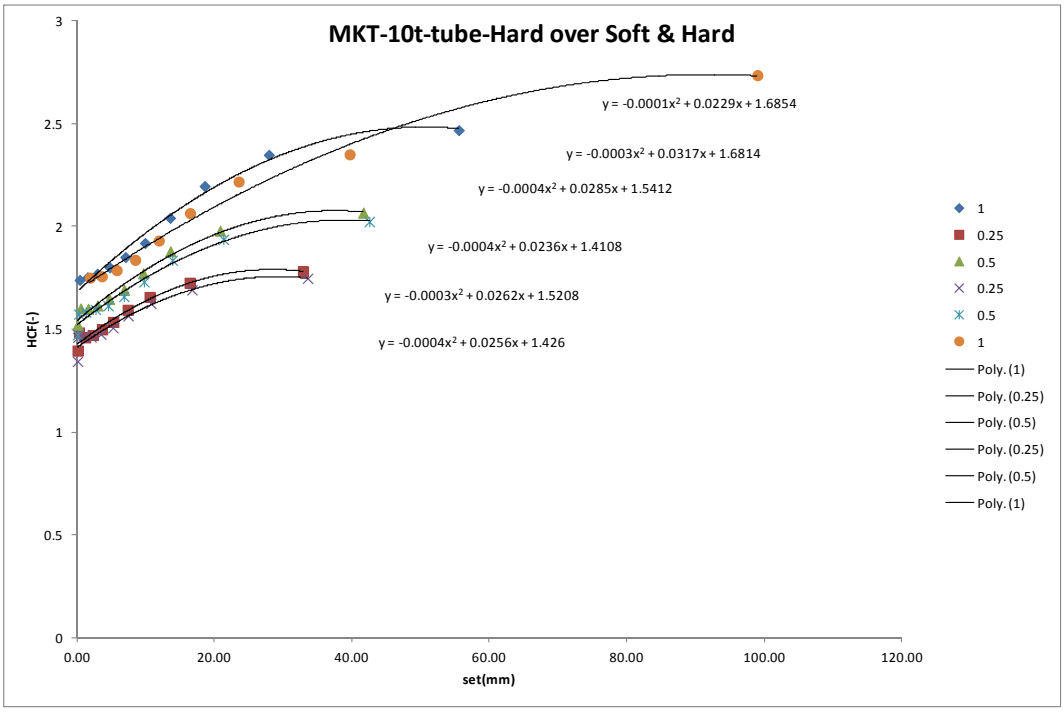

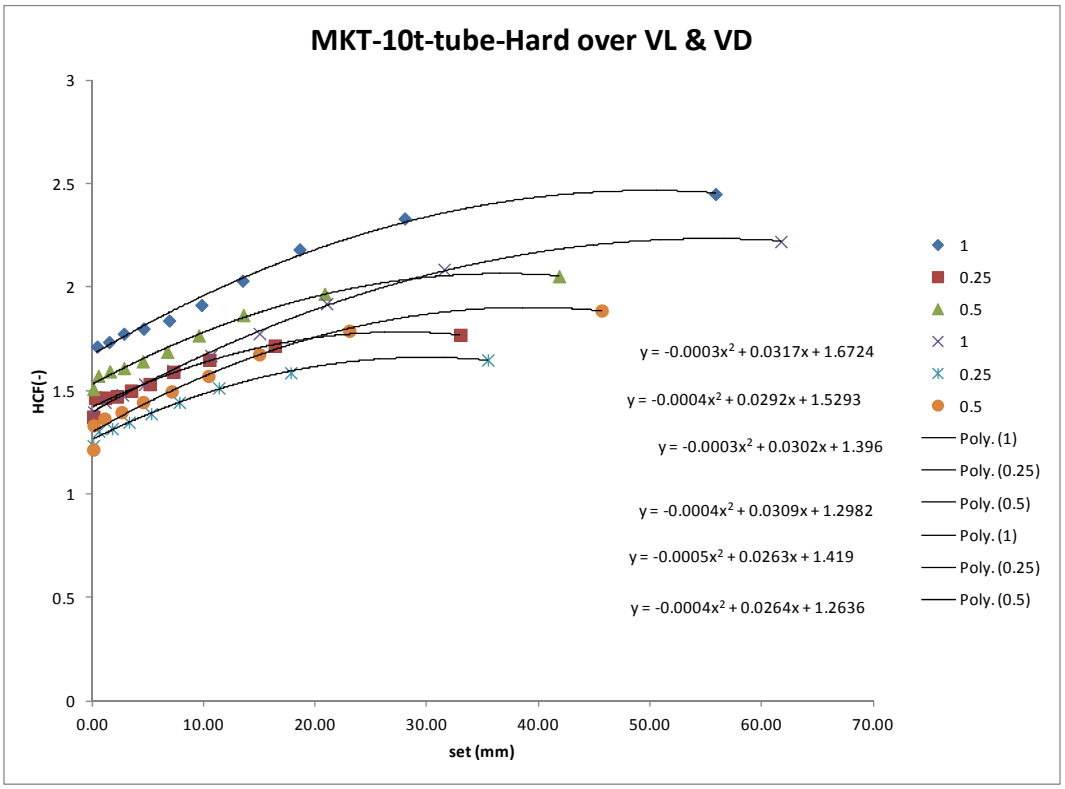
MKT-10t-tube-Hard over VL & VD
HCF(-)
set (mm)
y = -0.0003x² + 0.0317x + 1.6724
y = -0.0004x² + 0.0292x + 1.5293
y = -0.0003x² + 0.0302x + 1.396
y = -0.0004x² + 0.0309x + 1.2982
y = -0.0005x² + 0.0263x + 1.419
y = -0.0004x² + 0.0264x + 1.2636
1
0.25
0.5
1
0.25
0.5
Poly. (1)
Poly. (0.25)
Poly. (0.5)
Poly. (1)
Poly. (0.25)
Poly. (0.5)

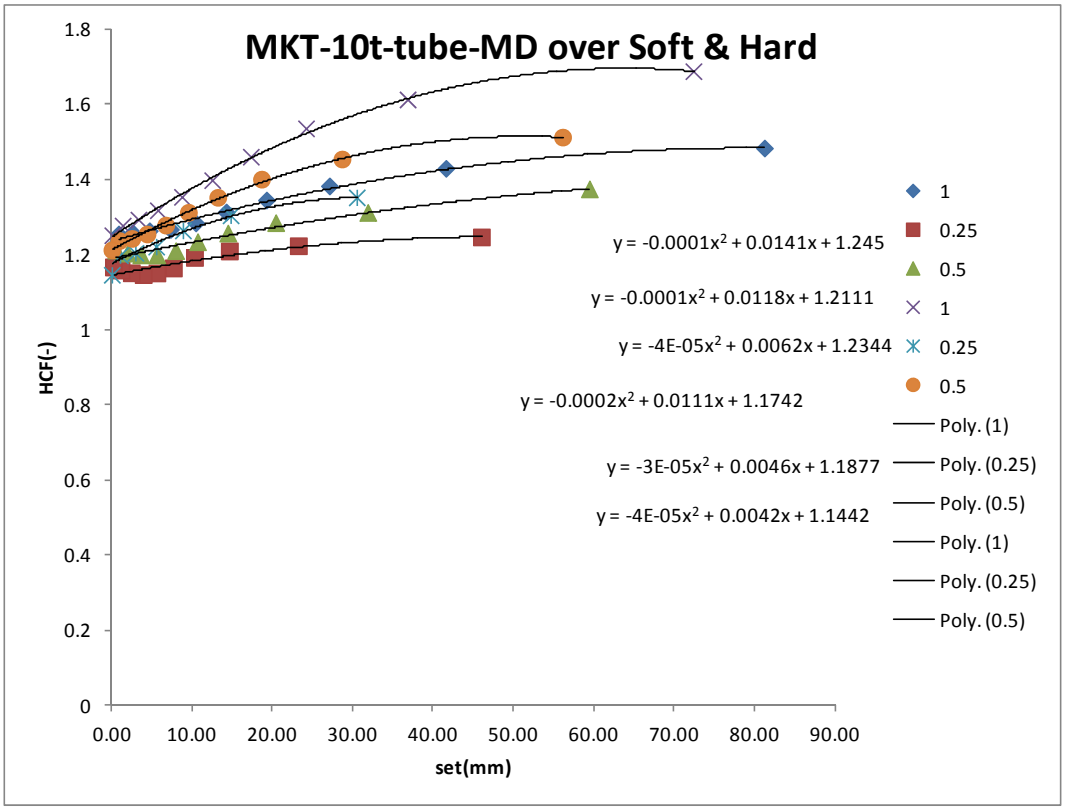
MKT-10t-tube-MD over Soft & Hard
HCF(-)
set(mm)
y = -0.0001x² + 0.0141x + 1.245
y = -0.0001x² + 0.0118x + 1.2111
y = -4E-05x² + 0.0062x + 1.2344
y = -0.0002x² + 0.0111x + 1.1742
y = -3E-05x² + 0.0046x + 1.1877
y = -4E-05x² + 0.0042x + 1.1442
1
0.25
0.5
1
0.25
0.5
Poly. (1)
Poly. (0.25)
Poly. (0.5)
Poly. (1)
Poly. (0.25)
Poly. (0.5)

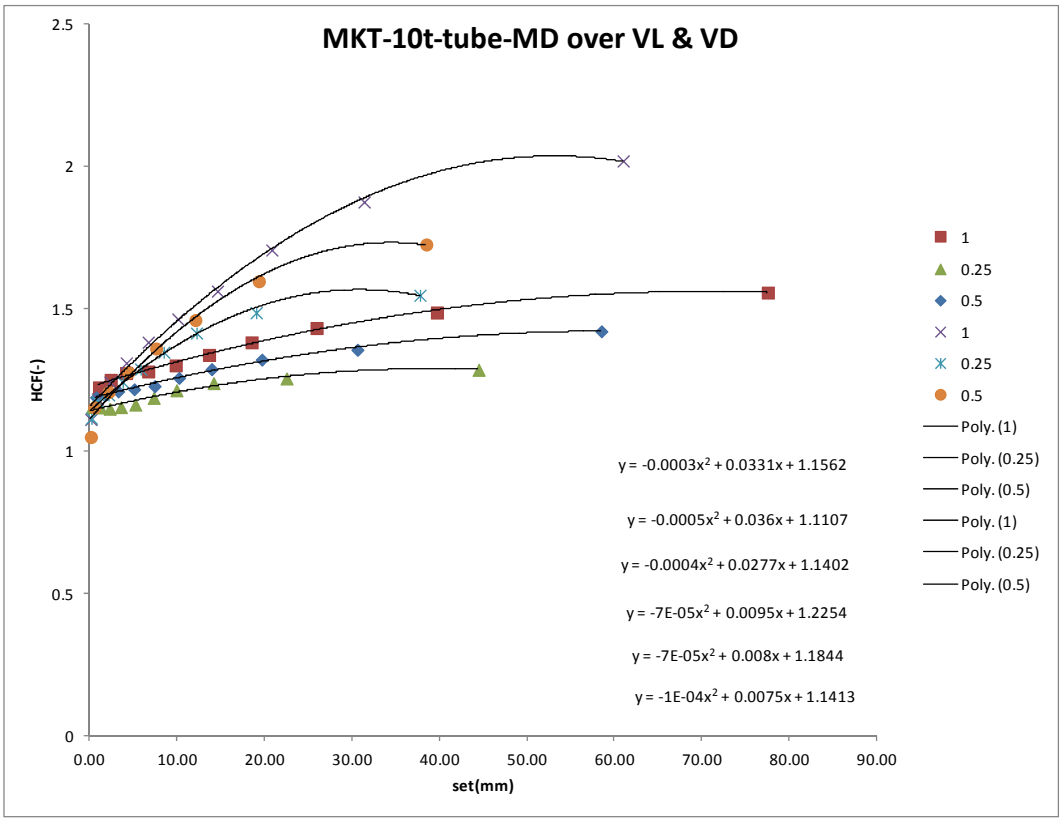
MKT-10t-tube-MD over VL & VD
HCF(-)
set(mm)
y = -0.0003x² + 0.0331x + 1.1562
y = -0.0005x² + 0.036x + 1.1107
y = -0.0004x² + 0.0277x + 1.1402
y = -7E-05x² + 0.0095x + 1.2254
y = -7E-05x² + 0.008x + 1.1844
y = -1E-04x² + 0.0075x + 1.1413
1
0.25
0.5
1
0.25
0.5
Poly. (1)
Poly. (0.25)
Poly. (0.5)
Poly. (1)
Poly. (0.25)
Poly. (0.5)

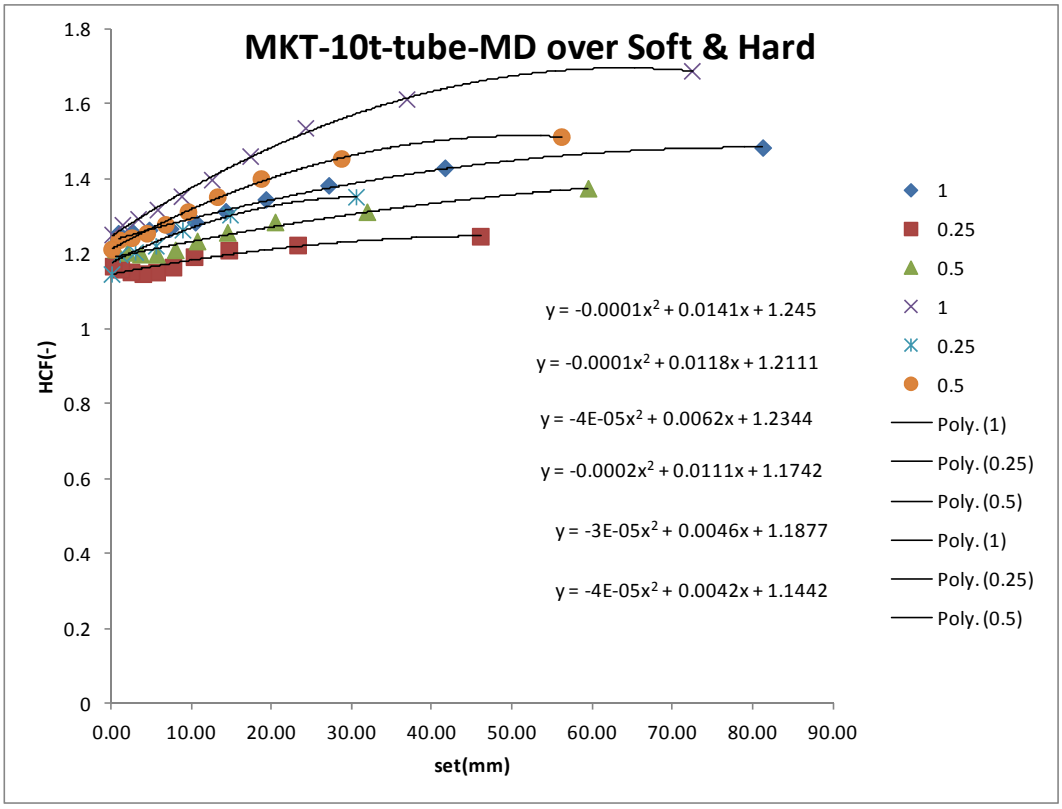
MKT-10t-tube-MD over Soft & Hard
HCF(-)
set(mm)
y = -0.0001x² + 0.0141x + 1.245
y = -0.0001x² + 0.0118x + 1.2111
y = -4E-05x² + 0.0062x + 1.2344
y = -0.0002x² + 0.0111x + 1.1742
y = -3E-05x² + 0.0046x + 1.1877
y = -4E-05x² + 0.0042x + 1.1442
1
0.25
0.5
1
0.25
0.5
Poly. (1)
Poly. (0.25)
Poly. (0.5)
Poly. (1)
Poly. (0.25)
Poly. (0.5)

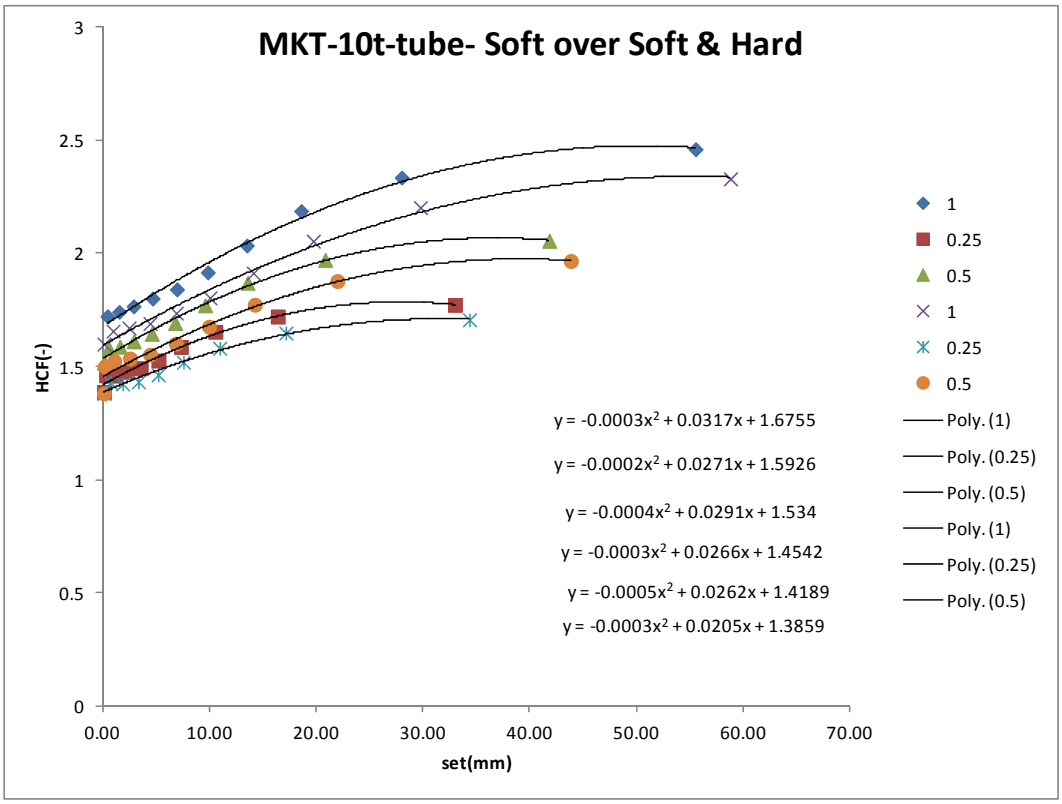
MKT-10t-tube- Soft over Soft & Hard
HCF(-)
set(mm)
y = -0.0003x² + 0.0317x + 1.6755
y = -0.0002x² + 0.0271x + 1.5926
y = -0.0004x² + 0.0291x + 1.534
y = -0.0003x² + 0.0266x + 1.4542
y = -0.0005x² + 0.0262x + 1.4189
y = -0.0003x² + 0.0205x + 1.3859
1
0.25
0.5
1
0.25
0.5
Poly. (1)
Poly. (0.25)
Poly. (0.5)
Poly. (1)
Poly. (0.25)
Poly. (0.5)

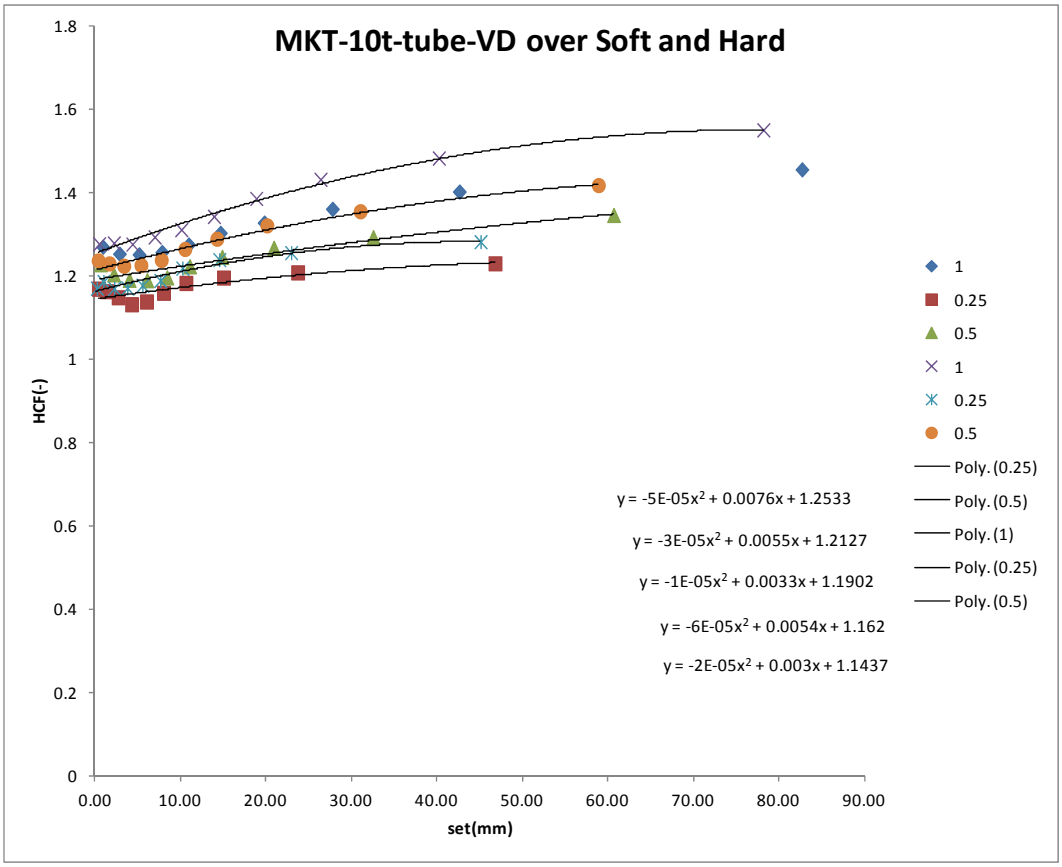
MKT-10t-tube-VD over Soft and Hard
HCF(-)
set(mm)
y = -5E-05x² + 0.0076x + 1.2533
y = -3E-05x² + 0.0055x + 1.2127
y = -1E-05x² + 0.0033x + 1.1902
y = -6E-05x² + 0.0054x + 1.162
y = -2E-05x² + 0.003x + 1.1437
1
0.25
0.5
1
0.25
0.5
Poly. (0.25)
Poly. (0.5)
Poly. (1)
Poly. (0.25)
Poly. (0.5)

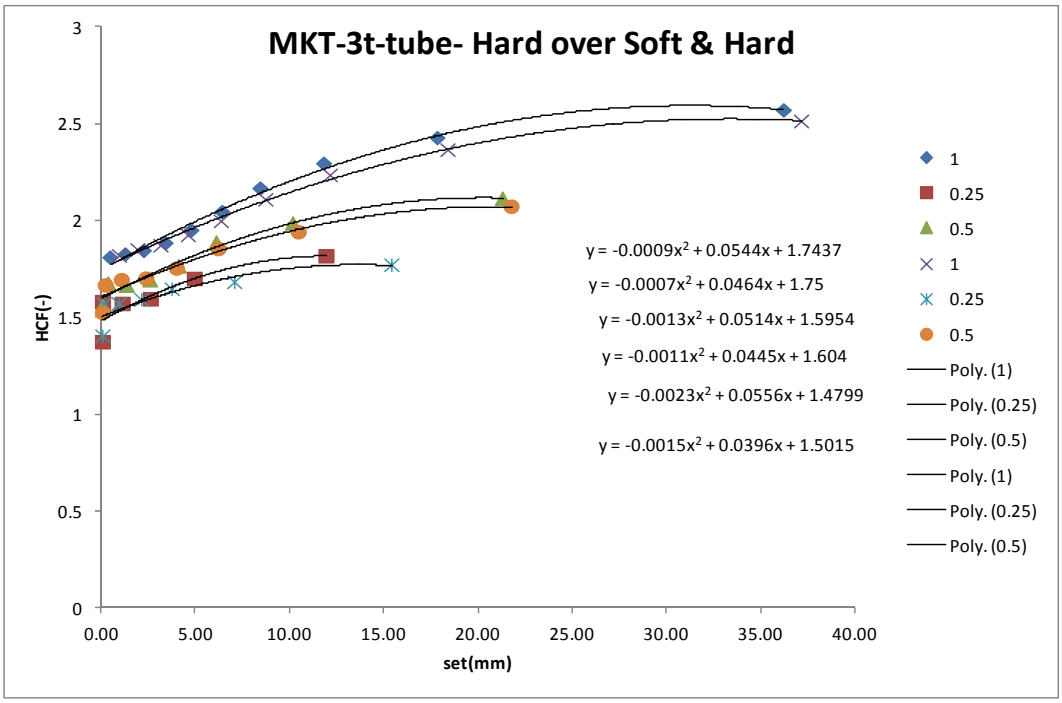
MKT-3t-tube- Hard over Soft & Hard
HCF(-)
set(mm)
y = -0.0009x² + 0.0544x + 1.7437
y = -0.0007x² + 0.0464x + 1.75
y = -0.0013x² + 0.0514x + 1.5954
y = -0.0011x² + 0.0445x + 1.604
y = -0.0023x² + 0.0556x + 1.4799
y = -0.0015x² + 0.0396x + 1.5015
1
0.25
0.5
1
0.25
0.5
Poly. (1)
Poly. (0.25)
Poly. (0.5)
Poly. (1)
Poly. (0.25)
Poly. (0.5)

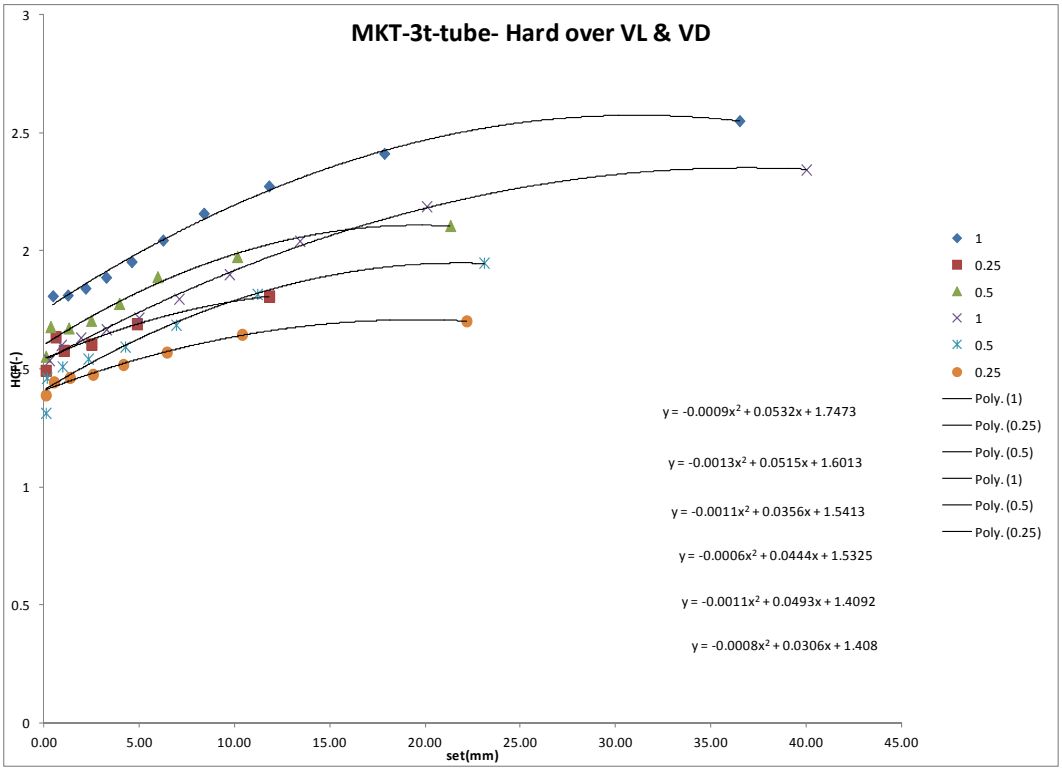
MKT-3t-tube- Hard over VL & VD
H(F(-)
set(mm)
y = -0.0009x² + 0.0532x + 1.7473
y = -0.0013x² + 0.0515x + 1.6013
y = -0.0011x² + 0.0356x + 1.5413
y = -0.0006x² + 0.0444x + 1.5325
y = -0.0011x² + 0.0493x + 1.4092
y = -0.0008x² + 0.0306x + 1.408
1
0.25
0.5
1
0.5
0.25
Poly. (1)
Poly. (0.25)
Poly. (0.5)
Poly. (1)
Poly. (0.5)
Poly. (0.25)

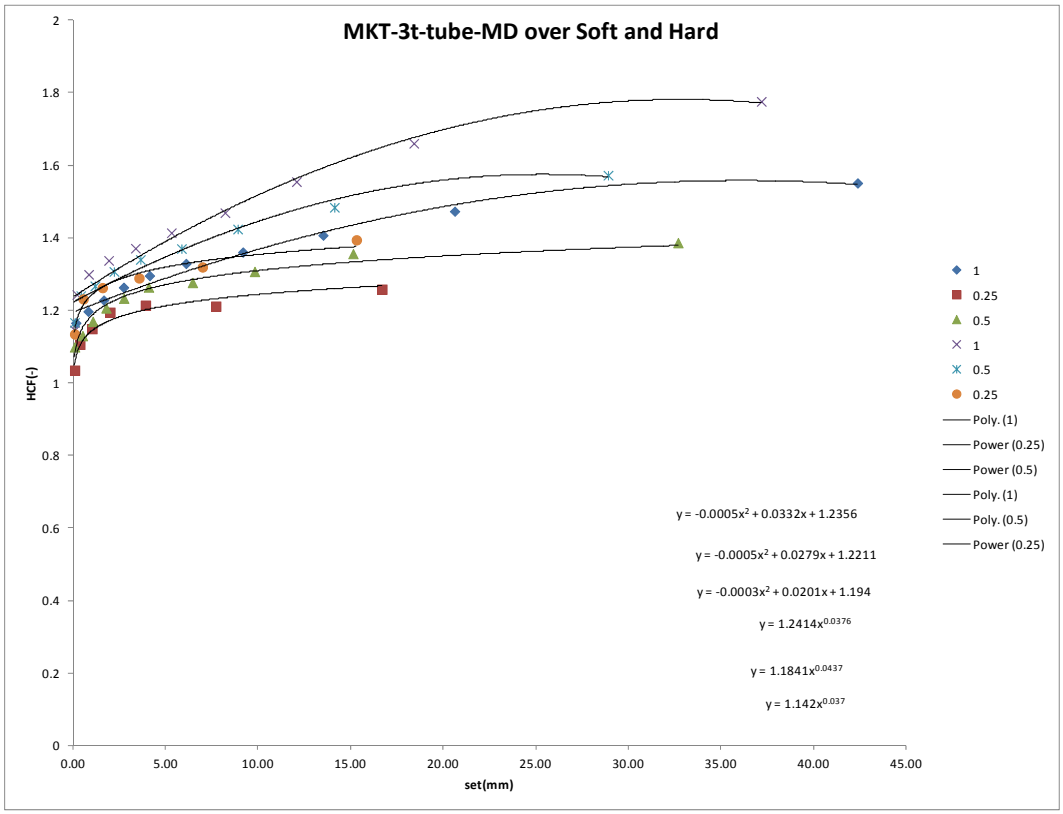
MKT-3t-tube-MD over Soft and Hard
HCF(-)
set(mm)
y = -0.0005x² + 0.0332x + 1.2356
y = -0.0005x² + 0.0279x + 1.2211
y = -0.0003x² + 0.0201x + 1.194
y = 1.2414x^0.0376
y = 1.1841x^0.0437
y = 1.142x^0.037
1
0.25
0.5
1
0.5
0.25
Poly. (1)
Power (0.25)
Power (0.5)
Poly. (1)
Poly. (0.5)
Power (0.25)

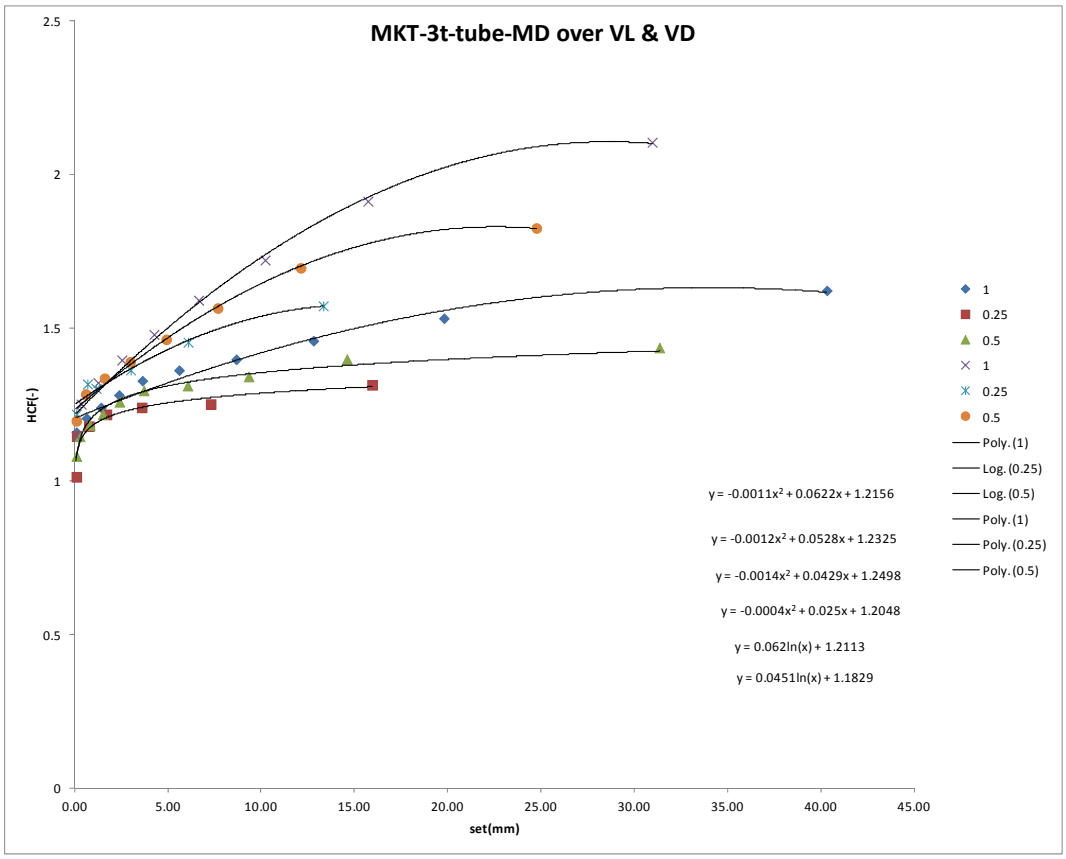
MKT-3t-tube-MD over VL & VD
HCF(-)
set(mm)
y = -0.0011x² + 0.0622x + 1.2156
y = -0.0012x² + 0.0528x + 1.2325
y = -0.0014x² + 0.0429x + 1.2498
y = -0.0004x² + 0.025x + 1.2048
y = 0.062ln(x) + 1.2113
y = 0.0451ln(x) + 1.1829
1
0.25
0.5
1
0.25
0.5
Poly. (1)
Log. (0.25)
Log. (0.5)
Poly. (1)
Poly. (0.25)
Poly. (0.5)

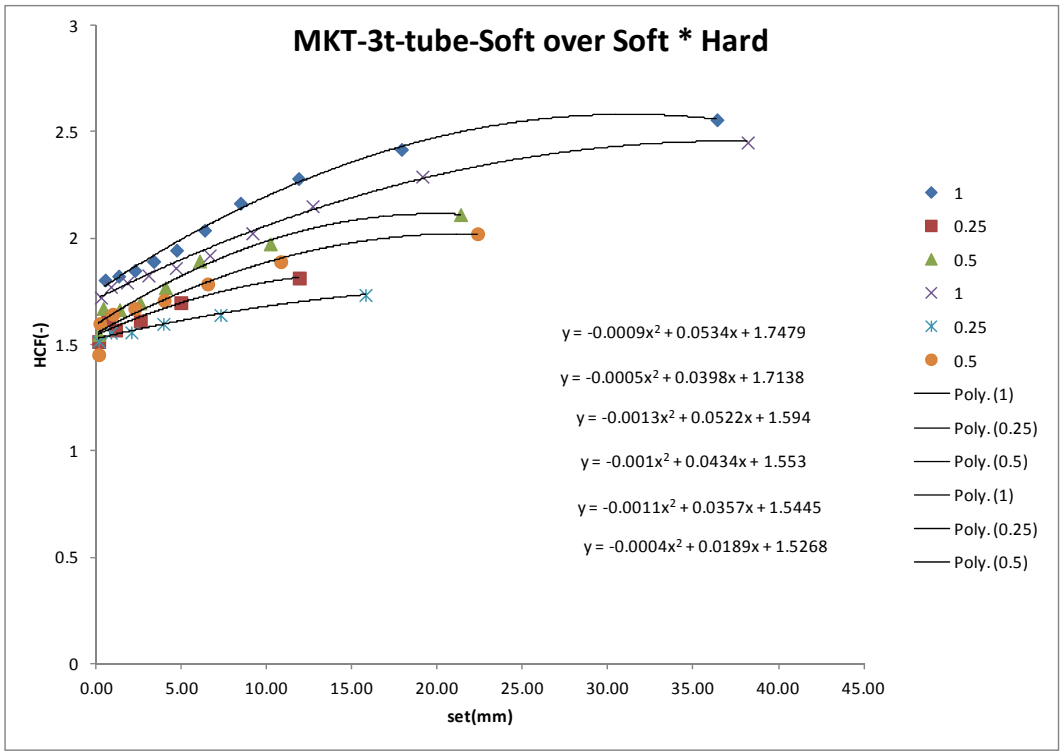
MKT-3t-tube-Soft over Soft * Hard
HCF(-)
set(mm)
y = -0.0009x² + 0.0534x + 1.7479
y = -0.0005x² + 0.0398x + 1.7138
y = -0.0013x² + 0.0522x + 1.594
y = -0.001x² + 0.0434x + 1.553
y = -0.0011x² + 0.0357x + 1.5445
y = -0.0004x² + 0.0189x + 1.5268
1
0.25
0.5
1
0.25
0.5
Poly. (1)
Poly. (0.25)
Poly. (0.5)
Poly. (1)
Poly. (0.25)
Poly. (0.5)

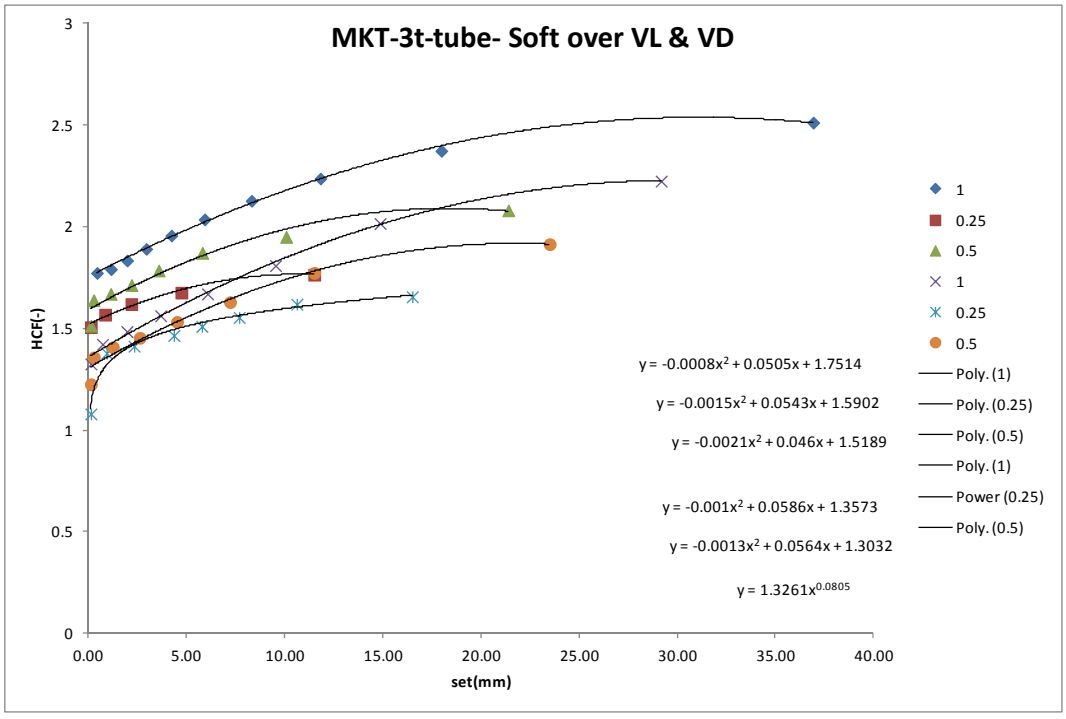
MKT-3t-tube- Soft over VL & VD
HCF(-)
set(mm)
y = -0.0008x² + 0.0505x + 1.7514
y = -0.0015x² + 0.0543x + 1.5902
y = -0.0021x² + 0.046x + 1.5189
y = -0.001x² + 0.0586x + 1.3573
y = -0.0013x² + 0.0564x + 1.3032
y = 1.3261x^0.0805
1
0.25
0.5
1
0.25
0.5
Poly. (1)
Poly. (0.25)
Poly. (0.5)
Poly. (1)
Power (0.25)
Poly. (0.5)

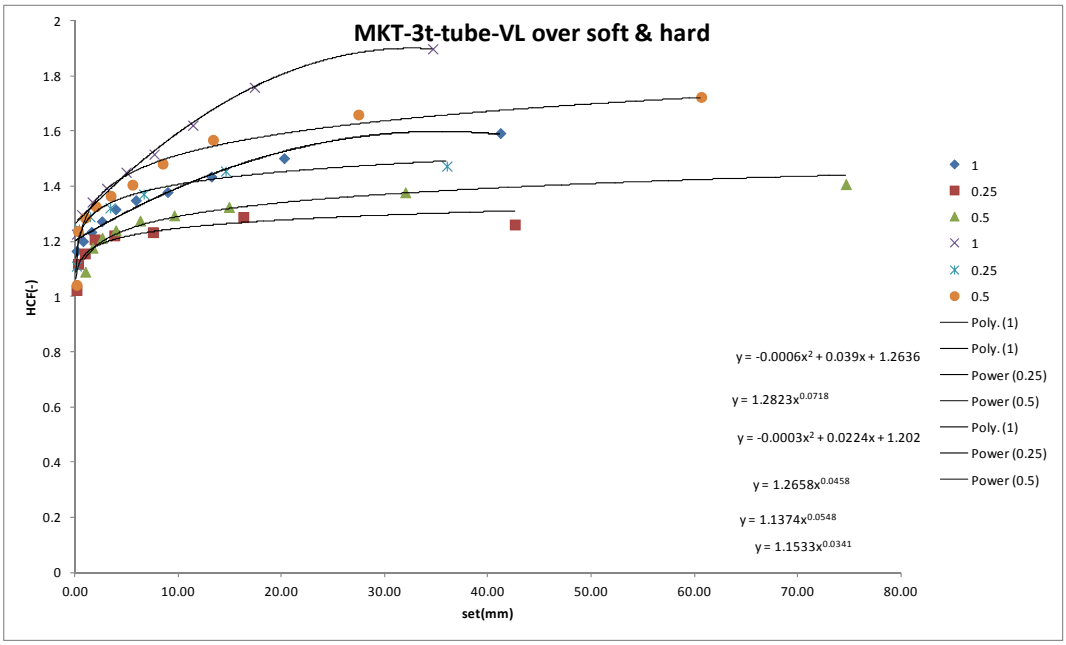
MKT-3t-tube-VL over soft & hard
HCF(-)
set(mm)
y = -0.0006x² + 0.039x + 1.2636
y = 1.2823x^0.0718
y = -0.0003x² + 0.0224x + 1.202
y = 1.2658x^0.0458
y = 1.1374x^0.0548
y = 1.1533x^0.0341
1
0.25
0.5
1
0.25
0.5
Poly. (1)
Poly. (1)
Power (0.25)
Power (0.5)
Poly. (1)
Power (0.25)
Power (0.5)

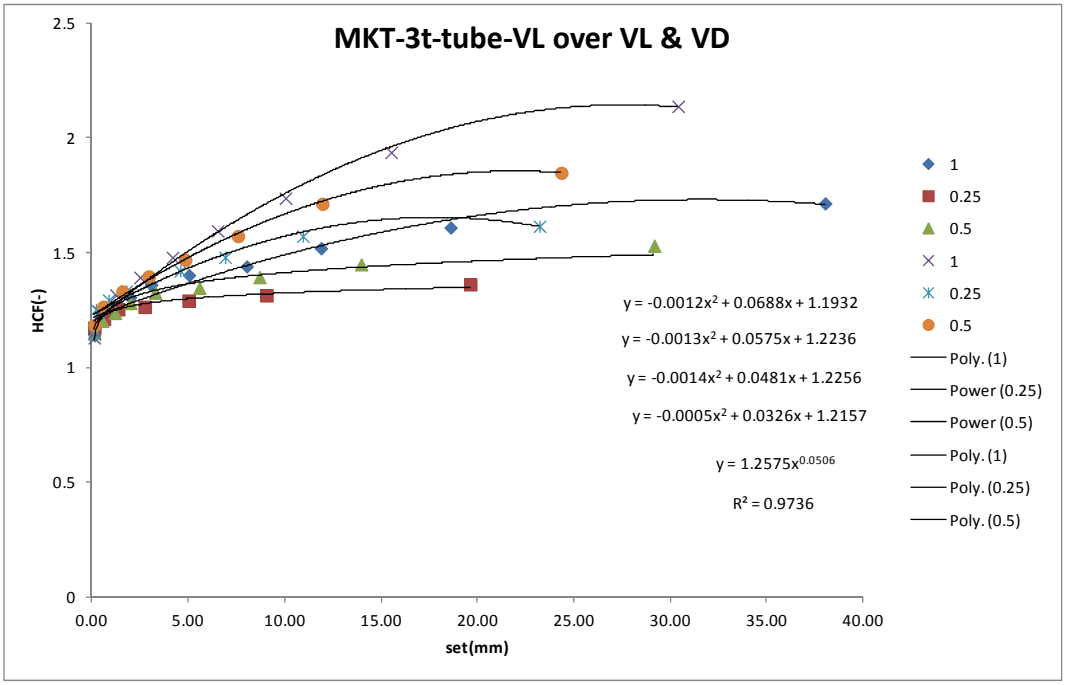
MKT-3t-tube-VL over VL & VD
HCF(-)
set(mm)
y = -0.0012x² + 0.0688x + 1.1932
y = -0.0013x² + 0.0575x + 1.2236
y = -0.0014x² + 0.0481x + 1.2256
y = -0.0005x² + 0.0326x + 1.2157
y = 1.2575x^0.0506
R² = 0.9736
1
0.25
0.5
1
0.25
0.5
Poly. (1)
Power (0.25)
Power (0.5)
Poly. (1)
Poly. (0.25)
Poly. (0.5)

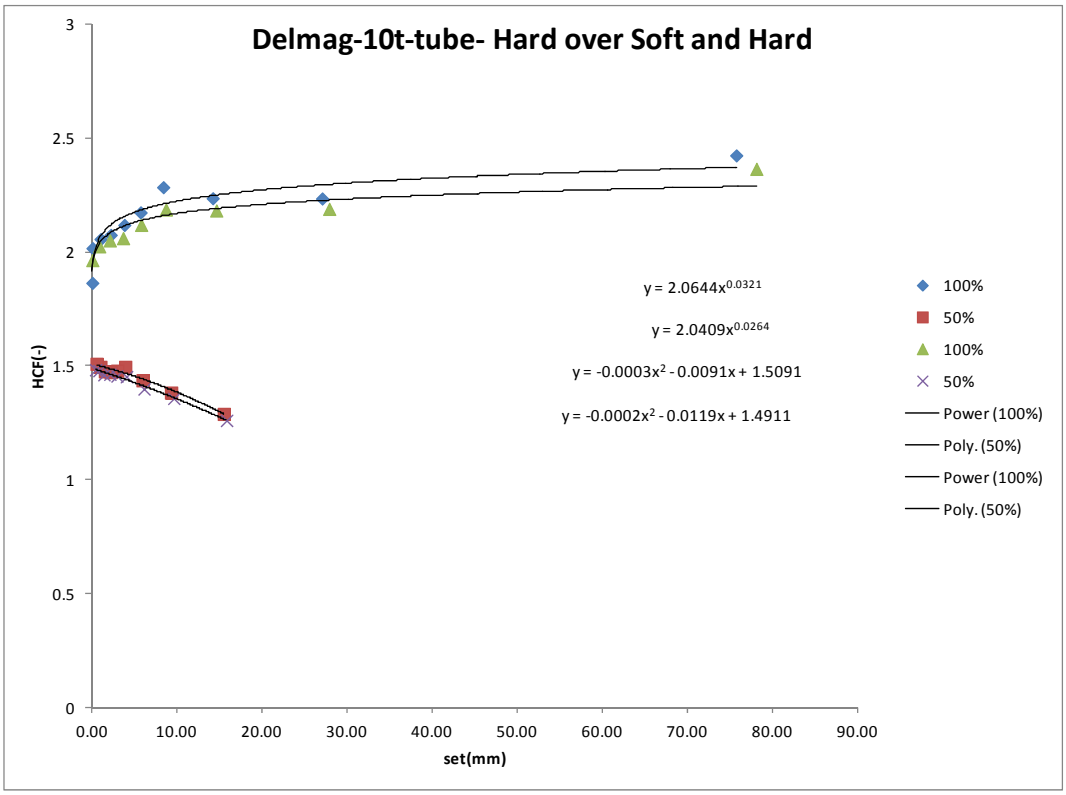
Delmag-10t-tube- Hard over Soft and Hard
HCF(-)
set(mm)
y = 2.0644x^0.0321
y = 2.0409x^0.0264
y = -0.0003x² - 0.0091x + 1.5091
y = -0.0002x² - 0.0119x + 1.4911
100%
50%
100%
50%
Power (100%)
Poly. (50%)
Power (100%)
Poly. (50%)

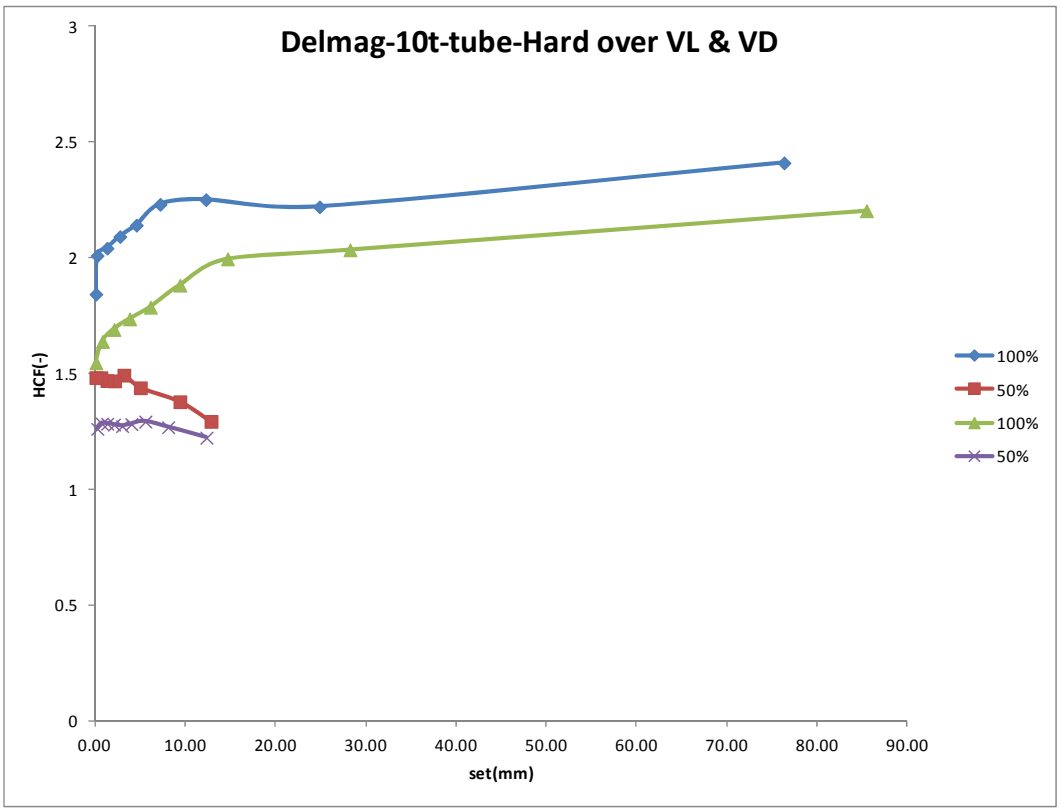
Delmag-10t-tube-Hard over VL & VD
HCF(-)
set(mm)
100%
50%
100%
50%

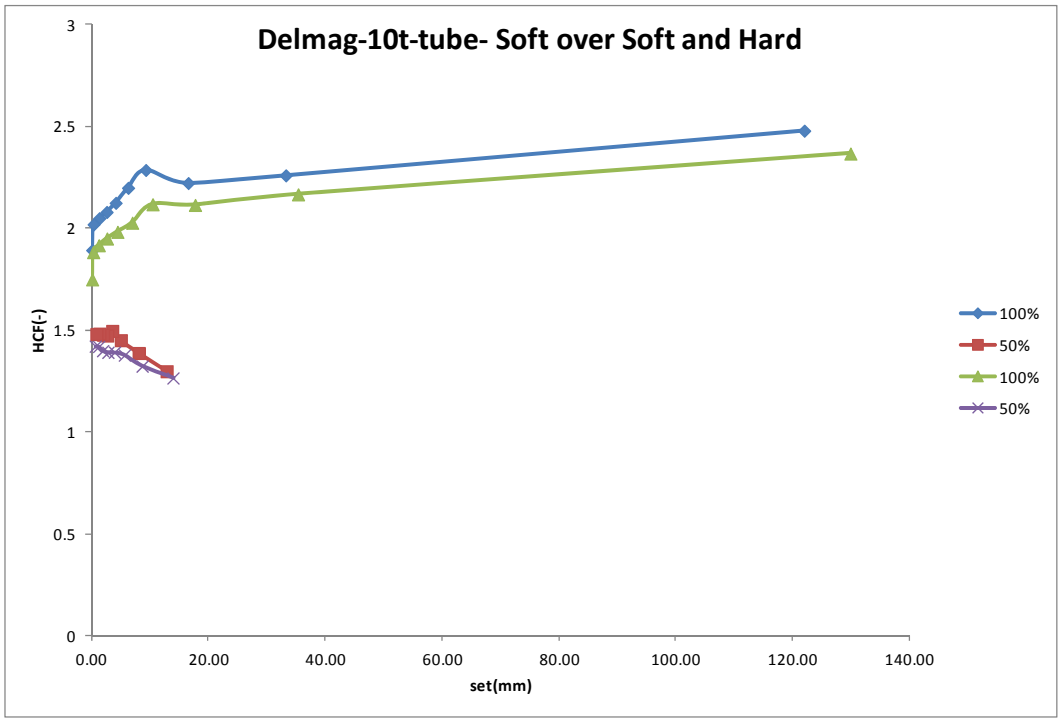
Delmag-10t-tube- Soft over Soft and Hard
HCF(-)
set(mm)
0
0.5
1
1.5
2
2.5
3
0.00
20.00
40.00
60.00
80.00
100.00
120.00
140.00
100%
50%
100%
50%

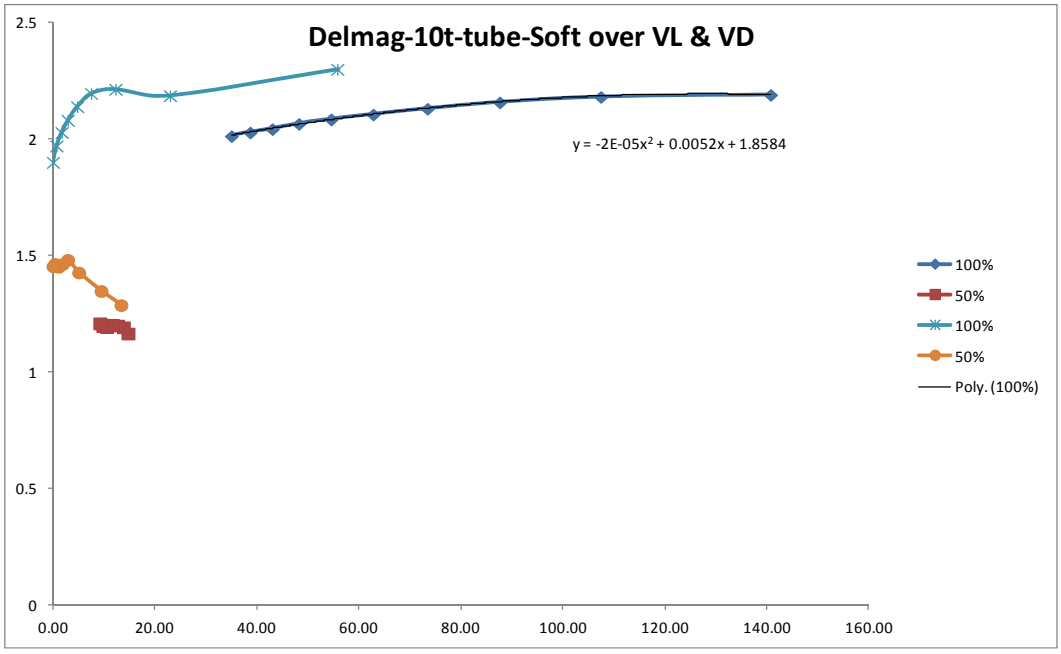
Delmag-10t-tube-Soft over VL & VD
y = -2E-05x² + 0.0052x + 1.8584
0
0.5
1
1.5
2
2.5
0.00
20.00
40.00
60.00
80.00
100.00
120.00
140.00
160.00
100%
50%
100%
50%
Poly. (100%)

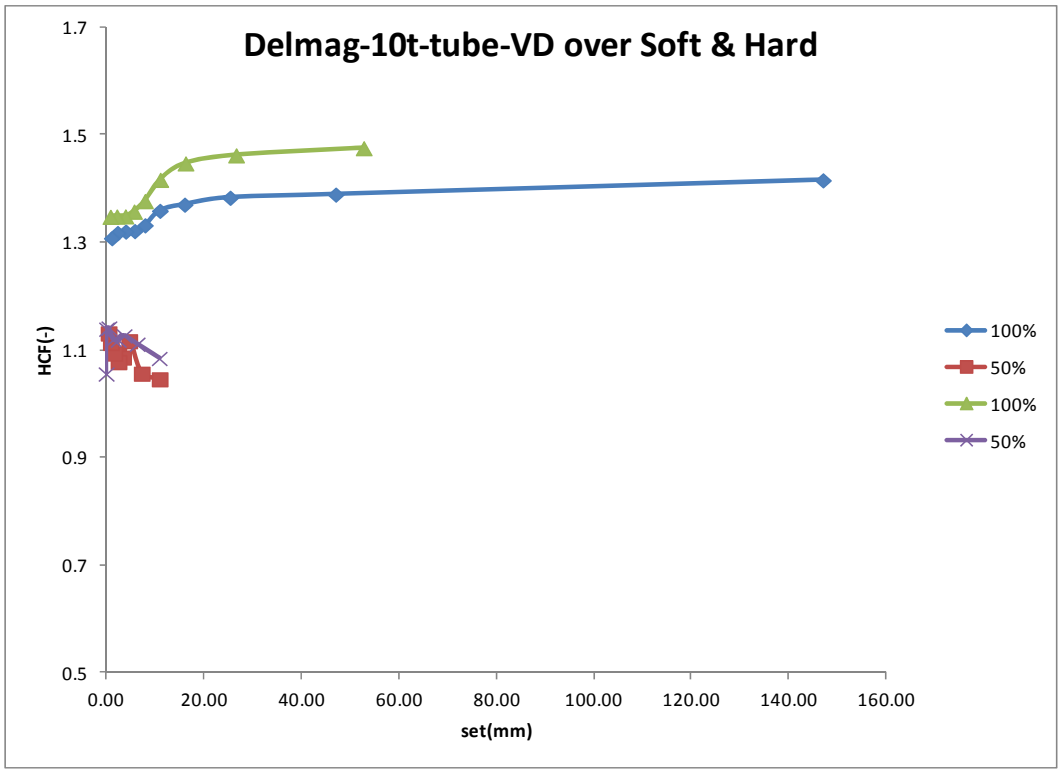
Delmag-10t-tube-VD over Soft & Hard
HCF(-)
set(mm)
1.7
1.5
1.3
1.1
0.9
0.7
0.5
0.00
20.00
40.00
60.00
80.00
100.00
120.00
140.00
160.00
100%
50%
100%
50%

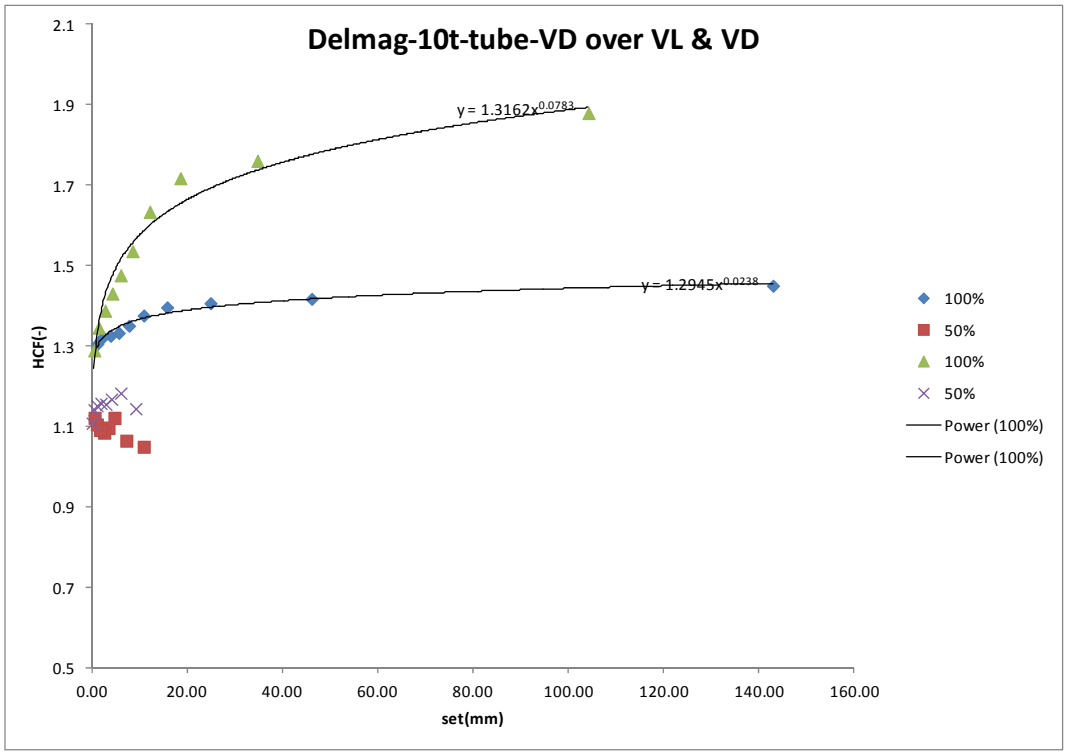
Delmag-10t-tube-VD over VL & VD
y = 1.3162x^0.0783
y = 1.2945x^0.0238
HCF(-)
set(mm)
2.1
1.9
1.7
1.5
1.3
1.1
0.9
0.7
0.5
0.00
20.00
40.00
60.00
80.00
100.00
120.00
140.00
160.00
100%
50%
100%
50%
Power (100%)
Power (100%)

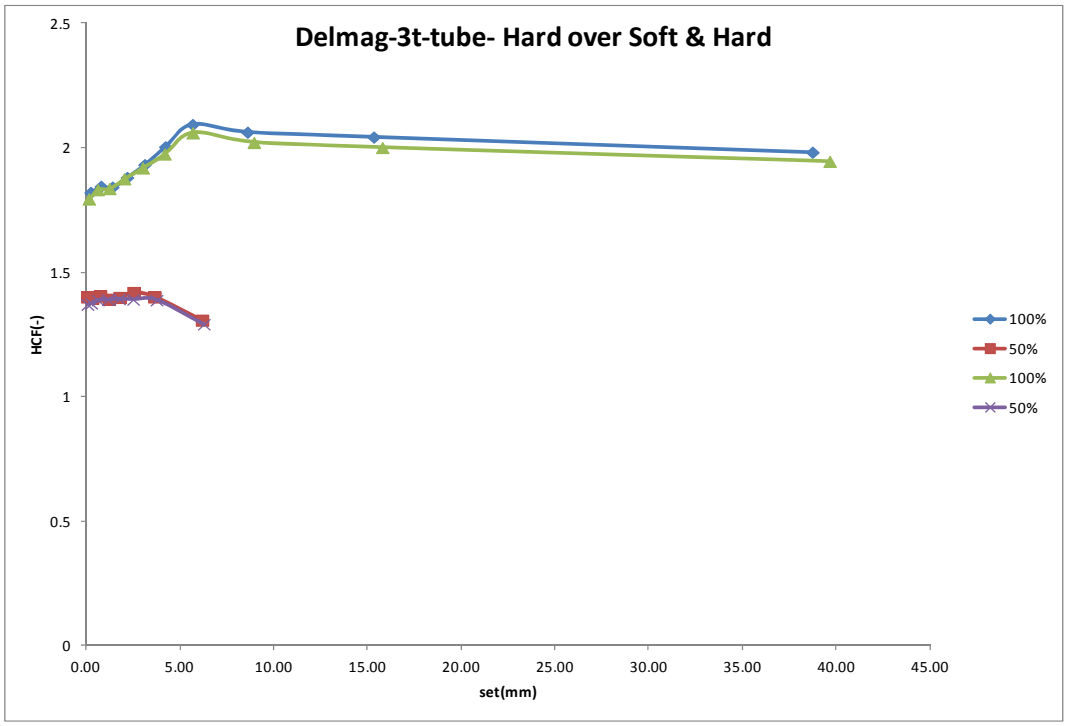
Delmag-3t-tube- Hard over Soft & Hard
HCF(-)
set(mm)
0
0.5
1
1.5
2
2.5
0.00
5.00
10.00
15.00
20.00
25.00
30.00
35.00
40.00
45.00
100%
50%
100%
50%

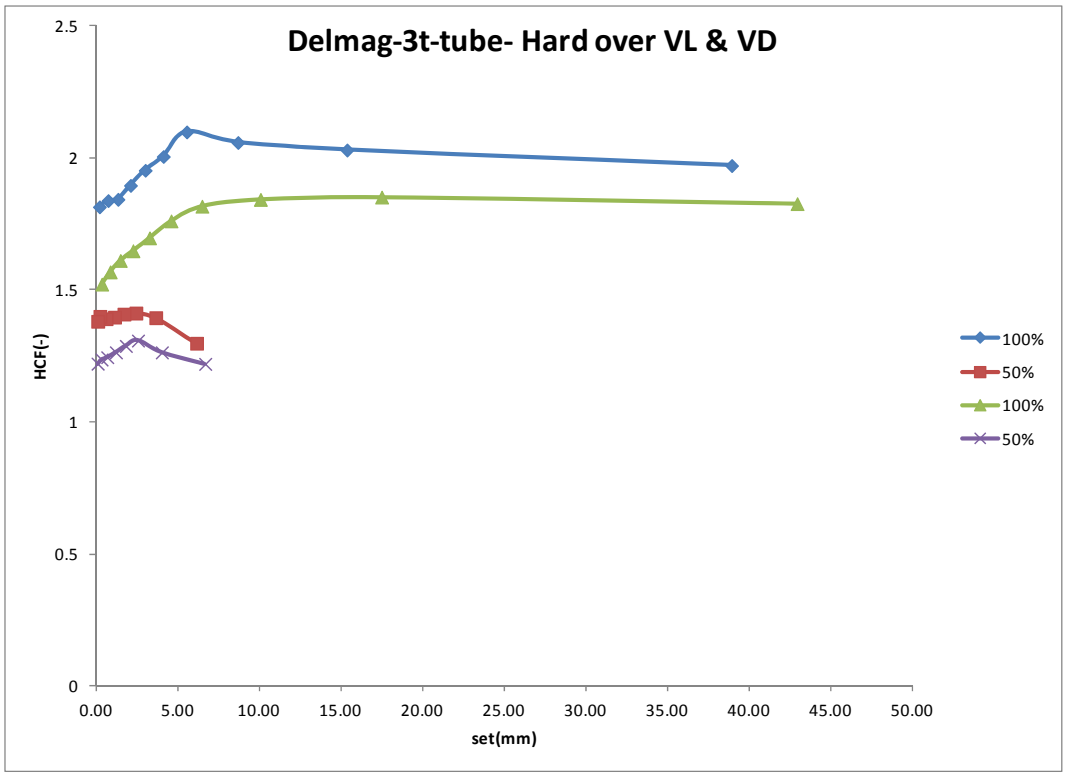
Delmag-3t-tube- Hard over VL & VD
HCF(-)
set(mm)
0
0.5
1
1.5
2
2.5
0.00
5.00
10.00
15.00
20.00
25.00
30.00
35.00
40.00
45.00
50.00
100%
50%
100%
50%

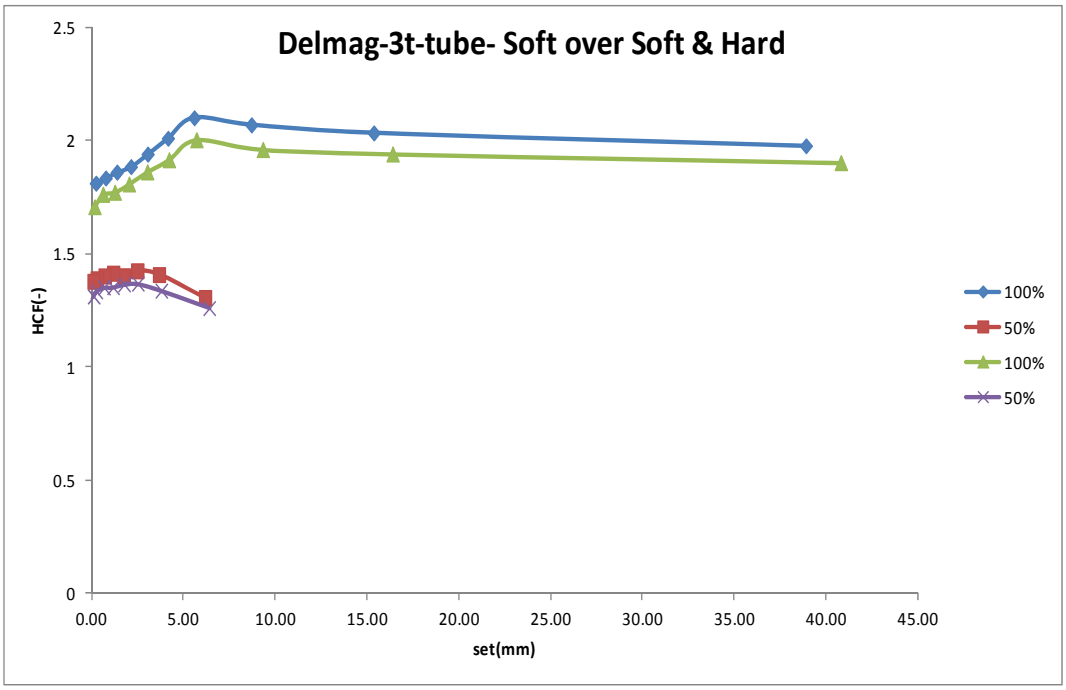
Delmag-3t-tube- Soft over Soft & Hard
HCF(-)
set(mm)
0
0.5
1
1.5
2
2.5
0.00
5.00
10.00
15.00
20.00
25.00
30.00
35.00
40.00
45.00
100%
50%
100%
50%

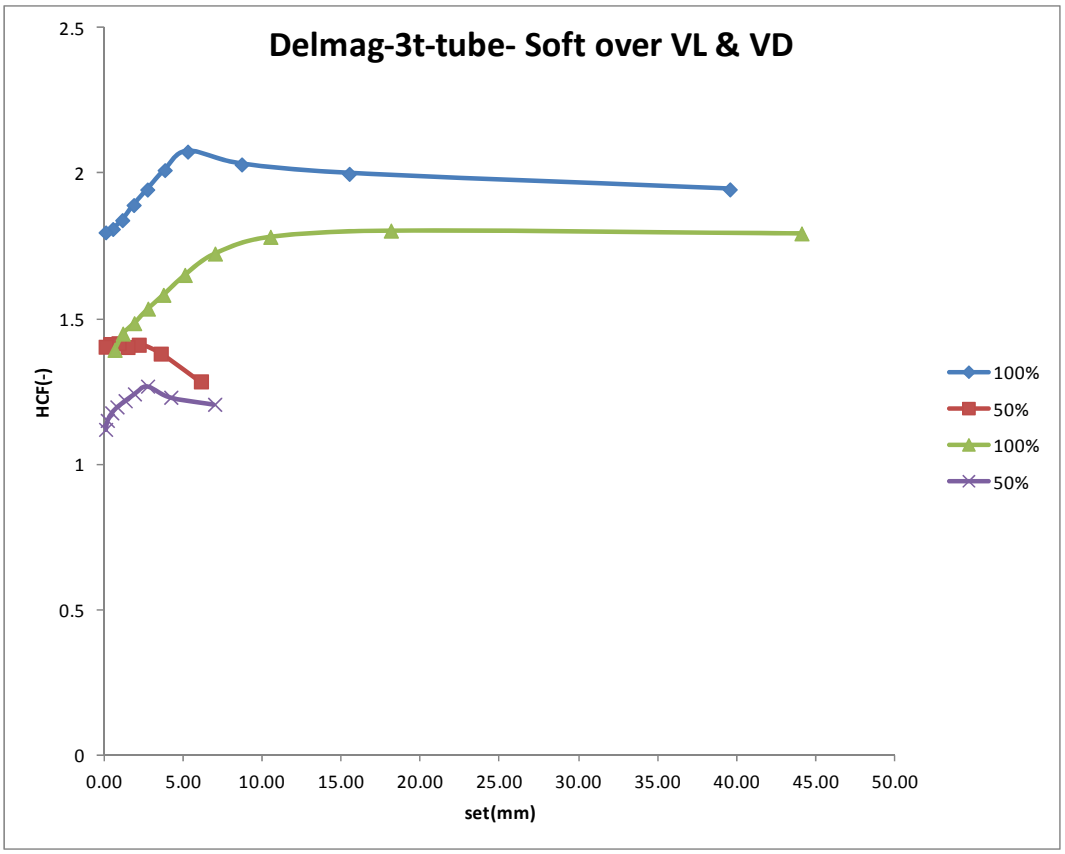
Delmag-3t-tube- Soft over VL & VD
HCF(-)
set(mm)
0
0.5
1
1.5
2
2.5
0.00
5.00
10.00
15.00
20.00
25.00
30.00
35.00
40.00
45.00
50.00
100%
50%
100%
50%

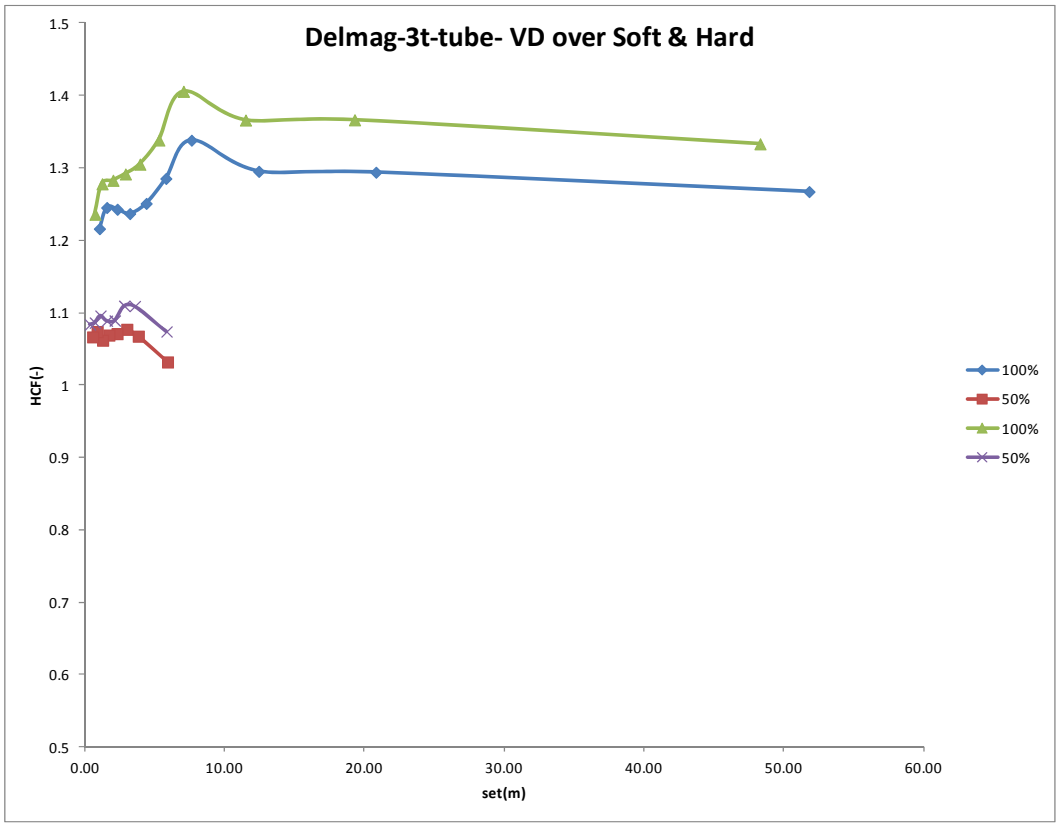
Delmag-3t-tube- VD over Soft & Hard
HCF(-)
set(m)
100%
50%
100%
50%

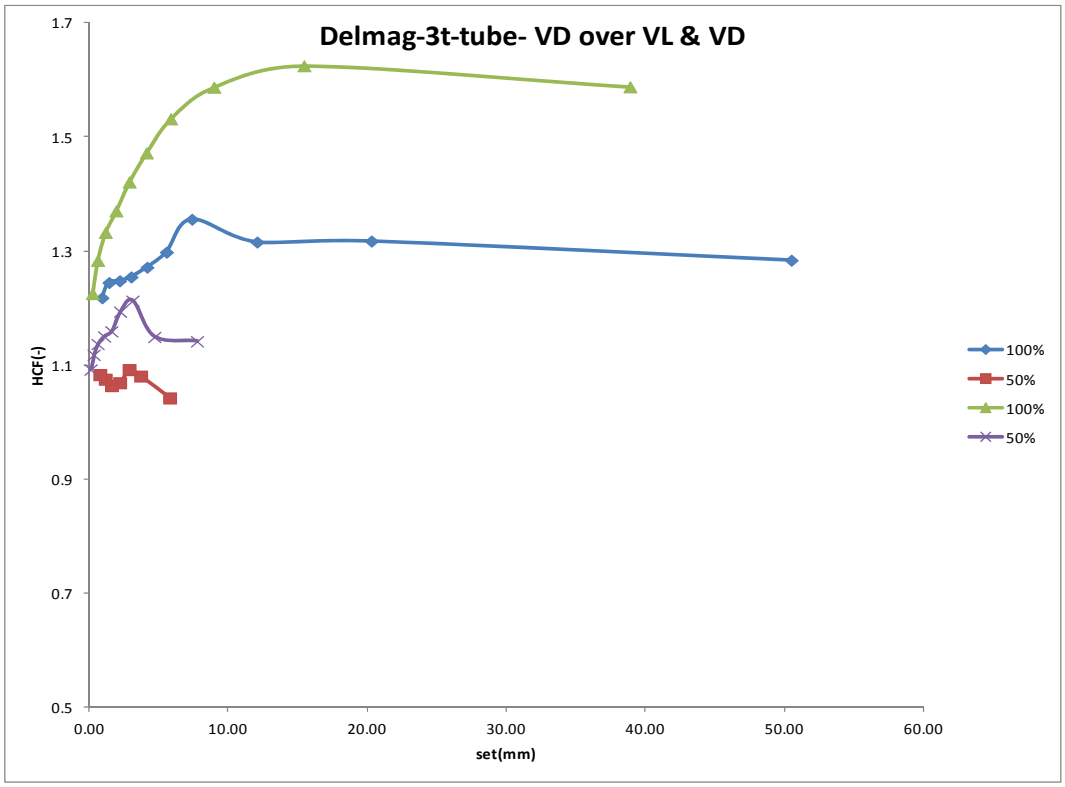
Delmag-3t-tube- VD over VL & VD
HCF(-)
set(mm)
100%
50%
100%
50%

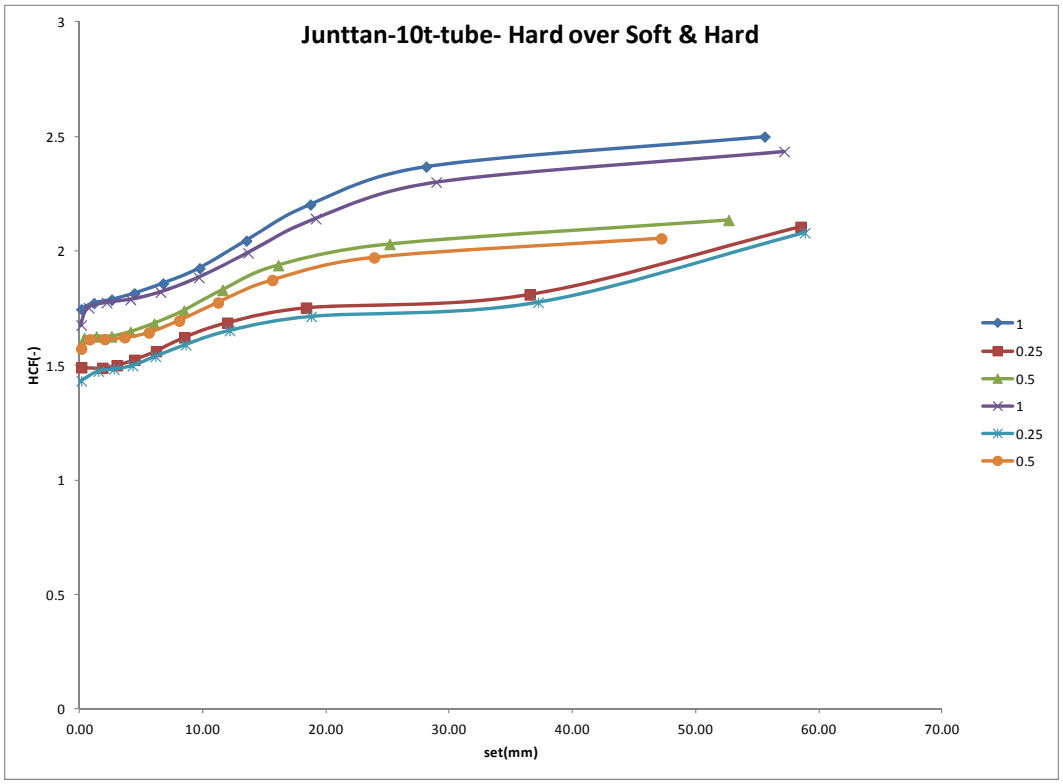
Junttan-10t-tube- Hard over Soft & Hard
HCF(-)
set(mm)
0
0.5
1
1.5
2
2.5
3
0.00
10.00
20.00
30.00
40.00
50.00
60.00
70.00
1
0.25
0.5
1
0.25
0.5

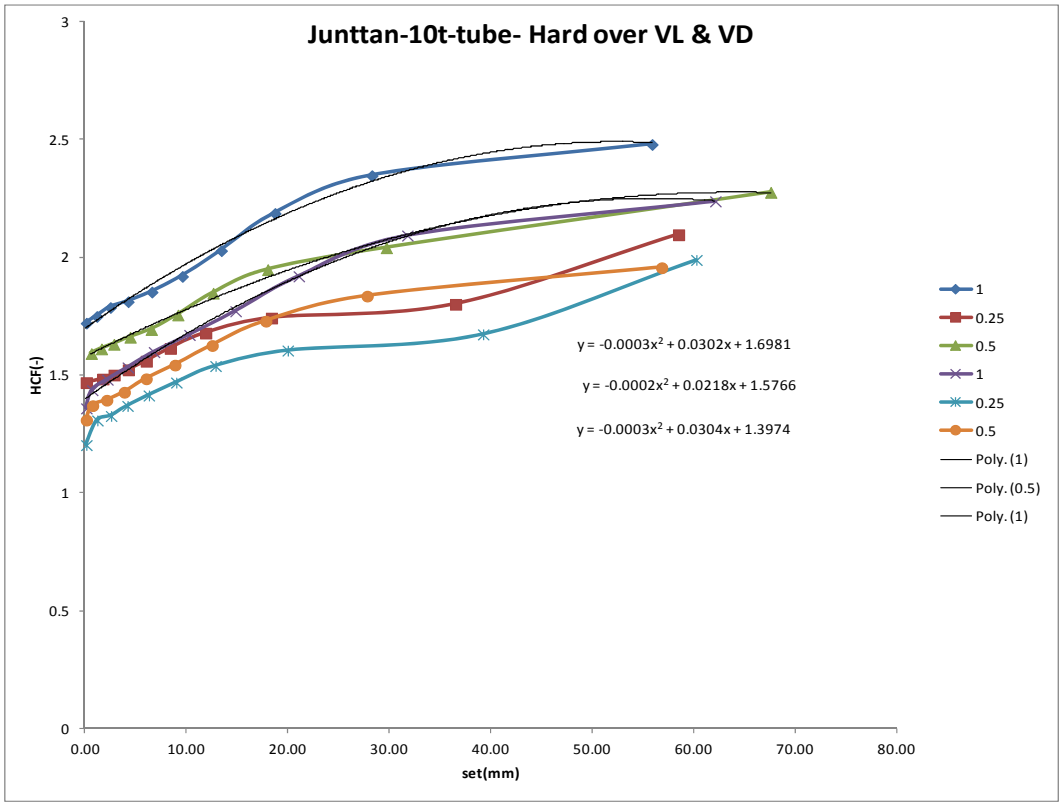
Junttan-10t-tube- Hard over VL & VD
HCF(-)
set(mm)
y = -0.0003x² + 0.0302x + 1.6981
y = -0.0002x² + 0.0218x + 1.5766
y = -0.0003x² + 0.0304x + 1.3974
0
0.5
1
1.5
2
2.5
3
0.00
10.00
20.00
30.00
40.00
50.00
60.00
70.00
80.00
1
0.25
0.5
1
0.25
0.5
Poly. (1)
Poly. (0.5)
Poly. (1)

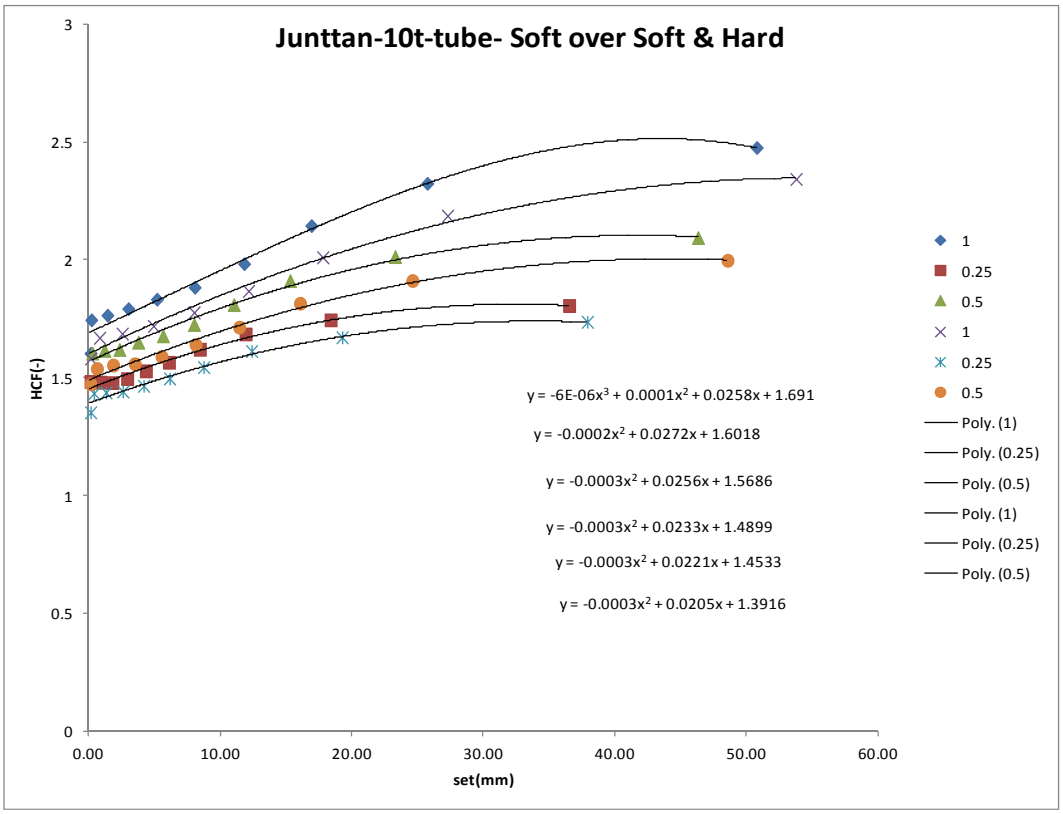
Junttan-10t-tube- Soft over Soft & Hard
HCF(-)
set(mm)
y = -6E-06x³ + 0.0001x² + 0.0258x + 1.691
y = -0.0002x² + 0.0272x + 1.6018
y = -0.0003x² + 0.0256x + 1.5686
y = -0.0003x² + 0.0233x + 1.4899
y = -0.0003x² + 0.0221x + 1.4533
y = -0.0003x² + 0.0205x + 1.3916
1
0.25
0.5
1
0.25
0.5
Poly. (1)
Poly. (0.25)
Poly. (0.5)
Poly. (1)
Poly. (0.25)
Poly. (0.5)

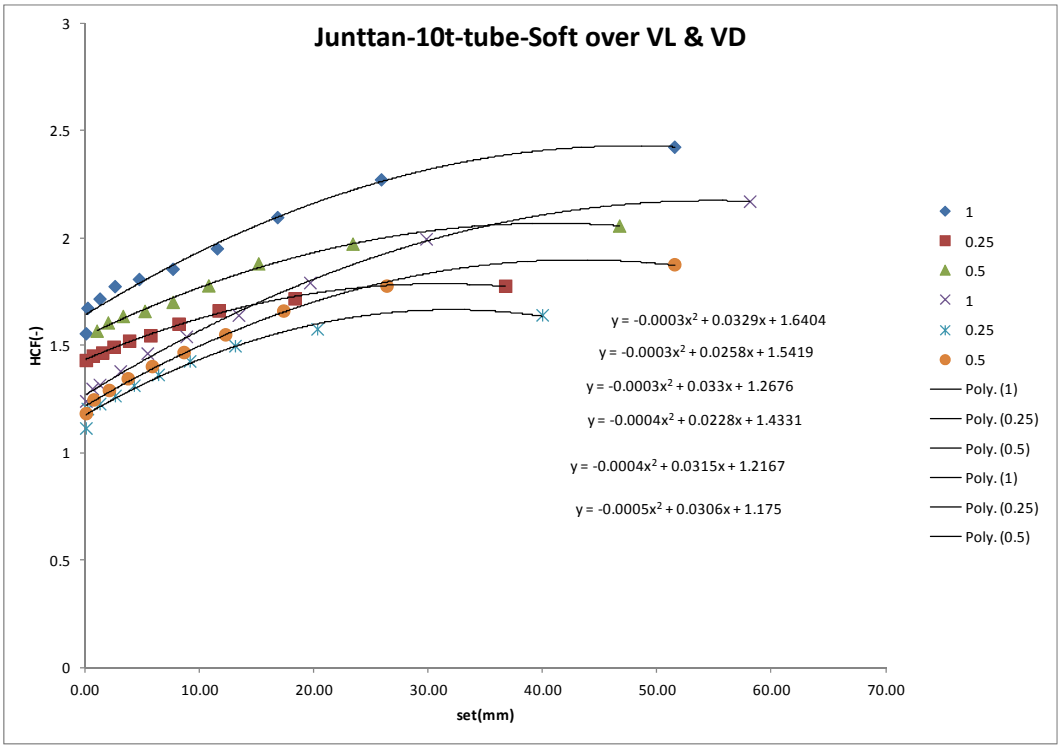
Junttan-10t-tube-Soft over VL & VD
HCF(-)
set(mm)
y = -0.0003x² + 0.0329x + 1.6404
y = -0.0003x² + 0.0258x + 1.5419
y = -0.0003x² + 0.033x + 1.2676
y = -0.0004x² + 0.0228x + 1.4331
y = -0.0004x² + 0.0315x + 1.2167
y = -0.0005x² + 0.0306x + 1.175
1
0.25
0.5
1
0.25
0.5
Poly. (1)
Poly. (0.25)
Poly. (0.5)
Poly. (1)
Poly. (0.25)
Poly. (0.5)

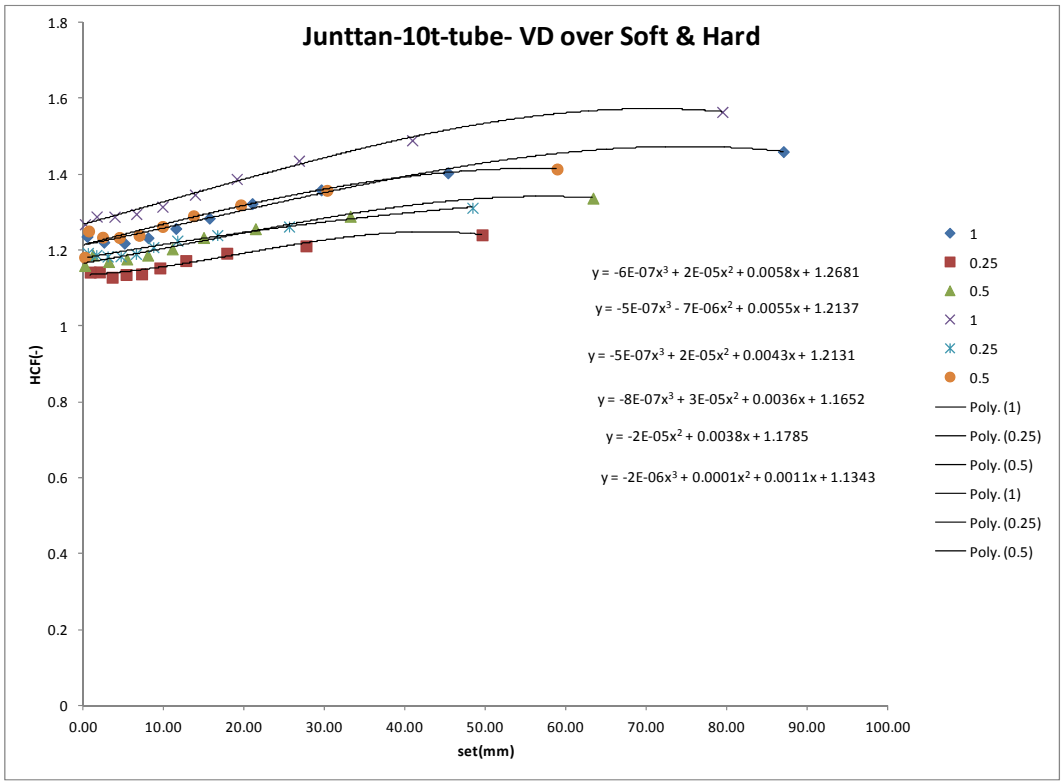
Junttan-10t-tube- VD over Soft & Hard
HCF(-)
set(mm)
y = -6E-07x³ + 2E-05x² + 0.0058x + 1.2681
y = -5E-07x³ - 7E-06x² + 0.0055x + 1.2137
y = -5E-07x³ + 2E-05x² + 0.0043x + 1.2131
y = -8E-07x³ + 3E-05x² + 0.0036x + 1.1652
y = -2E-05x² + 0.0038x + 1.1785
y = -2E-06x³ + 0.0001x² + 0.0011x + 1.1343
1
0.25
0.5
1
0.25
0.5
Poly. (1)
Poly. (0.25)
Poly. (0.5)
Poly. (1)
Poly. (0.25)
Poly. (0.5)

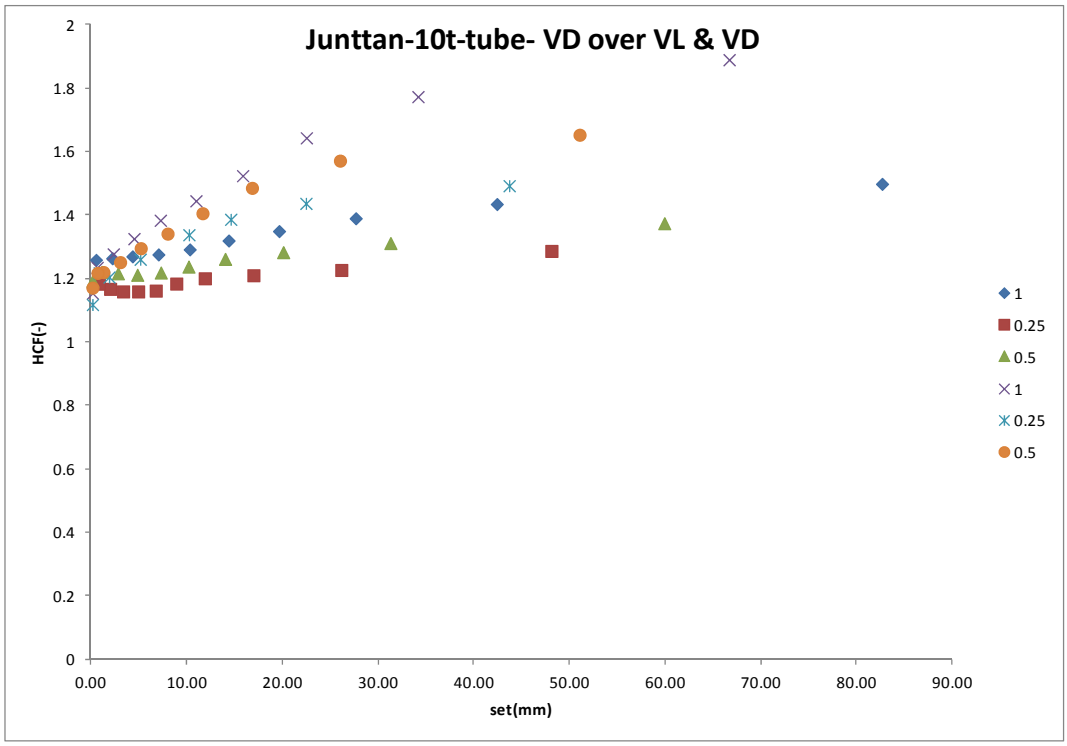
Junttan-10t-tube- VD over VL & VD
HCF(-)
set(mm)
1
0.25
0.5
1
0.25
0.5

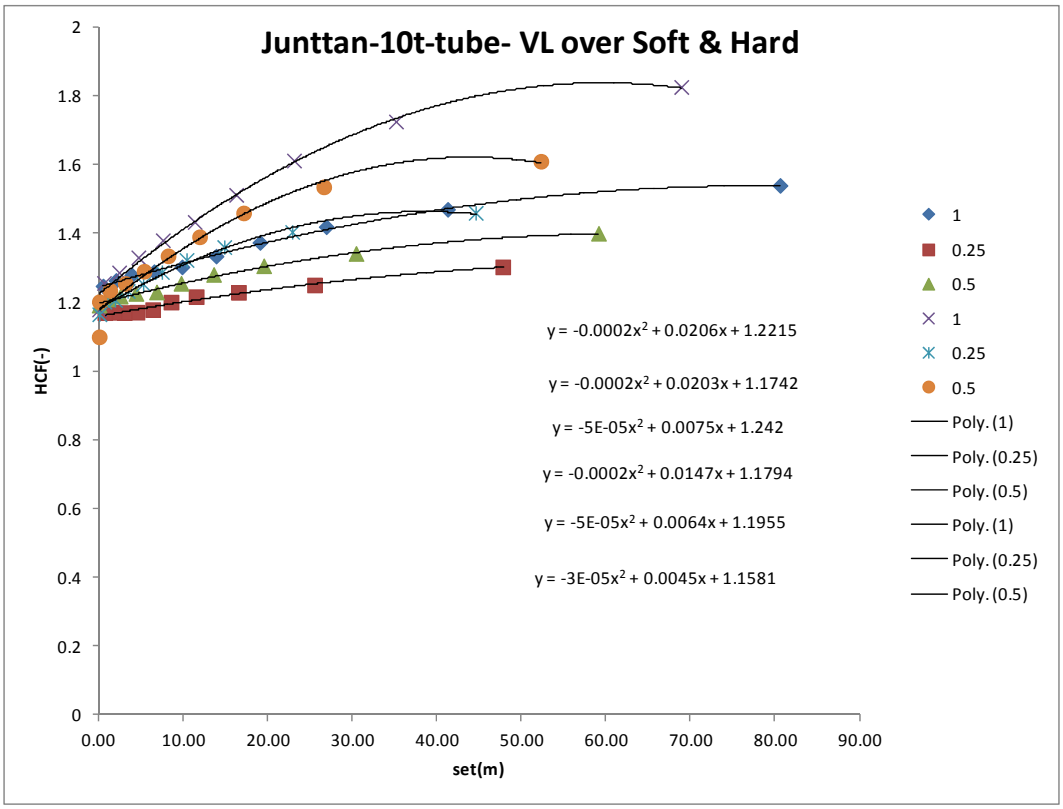
Junttan-10t-tube- VL over Soft & Hard
HCF(-)
set(m)
y = -0.0002x² + 0.0206x + 1.2215
y = -0.0002x² + 0.0203x + 1.1742
y = -5E-05x² + 0.0075x + 1.242
y = -0.0002x² + 0.0147x + 1.1794
y = -5E-05x² + 0.0064x + 1.1955
y = -3E-05x² + 0.0045x + 1.1581
1
0.25
0.5
1
0.25
0.5
Poly. (1)
Poly. (0.25)
Poly. (0.5)
Poly. (1)
Poly. (0.25)
Poly. (0.5)

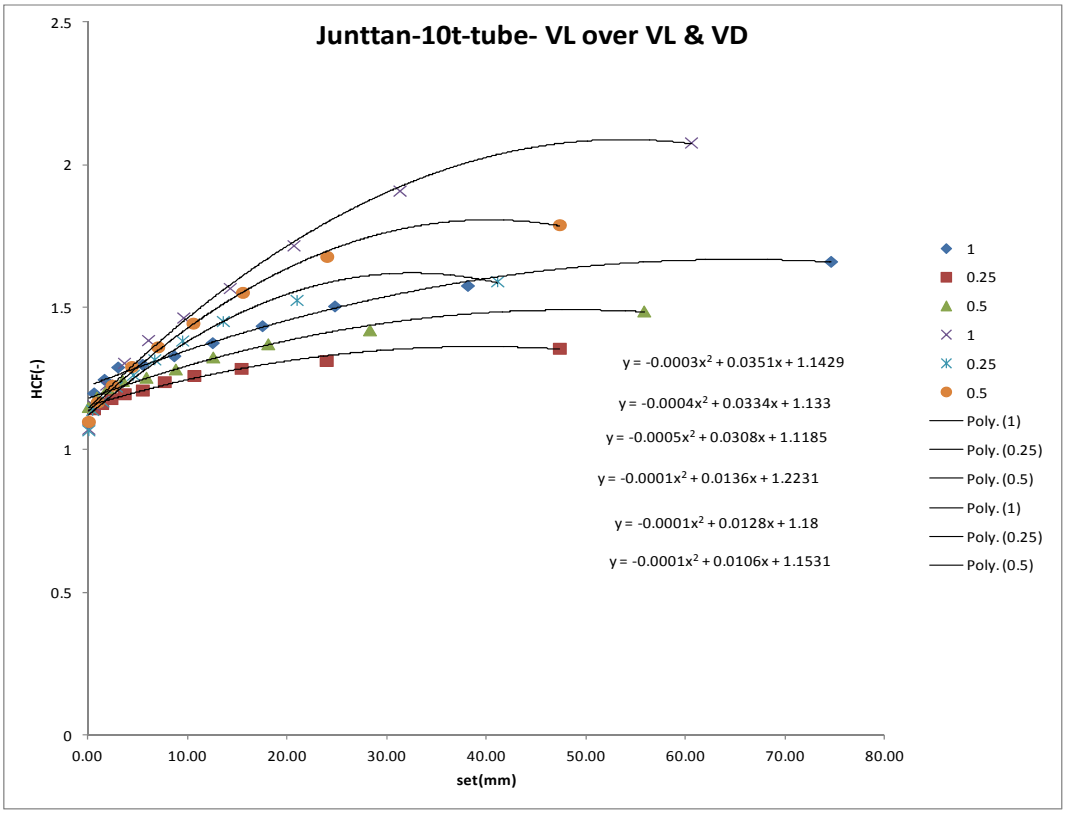
Junttan-10t-tube- VL over VL & VD
HCF(-)
set(mm)
y = -0.0003x² + 0.0351x + 1.1429
y = -0.0004x² + 0.0334x + 1.133
y = -0.0005x² + 0.0308x + 1.1185
y = -0.0001x² + 0.0136x + 1.2231
y = -0.0001x² + 0.0128x + 1.18
y = -0.0001x² + 0.0106x + 1.1531
1
0.25
0.5
1
0.25
0.5
Poly. (1)
Poly. (0.25)
Poly. (0.5)
Poly. (1)
Poly. (0.25)
Poly. (0.5)

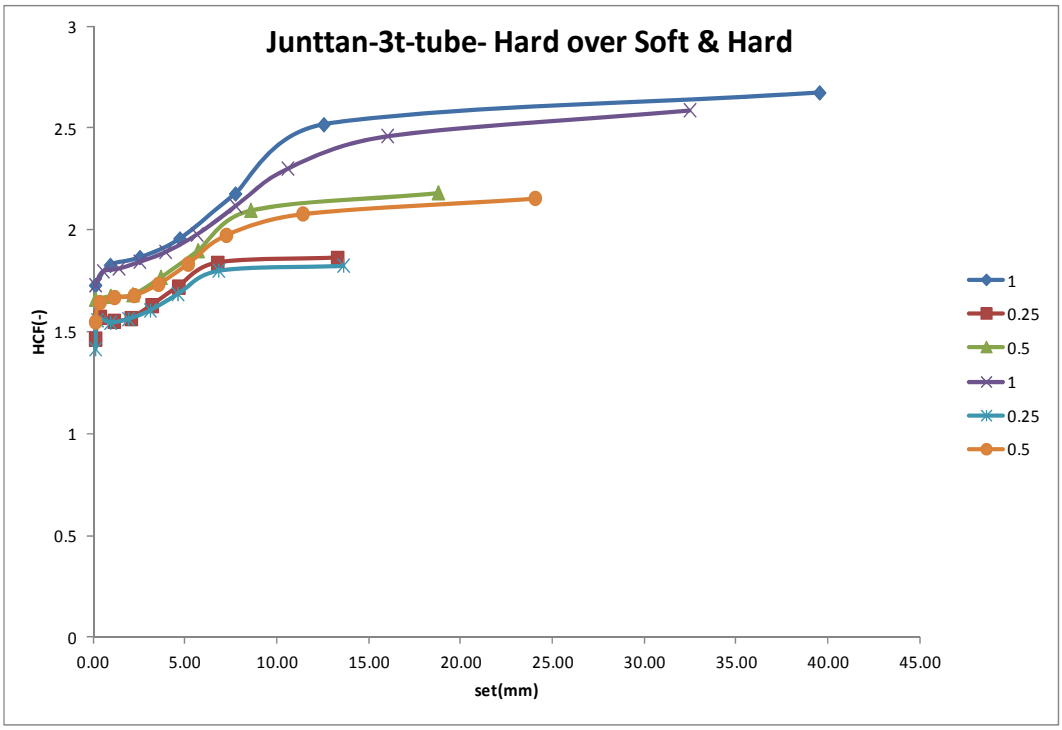
Junttan-3t-tube- Hard over Soft & Hard
HCF(-)
set(mm)
0
0.5
1
1.5
2
2.5
3
0.00
5.00
10.00
15.00
20.00
25.00
30.00
35.00
40.00
45.00
1
0.25
0.5
1
0.25
0.5

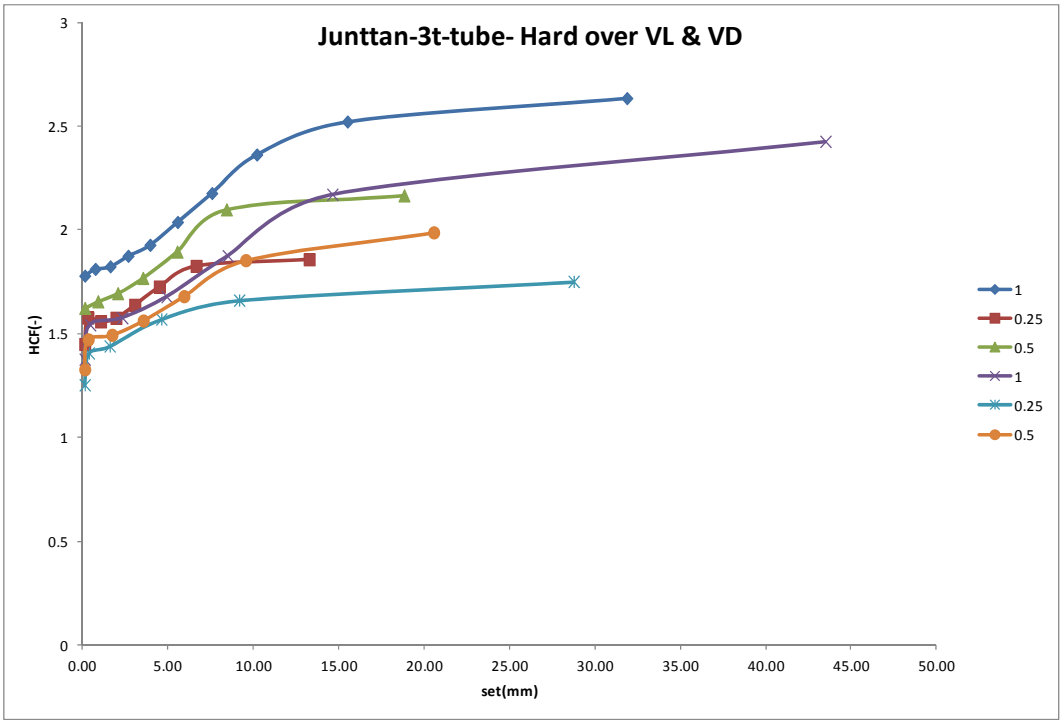
Junttan-3t-tube- Hard over VL & VD
HCF(-)
set(mm)
0
0.5
1
1.5
2
2.5
3
0.00
5.00
10.00
15.00
20.00
25.00
30.00
35.00
40.00
45.00
50.00
1
0.25
0.5
1
0.25
0.5

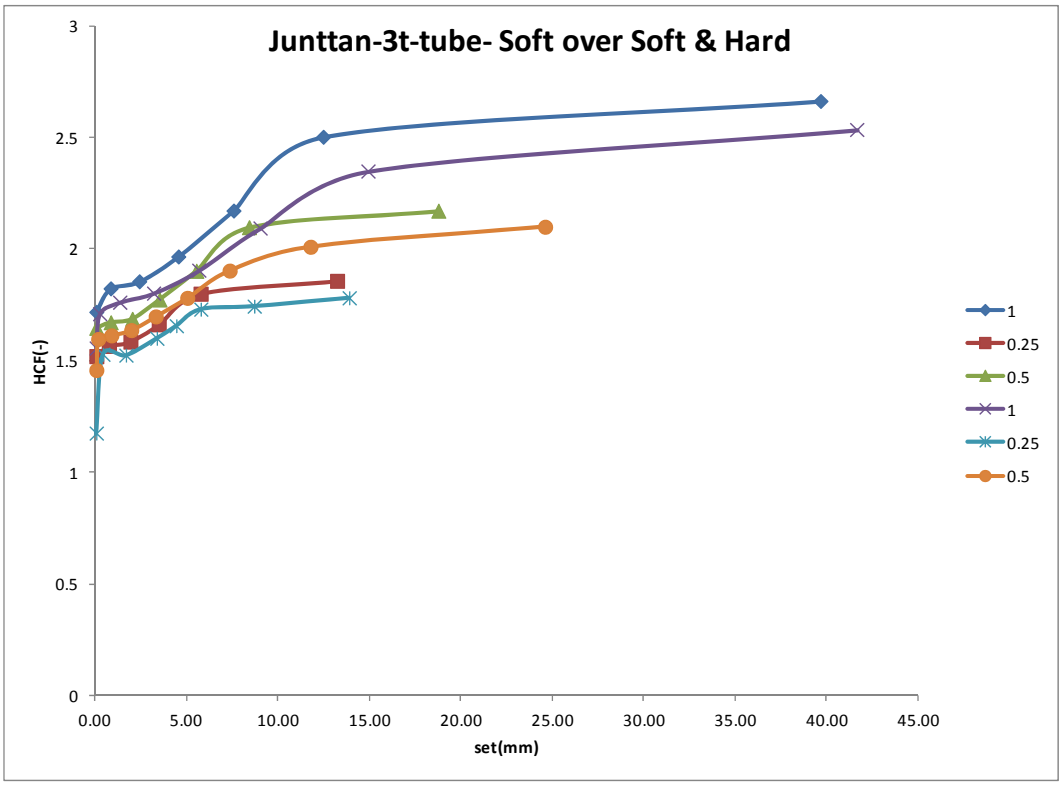
Junttan-3t-tube- Soft over Soft & Hard
HCF(-)
set(mm)
0
0.5
1
1.5
2
2.5
3
0.00
5.00
10.00
15.00
20.00
25.00
30.00
35.00
40.00
45.00
1
0.25
0.5
1
0.25
0.5

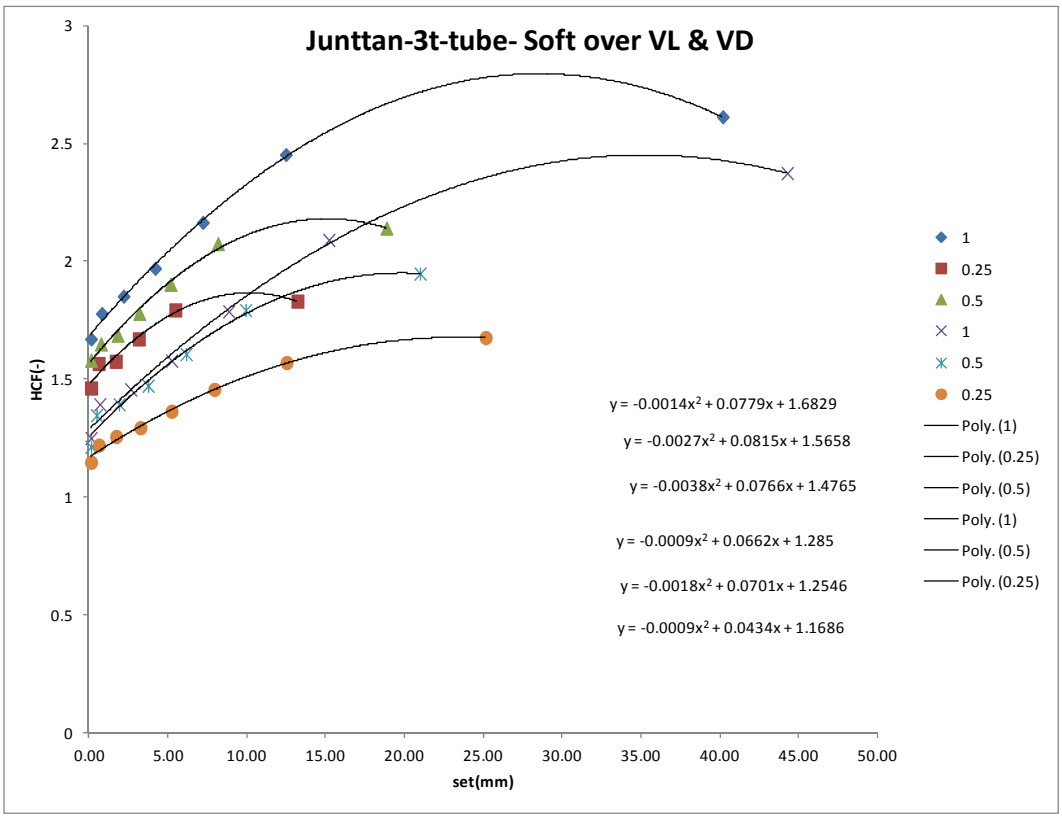
Junttan-3t-tube- Soft over VL & VD
HCF(-)
set(mm)
0
0.5
1
1.5
2
2.5
3
0.00
5.00
10.00
15.00
20.00
25.00
30.00
35.00
40.00
45.00
50.00
y = -0.0014x² + 0.0779x + 1.6829
y = -0.0027x² + 0.0815x + 1.5658
y = -0.0038x² + 0.0766x + 1.4765
y = -0.0009x² + 0.0662x + 1.285
y = -0.0018x² + 0.0701x + 1.2546
y = -0.0009x² + 0.0434x + 1.1686
1
0.25
0.5
1
0.5
0.25
Poly. (1)
Poly. (0.25)
Poly. (0.5)
Poly. (1)
Poly. (0.5)
Poly. (0.25)

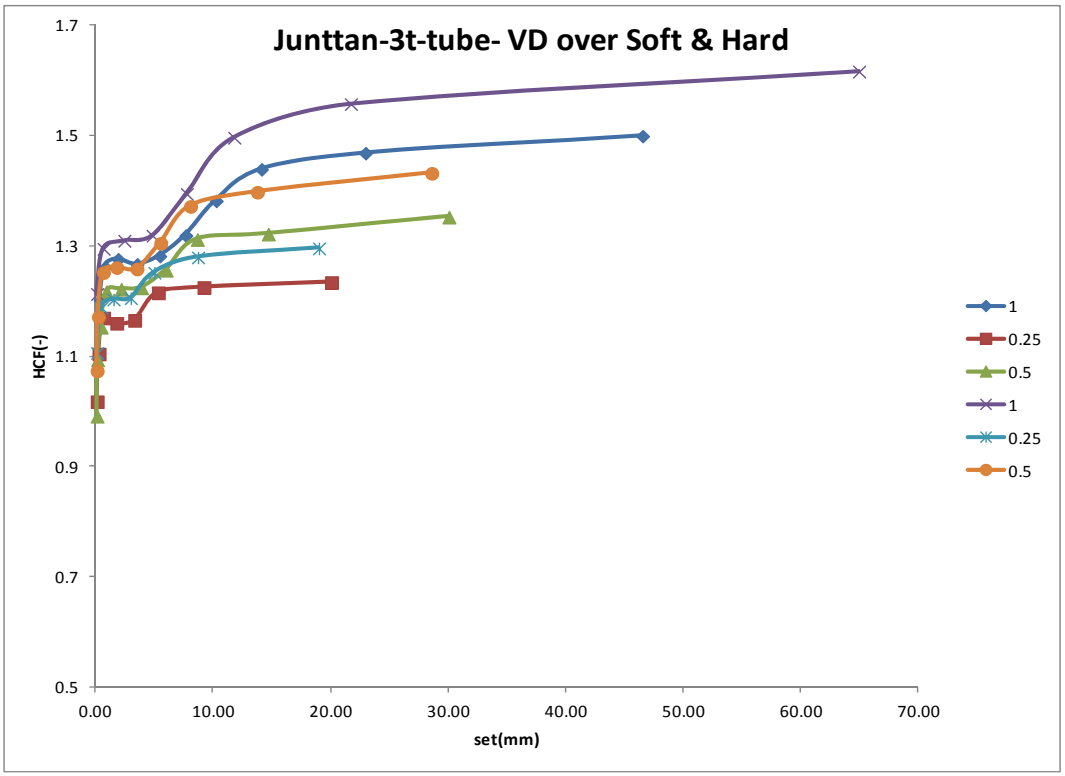
Junttan-3t-tube- VD over Soft & Hard
HCF(-)
set(mm)
1.7
1.5
1.3
1.1
0.9
0.7
0.5
0.00
10.00
20.00
30.00
40.00
50.00
60.00
70.00
1
0.25
0.5
1
0.25
0.5

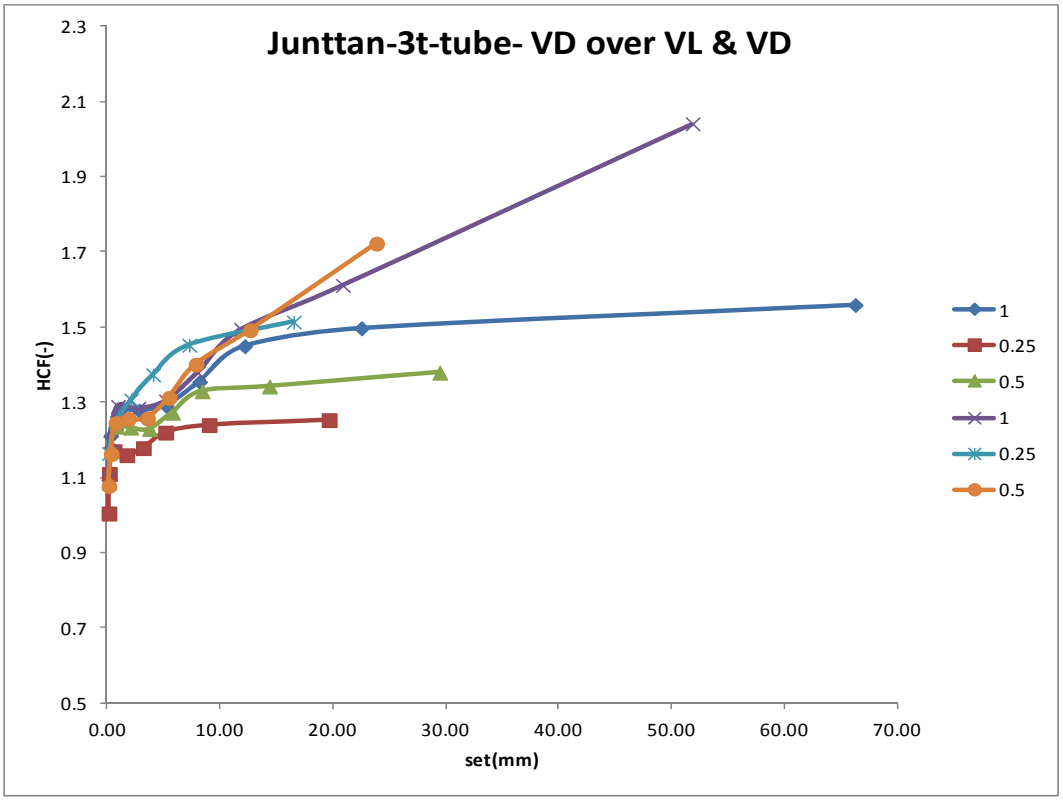
Junttan-3t-tube- VD over VL & VD
HCF(-)
set(mm)
2.3
2.1
1.9
1.7
1.5
1.3
1.1
0.9
0.7
0.5
0.00
10.00
20.00
30.00
40.00
50.00
60.00
70.00
1
0.25
0.5
1
0.25
0.5

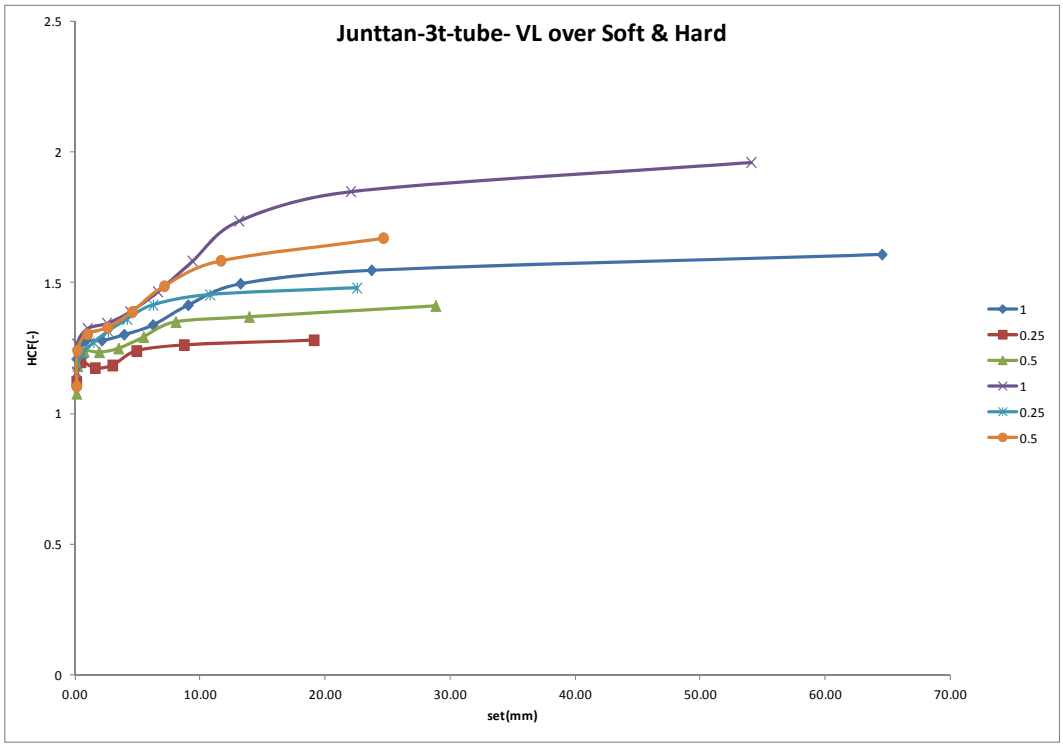
Junttan-3t-tube- VL over Soft & Hard
HCF(-)
set(mm)
2.5
2
1.5
1
0.5
0
0.00
10.00
20.00
30.00
40.00
50.00
60.00
70.00
1
0.25
0.5
1
0.25
0.5

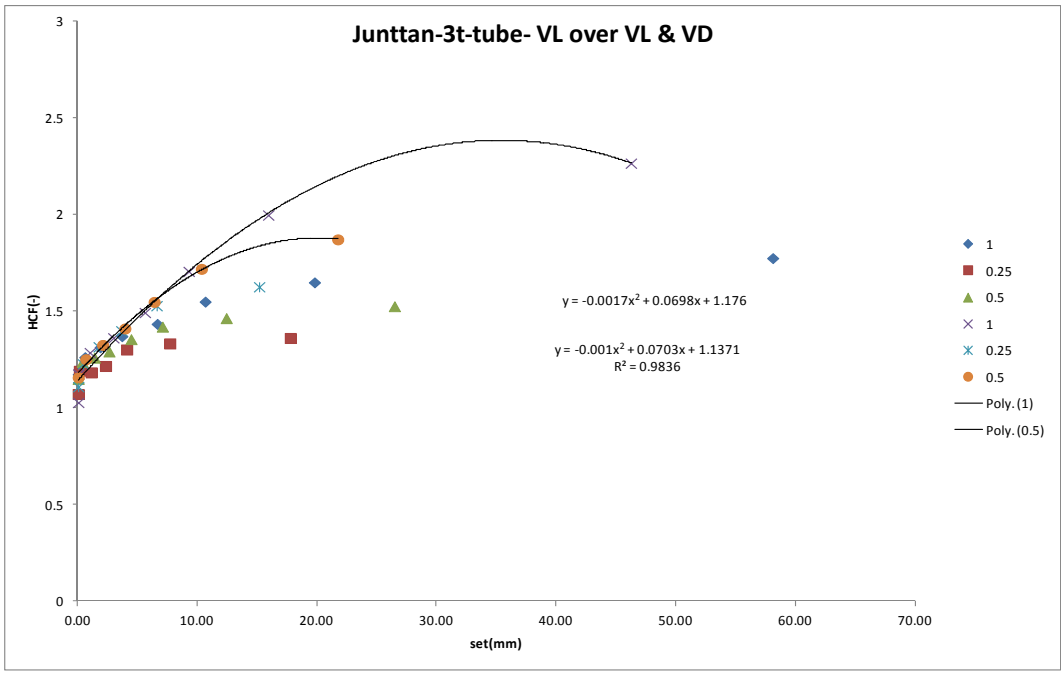
Junttan-3t-tube- VL over VL & VD
HCF(-)
set(mm)
3
2.5
2
1.5
1
0.5
0
0.00
10.00
20.00
30.00
40.00
50.00
60.00
70.00
y = -0.0017x² + 0.0698x + 1.176
y = -0.001x² + 0.0703x + 1.1371
R² = 0.9836
1
0.25
0.5
1
0.25
0.5
Poly. (1)
Poly. (0.5)

REFERENCES

AbdelSalam, S., S. Sritharan, et al. (2009). "Current design and construction practices of bridge pile foundations." Geotechnical Special Publication(186): 458-465.

Airhart T.P., Hirsch T.J., et al. (1967). Pile-Soil System Response in Clay as a Function of Excess Pore Water Pressure and Other Soil Properties. Texas, Texas Transportation Institute.

Allen T. M. (2005). Development of the WSDOT Pile Driving Formula and Its Calibration for Load and Resistance Factor Design (LRFD).

Allen T. M. (2007). "Development of New Pile-Driving Formula and Its Calibration for Load and Resistance Factor Design." Transportation Research Record: Journal of the Transport Research Board(No.2004): pp20-27.

Alvarez C., Zuckerman B. and Lemke J. (2006). Dynamic Pile Analysis Using CAPWAP and Multiple Sensors. ASCE GEO Congress, Atlanta, Georgia.

Baker C., Parikh G., et al. (1993). Drilled shafts for bridge foundations, Federal Highway Administration.

Bernardini G., De Pasquale G., et al. (2007). Microwave interferometer for ambient vibration measurement on civil engineering structures: 1. Principles of the radar technique and laboratory tests. EVACES'07 Experimental Vibration Analysis for Civil Engineering Structures. Porto, Portugal 2007: pp.1-9.

Broms B. (1981). Precast Piling Practice, Thomas Telford.

Broms B. , P.C. Lim (1988). A simple pile driving formula based on stress-wave measurements. Application of stress-wave theory to piles, 3rd international conference. Vancouvar, Canada: 591-600.

Bruno, D. and M. F. Randolph (1999). "Dynamic and Static Load Testing of Model Piles Driven into Dense Sand." Journal of Geotechnical and Geoenvironmental Engineering 125(11): 988-998.

Bullock P.J., Schmertmann J.H., McVay M.C. and Townsend F.C. (2005). "Side Shear Setup. I: Test Piles Driven in Florida." Journal of Geotechnical Geoenvironmental Engineering ASCE vol.131(3): pp292-300.

Casagrande A. (1964). "Karl Terzaghi." Geotechnique Vol.14(Issue 1): pp.1-14.

Chellis, R. D. (1951). Pile foundations: theory, design, practice, McGraw-Hill.

Chellis, R. D. (1961). Pile foundations, McGraw-Hill.

Chen D. D. S., Wong I. H. and Toto J. V. (1979). "Field Evaluation of Hammer Efficiency and Pile Driving Criteria." American Society of Civil Engineers Proceedings, Journal of the Soil Mechanics and Foundations Division: 64-74.

Chow Y.K., Yu C.L., Wong K.Y. and Lee S.L. (1989). "Relation between Peak Driving Force and the Bearing Capacity of Driven Piles." Journal of Southeast Asian Geotechnical Society vol.20(no.2): pp103-109.

Davie J.R., Bell K.R. (1991). A pile relaxation case history. International Conference " Fondations Profondes". Paris, France: 421-429.

Deeks A.J. (1992). Numerical Analysis of Pile Driving Dynamics. Doctor of Philosophy PhD, University of Western Australia.

Engel R.L. (1988). "Discussion of Procedures for the Determination of Pile Capacity " Transportation Research Record, Geotechnical Instrumentation No. 1169: p. 54-61,(Ohio Department of Transportation ODOT).

F. Tavenas, R. Audy (1972). "Limitations of the Driving Formulas for Predicting the Bearing Capacities of Piles in Sand." Canadian Geotechnical Journal 9(1): 47-62.

FABER O. and ANDREWS E. S. (1947). "DISCUSSION ON A NEW PILING FORMULA." Journal of the ICE Volume 28(Issue 8): pp. 422.

FELLENIUS B.H. (1988). Variation of CAPWAP results as a function of the operator. Proceedings of the Third International Conference on the Application of Stress-Wave Theory to Piles. Ottawa: pp.814 - 825.

Fischer H.C. (1984). Stree Wave Theory for Pile Driving Application. Second International Conference on the Application of Stress Wave Theory on Piles, Stockholm, Sweden, Commission of Pile Research, Royal Swedish Academy of Engineering Sciences.

Fleming K., Weltman A., et al. (2008). Piling Engineering, Taylor & Francis.

Fragaszy R.J. , Higgins J.D., Argo D.E. (1988). Comparison of Methods for Estimating Pile Capacity, Washington State Department of Transportation. Research Project Final Report 2.

Fragaszy Richard J. , Argo Douglas, Higgins, Jerry D. (1989). "Comparison of formula predictions with pile load tests." Transportation Research Record(n 1219): p 1-12.

Fung W.K., Wong C.T., Wong M.K. (2004). "A study on capacity predictions for driven piles." Transactions, HKIE Vol 11(Iss.no. 3).

Fung W.K., Wong C.T., Wong M.K. (2005). "Observations on using the energy obtained from stress-wave measurements in the hiley formula." Transactions Hong Kong Institution of Engineers v 12(n 4): p 19-22.

Fung W.K., Wong C.T., Wong M.K. (2006). "Discussion on observations on using the energy obtained from stress-wave measurements in the Hiley formula." Transactions Hong Kong Institution of Engineers v13(n 2): p 63-64.

Fung W.K., Wong C.T.,Wong M.K. (2006). "Response to discussion by Victor Li and Joley Lam on observations on using the energy obtained from stress-wave measurements in the Hiley formula." Transactions Hong Kong Institution of Engineers v 13(n 2): p 65-69.

Gates, M. (1957). "Empirical Formula for Predicting Pile Bearing Capacity." Civil Engineering Vol.27(No. 3): pp 65-66.

Goble G.G. and Rausche F. (1970). "Pile Load Test by Impact Driving." Highway Research Record(No.333).

Goble G.G., Scalan R.H., Tomko J.J. (1967). "Dynamic Studies on the Bearing Capacity of Piles " Highway Research Record (no.167): pp.46-47.

Goble G.G. & Aboumatar H. (1992). Determination of wave equation soil constants from the standard penetration test. Application of Stress-Wave Theory to Piles. F. B. J. Barends. Balkema, Rotterdam: 99-103.

Gozeling F.T.M and Van Der Velde E.G. (1996). Application of stress-wave theory to piles: test results ; proceedings of the Fourth International Conference on the Application of Stress-wave Theory to Piles, The Hague, Netherlands, 21-24 September 1992, A.A. Balkema.

Hajduk E., Paikowsky S., Hölscher P., Barends F. (2000). Accelerations of a Driven Pile and the Surrounding Soil. . Proceedings of the 6th International Conference on the Applications of Stress-Wave Theory to Piles. J. B. S. Niyama. São Paulo, Brazil, Balkema, Rotterdam-the Netherlands: 541-548.

Hannigan P.J., Goble G.G. , Likins G.E. and F. Rausche. (1998). Design and Construction of Driven Pile Foundations - Workshop Manual Volumes 1 and 2. Publication Numbers FHWA-HI-97-013 & 14. Washington, D.C., US Department of Transportation, Federal Highway Administration. Volume 2.

Hereema E.P. (1979). "Relationships between wall friction, displacement velocity and horizontal stress in clay and in sand, for pile driveability analysis." GROUND ENGINEERING Volume: 12(Issue Number: 1): pp. 55-65.

Hertlein B., Davis A., (2006). Nondestructive Testing of Deep Foundations, John Wiley & Sons.

Hiley A. (1925). "Rational Pile-Driving Formula and its Application in Piling Practice Explained." Engineering 657(721).

Hiley A. (1930). "Pile Driving Calculations with Notes on Driving Forces and Ground Resistance." The Structural Engineer Vol.8.

Hirsch T.J. and Samson C.H. Jr (1966). Driving Practices for Prestressed Concrete Piles. Texas, Texas Transportation Institute.

Ho C.E., Lim C.H. (2004). "Dynamic measurement and analysis of pile driving through thick soft clay." Geotechnical Special Publication (125): 329-347.

Hölscher, P. (1995). Dynamical Response of Saturated and Dry Soils. Delft, The Netherlands, Delft University Press.

Hölscher, P., and Barends, F. (1996). In-situ Measurement of Soil-Motion near the Toe of a Dynamically Loaded Pile. 5th International Conference of the Application of Stress-Wave Theory to Piles, Orlando, FL

Holscher P. (1995). Dynamic Response of Saturated and Dry Soils. Delft, Netherland, Delft University Press.

Hussein M.H. (2004). A Brief History of the Apllication of Stress Wave Theory to Piles: Current Practices and Future Trends in Deep Foundation. Deep Foundations.

IDS (2008). "IBIS-S CONTROLLER v2.0 - User Manual." (MN/2007/024): pp.1-47.

IDS Australia (2009). "Georadar Division - General Presentation Slides." pp.1-147.

Isaac, D. V. (1931). "Reinforced Conckrete Pile Formulae." Transactions, Institute of Engineers, Australia Vol.12 (no.370): pp.305-324.

J.F., P. (1970). MECHANICS OF IMPACT PILE DRIVING. Ph.D., University of Illinois.

Komurka V. E., A. B. Wanger, et al. (2003). Estimating Soil/Pile Set-up. Prepared for The Wisconsin Department of Transportation. Wisconsin Highway Research Program #0092-0014

Liang R. Y. (2003). "New Wave Equation Technique for High Strain Impact Testing of Driven Piles." Journal of Geotechnical Testing vol.26(no.1): pp.111-117.

Liang R. Y., Zhou J. (1997). "Probability Method Applied to Dynamic Pile-Driving Control." Journal of Geotechnical Engineering, ASCE Vol 123(No.2): pp137-144.

Liang, R. Y. (1992). "Determination of wave equation soil parameters using in-situ testing techniques." Determination of wave equation soil parameters using in-situ testing techniques: 307.

Liang, R. Y., ,Sheng, Y. J. (1992). "THEORETICAL INTERPRETATION OF SMITH MODEL PARAMETERS." APPLICATION OF STRESS-WAVE THEORY TO PILES: 111-116.

Likins G. E. (1988). "The Pile Driving Analyzer: Field Testing and Data Interpretation." PDA User's Day: Cleveland, OH.

Likins G. E., Hussein M.H. (1988). "A Summary of the Pile Driving Analyzer Capacity Methods - Past and Present." PDA User's Day: Cleveland, OH.

Likins, G. E. (1994). "Helpful Hints for Field Testing and Data Interpretation Using the Pile Driving Analyzer." Users Days: Orlando, FL.

Lim C. H., Broms B.B. (1990). "Influence of Pile Driving Hammer Performance on Driving Criteria." Journal of Southeast Asian Geotechnical Society vol.21(no.1): pp63-69.

Litkouhi S., Poskitt T.J. (1980). "Damping constants for pile driveability calculations." Geotechnique vol.30(no.1): pp.77-86.

Long J.H (2002). Resistance Factor for Driven Piling Developed from Load Test Databases. Internation Deep Foundation Congress Geotech Special Publication ASCE: 944-960.

Lowery L.L. J r . (1967). Dynamic Behavior of Piling. PhD, Texas A&M University.

Lowery L.L. J r ., Finley J.R., et al. (1968). A Comparison of Dynamic Pile Driving Formulas with the Wave Equation. Texas, Texas Transportation Institute, Texas A&M University.

Lowery L.L. J r ., Hirsch T.J., et al. (1969). Pile Driving Analysis - State of the Art. Texas, Texas Transportation Institute.

McVay M. C. and Kuo C. L. (1999). ESTIMATE DAMPING AND QUAKE BY USING TRADITIONAL SOIL TESTINGS, University of Florida, Department of Civil Engineering: 1-94.

McVay, M. C., B. Birgisson, et al. (2000). "Load and Resistance Factor Design (LRFD) for Driven Piles Using Dynamic Methods - A Florida Perspective." Geotechnical Testing Journal 23(1): 55-66.

Middendorp P. and Verbeek G.E.H. (2005). Thirty Years of Experience with the Wave Equation Solution Based on the Method of Characteristics Proceedings of the 30th Annual Conference on Deep Foundations, Chicago, Illinois, USA, Deep Foundation Institute.

Mitchell J.K. (1960). "Fundamental aspects of thixotropy in soils." Journal of Soil Mechanics and Foundation Division, ASCE Vol.86(No.8M3): p19-52.

Morgano C.M, White B.A. & Allin R.C. (2008). Dynamic testing in sensitive & difficult soil conditions. Application of Stress Wave Theory to Piles. J. A. Santos. Lisbon: 135-138.

Olsen R., Flaate K. (1967). "Pile Driving Formulas for Friction Piles in Sand." Journal of Soil Mechanics and Foundation Engineering, JSMFE Vol. 93(SM6): 279-297.

Paikowsky, S. (1984). Use of Dynamic Measurements for Pile Analysis. Including PDAP-Pile-Driving Analysis Program. Newton, Massachusetts, GZA Inc.

Paikowsky, S. (1995). "Using Dynamic Measurements for the Capacity Evaluation of Driven Piles. ." Journal of the Boston Society of Civil Engineers Section/ASCE Vol.10(No. 2): pp. 61-76.

Paikowsky S (2004). Load and Resistance Factor Design (LRFD) for Deep Foundation. Lowell, Masssachusetts, University of Massachusetts.

Paikowsky, S., and Stenersen, K. (2000). The Performance of the Dynamic Methods, their Controlling Parameters and Deep Foundation Specifications. Keynote lecture in Stress Wave 2000, Proceedings of the Sixth International Conference

on the Application of Stress-Wave Theory to Piles. a. J. B. S. Niyama. São Paulo, Brazil, Balkema, Rotterdam-the Netherlands: 281-304.(Paikowsky 1982).

Paikowsky, S. and L. Chernauskas (1996). Soil Inertia and the Use of Pseudo Viscous Damping Parameters. Proceeding of the 5th International Conference on the Application of Stress-Wave Theory to Piles. M. H. F.C. Townsend, and M.C. McVay. Orlando, FL: 203-216.

Paikowsky, S., LaBelle, V., and Hourani, N. (1996). Dynamic Analyses and Time Dependent Pile Capacity. Proceedings of the 5th International Conference on the Application of Stress-Wave Theory to Piles. M. H. F.C. Townsend, and M.C. McVay eds. Orlando, FL: 325-339.

Paikowsky, S., Regan, J., and McDonnell, J. (1994). A Simplified Field Method for Capacity Evaluation of Driven Piles, FHWA.

Paikowsky S., C.M. Marchionda, C.M. O'Hearn, M.C. Canniff (2009). Developing a Resistance Factor for Mn/DOT's Pile Driving Formula. Lowell, University of Massachusetts.

Paikowsky S. and Chernauskas L. (1992). Energy Approach for Capacity Evaluation of Driven Piles. Proceedings of the 4th International Conference on the Application of Stress-Wave Theory to Piles. F. B. Barends. The Hague, The Netherlands: pp. 595-601.

Paikowsky S., Hajduk E. (2000). Theoretical Evaluation and Full Scale Field Testing Examination of Pile Capacity Gain with Time: Research Report submitted to the Massachusetts Highway Department. Massachusetts-Lowell, MA., University of Massachusetts-Lowell.

Paikowsky S. and LaBelle V. (1994). Examination of the Energy Approach for Capacity Evaluation of Driven Piles. Proceedings of the International Conference on Design and Construction of Deep Foundations, Orlando, FL.

Paikowsky S., LaBelle V. and Mynampaty R. (1995). Static and Dynamic Time Dependent Pile Behavior: Research Report submitted to the Massachusetts Highway Department, University of Massachusetts-Lowell, MA.

Paikowsky S.G., Hajduk E.L. (2004). "Design and Construction of Three Instrumented Test Piles to Examine Time Dependant Pile Capacity Gain." Geotechnical Testing Journal vol.27(no.6): pp.515-531.

Paikowsky, S. G., ,, Hajduk E. L. , et al. (2005). Comparison between Model and Full Scale Pile Capacity Gain in the Boston Area, ASCE.

Paquet J. (1988). Checking Bearing Capacity by Dynamic Loading - Choice of a Method. 3rd Conference on the Application of Stress Wave Theory on Piles, Ottawa, Canada.

Pile Dynamics Inc. (2006). CAPWAP Case Pile Wave Analysis Program: Background Report Manual, Version 2006. Cleveland, Oh.

Pile Dynamics Inc. (PDI) (2005). GRLWEAP Wave equation analysis of pile driving: Procedures and Models Manual. Cleveland, Oh.

Pile Dynamics Inc.(PDI) (1992). PDA-W Users Manual. Cleveland, Oh.

Poulos H.G. (1989). "Pile Behaviour-theory and application." Geotechnique vol.39(no.3): pp365-415.

Raamot T. (I967). Analysis of Pile Driving by the Wave Equation. Foundation Facts, Raymond International Inc. Vol.lIl, No. I: pp10-12.

Randolph M.F., Carter J.P. and Wroth C.P. (1979). "Driven Piles in clay-the effects of installation and subsequent consolidation." Geotechnique vol.29(no.4): pp361-393.

Rausche, F., G. Thendean, et al. (1997). Determination of pile driveability and capacity from penetration tests: volume II: appendixes. McLean, Virginia, USA, United States. Federal Highway Administration (FHWA). Office of Engineering R and D: 393.

Rausche, F., G. Thendean, et al. (1997). Determination of pile driveability and capacity from penetration tests: volume III: literature review, data base and appendixes. McLean, Virginia, USA, United States. Federal Highway Administration (FHWA). Office of Engineering R and D: 128.

Rausche, F., G. Thendean, et al. (1997). Determination of pile driveability and capacity from penetration tests; volume 1: final report. McLean, Virginia, USA, United States. Federal Highway Administration (FHWA). Office of Engineering R and D: 204.

Rausche F. (1978). "A Critical Examination of the Wave Equation." Transportation Research Record No. 665, Bridge Engineering, proceeding of a conference

conducted by the Transportation Research Board, September 25-27, 1978. Volume 2: pp.209-213.

Rausche F. (2000). Pile Driving Equipment: Capabilities and Properties [keynote lecture]. Proceedings of the Sixth International Conference on the Application of Stress-wave Theory to Piles, São Paulo, Brazil.

Rausche F., G.G. Goble & G. Likins (1985). "Dynamic determination of pile capacity." Journal of Geotechnical Engineering, ASCE. 111(3): 367-383.

Rausche F., Goble G.G., et al. (1988). Recent WEAP Developments. Third International Conference on the Application of Stress-Wave Theory to Piles. Ottawa, Canada: 164-173.

Rausche F. and Klesney A. (2007). Hammer Types, Efficiencies and Models in GRLWEAP. PDCA 11th Annual International Conference and Exposition: Nashville, TN, Cleveland, Ohio, GRL Engineers Inc.

Rausche F., Liang L., Allin R., Rancman D., (2004). Applications and Correlations of the Wave Equation Analysis Program GRLWEAP. Proceedings of the Seventh International Conference on the Application of Stresswave Theory to Piles, Petaling Jaya, Selangor, Malaysia.

Rausche F., Likins G.E., et al. (1986). The performance of Pile Driving Systems Inspection Manual. Washington DC, FHWA.

Rausche F., Likins G.E., Goble G.G, Hussein M. (1986). The performance of Pile Driving Systems.

Rausche F., Webster S., et al. (2009). CAPWAP and Refined Wave Equation Analyses for Driveability Predictions and Capacity Assesmnet of Offshore Pile Installations. Proceedings of the ASME 28TH International Conference on Ocean, Offshore and Arctic Engineering, Honolulu, Hawaii, USA, ASME.

Rausche F., M. F., Goble G. G. (1972). "Soil Resistance Predictions From Pile Dynamics." Journal of the Soil Mechanics and Foundations Division, American Society of Civil Engineers. Reprinted in Current Practices and Future Trends in Deep Foundations, Geotechnical Special Publication No. 125, DiMaggio, J. A., and Hussein, M. H., Eds, August, 2004. American Society of Civil Engineers: Reston, VA; 418-440.

Sakai T., Sawai H. and Shioi Y. (1996). Theoretical Analysis of the Pile Driving Formula. Proceeding of 5th International Conference on the Application of Stress

Wave Theory to Piles. F.C Townsend, M. Hussein and M.C. McVay. Orland, FL: 81-88.

Salgado R. (2006). The Engineering of Foundations, McGraw-Hill Science.

Skov R., Denver H. (1988). Time Dependance of Bearing Capacity of Piles. Proceedings of the Third International Conference on the Application of Stress-Wave Theory to Piles. Ottawa, Canada, BiTech Publishers: 879-888.

Smith E.A.L. (1950). Pile Driving Impact. Industrial Computation Seminar. New York, N.Y., International Business Machine Corp.

Smith E.A.L. (1960). "Pile Driving Analyses by the Wave Equation." Journal of the Soil Mechanics and Foundation Division, ASCE. Vol. 86(1960): 35-61.

Smith, E. A. L. (1955). "Impact and Longitudinal Wave Transmission." Transactions of the American Society of Mechanical Engineers: pp 963-973.

Smith, E. A. L. (1957). "What Happens When Hammer Hits Pile." Engineering News Record: pp 46-48.

Smith, E. A. L. (1962). "Pile-Driving Analysis by the Wave Equation." Transactions of the American Society of Civil Engineers Vol 127(Part 1): pp 1145-1193.

Soderberg L. O. (1962). "Consolidation Theory Applied to Foundation Pile Time Effects." Géotechnique Vol.12(Issue 3): pages 217 -225.

Stain R. T. (2005). SIMBAT Dynamic Pile Testing – Results of an Independent Pile Capacity Prediction Event 30th Annual Conference on Deep Foundations, Chicago, Illinois, USA.

Stevens R.F. (2000). Pile acceptance based on combined CAPWAP analysis. Proc. Conf. on Application of Stress-Wave Theory to Piles. Sao Paulo, Brazil, Balkema.

Svinkin M.R., Morgano C.M (1994). Pile Capacity as a Function of Time in Clayey and Sany Soils. Fifth International Conference and Exhibition on Piling and Deep Foundations, Belgium.

Svinkin, M. R. (1996). Soil damping in wave equation analysis of pile capacity. Proceedings of Fifth International Conference on the Application of Stress-Wave Theory to Piles. M. H. M. M. F. Townsend. Rotterdam, Balkema.

Svinkin, M. R. (2002). "Engineering judgement in determination of pile capacity by dynamic methods." Geotechnical Special Publication ISSU(116): 898-914.

Tavenas F. and Audibert J.M.E. (1977). "Application of the wave equation analysis to friction piles in sand." Canadian Geotechnical Journal Vol.14: pp.34-51.

Tavenas F. and Audy R. (1972). "Limitations of the Driving Formula for Predicting the Bearing Capacities of Piles in Sand." Canadian Geotechnical Journal Vol.9: pp.47-62.

Tejchman, A., , Klos, J. (1984). An example of dynamic formulae determined on the basis of field tests. Application of Stress-Wave Theory to Piles, Swedish Pile Commission.

Testconsult Limited. "SIMBAT Test Equipment - Hardware and Software Specification." www.testconsult.co.uk.

The Wave Equation Page for Piling. (1997). "Efficiency and Energy Transfer in Pile Driving Systems."

The Wave Equation Page for Piling. (1997). "An Overview of Pile Driving Equipment." December 1999.

Thompson, C. D. and D. E. Thompson (1985). "Real and Apparent Relaxation of Driven Piles." Journal of Geotechnical Engineering 111(2): 225-237.

Timoshenko S.P., Goodier J. N. (1951). Theory of Elasticity. New York, McGRaw-Hill Book Company.

Tomlinson, M. (2001). Foundation Design and Construction.

Triantafyllidis, T. (2001). "On the application of the Hiley formula in driving long piles." Geotechnique v 51(n 10): p 891-895.

Uto K., Aso T., Tsutsumi and Matsui K., (1981). A New Method for Estimating the Bearing Capacity of A Cast-In-Place Pile. Application of Stress Wave Theory to Piles. H. Bredenberg. Balkema/Rotterdam: 345-350.

Uto K., Fuyuki M., Ninomiya K. and Omori H. (1992). New Development of Pile Driving Management System. Application of Stress Wave Theory to Piles. Balkema/Rotterdam/Brookfield: 351-356.

Verruijt A. (2005). Waves in Piles. Soil Dynamics. Delft, Delft University of Technology.

Voitus van Hamme, Jansz J.W., et al. (1975). "Hydroblok and Improved Pile-driving Analysis." International Civil Engineering Vol.3(no.4): pp167-179.

Vulcanhammer Guide to Pile Driving (Vulcan Iron Works Inc.). (2011). "www.vulcanhammer.info." Retrieved 2010, 2010, from www.vulcanhammer.info.

Warrington D.C. (1996). Development and Potential of the Wave Equation In Closed Form as applied to Pile Dynamics. Fifth International Conference on the Application of Stress-Wave Theory to Piles. Orlando, FL.

Warrington D.C. (1997). Closed Form Solution of the Wave Equation for Piles. Master's Thesis, University of Tennessee at Chattanooga.

Whitaker, T. (1970). The Design of Pile Foundation.

Wu A.K.H (1985). "Validity of Smith Model in Pile Driving Analysis." Journal of Geotechnical Engineering Vol.115(No.9): pp1285-1302.

Yang, L. and R. Liang (2009). "Incorporating setup into load and resistance factor design of driven piles in sand." Canadian Geotechnical Journal 46(3): 296-305.

Zadroga B., Gwizdala K. (1992). Determination of bearing capacity of piles using modified Delmag dynamic formula. Application of Stress-Wave Theory to Piles, Balkema.

Zhang B., Yu X. (Bill), et al. (2009). The Dynamic Components of End Bearing in Highly Cohesive Clay during Pile Driving Process. ASCE Conf. Proc. M. Iskander, D. F. Laefer and M. H. Hussein. Orlando, Florida, ASCE. 336.

Zhang L., Shek M.P, Ng M.Y. (2004). Wave Equation Parameters for Long Steel H-Piles Founded in Decomposed Granite. Proceedings of the Seventh International Conference on the Application of Stresswave Theory to Piles. Petalling Jaya, Selangor, Malaysia.

Zhang L.M (2005). "Pile Driving Process Monitoring Based on Field Energy Measurements." Soil and Foundations - Japanese Geotechnical Society Vol.45(No.6): pp31-41.

Zhou L. and Lao W. (2006). "Studying of the Dynamic Behavior of Pile Cushioning Materials in Pile Driving." Journal of Testing and Evaluation vol.34(no.5): pp1-6.